

**UNRAVELLING FORESHORE ECOSYSTEM DYNAMICS:
APPLICATIONS FOR ECOSYSTEM-BASED
COASTAL DEFENCE**

Beatriz Marin-Diaz

Marin-Diaz, B. (2022). Unravelling foreshore ecosystem dynamics: applications for ecosystem-based coastal defence. PhD thesis, Royal Netherlands Institute for Sea Research, The Netherlands and University of Groningen, The Netherlands

The research presented in chapter 2, 3, 4, 6 and 7 was conducted as part of the Perspectief Research Programme 'All- Risk', project number P15- 21 B1, which is cofinanced by NWO Domain Applied and Engineering Sciences, in collaboration with the Dutch Ministry of Infrastructure and Water Management (RWS), Deltares, STOWA, the regional water authority Noorderzijlvest, the regional water authority Vechtstromen, it Fryske Gea, HKV consultants, Natuurmonumenten and the waterboard HHNK. Chapter 5 was part of my MSc project funded by Erasmus+ and MOBINT grants, together with the FORMAS grant Dnr. 231-2014-735 from E. Infantes in the University of Gothenburg.

All work was conducted with the support of the Department of Estuarine & Delta Systems (Royal Netherlands Institute for Sea Research, NIOZ), the Faculty of Science and Engineering (University of Groningen) and the Department of Marine Sciences, University of Gothenburg.

Cover : Beatriz Marin-Diaz (painting) and Lisa Sanchez Aguilar (layout)

Layout: Beatriz Marin-Diaz

Pictures: Beatriz Marin-Diaz

Printed by: GVO drukkers en vormgevers

Correspondence: bea.marin.diaz@gmail.com

©2022, Beatriz Marin-Diaz, all rights reserved. No part of this thesis may be reproduced, stored or transmitted in any form or by any means without prior written permission of the author



university of
 groningen

Unravelling foreshore ecosystem dynamics: applications for ecosystem-based coastal defence

PhD thesis

to obtain the degree of PhD at the
University of Groningen
on the authority of the
Rector Magnificus Prof. C. Wijmenga
and in accordance with
the decision by the College of Deans.

This thesis will be defended in public on

Tuesday 28 June 2022 at 14.30 hours

by

Beatriz Marin Diaz

born on 23 January 1992
in Ripollet, Spain

Supervisors

Prof. T.J. Bouma
Prof. H. Olff
Prof. D. van der Wal

Co-supervisor

Dr. L.L. Govers

Assessment Committee

Prof. J. Van De Koppel
Prof. K.R. Timmermans
Prof. E.S. Bakker

Paranymphs

Lisa Sanchez Aguilar
Isabelle Buyens

For my dear family, Pol and friends

Contents

CHAPTER 1	General introduction	11
CHAPTER 2	Using salt marshes for coastal protection: effective but hard to get where most needed	31
CHAPTER 3	The importance of marshes providing soil stabilization to resist fast-flow erosion in case of a dike breach	65
CHAPTER 4	Quantifying the resistance to cliff and sheet erosion across vegetation zones in a sandy back-barrier island	99
CHAPTER 5	Role of eelgrass on bed-load transport and sediment resuspension under oscillatory flow	121
CHAPTER 6	How grazing management can maximize erosion resistance of salt marshes	141
CHAPTER 7	On the use of large-scale biodegradable artificial reefs for intertidal foreshore stabilization	173
CHAPTER 8	Synthesis	195
	References	217
	Summary	235
	Samenvatting	241
	Resumen	247
	Acknowledgments	255
	Curriculum Vitae	263
	List of publications	267



Chapter 1

General introduction

INTRODUCTION

Many coastal communities are currently facing flood risks worldwide (Nicholls et al. 2007) due to accelerating sea level rise (IPCC 2014), land subsidence (Syvitski et al. 2009; Weston 2014) and extreme events such as storms surges (Kiesel et al. 2021), which will probably become more frequent with climate change (Menéndez and Woodworth 2010; IPCC 2014; Vousdoukas et al. 2018). Extreme sea levels have become more frequent worldwide since the 1970s (Woodworth et al. 2011; IPCC 2014), and while changes in mean sea level are long term slowly increasing, extreme sea level events have immediate impacts on the coast (Menéndez and Woodworth 2010). Particularly, extreme sea levels may become more important in areas with high flooding risk due to low land elevations and constructions near the coastline, as is the case in the Netherlands (Bouwer and Vellinga 2007).

As a result, increasing investment in coastal defence structures is needed worldwide (Temmerman et al. 2013). Hard engineering structures such as dikes, sea walls, breakwaters and storm surge barriers, also called 'grey' solutions, are commonly used for coastal protection (Fig. 1). Nevertheless, conventional hard engineering is often associated with negative impacts on natural functioning and biodiversity of coastal ecosystems and their ecosystem services (e.g. Lai et al., 2015). Furthermore, because conventional hard engineering is static, it can be increasingly challenged by climate change and the maintenance may become very costly (Temmerman et al. 2013; Bouma et al. 2014; Morris et al. 2020).



Fig. 1. Examples of types of coastal defence, from 'grey' (human based) to 'green' (nature-based). Green solutions leave space for natural ecosystems to develop and migrate inland, therefore is paired with not building right next to the sea.

COASTAL PROTECTION BY NATURAL FORESHORE ECOSYSTEMS

An alternative to the 'grey' solutions is the ecosystem-based coastal defence, also called nature-based coastal protection or 'green' solutions (Fig. 1). Hybrid ecosystem-based coastal defence combines conventional hard engineered barriers with coastal ecosystems (Fig. 1 and 2) and can be a more sustainable, ecologically valuable and cost effective alternative to hard engineering alone (Shepard et al. 2011; Temmerman et al. 2013; Morris et al. 2018; Schoonees et al. 2019; Vuik et al. 2019; van Zelst et al. 2021). In contrast to engineered solutions, ecosystems can be capable to spontaneously recover from storm disturbances and

be resilient against sea-level rise (Feagin et al. 2015; Kirwan et al. 2016; Fagherazzi et al. 2020; Morris et al. 2020). In addition, they provide a broad range of ecosystem services (Orth et al. 2006; Gedan et al. 2009; Barbier et al. 2011). These include biodiversity conservation (e.g. Terrados and Borum 2004; Spencer and Harvey 2012), nutrient cycling (e.g. Human et al. 2015), support for fisheries (e.g. Lilley and Unsworth 2014; Christianen et al. 2017), water purification (e.g. Andrews et al. 2006) and carbon sequestration (Duarte et al. 2013).

Sand dunes, marshes, mangroves, seagrass, kelp forest, coral and shellfish reefs are coastal ecosystems recognised for their coastal protection value, especially along soft-bottom coasts (Temmerman et al. 2013; Schoonees et al. 2019). This thesis is focused on tidal flats, seagrass, shellfish reefs, dunes and with most emphasis on salt marshes (Box 1). These so-called foreshore ecosystems are able to attenuate waves and currents and stabilise the soil (Shepard et al. 2011; Bouma et al. 2014). For example, salt marshes have been found to reduce waves even under storm surge conditions (Möller et al. 2014; Willemsen et al. 2020), lower the wave run-up on the dikes compared to dikes with bare tidal flat in front (Vuik et al. 2016; Zhu et al. 2020), reduce the chance of dike breaching during extreme events, and reduce the size of dike breaches when dikes fail (Zhu et al. 2020). Furthermore, the protection by coastal ecosystems may be the result of long-distance interactions and facilitation effects (Bos and Van Katwijk 2007; Bouma et al. 2014; van de Koppel et al. 2015; Schoonees et al. 2019). For example, mussel or oyster beds may act as natural wave breakers behind which seagrass beds can establish, which in return may affect tidal flat morphology promoting marsh development, and finally the salt marsh may protect the seawall or dike (Fig. 2).

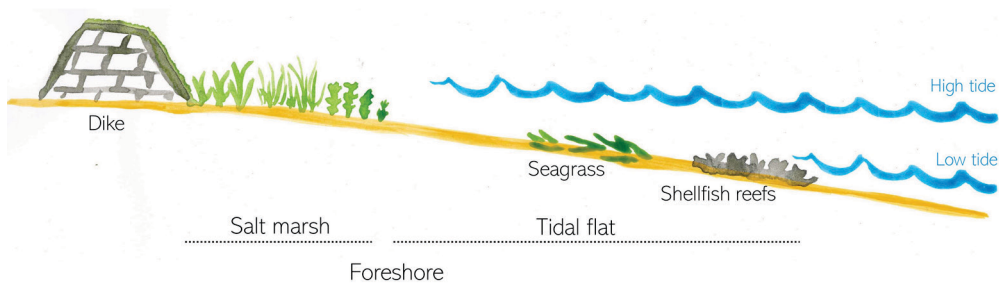


Fig. 2. Representation of ecosystem-based coastal protection in soft-bottom coastal zones. Natural ecosystems in front of hard engineer structures can reduce wave loads arriving to the foreshore and therefore increase safety value and simultaneously increase the ecological value of the foreshore.

Although there is mounting evidence for ecosystem-based coastal defence being a cost-effective and ecological valuable alternative to 'grey' infrastructure alone, uncertainties about the actual effectiveness still hampers the practical implementation of these ecosystem-based measures. There is not a one-size-fits-all 'green' solution and each situation requires a tailor-made approach but based on common principles. For instance, natural ecosystems can adapt to sea level rise by landward migration. However, in urbanized areas, this migration may be prevented by hard structures constructed along the coastline (i.e. urbanization, roads, dikes, seawalls), a process called coastal squeeze (Doody 2013). Therefore, there are coastal settings

INTRODUCTION

where nature-based solutions alone can be enough, while in other situations, with harsher environmental conditions and where landward migration of the ecosystems is not possible, hard engineering may be needed (Morris et al. 2018, 2020; Schoonees et al. 2019) (Fig. 1). On top of that, coastal ecosystems are degrading due to anthropogenic pressures and climate change (Orth et al. 2006; Syvitski et al. 2009; Murray et al. 2019). Therefore, there is an urgent need to advance the understanding of coastal ecosystem dynamics in space and time, and how management can affect these systems in order to optimize their coastal protection function (Bouma et al. 2014).

BOX 1. SYSTEMS INCLUDED IN THIS THESIS

SALT MARSHES

Found at relatively sheltered locations, salt marshes are salt-tolerant vegetated areas at the transition between land and sea, subject to periodic flooding (Allen 2000). Salt marshes can attenuate hydrodynamics (i.e. waves and currents) and create stable and elevated soils by trapping sediment and accumulating organic matter. This leads to a positive feedback by creating suitable conditions for the growth of more vegetation and in return attenuate more hydrodynamics (Allen 2000, Koppel et al. 2005).

Salt marshes can be found in the mainland (i.e. mainland marshes), or in barrier islands, growing behind the shelter of a dune or chenier ridge (i.e. back-barrier marsh) (Bakker 2014). In mainland marshes, the elevation gradient goes from the dike toe to the tidal flats, while in back-barrier marshes, the elevation gradient goes from the dune toe to the tidal flats (Bakker et al. 2015). Due to intrinsic feedbacks (Koppel et al. 2015) or factors such as changing exposure or sediment supply (e.g. Wang et al. 2017, Ladd et al. 2019), marshes can retreat landwards. This process is also called cliff or lateral erosion.



TIDAL FLATS

Tidal flats are soft-sediment environments regularly flooded by the tides that form in intertidal areas where sediment is deposited by the tides or rivers (Murray et al. 2019). They can be found in front of salt marshes, mangroves or directly in front of the dikes or seawalls and extend until the mean low-tide elevation. When composed of mud, they are also referred as mudflats. Tidal flats can host high biodiversity of benthic species (Christianen et al. 2017b) and are important for migratory birds (Boere and Piersma 2012).



MUSSEL BEDS

Mussel beds are a type of shellfish reef that occurs in subtidal (always below water) and intertidal (flooded during high tide) zones along the coast (Folmer et al. 2017). They provide hard substrate in soft-sediment environments and can accrete sediment, which is related to waves and currents attenuation (Donker, Vegt, & Hoekstra 2013). Mussel beds were not directly studied in this thesis, but the description serves as a background for the chapter 7, where we utilised biodegradable artificial reefs aimed at mussel bed restoration.



SEAGRASS BEDS

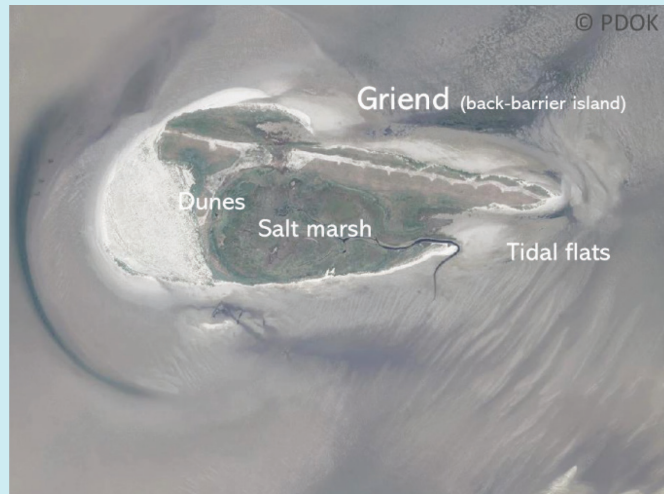
Seagrasses are aquatic flowering plants that evolved from freshwater plants to grow on marine or brackish environments. They can grow in the intertidal to subtidal zones along the coast, always at lower tidal elevations than the salt marshes (Short et al. 2007). They can trap sediment and attenuate waves and currents, which makes them valuable for coastal protection (Ondiviela et al. 2014). *Zostera marina*, also known as eelgrass,

is the species studied in this thesis and the most wide-ranging marine flowering plant in the Northern Hemisphere (Short et al. 2007).



SOFT-SEDIMENT BARRIER ISLANDS

Barrier islands are migrating and dynamic soft-sediment coastal landscapes that accommodate both sandy dune barriers and silty back-barrier marshes in their wake (Oertel 1985). Dune formation occurs above the mean high-tide level and it is mostly driven by aeolian sand deposition facilitated by vegetation (Otvos, 2020). Situated parallel to the mainland coast, barrier islands are the first barrier attenuating waves coming towards the coast from the open seas (Otvos, 2020). Back-barrier islands, like Griend in the Netherlands, are a type of smaller barrier islands that can be found behind oceanic barrier islands (Cooper et al. 2007). In contrast to the ocean barrier islands, back-barrier islands do not often form a dune through aeolian sand transport (Pilkey et al. 2009). Instead, they present a beach, small dunes or a chenier ridge on the exposed side formed during strong storm events (Pilkey et al. 2009).



FORESHORE ECOSYSTEM IMPACTS ON WAVE ATTENUATION AND RUN-UP

After storms, the maximum height that waves reach onto the dikes can be measured as the vertical elevation at which beach wrack is left on the dike (Spencer et al. 2015; Vuik et al. 2016; Zhu et al. 2020) (Fig. 3). The actual wave run-up onto a dike is the distance from the storm-surge water level to the beach wrack level (Fig. 3). Therefore, beach wrack levels depend on the wave properties and storm-surge levels, with large waves combined with high water levels resulting in the highest beach wrack levels (Vuik et al. 2016; Zhu et al. 2020). The probability of water overtopping the dike (i.e. water flowing over the dike) increases if storm-surge levels and thus wave run-up increase due to global change. Dike overtopping risk may be reduced by the use of ecosystem-based coastal defence, where natural ecosystems in front of dikes would reduce wave heights leading to lower wave run-up onto the dike (Vuik et al. 2016). Furthermore, the reduction of wave energy arriving to the dikes may also prevent dike failures (Vuik et al. 2019; Zhu et al. 2020).

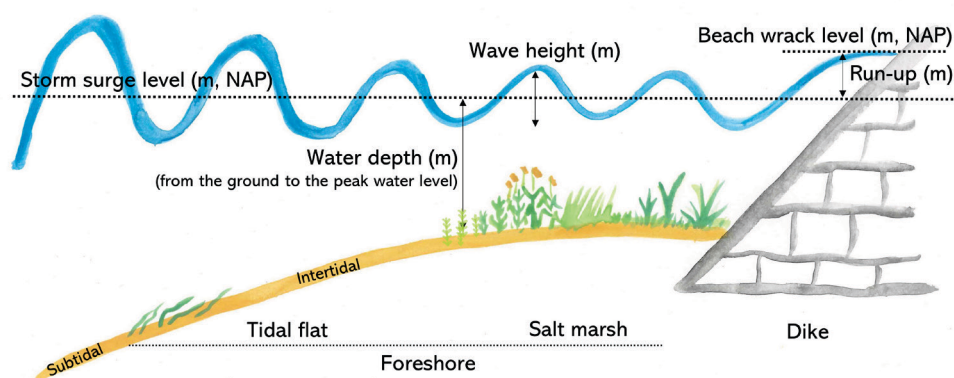


Fig. 3. Diagram describing the terms related to the run-up on the dikes. Below, a photo of a beach wrack in a dike fronted by a salt marsh. NAP is the Dutch Ordinance Level, similar to mean sea water level.

Bare tidal flats can attenuate waves and currents (Le Hir et al. 2000; Hu et al. 2015). Particularly, wave forcing is more efficiently dissipated in higher, wider, convex and gentler sloping tidal flat profiles than concave and steep profiles (Le Hir et al. 2000; Hu et al. 2015). In addition, structures on tidal flats such as reefs, macroalgae, seagrasses or annual saltmarsh plants will promote further waves and flow attenuation by the creation of drag forces (Pinsky et al. 2013; Walles et al. 2015; Leonardi et al. 2018). Such communities at low elevations along the foreshore can attenuate hydrodynamics (e.g. waves and currents) and trap sediment, thus changing the tidal flat morphology (e.g. Bos et al. 2007; Christianen et al. 2013; Walles et al. 2015), which may ultimately facilitate the establishment and stability of communities at higher elevations such as salt marshes and mangroves (Gillis et al., 2014; van de Koppel et al., 2015). Communities higher in the intertidal zone such as perennial salt marsh vegetation, mangroves or dune vegetation will attenuate more hydrodynamics than communities at lower elevations (Bouma et al. 2014) as a result of their persistent and higher foreshore which enhances wave attenuation combined with vegetation friction (Möller et al. 1999; Vuik et al. 2016; Gracia et al. 2018; Leonardi et al. 2018; Brooks et al. 2020).

The ratio of water depth to structure height is an important variable for wave attenuation. The lower the water levels are relative to the structure height, the more attenuation will occur (e.g. Möller et al. 1999; Ysebaert et al. 2011; Yang et al. 2012; Chowdhury et al. 2019). This is one of the reasons why marsh vegetation is more effective in the overall wave attenuation than seagrass beds or biogenic reefs which are generally associated with deeper water levels (Bouma et al., 2014). In the case of salt marshes, the promotion of sediment accretion by the vegetation and resulting increase in soil elevation, will in return enhance wave attenuation and promote better conditions for vegetation, since plants become less exposed to inundation (Redfield et al. 1972; Morris et al. 2002; Van de Koppel et al. 2005; Bouma et al. 2009b). Vegetation may also increase the soil elevation by belowground biomass production (Morris et al. 2002; Cahoon et al. 2006; Kirwan and Guntenspergen 2012). Marshes where organic accumulation dominates the vertical accretion and have low sediment input can be classified as organogenic marshes (e.g. found in the United States and microtidal marshes) (Nolte et al. 2013; Kearney and Turner 2016). In contrast, vertical accretion in minerogenic marshes depends mainly on sediment supply from tidal flooding (common in Europe and south-east USA) (Bakker et al. 2015). In general, organogenic marshes will have higher rates of subsidence as their sediment is compacted or decomposed faster than in minerogenic marshes (Nolte et al. 2013).

Wave attenuation by vegetation friction will also depend on the vegetation characteristics as the number of structures (leaves or branches), stem density and stiffness (Möller 2006; Bouma et al. 2005, 2010; Ysebaert et al. 2011). Stiffer plants such as *Spartina* sp. (marsh species) will pose more friction to the water, therefore dissipating more waves and currents compared to more flexible vegetation such as *Zostera* sp. (seagrass species) (Bouma et al. 2005b; Schwarz et al. 2015). Wave attenuation will also vary over the seasons, with greater attenuation in summer due to the higher density of vegetation (Vuik et al. 2016, 2017).

INTRODUCTION

Nevertheless even for the considerable inundation depths that occur during storms and with winter state vegetation, saltmarshes can be efficient in reducing wave impacts, especially due to their elevated and stable foreshores (Möller et al. 2014; Vuik et al. 2016; Willemsen et al. 2020). Finally, wider marshes are expected to attenuate more waves and therefore provide more protection compared to narrow marshes or bare tidal flats (Shepard et al. 2011). For this reason, marsh width is one of the most important factors related to the coastal defence function of marshes (Shepard et al. 2011; Bouma et al. 2014).

The effect of (vegetated) foreshores in wave run-up can be modelled based on wave properties and storm surge levels (e.g. Vuik et al. 2016). However, experimental evidence on how (vegetated) foreshores affect wave run-up including contrasting foreshore types (i.e. different wind exposure, vegetation, tidal range and bathymetry) remains scarce (Spencer et al. 2015; Zhu et al. 2020). Understanding the effect of foreshores on run-up requires in depth understanding of *i)* at which locations you can have salt marshes and *ii)* how effective such (vegetated) foreshores are in reducing wave run-up onto a seawall. This will be addressed in **chapter 2**.

FORESHORE SEDIMENT STABILITY

Sediment erosion can occur on the soil surface or on the lateral of a cliff (Box 1, Fig. 4). Soil surface erosion, hereafter called top erosion, can be caused by the initiation of horizontal sediment transport (i.e., bed load) or by sediment resuspension (i.e., suspended load) (Einstein et al. 1940; Brown et al. 1995) due to increased bed shear stress by currents or waves (Van Rijn 1984a; b; Brown et al. 1995; Ganthy et al. 2015). Bed load occurs when sediment particles move along the bottom horizontally by rolling whereas sediment resuspension occurs when the sediment particles are lifted vertically into the water column creating turbidity and reducing light (Einstein et al. 1940; Brown et al. 1995). Lateral erosion, also called cliff erosion, can be in form of gradual detachment of soil particles from the sediment due to hydraulic pressure (e.g. Feagin et al. 2009; Twomey et al. 2021) (Fig. 4). Lateral erosion can also occur in form of big blocks or “mass failure”, which can occur due to undercutting, normally by wave swash, and the creation of tension cracks (Schwimmer et al. 2001; Francalanci et al. 2013; Priestas et al. 2015). Undercutting can occur in marsh cliffs when the sediment below the cohesive top layer of the marsh starts to erode, and the top layer with roots overhangs until it breaks off and collapses (Fig. 4).

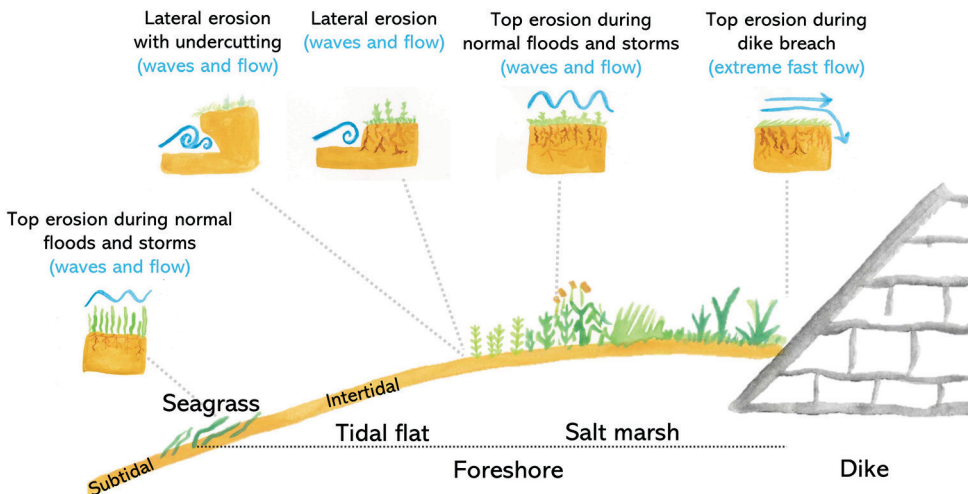


Fig. 4. Types of sediment erosion present in foreshores. Same erosion as represented for a salt marsh can be applied to bare tidal flats. Seagrass can be subtidal (always below water) or intertidal (flooded daily).

Fine grained soils with silt, clay and organic matter are more cohesive and less erodible (Brown et al. 1995; Gailani et al. 2001; Grabowski et al. 2011). In contrast, sandy soil is much less cohesive and therefore less resistant to erosion (Brown et al. 1995). On the other hand, even small percentages of clay (5-10%), will make the sediment more cohesive, having a significant effect on erosion reduction (Brown et al. 1995; Gailani et al. 2001; Grabowski et al. 2011). Silty sediment without clay, even being very fine, can be non-cohesive and be easily eroded (Brown et al. 1995). Clay fraction can be more time consuming to determine, and commonly used instruments to determine the grain size, such as Malvern Laser Particle Sizer®, can underestimate the clay content (Vroom et al. 2014). In some regions, like in the Wadden Sea, which is one of our study sites, the clay-silt fraction in marine soils, also called mud, correlates to the clay fraction (Van Ledden et al. 2004). For example, sandy sediment with more than 20% of mud was found to be more cohesive and had lower erosion rates than sandy sediment with low percentage of mud (Houwing 1999; Lo et al. 2017). For these reasons, in many studies on erosion, the clay-silt fraction or 'mud' has been used as a variable to relate to erosion instead of clay alone.

Sediment particles can be classified according to their size, from the finest to the coarser sizes:

- clay ($< 2 \mu\text{m}$)
- silt ($< 62.5 \mu\text{m}$)
- sand ($62.5 \mu\text{m} > 2 \text{ mm}$)
- gravel ($2 \text{ mm} > 25 \text{ cm}$)
- boulders ($> 25 \text{ cm}$)

Coastal vegetation can reduce erosion by waves and currents (Ward et al. 1984; Christianen et al. 2013; Brooks et al. 2020), which is normally attributed to a reduction of the hydrodynamics within the canopy and hence lower shear stress on the soil (Bos et al. 2007; Infantes et al. 2012; Möller et al. 2014; Feagin et al. 2019; Türker et al. 2019). However,

INTRODUCTION

vegetation with little or no aboveground biomass, such as in winter-state, due to grazing (Christianen et al. 2013; Paul and Kerpen 2021) or with the leaves broken or flattened due to wave energy (Möller et al. 2014; Spencer et al. 2016), has been observed to still limit erosion. This suggests that changes induced in the sediment as a result of vegetation presence and the belowground biomass (i.e. roots and rhizomes, Fig. 4) can increase soil resistance to erosion.

Vegetation is able to accumulate fine sediment (silt and clay) and organic matter (Allen 2000; Feagin et al. 2009; Marani et al. 2013), thus enhancing properties that can make the sediment more cohesive and less erodible (Brown et al. 1995; Gailani et al. 2001; Grabowski et al. 2011). In terrestrial ecosystems, top erosion by runoff is reduced with increasing fine root density (below 1 or 0.5 mm Ø, depending on the author) compared to bare soils (Li et al. 1991; Baets et al. 2006, 2007; Burylo et al. 2012). Studies on salt marshes show that higher belowground biomass is related to less top erosion (Coops et al. 1996; Spencer et al. 2016), even with the vegetation in winter state (Paul and Kerpen 2021). Belowground biomass has been also related to a reduction in lateral erosion in marshes (Ford et al. 2016; Wang et al. 2017), with the strongest effects found in sandy soils (Lo et al. 2017; De Battisti et al. 2019). However, the soil stability of the marshes under fast flow conditions like would occur during a dike breach, has not yet been studied (Fig. 4). This is becoming increasingly important when dikes protect people living in low-lying areas that are being faced with sea level rise (Zhu et al. 2020). Hence, there is urgent need to gain in depth understanding of the erosion resistance of foreshores fronting dikes against fast flow running over the soil surface (**chapter 3**).

Sandy systems such as sandy barrier islands and back-barrier islands, are also an important part of coastal protection in shallow soft-bottom coasts like the Wadden Sea as they are the first barrier attenuating waves coming towards the coast from the open seas (Cooper et al. 2007; Otvos 2020). Sandy islands can include dunes, marshes and tidal flats (Box 1). These sandy systems can be vulnerable to erosion due to their low cohesive soils, especially if there is not enough recovery time in between storms (Timmons et al. 2010; Cooper 2013; Durán Vinent and Moore 2015; Vinent et al. 2021). For this reason, these systems are increasingly being managed to prevent their complete erosion (Govers and Reijers 2021). However studies testing their erodibility are scarce, especially in back-barrier islands. Hence, it is important to understand their stability to better understand how to manage them (**chapter 4**). Furthermore, this knowledge is important for being able to integrate sandy coastal systems into ecosystem-based, sustainable flood defence systems. As mentioned above, marsh vegetation can reduce cliff and top erosion. Regarding dune vegetation, to the best of our knowledge, studies on the effect of belowground biomass on top erosion have not been done yet, but belowground biomass has been related to a reduction in lateral erosion (De Battisti et al. 2020).

Finally, seagrass beds are also known to stabilize soils and attenuate waves which are valuable properties for coastal protection (Bouma et al. 2014; Ondiviela et al. 2014). However the effect of belowground biomass on soil stability is still relatively poorly studied (Bouma et al. 2014). Christianen et al. (2013) found that seagrass rhizomes and roots seem to play a major

role in topsoil erosion, but to the best of our knowledge, there are no mechanistic studies that directly quantify the effect of belowground biomass. Understanding the effect of seagrass on sediment erosion is important to maintain the water clarity, necessary for seagrass development (Dennison 1987; Duarte 1991), and to retain the sediment in coastal areas (Christianen et al. 2013; Ganthy et al. 2015). The role of eelgrass on top erosion under wave conditions will be studied in **chapter 5**.

GRAZING MANAGEMENT ON SALT MARSHES FOR COASTAL PROTECTION

Biophysical (grain size, compaction, rooting) properties of marsh soils can change with grazing management in combination with marsh age and elevation (Davidson et al. 2017 and references therein). In turn, these changes may affect the lateral erodibility of marshes. For example, marshes which develop from initially sandy intertidal flats and sand banks, will develop a cohesive fine-grained top layer over time during vegetation succession which will be even thicker at lower elevations due to higher flooding frequency and hence higher sediment imports (Olff et al. 1997; Van de Koppel et al. 2005; Elschot et al. 2013). Livestock grazing, which is often used for managing biodiversity in salt marshes, can modify these soil properties (Howison et al. 2015; Davidson et al. 2017 and references therein), thereby potentially also reducing erosion (Pagés et al. 2018). Small grazers such as hare and geese have also shown to structure salt marsh vegetation communities (Kuijper and Bakker 2005; Chen et al. 2019), although previous studies showed no significant effects of these small grazers on soil properties (Elschot et al. 2013). However, as different plant species have different amount of belowground biomass, we could expect differences on erosion depending on the vegetation species (Lo et al. 2017; Wang et al. 2017). Understanding how grazing management on salt marshes can affect soil resistance to lateral erosion is important especially in face of climate change. The frequency and intensity of storms and storm surges are expected to increase (IPCC 2014). Extreme storms may induce the formation of a marsh cliff (Bouma et al. 2016), where especially frequently occurring moderate (winter) storms will determine the rate of lateral retreat (Leonardi et al. 2016). Hence, understanding the susceptibility of salt marshes to lateral erosion is of key importance for being able to integrate marshes as sustainable flood defence strategies. An integrated view on how grazing management in combination with abiotic factors, such as marsh age, marsh elevation and sediment layering, affect the susceptibility of marsh edges to lateral erosion, will be addressed in **chapter 6**.

MANAGEMENT OPTIONS FOR TIDAL FLATS TO PROMOTE MARSH EXPANSION

Salt marsh presence and expansion depends on different factors such as

- i) soil elevation relative to the mean sea level (Balke et al. 2016), which is directly related to the flooding frequency and duration (Cox, Wadsworth and Thomson, 2003; Mateos-Naranjo *et al.*, 2008; Wang and Temmerman, 2013; Silinski *et al.*, 2016),
- ii) the presence of undisturbed periods of time (windows of opportunity) for the seedlings to establish and develop before a disturbance occurs (Balke et al. 2011; Hu et al. 2015),
- iii) the wind exposure of the area, which is related to increased waves and currents and in turn to less seedling establishment even having enough soil elevation (Silinski et al. 2015; Wang et al. 2017)
- iv) bed level changes at the transition of tidal flats and salt marshes (Bouma et al. 2016; Willemsen et al. 2017) and
- v) having enough sediment supply to sustain or create new elevated tidal flats for marsh expansion and keep up with sea level rise (Ladd et al. 2019; Fagherazzi et al. 2020; Liu et al. 2021).

Creating higher and convex foreshores may lead to higher wave dissipation and longer distance from wave breaking points toward the potential pioneer marsh zone (Mariotti and Fagherazzi 2013; Hu et al. 2015; Bouma et al. 2016). This would reduce erosion in the pioneer vegetation zone of a salt marsh and promote marsh establishment (Mariotti and Fagherazzi 2013; Hu et al. 2015; Bouma et al. 2016; Willemsen et al. 2017; Hu et al. 2021). Promotion of marsh expansion is often managed with manmade interventions in the tidal flats in front of the marshes such as building wave-breaking brushwood groynes and digging drainage channels (Dijkema et al. 2011; Siemes et al. 2020), hard-engineered coastal structures such as groynes and breakwaters (Schoonees et al. 2019; Siemes et al. 2020), stone dams (Van Loonsteensma and Slim 2013) or concrete reefs (Chowdhury et al. 2019). These structures can attenuate waves and increase soil elevation as a result of sediment trapping in front of the marshes, thus creating favourable conditions for marsh expansion.

An alternative nature-based approach to change the morphology, width and elevation of the tidal flats in front of the salt marshes and simultaneously increase ecological value may be the restoration of adjacent foundation species such as seagrass meadows or shellfish reefs (e.g. oyster or mussels) (Angelini et al. 2011; van de Koppel et al. 2015; Schoonees et al. 2019) (Fig. 1). These communities found in the tidal flats can also attenuate waves and stabilise and/or accrete sediment in the tidal flat (e.g. Meyer et al. 1997; Borsje et al. 2011; Donker et al. 2013; Walles et al. 2015; Chowdhury et al. 2019). Trials of more environmentally friendly options, such as the restoration of biogenic reefs (e.g. dominated by oysters or mussels) at a large scale and at exposed sites remain scarce (Bouma et al. 2014; Morris et al. 2018). **Chapter 7** will investigate the effects of an alternative management measure using ecoengineering solutions (i.e. biodegradable artificial reefs) on unvegetated intertidal flats to shape the foreshores by restoring mussel beds, which ultimately may reduce marsh retreat and/or facilitate marsh expansion.

MAIN OBJECTIVES OF THIS THESIS

As described above, the main objectives of this thesis are to assess *i)* the distribution and development of salt marshes in relation to the foreshore bathymetry (chapter 2), *ii)* the effectiveness of such (vegetated) foreshores in reducing wave run-up onto a seawall (chapter 2), *iii)* topsoil and lateral erosion resistance across foreshore ecosystems and management types (chapters 3, 4, 5 and 6) and *iv)* the use of 'green' management measures to stabilise tidal flats and thereby facilitate marsh expansion (chapter 7) (Fig. 5). The questions addressed in this thesis are summarized in box 2 and the embedding in the AllRisk project is summarized in box 3.

Chapter 2: Using salt marshes for coastal protection: effective but hard to get where most needed

Chapter 3: The importance of marshes providing soil stabilization to resist fast-flow erosion in case of a dike breach

Chapter 4: Quantifying the resistance to cliff and sheet erosion across vegetation zones on a sandy back-barrier island

Chapter 6: How grazing management can maximize erosion resistance of salt marshes

Chapter 5: Role of eelgrass on bed-load transport and sediment resuspension under oscillatory flow

Chapter 7: On the use of large-scale biodegradable artificial reefs for intertidal foreshore stabilization

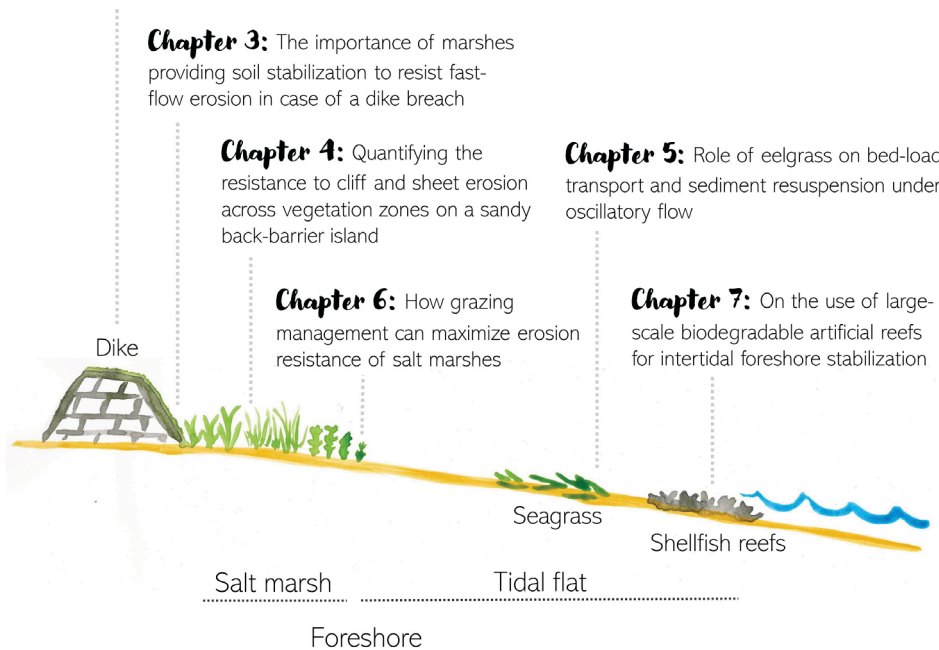


Fig. 5. Illustration of the parts included in this thesis.

BOX 2. THESIS OUTLINE

Chapter 2

Questions: Are marshes growing where we need them most? Which factors drive differences of run-up and beach wrack levels across different foreshore types?

Through the analysis of vegetation and bathymetry maps of the last two decades, in chapter 2 I study *i)* at which locations are the salt marshes found in the Dutch Wadden Sea in relation to the foreshore bathymetry and *ii)* the salt marsh expansion in relation to the sediment dynamics in the adjacent tidal flats. Simultaneously I study how effective are salt marshes with different settings in reducing wave run-up onto the dikes compared to bare tidal flats by conducting field measurements for 3 years.

Chapter 3

Questions: How do different foreshore types resist to fast flow erosion, which could occur during a dike breach?

In chapter 3 I conduct a fast-flow flume experiment to study the resistance of salt marshes and tidal flats with different soil and vegetation properties to fast flow erosion, which could occur during a dike breach.

Chapter 4

Questions: How resistant are soft-sediment ecosystems from a fetch-limited back-barrier island to top and lateral erosion in relation to its management?

In chapter 4 I investigate how the management of a sandy island can affect its stability. I do that by experimentally testing the top and lateral erosion resistance of dunes, marshes and tidal flats soils found in the island, using wave mesocosms and a fast-flow flume. Then, the soil properties and erosion results are related to the past management and development of the island.

Chapter 5

Questions: What is the role of eelgrass on bed-load transport and sediment resuspension under wave conditions?

Using a wave flume, in chapter 5 I experimentally test the role of eelgrass, with and without canopy, on sediment resuspension and top erosion under controlled wave conditions.

Chapter 6

Questions: How does grazing management in combination with abiotic factors, such as marsh age, marsh elevation and sediment layering, affect the susceptibility of marsh edges to lateral erosion?

In chapter 6 I conduct a wave flume experiment to test the lateral erodibility of marsh soils collected in areas with different grazing management, marsh age and marsh elevation.

Chapter 7

Questions: Can we develop nature-based management on the tidal flats to stabilize the marshes?

In chapter 7 I assess the effects of artificial reefs on tidal flat morphology, which may ultimately be beneficial for marsh stability. A large scale experiment is performed where artificial reefs are deployed in a bare tidal flat. The effect of the reefs on the tidal flat is assessed by measuring their wave attenuation capacity, soil elevation changes and soil properties changes on the tidal flat.

BOX 3. EMBEDDING IN THE ALLRISK PROJECT

This thesis is part of the large integrated multidisciplinary AllRisk project, funded by STW and led by Prof.dr.ir. M. Kok (Delft University of Technology), which employs several PhD's, post-docs and technicians. The AllRisk project aimed to support the Dutch Flood Protection Program (HWBP) by investigating key knowledge gaps in flood risk assessment and the use of flood defences to reduce this risk. More specifically, the AllRisk project aimed to make improvements in the assessment of flooding probability and in the design measures by i) reducing statistical and model uncertainty by adding new knowledge on hydraulic loads, subsoil characteristics and the strength of flood defences, ii) evaluating measures to reduce hydraulic loads on the dikes or strengthen flood defences (e.g. eco-engineered foreshore measures to reduce waves) and iii) exploring opportunities for other utilization of flood defences in the 'new flood risk approach'. Another aim of the AllRisk project was to create connections between science (i.e. researchers) and practice (i.e. end users). This imposed questions ranging from legal, governance, engineering to ecology. The research reported in this thesis is the subproject B1 "Uncertain foreshore ecosystem dynamics", which is part of the project B: Dynamics in hydraulic loads.

The joined NIOZ-RUG subproject B1 was focussed on the ecological part and addressed uncertainties about foreshore ecosystem dynamics of the Wadden Sea and Scheldt Estuary coasts and how to manage the foreshore ecosystems to gain both coastal protection and ecological value. Adequate management of foreshores along the Wadden Sea dikes may save huge costs of 'hard' coastal protection through higher and stronger dikes (Temmerman et al. 2013; van Wesenbeeck et al. 2016). However, uncertainties about the actual effectiveness still hampers the practical implementation of these ecosystem-based measures. The aims of this project were to reduce these uncertainties by providing thorough understanding of coastal ecosystem dynamics in relation to their coastal protection role, as well as investigating nature management strategies in order to optimize both the coastal protection services and the ecological value of these ecosystems.





Chapter 2

Using salt marshes for coastal protection: effective but hard to get where most needed

Beatriz Marin-Diaz, Daphne van der Wal, Leon Kaptein, Pol Martinez-Garcia,
Christopher H. Lashley, Kornelis de Jong, Jan Willem Nieuwenhuis,
Laura L. Govers, Han Olff, Tjeerd J. Bouma

Under review

ABSTRACT

Salt marshes fronting sea walls and dikes may offer important ecosystem-based coastal defence by reducing the wave loading and run-up levels during storms. We analysed 20 years of vegetation and bathymetry maps along the whole Dutch Wadden Sea coast in combination with detailed process-based measurements at 5 locations during three years in order to understand where salt marshes form and what features determine their contribution to coastal protection value. The horizontal extent of marshes along dikes remained relatively stable over the past two decades. The presence of marshes was associated with higher elevations of adjacent tidal flats (above ~ 0.5 m NAP), while landward retreat was associated with surface erosion lowering the fronting tidal flats. Wave run-up onto sea dikes during storms (enhancing dike failure risk) was lower in sites with wider marshes and higher foreshore elevations. In turn, run-up was mainly explained by a reduction in wave heights at the toe of the dike. Furthermore, larger tidal ranges led to higher high-tide water levels, causing higher wave run-up. Overall, we found that marshes effectively protected dikes from wave loading across all locations, but also that sites that are most vulnerable to high wave run-up were found in those areas where marshes typically do not develop spontaneously. This catch-22 problem implies that increasing reliance on nature-based coastal defences along soft-bottom coasts may require human interventions to stimulate marsh formation in locations where it is most needed. Alternatively, 'hard engineering' solutions may remain necessary where nature-based solutions are too costly, not achievable, or going at the expense of other ecological values, such as causing the loss of mudflats that are important for migratory birds.

INTRODUCTION

Salt marshes are intertidal ecosystems characterized by salt and flooding tolerant vegetation growing at temperate latitudes (Bakker 2014). Salt marshes provide valuable ecosystem services (Barbier et al. 2011) such as carbon sequestration (Duarte et al. 2013), water purification (Andrews et al. 2006), biodiversity conservation (Spencer and Harvey 2012) and coastal protection by stabilizing the foreshore (Brooks et al. 2020; Zhu et al. 2020, chapter 3) and attenuating waves (Möller et al. 2014; Leonardi et al. 2018; Zhu et al. 2020). The combination of these natural ecosystems with hard engineering like sea-walls or dikes for the purpose of coastal protection is also known as ecosystem-based coastal defence, and can be a more sustainable and cost-effective alternative compared to hard engineering alone (Temmerman et al. 2013; Schoonees et al. 2019; Vuik et al. 2019). Ecosystem-based coastal defence is becoming increasingly important in face of sea level rise and potentially increasing storminess (IPCC 2014; Morris et al. 2020). Implementation of such solutions requires in depth understanding of *i)* at which location you can have salt marshes and *ii)* how effective such (vegetated) foreshores are in reducing wave run-up onto a dike.

The applicability of marshes for ecosystem-based coastal defence strongly depends on where they can develop. Marsh presence depends on the soil elevation relative to the mean sea level (Balke et al. 2016), the sediment supply (Ladd et al. 2019; Fagherazzi et al. 2020; Liu et al. 2021) and the wind-exposure of the location (Wang et al. 2017). Bed level change and inundation period will drive the location of the marsh edge: at lower elevations with longer inundation periods, a more stable bed will be needed to preserve seedlings. Vice versa, more dynamic areas require lower inundation frequency for the seedlings to outgrow the disturbance (Bouma et al. 2016; Willemsen et al. 2017). As wind-driven waves can cause sediment dynamics, they may impede seedling establishment, causing marshes to be restricted to higher elevations at exposed locations and sometimes even causing cliff formation and retreat (Bouma et al. 2014, 2016; Wang et al. 2017). Despite the growing understanding of marsh establishment, we lack quantitative landscape-scale analyses relating the long-term marsh occurrence at the regional scale to the long-term morphological development of bare foreshores.

The applicability of marshes for ecosystem-based coastal defence strongly depends on the effectivity of marshes in attenuating waves. Dike overtopping by waves forms a major flood-safety risk, as it may induce sea-wall breaching by eroding the back of the dike (Schüttrumpf and Oumeraci 2005; Zhu et al. 2020). Hence, the seawall or dike height is typically designed to resist high water levels during a storm surge and the corresponding wave run-up height (Altomare et al. 2016; EurOtop 2018). The probability of dike overtopping obviously increases if storm-surge levels and wave run-up increase due to global change. The wave-attenuating capacity of foreshores can be derived from measuring the maximum height where storm waves deposit debris/beach wrack on a dike (Spencer et al. 2015; Zhu et al. 2020), also called 'flotsam' in previous studies (Vuik et al. 2016; Zhu et al. 2020) (Fig. 1). The actual wave run-up onto a dike is the distance from the storm-surge water level to the beach wrack level (Fig.

MARSHES AND RUN-UP

1). Measured beach wrack levels thus depends both on the wave properties and storm-surge levels, with large waves combined with high water levels resulting in the highest beach wrack levels (Vuik et al. 2016; Zhu et al. 2020). At this moment, little data exists on how the attenuating effect of marshes on wave run-up varies at the regional scale, due to variation in properties like foreshore bathymetry, marsh vegetation, the tidal range and the wind exposure.

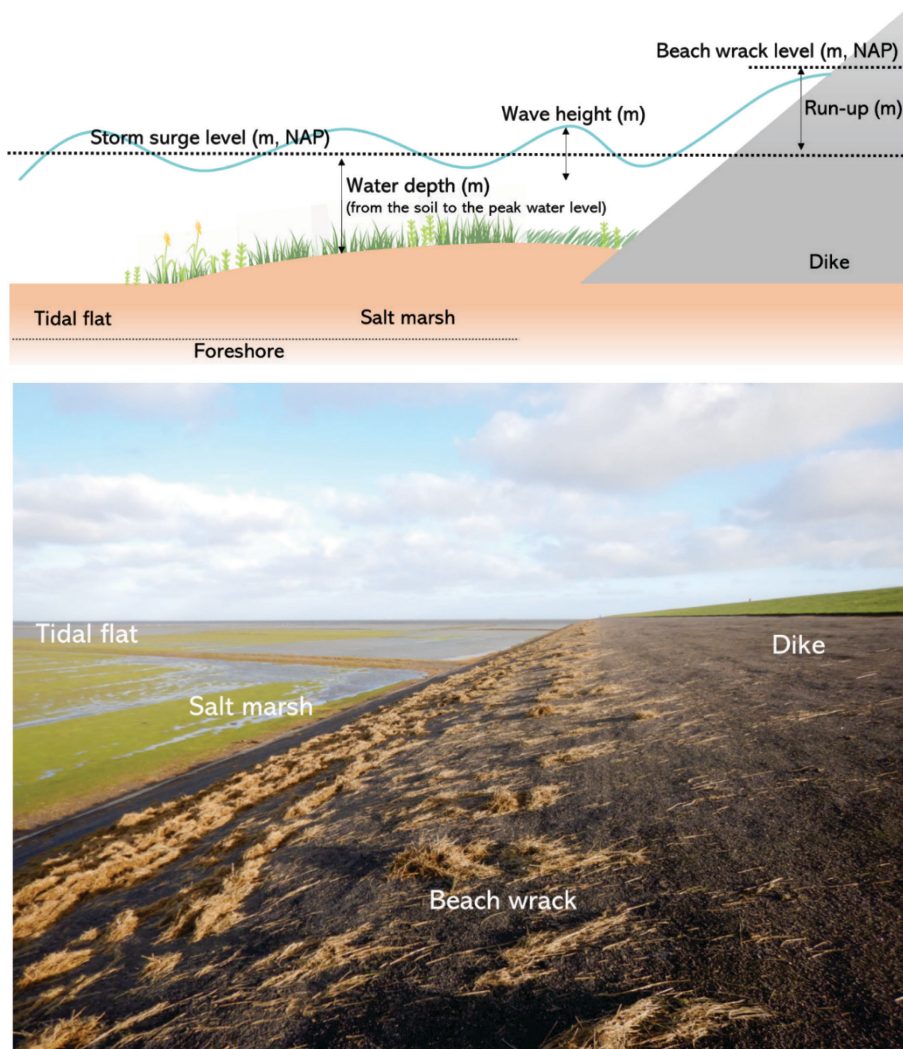


Fig. 1. Illustration of the terms utilised in this study and image of the beach wrack left in a dike near Uithuizen after the storm of the 8th of January 2019. NAP is the Dutch Ordinance Level, similar to mean sea water level.

All elevated foreshores fronting a dike will attenuate waves because the maximum wave height is depth limited (Bouma et al. 2014; Brooks et al. 2020). Thus, both bare tidal flats and salt marshes can attenuate waves (Le Hir et al. 2000; Leonardi et al. 2018; Willemsen et al. 2020). However, salt marshes will be more effective in wave attenuation as a result of both having a higher bathymetric elevation, combined with imposing vegetation friction to the orbital water motion (e.g. Möller et al. 1999, 2014; Bouma et al. 2014; Vuik et al. 2016; Leonardi et al. 2018). The magnitude of vegetation friction may vary in space and time, as it depends on vegetation characteristics like plant height, structural complexity (leaves or branches complexity), stem density and stiffness (Bouma et al. 2005b, 2010b; Möller 2006; Ysebaert et al. 2011). Obviously, the tidal range also varies between locations, even at a regional scale (Nieuwhof and Vos 2018). Locations with higher tidal water levels may be expected to attenuate less waves during storms (Yang et al. 2012), ultimately resulting in higher wave run-up (Keimer et al. 2021) and beach wrack levels. Finally, locations that are more directly exposed to the wind direction of a storm, are likely to experience higher waves (Leonardi and Fagherazzi 2015; Vuik et al. 2016). Hence it would be logical to expect higher wave run-up and beach wrack levels at wind-exposed than at more sheltered locations.

Currently, we lack measurements on how wave run-up varies at the regional scale, due to variation in foreshore properties like bathymetry, vegetation characteristics, tidal range and wind exposure. To our knowledge, most work is modelled (e.g. Vuik et al. 2016), tested in wave flumes using artificial vegetation (Keimer et al. 2021), or applied to beaches (e.g. Polidoro 2014; Didier et al. 2020). Hence, field measurements regarding the effects of marsh foreshores on wave run-up remains scarce (Spencer et al. 2015; Zhu et al. 2020). Moreover, run-up measurements have not been related to the ability of marshes to establish at those locations. To deepen our insight in the applicability of marshes for ecosystem-based coastal defence, we studied at the regional scale *i*) how the long-term salt marsh development in the Dutch Wadden Sea relates to the tidal flat foreshore bathymetry and *ii*) how the wave run-up onto dikes depends on foreshore bathymetry, the presence/absence of marshes, marsh vegetation properties, tidal range and wind exposure (Fig. 2).

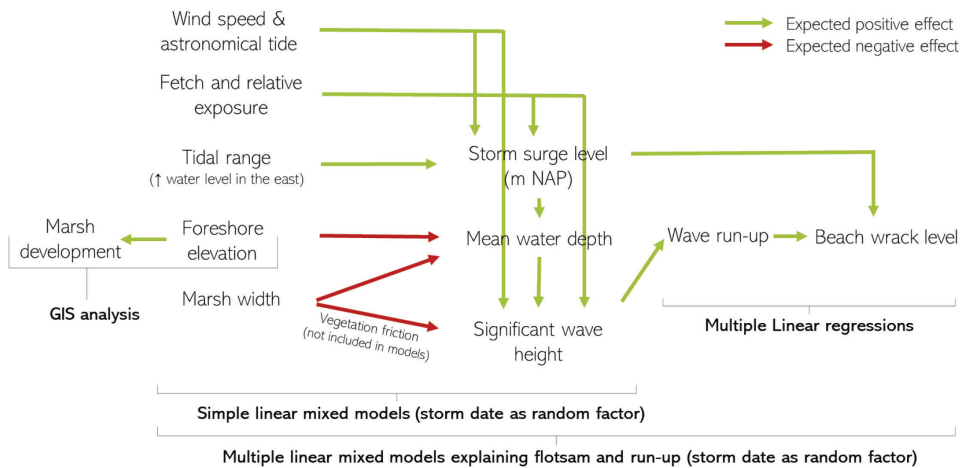


Fig. 2. Conceptual diagram of the relationships between the variables analysed in this study, the methods utilised in the analysis and the expected positive or negative effect.

METHODS

Description of the field location: Dutch Wadden Sea coast

The Wadden Sea is a large intertidal area, part of the Natura 2000 and declared world Heritage Site by the UNESCO since 2009. Our study focuses on the stretch of mainland coast between Harlingen (53°10'46.2' N, 5°24'34.3' E) and Eemshaven (53°27'53.1' N 6°45'33.7' E), in the Netherlands (Fig. 3a). This area is micro to meso-tidal, with a normal tidal range varying from ~ 190 m in the west (Harlingen) to ~ 260 m in the east (Eemshaven) (RWS 2013). The Dutch Wadden Sea is bordered by barrier islands which dampen waves coming from the North Sea (Reise et al. 2010). The mainland coast is protected against flooding by dikes of 8 to 10 m high and slope at an average gradient of ~ 1:5 at the seaward side (van Loon-Steensma et al. 2014b; a). After the construction of the 'Afsluitdijk' (a dike closing off lake IJssel from the Wadden Sea) in the 1930s, changes in the currents and bathymetry of the Dutch Wadden Sea led to the current distribution of tidal flats and marshes (Jonge et al. 1993). Stable marshes are currently present in some areas along the dike as a result of accretion works aimed at land reclamation (Bakker 2014). These accretion works consisted of drainage ditches and sedimentation fields surrounded by brushwood groynes. From 1960, land reclamation was ceased. From 1990 onwards, human interventions were reduced by abandoning the most seaward sedimentation fields and reducing artificial drainage to enhance more natural development of the marshes and intertidal flats (Bakker 2014).

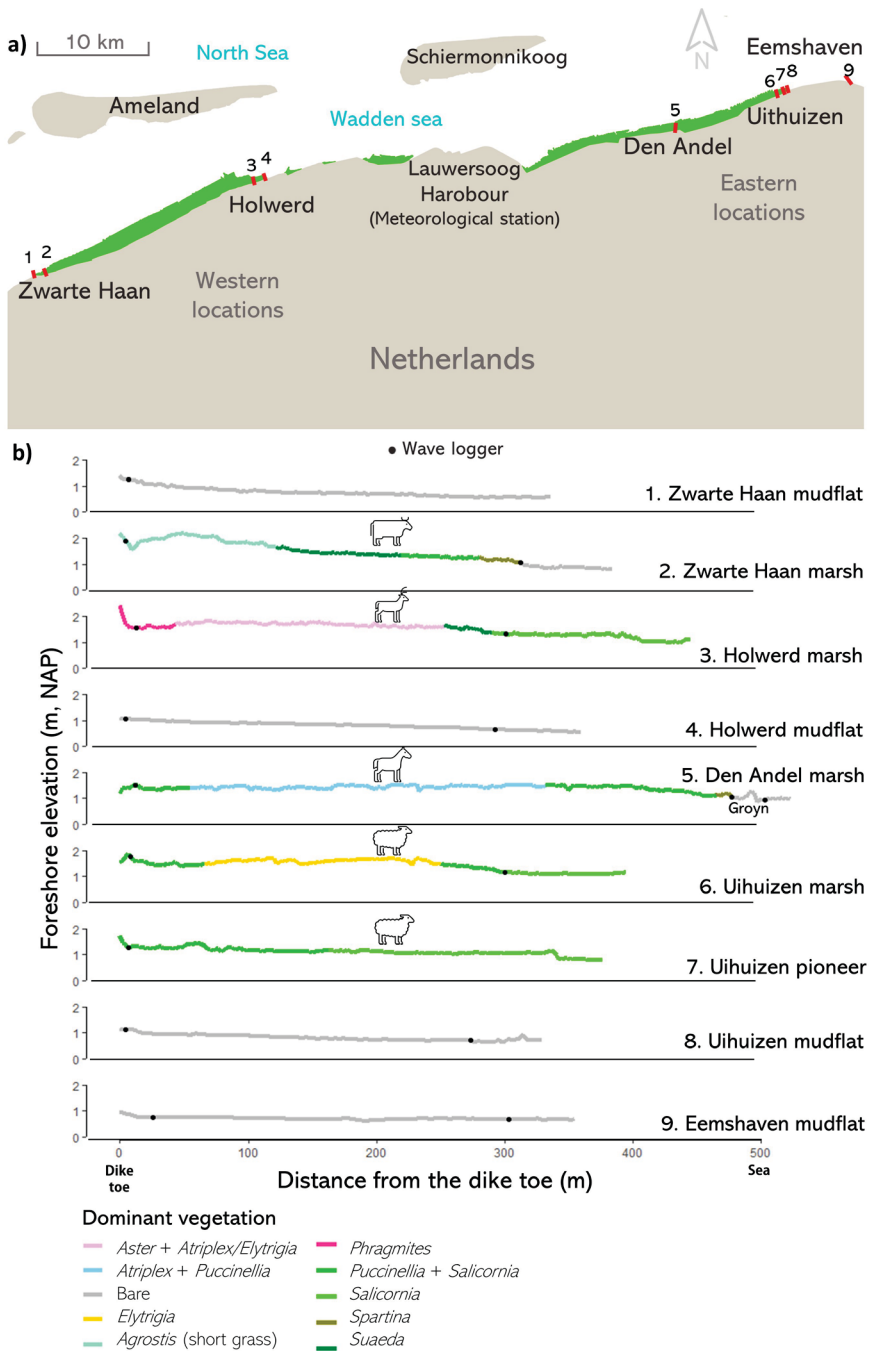


Fig. 3. a) Location of the study sites. Locations of the transects with wave loggers are indicated in red. and b) elevation profiles of the transects with wave loggers, including the dominant vegetation. Animal shapes indicate the type of large herbivores present.

Tidal flat and marsh decadal development (GIS analysis)

Marsh development was investigated using contour lines at 1 m NAP (i.e. the Dutch ordnance level, similar to mean sea level) extracted from two sets of intertidal elevation maps of the study area: for 2004 (5 m resolution) and 2012-2017 (2 m resolution). The intertidal elevation maps were derived from LiDAR data and provided by Rijkswaterstaat. As in Janssen-Stelder (2000), contour lines at 1 m NAP corresponded to the pioneer marsh edge (excluding pre-pioneer vegetation), which was contrasted with vegetation polygon maps from 2002 and 2014 respectively. Vegetation polygons maps are based on 1:5000 false colour aerial photographs and vegetation surveys and were also obtained from Rijkswaterstaat.

Contour lines, rather than polygon maps, were used for the analysis because it was a more objective representation of the marsh edge in addition to being related to the bathymetry of the area. Contour lines at 0.5 m NAP (hereafter called "upper tidal flat") and 0 m NAP were obtained to visualize the location of the most elevated tidal flats in relation to the marsh presence. Marsh expansion offshore or landward retreat was calculated with the Digital Shore-line Analysis System (DSAS) from ArcGIS (Himmelstoss et al. 2018). Transects perpendicular to the dike with spacing of 500 m were drawn with DSAS, and the length of the marsh for each transect was calculated until the intersection with the 1 m NAP marsh contour for the two time steps (2004 and 2012/2017). The same procedure was done but from the marsh contour of 2004 to the contour lines at 0.5 m NAP of both time steps, to obtain the change in width of the upper tidal flat in front of the marshes. Changes in elevation of the tidal flats fronting the marsh were obtained by subtracting the intertidal elevation maps from both time steps using the package "raster calculator" from QGIS. The mean of the accretion/erosion values of the first 100 m of each transect perpendicular to the dike used previously with the DSAS was used as a value of tidal flat elevation change. Changes in marsh width were related to the changes in width and elevation of the upper tidal flat in front.

Description of the wave run-up monitoring locations (field study)

Five locations were selected along the dikes of the Dutch Wadden Sea to be monitored during 3 years, including the tidal flat of Eemshaven (53°27'53.1"N 6°45'33.7"E), the interface marsh-mudflat from Uithuizen (53°27'26.8"N 6°40'14.0"E), the marsh from Den Anel (53°25'36.1"N 6°30'53.7"E), the interface marsh-mudflat from Holwerd (53°23'18.9"N 5°56'05.9"E) and Zwarte Haan (53°18'44.8"N 5°37'34.0"E) (Fig. 3a). Eemshaven, Uithuizen and Den Anel were the most eastern locations and this area is related to higher tidal ranges and mean high water neap (MHWN), and therefore higher water levels compared to Holwerd and Zwarte Haan which were located more to the west (RWS 2013) (Fig. 4).

All tidal flats had a lower bathymetric elevation than the marshes, with Eemshaven tidal flat having the lowest (Fig. 3b). Zwarte Haan was the highest marsh, followed by Holwerd, Den Anel and Uithuizen. All locations, except Zwarte Haan were framed by brushwood groynes of ~0.5 m high. Zwarte Haan was grazed by cows during summer and autumn and had the shortest vegetation (Fig. 3b). The marshes at Holwerd were dominated by taller vegetation and

have no active grazing management, but non-domesticated grazers like deer occur there occasionally (Fig. 3b). Den Andel was grazed by horses in summer and characterized by dense short vegetation (Fig. 3b). Uithuizen was grazed by sheep in summer and characterized by dense short vegetation. (Fig. 3b). Marsh edge was considered as the limit of the dense pioneer vegetation (including *Spartina sp.* and dense *Salicornia sp.* with *Puccinellia sp.*) and all the locations with exception of Zwarte Haan presented annual *Salicornia* following the marsh edge.

Waves and water depth measurements

Wave loggers transects were installed in all the locations to measure the water levels and wave heights (Fig. 3a). To calculate the total wave attenuation of the foreshore for each transect, one wave logger (OSS1-10-003C) was deployed at 10 cm from the ground next to the dike and one in the marsh edge or equivalent distance on the mudflat transect (~ 300 m) (Fig. 3b). The transect at Den Andel was longer than the previously mentioned transects because of the marsh width (~ 400 m). The Eemshaven transect was an exception, with the transect in diagonal instead of perpendicular to the dike (Fig. S1). One extra wave logger was deployed before the brushwood groyne in Den Andel. The wave loggers were deployed in December 2018 in Eemshaven, Uithuizen and Den Andel, and in November 2019 in Holwerd and Zwarte Haan. Therefore, not all the locations have wave data for all the storms measured. A total of 24 tides with high water inundating all the sensors were the subset from the recorded data that we focussed on in this paper. From these 24 high waters, beach wrack lines on the dike were measured for 9 tides (Table S1), and in only 2 of them the beach wrack reached onto the dike behind the marsh zones (8th of January 2019 and 11th of February 2020). However, for the 8th of January, the wave loggers were only installed in the eastern locations.

The recording settings utilised for the wave loggers were modified during the monitoring period, due to the requirements for other purposes than this study, but did not affect the wave statistics that we calculated (Table S2). Mean water depth and significant wave height were calculated for each sensor as described in the script in Marin-diaz et al. (2021). Values of significant wave height and mean water depth during the hour with higher water levels for each storm surge were averaged and used as reference values for the analysis. Wave attenuation by the foreshore was calculated as the percentage of significant wave height reduction between the wave logger in the edge of the marsh or equivalent distance in the tidal flats and the sensor in front of the dike.

Beach wrack levels and wave run-up monitoring

Nine beach wrack lines were measured with an rtk-DGPS (Leica GS12) on the dikes every ~ 30 m along 1 – 3 km in each location. Wave run-up was calculated by subtracting the water level measured by the wave loggers at each location from the beach wrack level measured in the field. Run-up in Holwerd and Zwarte Haan could be only calculated from November 2019 onwards (when wave loggers were installed).

Foreshore elevation characterization and seasonal monitoring

Soil elevation in front of the dikes to relate to the beach wrack measurements along the coast were obtained from the newest intertidal elevation maps to date (2017-2019). These maps were derived from LiDAR data with 2 m resolution (source: Rijkswaterstaat). Profiles perpendicular to the dike and 100 m spacing were drawn in QGIS and the elevation data was obtained for each profile, with a resolution of 2 m. From each of these profiles, the elevation in front of the dike was calculated as the average elevation along 100 m measured from 40 m in front of the dike to avoid the ditches. In addition, the elevation at 400 m from the dike was obtained as a measure of the offshore elevation. Each elevation value was related the beach wrack measured at that same location of the dike. Seasonal elevation changes in the field were monitored with an rtk-DGPS (Leica GS12) every ~ 10 m along the transects with wave loggers to determine the stability of the marshes compared to the mudflats. The monitoring took place in December 2018 (except for Holwerd and Zwarte Haan); January, September and December 2019 and March, August and December 2020. Variability in elevation change was calculated as the standard deviation of the elevation for each transect.

Monitoring of vegetation properties

Vegetation was monitored along the wave logger transects in September and November 2019; February, March, August and December 2020 and February 2021. Measurements were taken in the most dominant vegetation along the transects (Fig. 3b). In the field, overall ground cover percentage of vegetation was visually assessed for each area. Overall vegetation height was measured with a ruler with 6 replicates per vegetation zone. For September and November 2019 and February and March 2020, stem density was counted from three 20 x 20 cm plots collected in each vegetation zone. For a subset of 10-20 stems per plot, the stem and diameter from the dominant species were measured in the laboratory. From a subset of 2-5 stems per plot, the structures (leaves or branches) were measured as in Bouma et al. (2005). Samples were then dried at 60 degrees until constant weight to obtain the dry biomass. In winter, vegetation measurements represent only the vegetation in the standing tussocks therefore the general ground cover should be taken into account.

Calculation of wind exposure and fetch

Wind direction and wind speed during the selected storms were obtained from the Royal Dutch Meteorological Institute (KNMI), recorded in the weather station of Lauwersoog, which is in between of our study sites. Fetch for each beach wrack point and for every storm, was calculated with the *waver* package from R (Marchand and Gill 2018). Fetch is typically defined as the distance of open water over which the wind can blow in a specific direction. In this study, fetch was considered as the distance over the intertidal area from a specific location of the dike to the system of Wadden barrier islands for a specific wind direction. The inputs needed were the wind direction during the peak of each storm surge level, a shapefile with the locations along the dike where the beach wrack was measured and a shapefile with the foreshore and barrier

islands obtained from the European Environment Agency (EEA). Relative exposure (RE) was calculated as the fetch multiplied by the wind speed.

Statistical analysis

One-way ANOVA followed by Tukey HSD post hoc test was used to test differences between transects in variability of soil elevation (measured in the field). Spearman correlations were used to analyse the relationships between mean water depth and significant wave heights. Pearson correlations were used to analyse the relationships between significant wave height and wave run-up. The relationship between run-up and beach wrack levels was determined with a multiple linear regression including the storm date as independent variable. Differences in elevation change, beach wrack levels, run-up, storm surge water level and wave heights among each wave logger transect were tested with linear mixed models (LMM) with date as random factor followed by post-hoc Tukey HSD tests. Water level, wave heights and run-up differences between transects were tested using data from dates where all the locations had wave loggers installed (see Fig. S2 for details). Beach wrack levels could be compared including more storms dates without wave loggers because water level from the wave sensors was not needed for the calculation, in contrast to the run-up calculation (Fig. S2). LMM with date as random factor were used to investigate the effects of marsh width, foreshore elevation, offshore elevation, storm surge level, relative exposure and fetch on the response variables beach wrack levels and run-up. Vegetation was represented by marsh width in the models. First, a simple model for each explanatory variable was run to obtain the effect of isolated variables. Secondly, the most parsimonious model explaining run-up and beach wrack levels was selected based on lowest AIC. Finally, we explored how these variables affected the water level and wave height, which were the underlying variables explaining most of the run-up and beach wrack levels, again using LMM with random date (Fig. 2). Values with zero run-up were excluded from the analysis. Significance of the fixed effects was tested using the Type II Wald Chi-square tests. Marginal and conditional R^2 of the LMM were obtained with the package *sjstats* from R. Normality and homogeneity were checked with residuals plots, and data was log transformed when necessary to comply with the assumptions. Statistical analyses were performed using R 3.5.0 (R Development Core Team 2018).

RESULTS

Distribution and decadal development of marshes and tidal flats (GIS analysis)

Salt marshes were only present in areas with elevated tidal flats in front of the marsh (> 0.5 m NAP), hereafter called 'upper tidal flats', and strongly related to human interventions (groynes/sedimentation fields) (Fig. 4a and S3). Salt marsh extension along the dike has remained stable over the past two decades (Fig. 4a and S1). The marsh edge in the eastern locations coincided with the mean high-water neap (MHWN), which was around 1 m in this area (Fig. 4a). In the most western area, the calculated MHWN was slightly lower (around 0.8 m). However, the marsh edge from the polygons also coincided with the tidal flat contour at 1 m (Fig. 4a). Overall, marsh landward retreat was related to erosion or retreat of the upper tidal flats fronting the marsh (Fig. 4bc). Vice versa, offshore marsh expansion was related to the accretion and expansion of the upper tidal flats fronting the marsh. Most of the erosion occurred in the west area, which includes location 'Zwarte Haan', which was also confirmed by field observations (Fig. 4bc, S1 and S4). This area was more directly exposed to predominant wind directions from 2002 to 2017 (Fig. 4d).

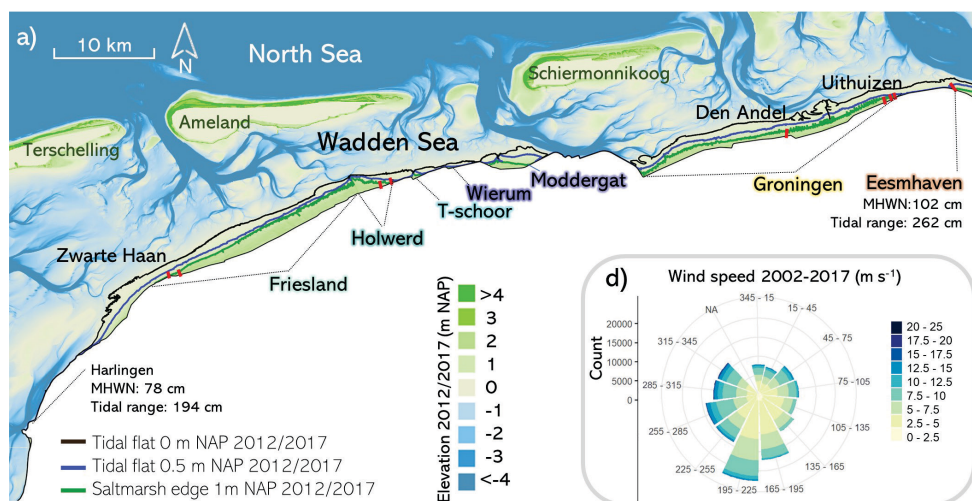


Fig. 4 Part I. a) elevation map of the Wadden Sea with contour lines at 0, 0.5 (upper tidal flat) and 1 (marsh edge) m NAP. Red lines indicate the transects with wave loggers, colours in the text relates to panel b and c.

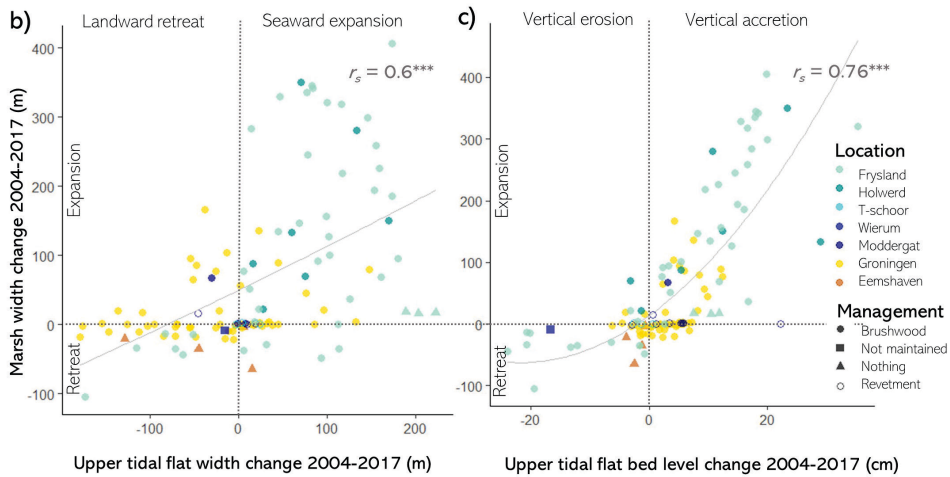


Fig. 4 Part II. b) relationship between marsh expansion and upper tidal flat seaward expansion/landward retreat, c) relationship between marsh expansion and change in vertical elevation of the first 100 m of the upper tidal flat. Colours indicate different regions shown in panel a. And d) wind speed and wind direction during 2002 until 2017. Significant codes refer to $p < 0.001$ (***)

Seasonal variability of foreshore characteristics monitored in the field: bathymetry and vegetation

The variability in elevation measured with the rtk-DGPS during the 3 year monitoring period was higher in the bare tidal flats than in the marshes, which remained mostly stable (the average standard deviation in tidal flat transects was 3.1 cm while in marsh transects was 1.5 cm) (ANOVA: $F_{8,90} = 7.5$, $p < 0.001$) (Fig. S5). The tallest vegetation was found in Holwerd throughout all the seasons (e.g. *Phragmites* and *Aster*), mainly attributed to not being grazed by livestock (Fig. 5). The vegetation height, ground cover and biomass declined during winter, with the lowest vegetation properties in March. Shoot density declined in all species with the exception of *Atriplex* and *Spartina*, which lost the flowering stems but not the basal stems (Fig. 5). Stem diameter remained constant except in succulent plant species such as *Salicornia* (Fig. S6a). Vegetation structures (leaves and branches) declined during winter, especially after freezing days, in all the species, even when the total height had not significantly varied (for example in *Phragmites*) (Fig. S6bc).

MARSHES AND RUN-UP

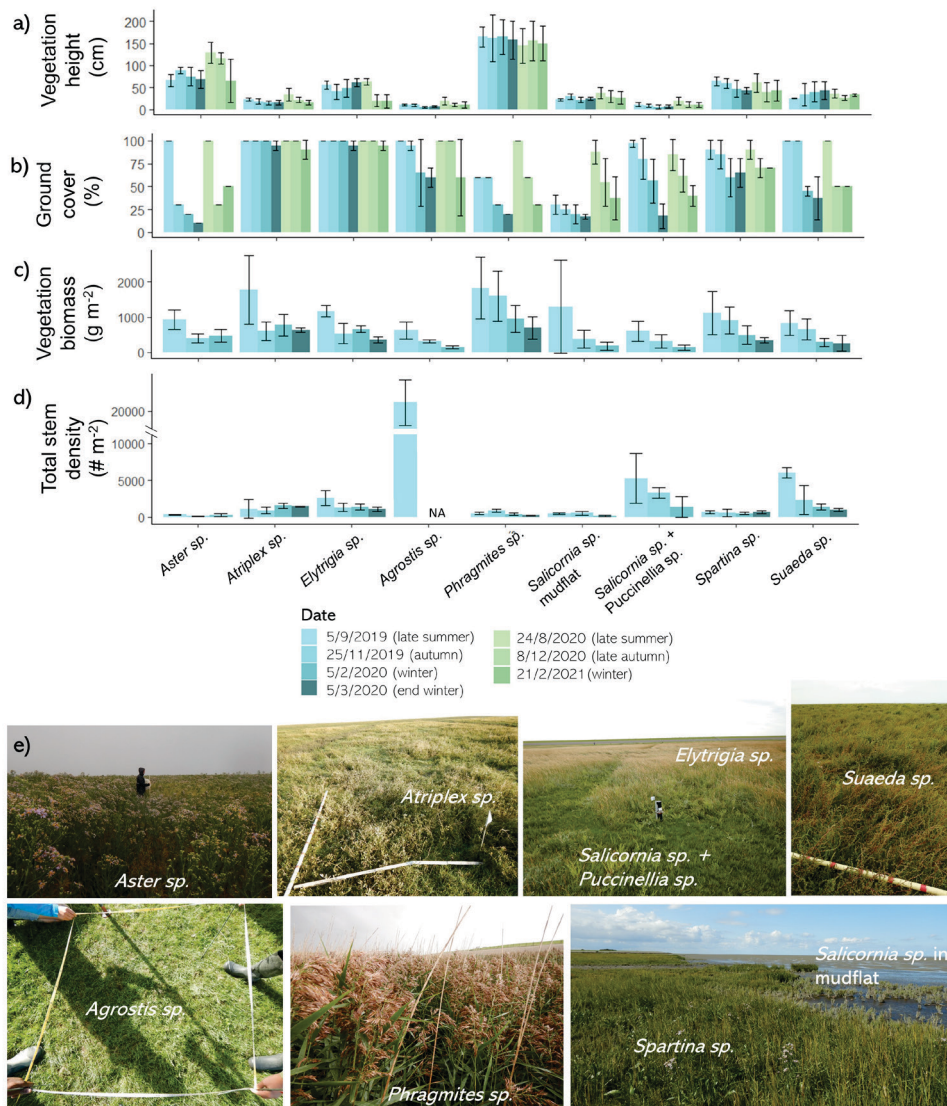


Fig. 5. Seasonal changes in a) vegetation height, b) vegetation ground cover, c) vegetation biomass and d) total stem density; for the dominant vegetation species. Error bars represent standard deviations. E) images of the dominant vegetation species in summer state.

Wave run-up, beach wrack levels and their relationship with water level and wave height

Higher waves were observed with increasing water depths (i.e., with high storm surge levels and in locations with lower elevations) (Fig. 6a and 7bef). Wave run-up on the dike, as obtained by correcting the beach wrack level for the storm surge water level, increased with higher waves measured at the toe of the dike (Fig. 6b). Differences of water level and wave heights between different storms were explained by astronomical tides and wind (Fig. S7). Wave run-up on the dikes was strongly correlated to measured beach wrack levels (MLR: $R^2 = 0.99$, $p < 0.001$). Therefore, locations with higher run-up also had higher beach wrack levels (Fig. S8). However, for the same run-up values, eastern locations had ~20 cm higher beach wrack levels than western locations independently of the wind direction and speed. This could be attributed to the higher tidal amplitudes and thus storm surge levels found in the east compared to the west (LMM: $\chi^2 = 192.03$, $p < 0.001$) (Fig. 7a). Given the differences in storms surge levels between western and eastern locations, beach wrack and run-up were always higher at dikes fronted directly by mudflats, compared to dikes fronted by marshes (LMM beach wrack: $\chi^2 = 397.12$, $p < 0.001$, run-up: $\chi^2 = 155.6$, $p < 0.001$) (Fig. 7cd).

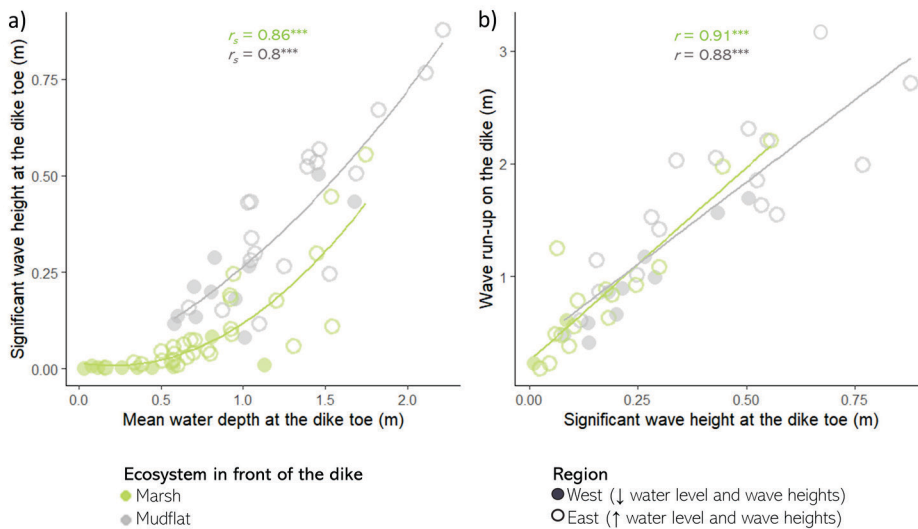


Fig. 6. Relationships between a) mean water depth and significant wave height separated by salt marshes and bare tidal flats, including all the storm dates with wave run-up measured; and b) significant wave height and wave run-up on the dike, excluding points with zero run-up, which occurred in cases where the waves were completely attenuated. Significant codes refer to $p < 0.001$ (***).

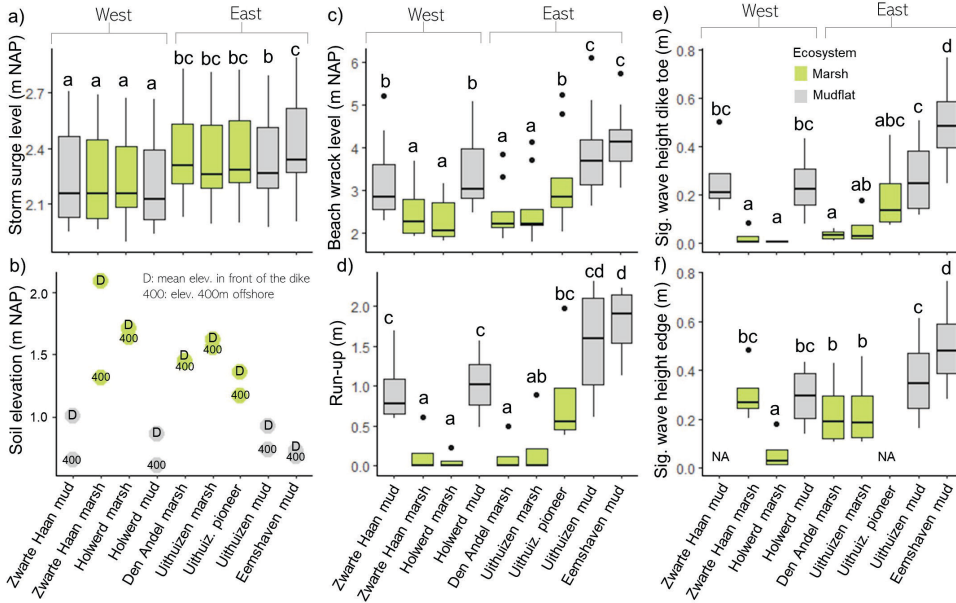


Fig. 7. Differences among transects with wave loggers for a) storm surge water levels; b) soil elevation in front of the dike and at 400m from the dike; c) beach wrack levels on the dike; d) run-up on the dike, e) significant wave height at the dike toe; and f) significant wave height at the marsh/mud edge (300 m offshore except for Den Andel at 400 m). Note that sensors were not present in the mudflat of Zwarte Haan edge and Uithuizen pioneer edge. See Fig. S1 for specifications on the storm dates used for the analysis of each variable.

Processes controlling spatial variability of wave run-up & beach wrack: field measurements

Variability on beach wrack levels and run-up between locations was best explained by the bathymetric elevation in front of the dike, the marsh plateau width and the storm surge level, with the latter accounting for the differences of tidal range between locations in the west and east (Table 1, Fig. 7, 8 and 9a; model: $mR^2 = 0.78$, $cR^2 = 0.9$ and $mR^2 = 0.66$, $cR^2 = 0.85$ respectively). Higher foreshore elevations combined with wider marshes were related to lower water depths and therefore lower wave heights (LMM: $X^2(1) = 154$, $p < 0.001$ and $X^2(1) = 131$, $p < 0.001$ respectively), which explains the lower run-up and beach wracks (Fig. 9a and S9). Furthermore, run-up was close to zero in the marshes during storms with water levels < 2.5 m NAP (around 0.5 m water depth over the marsh soil), due to stronger wave attenuation related to depth limitation that was present in the marshes (Fig. 6). Given the differences in incoming waves between locations (Fig. 7f), mudflats attenuated the waves to a lesser extent when compared to marshes (average attenuation in mudflats \pm SD: 1.8 ± 9.8 % in Eemshaven, 13.5 ± 13.7 % in Holwerd and 22.4 ± 9.55 % in Uithuizen) (Fig. 7e and S10). Within marshes, wave attenuation in Den Andel (average attenuation: 80 ± 7.4 %) could be attributed to a wider marsh and in Zwarte Haan (average attenuation: 96 ± 5.36 %) to the higher elevation of the marsh in front of the dike and lower storm surge levels compared to

Uithuizen (average attenuation: $77 \pm 12.2\%$) (Fig. 3, 7b and S10). In the marsh of Holwerd, the waves were always completely attenuated, related to smaller incoming waves and lower storm surge levels (average attenuation: $86 \pm 17.6\%$) (Fig. 7f and S10). The higher run-up and beach wrack levels in the pioneer marsh of Uithuizen compared to other locations with the same marsh width were attributed to higher waves reaching the dike due to a lower foreshore both offshore and at the dike toe (Fig. 3 and 7). Surprisingly, nor wind exposure measured as fetch (m), nor relative exposure related to the islands could explain differences in beach wrack and run-up (Table. 2). Although incoming waves with western wind directions, such as during the storm of February 2020, were higher in Zwarte Haan and lower in Holwerd (which was sheltered by a harbour), the determining effects of bathymetry and differences in storm surge levels overruled wind exposure effects.

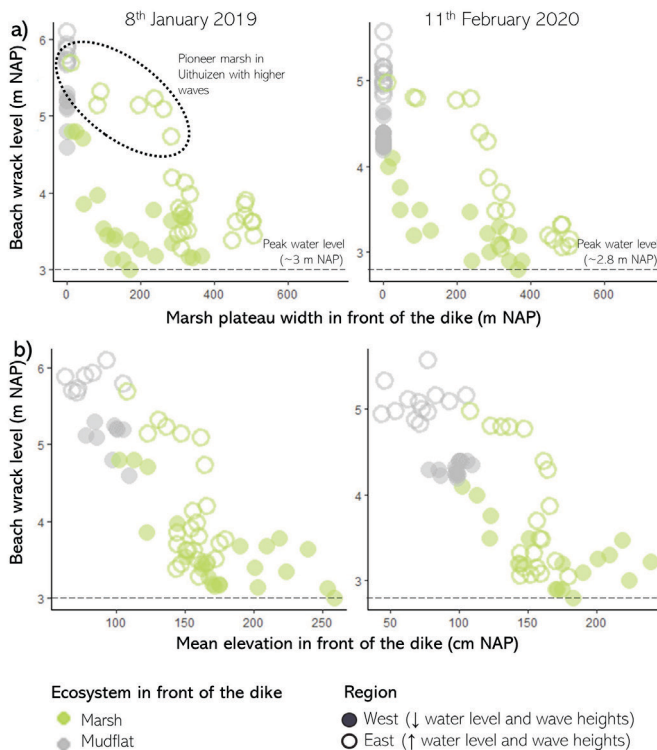


Fig. 8. Relationships between beach wrack levels during the two biggest storms measured and a) soil elevation in front of the dike and b) marsh plateau width. Run-up is not shown because wave loggers were missing in the west during in January, and therefore could not be calculated. However, beach wrack and run-up were closely correlated and similar relationships are found when plotting run-up (Fig. S11). Colours indicate if the dike was fronted by mudflat or marsh. Shapes indicate the region (west of east). Peak water level refers to the east region and was ~ 20 cm lower in the west.

In summary, for the 9 measured beach wrack lines, a marsh of ~ 300 m width and more than 1.5 m elevation, effectively reduced the wave run-up by up to 100 % in some cases (Fig. S1), so that the beach wrack level was approximately the same as the storm-surge water level. In marshes with higher elevations (i.e. Zwarte Haan, > 2 m NAP), or with lower incoming waves as a result of the presence of wider elevated tidal flats in front of the marsh (i.e. Holwerd), even a narrow width of ~ 100 m attenuated the run-up. On the other hand, the combination of

MARSHES AND RUN-UP

narrow pioneer marshes (< 300 m) with low elevation (< 1.5 m NAP) and high incoming waves (i.e. Uithuizen pioneer marsh), were not as effective.

Table 1. Set of linear mixed models explaining the relationships of bathymetry, tidal range and wind with the beach wrack level and run-up, with the storm date as random. The first two models are the most parsimonious models explaining beach wrack and run-up. The remaining models are the effects of each variable independently.

		χ^2	<i>df</i>	<i>p</i>	Conditional R^2	Marginal R^2
Selected beach wrack model					0.9	0.78
beach wrack ~	Elevation over 100 m in front of the dike	73.5	1	<0.001		
	Marsh plateau width	105.3	1	<0.001		
	Storm surge level	169	1	<0.001		
Selected run-up model					0.85	0.66
Run-up ~	Elevation over 100 m in front of the dike	73.5	1	<0.001		
	Marsh plateau width	105.3	1	<0.001		
	Storm surge level	68.1	1	<0.001		
Isolated variables						
beach wrack ~	Elevation over 100 m in front of the dike	540.03	1	<0.001	0.86	0.29
beach wrack ~	Elevation at 400m	336.8	1	<0.001	0.83	0.25
beach wrack ~	Marsh width	299.7	1	<0.001	0.82	0.23
beach wrack ~	Marsh plateau width	337	1	<0.001	0.83	0.24
beach wrack ~	Storm surge level	57.7	1	<0.001	0.49	0.42
beach wrack ~	Fetch	0.31	1	>0.05	0.42	0
beach wrack ~	Relative exposure	0	1	>0.05	0.43	0
Run-up~	Elevation over 100 m in front of the dike	593.6	1	<0.001	0.8	0.47
Run-up~	Elevation at 400m	445.9	1	<0.001	0.79	0.41
Run-up~	Marsh width	403.6	1	<0.001	0.77	0.39
Run-up~	Marsh plateau width	454.5	1	<0.001	0.78	0.41
Run-up~	Storm surge level	8.04	1	<0.05	0.19	0.09
Run-up~	Fetch	0.22	1	>0.05	0.14	0
Run-up~	Relative exposure	0	1	>0.05	0.16	0

DISCUSSION

The present study shows that salt marshes can protect the dikes independently of the vegetation species, the seasonal state of the vegetation, grazing management and wind exposure. This could simplify the considerations needed to include salt marshes and adjacent tidal flats into nature-based coastal protection schemes. Overall, differences in tidal range together with higher marsh elevations due to sediment trapping were the most important factors determining the run-up. Furthermore, the presence and expansion of a marsh was found to be related to the presence of elevated and accreting tidal flats, highlighting the importance of the management of ecosystems fronting the marshes for coastal protection.

Salt marsh development related to sediment dynamics

Our results show a relationship between the marsh lateral retreat (i.e., marsh narrowing) and the tidal flat erosion both vertically and in width. Furthermore, marsh presence along the Wadden Sea dikes was related to areas with elevated tidal flats (above 0.5 m NAP) which depends on where sediment is transported and deposited by the tides, waves and currents (Elias et al. 2012; Schuerch et al. 2014; Wang et al. 2018). Lower and narrower tidal flats can lead to higher waves exposure and therefore to more marsh erosion (Callaghan et al. 2010). This may be the case of the eroding marshes of Zwarte Haan (west area, Fig. S1), which had the largest incoming waves from all the marsh locations measured (Fig. 7) as a result of low-lying fronting tidal flats. Higher exposure could lead to increased sediment dynamics, which has been related to a reduction in seedling establishment opportunities, and therefore less marsh expansion (Bouma et al. 2016; Willemsen et al. 2017). Moreover, Leonardi et al. (2016) show that violent storms contribute less than 1% to the salt marsh erosion rates, while moderate storms cause most of the marsh erosion. This could also explain the greater erosion in Zwarte Haan, which has been more exposed to predominant wind direction and therefore to moderate storms than the other locations. Another example is the marsh of Wierum, where there was almost no elevated tidal flat in front of the marsh (Fig. 4bc and S1), and once the maintenance of the brushwood groynes work was stopped in the 1960s, the marsh started to erode (Siemes et al. 2020).

Marsh edge location in our study sites corresponded to an elevation of 1 m NAP, as found in the years previous to our study period (Janssen-Stelder 2000). Marsh edge has been previously related to the mean high water neap (MHWN), although more recent studies show that tidal range is not the only driver (e.g. van der Wal and Pye 2004; Balke et al. 2016; Bouma et al. 2016; Willemsen et al. 2017). In the eastern marshes, the MHWN coincided with ~ 1 m NAP (RWS 2013). However in the western locations the marsh edge did not coincide with the estimated MHWN, which is around 0.8 m (RWS 2013). The presence of elevated tidal flats did not explain this, because they were equally present in the west and east. However, the higher exposure to winds coming from the west might have caused larger bed level changes in this area, including erosion, which could lead to finding the marsh edge at higher elevations than expected based on the MHWN (van der Wal and Pye 2004; Balke et al. 2016; Bouma et al. 2016; Willemsen et al. 2017).

Wave run-up differences are driven mainly by the marsh presence

This study provides field evidence that salt marshes effectively protect the dikes across locations by reducing both the beach wrack levels (by up to ~ 3 m) and wave run-up (by up to 100 %), mainly due to forming higher and more stable foreshores (Fig. 7b and S5) which reduced wave heights (Fig. 8b). Furthermore, marshes fronted with a more elevated tidal flat experienced lower incoming waves, emphasizing that the elevation of the tidal flat in front of the marsh is also important.

Our study demonstrates that wave attenuation occurred even in winter when the vegetation was shorter and less dense. This is in agreement with previous studies on wave attenuation, although the effect may be less during stronger storms (Möller and Spencer 2002; Vuik et al. 2016, 2018; Willemsen et al. 2020). Furthermore, run-up was completely attenuated during moderate storms as a consequence of the elevated marsh foreshore which led to depth limited waves (Zhu et al. 2019). Although bathymetry explained most of the run-up attenuation across sites, part of this attenuation may be due to the vegetation friction (Vuik et al. 2016; Willemsen et al. 2020; Keimer et al. 2021). However, this was not tested in our model because the high variability of vegetation parameters in time and space, made it impossible to create a single vegetation variable to fit the statistics. For example, locations with taller and stiffer vegetation like Holwerd may have had a somewhat greater wave attenuating effect due to the higher ratio of vegetation to water depth and higher drag forces (e.g. Möller et al. 1999; Bouma et al. 2010; Ysebaert et al. 2011). On the other hand, lower wave attenuation could have been attributed to grazing in Uithuizen, Den Andel and Zwarte Haan, which kept the overall vegetation shorter (Yang et al. 2012). Nonetheless, in our field observations, these possible differences due to the vegetation friction were overruled by the marsh elevation as seen in locations with higher incoming waves and shorter vegetation (i.e. Uithuizen), which were still effective reducing run-up and beach wrack levels compared to bare tidal flats. Similarly, although higher waves were measured in Zwarte Haan (west) during western wind directions (for example during the storms of 11/2/20, Fig. S2de), the beach wrack and run-up were not higher than in the eastern marshes like Uithuizen (sheltered from western winds) because it was overruled by the lower bathymetry and higher tidal range in the east. Furthermore, wind fetch to the islands did also not explain differences on wave run-up. On the other hand, Holwerd was sheltered by the harbour with western winds, and this could have further reduced the beach wracks in this location.

The effectiveness of marshes during extreme conditions (1/1000 year storms, or worse) could not be measured during this field campaign, as we only encountered less intense winds. However, flume experiments (Möller et al. 2014) and models (e.g. Vuik et al. 2016; Willemsen et al. 2020) report that marshes remain effective in wave dampening even during such extreme conditions. Moreover, marshes would still be beneficial to protect the damage of the revetment during smaller but more frequent storms (chapter 3). Regarding the long term effectivity of the marshes, studies show that once a marsh is established, it can stand even if there is an increase in hydrodynamics (Van der Wal et al. 2008).

Are the marshes “where we need them most”? A catch-22 situation

Marshes effectively reduced the run-up on the dikes. However, locations currently more vulnerable to run-up (i.e., locations with lower bathymetry, therefore deeper water levels and higher waves), are also the locations where the marshes will not naturally occur (Fig. 9b). Marshes are not necessarily found only in the most sheltered locations, but where the sediment is deposited with sufficient elevation thus reducing wave loadings and providing adequate windows of opportunities for marsh establishment (Hu et al. 2015; Bouma et al. 2016; Hu et

al. 2021). In this sense, marshes can be both in exposed locations (“where we need them most”) if enough tidal flat is accreted in front of them; and in sheltered locations (“where we need them least”) where there are less hydrodynamics and sediment dynamics that facilitate marsh establishment. Large-scale sediment dynamics determining the presence of higher tidal flats may be affected by wave exposure, currents, storms surges, sediment supply, dredging activities as well as biotic factors (e.g. Elias et al. 2012; Mariotti and Fagherazzi 2013; Schuerch et al. 2014; Ladd et al. 2021), although this was not covered in this study.

Management of the local conditions on the tidal flats (e.g. sediment supply, sediment accretion and hydrodynamics) is key for marsh expansion (Mariotti and Fagherazzi 2013; Ladd et al. 2019; Hu et al. 2021). Enough sediment supply is a key factor for successful foreshore development specially to keep up with sea level rise and in situations where the ecosystems are not able to migrate inland due to human constructions like sea dikes (Doody 2013; Mariotti and Fagherazzi 2013; Ladd et al. 2019; Hu et al. 2021; Liu et al. 2021). Therefore foreshore management may also require actions in the land watershed such as opening upstream dams or reduce river dredging (Mariotti and Fagherazzi 2013). If this is not possible, sediment nourishments may be an option to consider (Baptist et al. 2019; Hu et al. 2021). Areas where sediment accretion is possible but marshes are not occurring naturally (e.g. Zwarte Haan and Eemshaven), management of the fronting tidal flats to reduce hydrodynamics and accrete more sediment to create windows of opportunity for marsh establishment may be an option (Mariotti and Fagherazzi 2013; Hu et al. 2015; Bouma et al. 2016; Hu et al. 2021). Common interventions like building wave-breaking brushwood groynes or applying dredging material to create a wave attenuating foreshore can promote marsh establishment (Dijkema et al. 2011; Hu et al. 2015; van Loon-Steensma 2015). An alternative approach to increase ecological value may be to restore adjacent ecosystems such as seagrass or shellfish reefs (van de Koppel et al. 2015; Schoonees et al. 2019), which can also attenuate waves and stabilise and/or accrete sediment in the tidal flat (e.g. Meyer et al. 1997; Borsje et al. 2011; Donker et al. 2013; Walles et al. 2015; Chowdhury et al. 2019). However the success of using ecosystem restoration will depend on factors such as the hydrodynamic forcing of the location and if there is enough space to develop (Morris et al. 2019; Schoonees et al. 2019; chapter 7). Finally, in the most vulnerable locations, exposed to higher wave loads and with insufficient tidal flat accretion, marsh development may not be possible even with human intervention (Schoonees et al. 2019). In this case, hard engineered solutions to protect from floods may be the only option (e.g. dike heightening).

Regarding specific marsh properties, the more elevated the marsh (e.g. above 2 m NAP), the more protection, even if it is narrow (~ 100 m width). However the species that could grow there could be different (Bakker 2014). On the other hand, low intensity grazing management may help preventing the dominance of high marsh species such as *Elytrigia atherica* (Davidson et al. 2017; Chen et al. 2020) and increase soil erosion resistance (Pagés et al. 2018, chapter 6). In any case, vegetation species are not a key factor for wave run-up attenuation purposes, as seen in this study where all marshes reduced the wave run-up independently of the vegetation

MARSHES AND RUN-UP

species and properties, although taller and stiffer species may attenuate the run-up even further. Regarding the width of the marsh, although our study shows that a 300 m width and ~1.5 m of elevation marsh was effective, wider marshes would guarantee wave dampening even with bigger storms (Zhu et al. 2020). Nevertheless, because the higher percentage of attenuation often occurs in the first meters of marsh plateau (the vegetation that resists during winter) (Möller and Spencer 2002; Ysebaert et al. 2011), even a narrow marsh will provide some protection to the dike, including protection of the dike revetment, compared to a bare tidal flat in front of a dike.

In summary, marshes effectively reduce run-up but are not necessarily developing “where we currently need them most”. This catch-22 problem means that engineering measures will always be needed in vulnerable locations: *either* to stimulate tidal flat accretion to induce marsh development at those exposed places where marshes cannot develop without our help *or* to strengthen exposed dikes where nature-based solutions are too costly, not achievable, or going at the expense of other ecological values, such as causing the loss of mudflats that are important for migratory birds (Boere and Piersma 2012).

a) Processes controlling variability of run-up between different locations

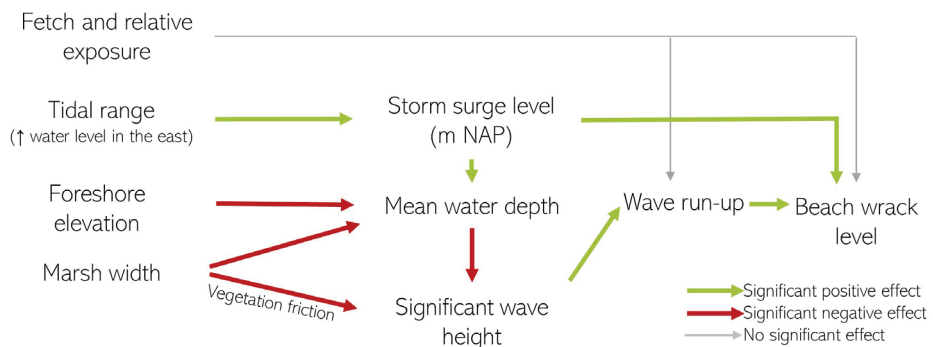


Fig 9 Part I. a) Mechanisms of the effect from the bathymetry, tidal range and vegetation investigated with LMM. Mechanisms of the wind were not further investigated because it was not related to the run-up and beach wrack levels. Green arrows indicate significant positive effect ($p < 0.001$), red arrows indicate significant negative effect ($p < 0.001$) and grey arrows indicate not significant effect ($p > 0.05$).

b) Integration foreshore development and run-up

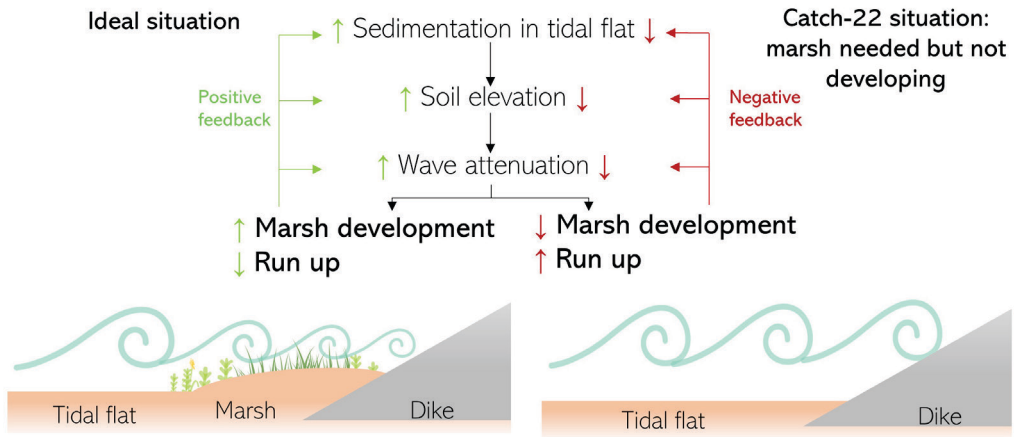


Fig 9 Part II. b) schematic diagram of catch-22 situation between the foreshore elevation (bathymetry), marsh formation and wave run-up attenuation.

ACKNOWLEDGEMENTS

This work is part of the Perspectief research programme All-Risk with project number P15-21 project B1 which is (partly) financed by NWO Domain Applied and Engineering Sciences, in collaboration with the following private and public partners: the Dutch Ministry of Infrastructure and Water Management (RWS), Deltares, STOWA, the regional water authority Noorderzijlvest, the regional water authority Vechtstromen, it Fryske Gea, HKV consultants, Natuurmonumenten, waterboard HHNK. L.L.G. was funded by NWO grant 016.Veni.181.087. In addition, we would like to thank Lennart van IJzerloo from the Nioz for technical assistance; Annette Wielemaker for helping with obtaining the GIS maps; Nelly Eck, Jacob Hogendorf and Panagiota Stergiou, Santiago Amaya for helping with vegetation measurements in the laboratory; Fabris van der Zee, Panagiotia Stergiou, Isabelle Buyens, Sarah Paulson, Lissie de Groot, Michelle Jongenelen, Thijs Zuidewind, Nadia Hijner and Lucia Irazabal Gonzalez for helping in the field. The authors declare no conflict of interest.

SUPPORTING INFORMATION

Table S1. Beach wrack measurement dates and the mean wind direction and speed during the highest water level.

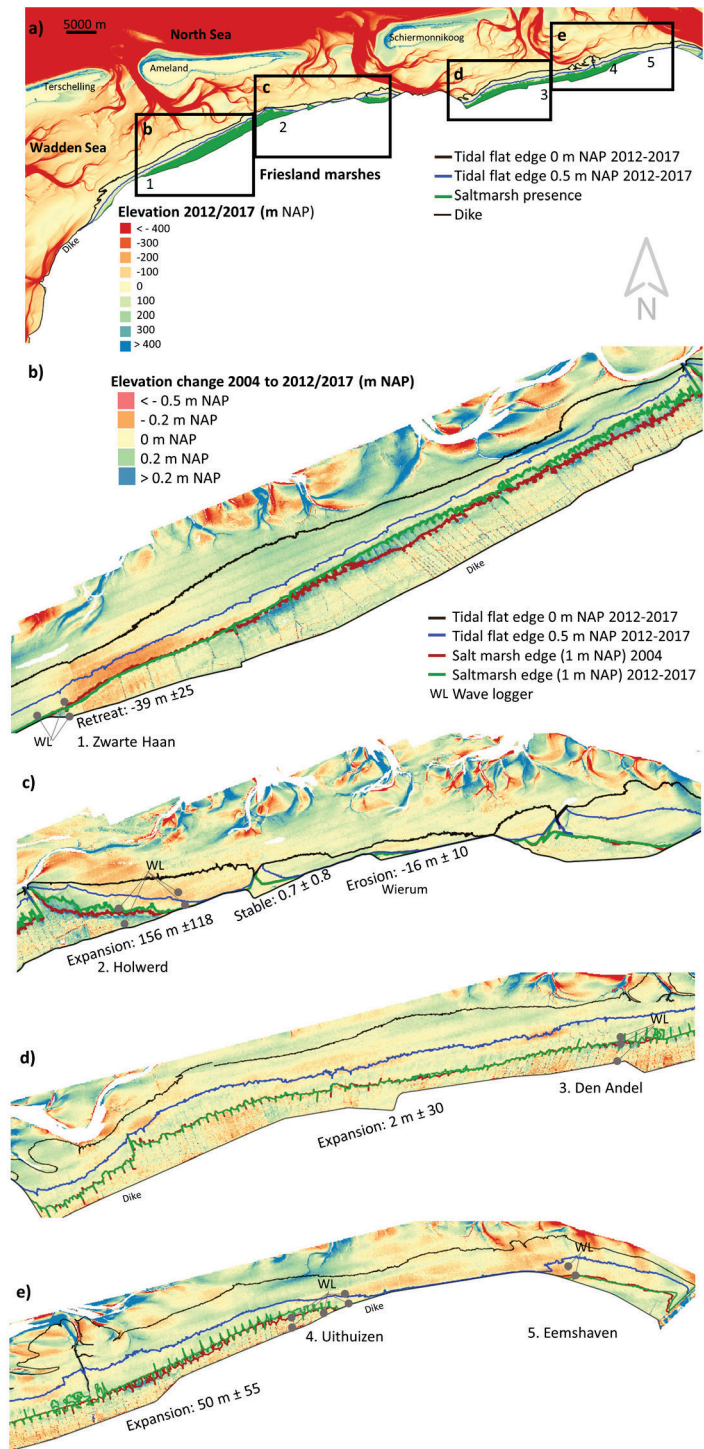
Date	Wind direction (degrees)	Wind speed (m/s)
8/1/2019	320	18
30/9/2019	300	13
9/12/2020	330	13
14/1/2020	210	14
11/2/2020	270	17
12/2/2020	270	15
20/11/2020	320	12
1/12/2020	10	12
5/4/2021	300	15

Table S2. Settings wave loggers.

Wave loggers settings Dec 2018 - June 2019	
Sample rate	10 Hz
New file interval	1 day
Burst length	7 min
Burst interval	15 min

Wave logger settings Sept 2019- Feb 2021	
Sample rate	5 Hz
New file interval	1 day
Burst length	20 min
Burst interval	30 min

Fig. S1. Intertidal elevation change with the marsh edge at 1 m NAP and the elevated mudflat edge for 2004 and 2012/2017. The 1 m NAP contour follows the shape of the groynes where marsh has established.



MARSHES AND RUN-UP

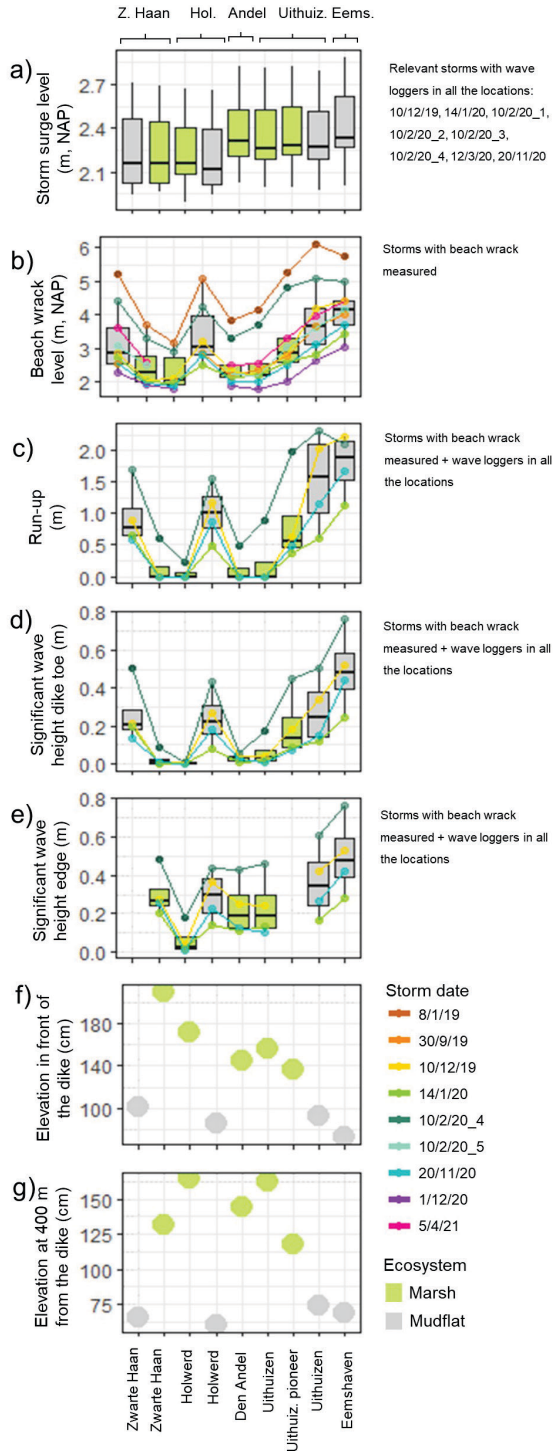


Fig. S2. Differences among transects with wave loggers for a) storm surge water levels; b) beach wrack levels on the dike; c) run-up on the dike, d) significant wave height at the dike toe; and e) significant wave height at the marsh/mud edge (300 m offshore except for Den Andel at 400 m). Water level, wave heights and run-up differences between transects were tested using data from dates where all the locations had wave loggers installed. Beach wrack levels and could be compared including more storms dates because water level from the wave sensors was not needed for the calculation like in the run-up. Storm surge levels were compared for more dates, including days without beach wrack measurements.

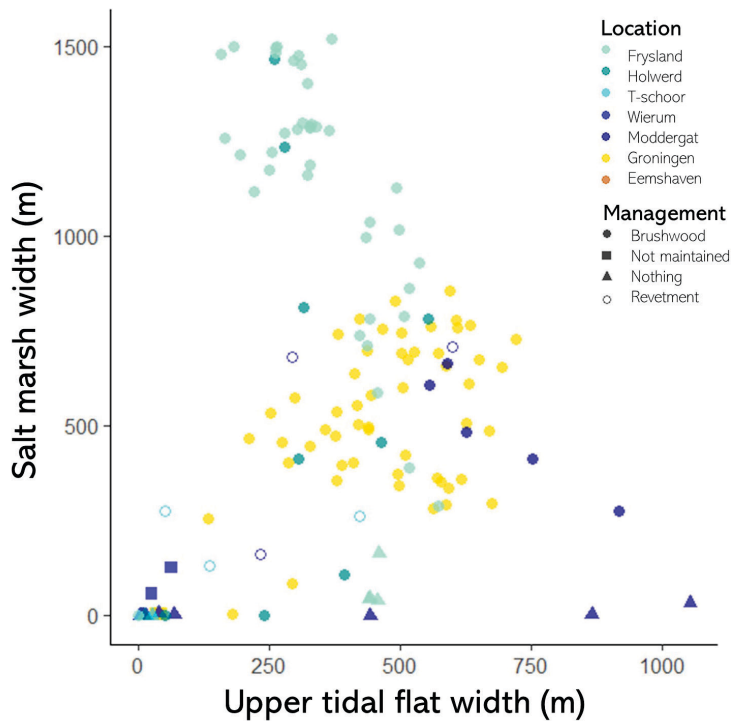


Fig. S3. Relationship between marsh presence and the upper tidal flat width. Upper tidal flat is considered to be above 0.5 m NAP. Marsh width is affected by the management, for example, marshes without management (i.e. brushwood groynes) or not maintained are narrower even though being fronted by a wide upper tidal flat. Note that in the 0 m width upper tidal flat (X axis) there are many overlapped points with zero marsh width (Y axis).



Fig. S4. Erosion observed at the marsh edge of Zwarte Haan in 2018.

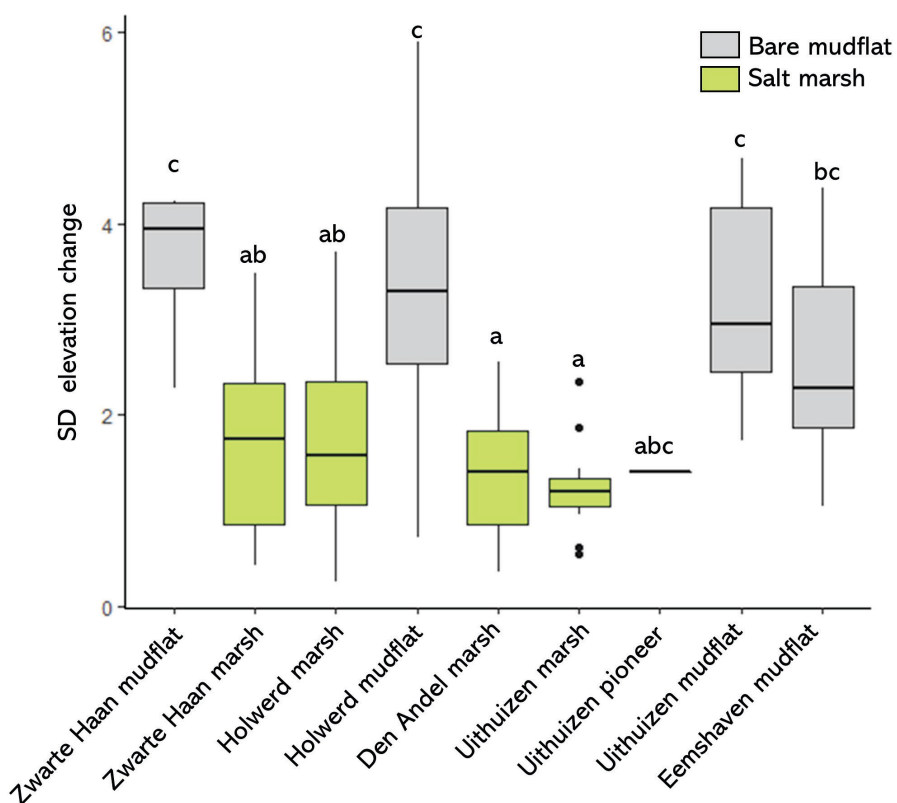


Fig. S5. Variability in elevation change along the transects with wave loggers during the monitoring period (December 2018 – February 2021). Variability in elevation was measured as the standard deviation of the mean elevation. Standard deviation of the elevation change of the transects with wave loggers during the monitoring period

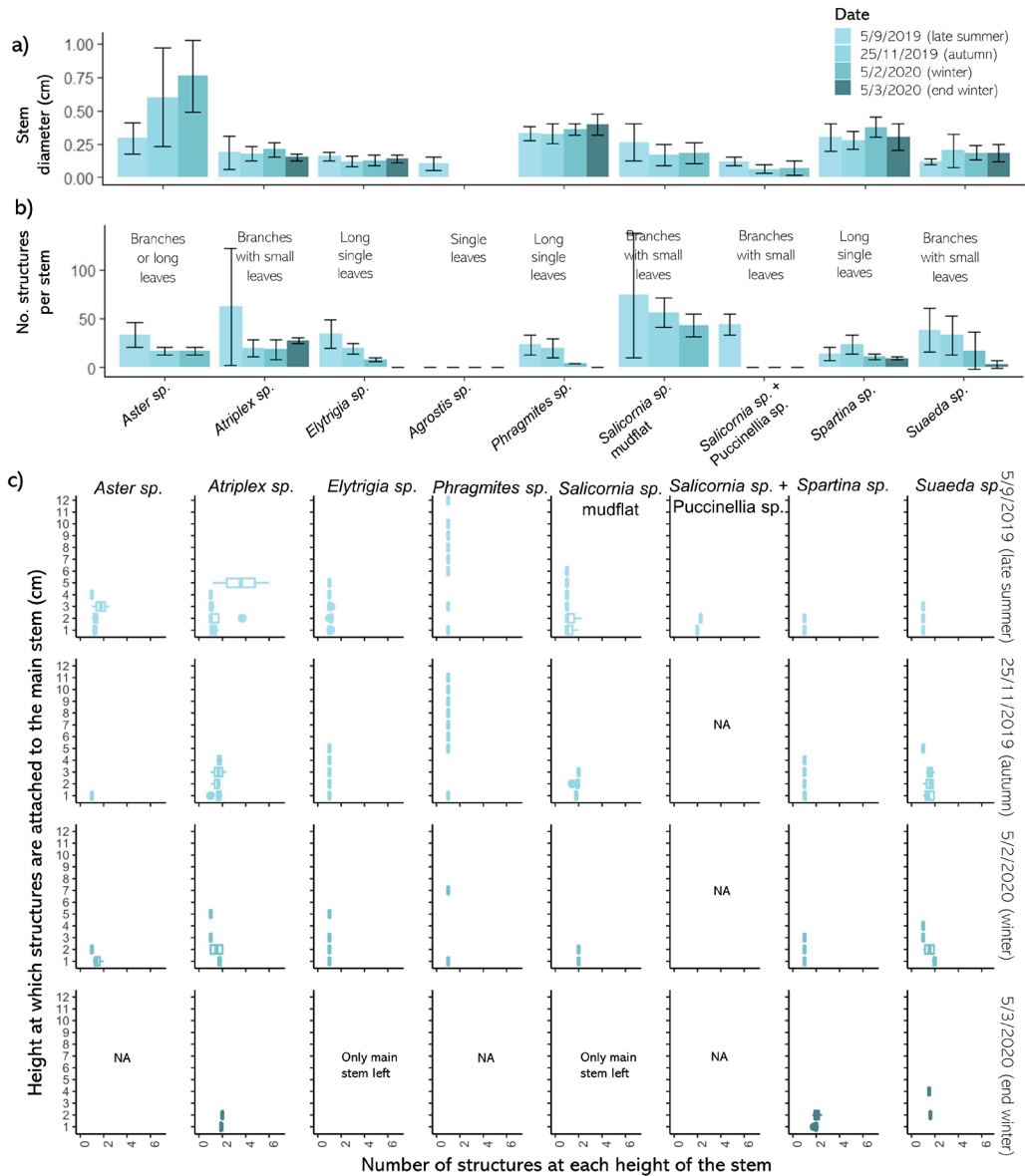


Fig. S6. Changes over the season of a) vegetation diameters, b) number of structures (leaves or branches) per stem, and c) height at which structures were attached per stem. Structures were not measured in *Agrostis* sp.

MARSHES AND RUN-UP

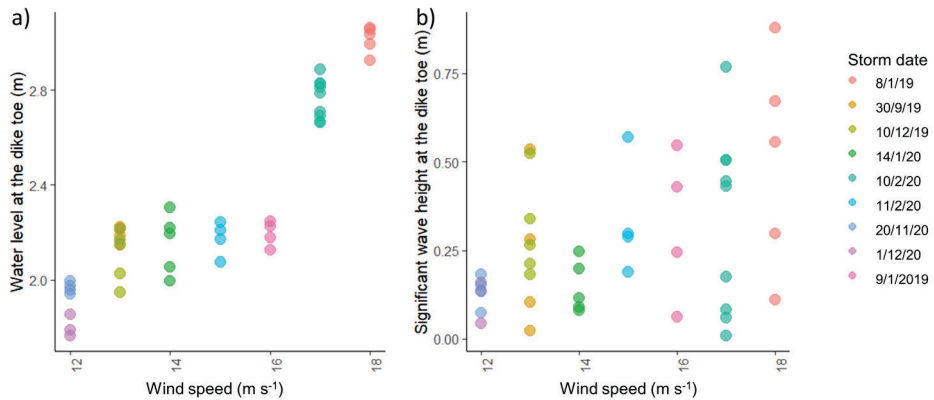


Fig. S7. Relationships between wind speed and a) water level in front of the dike and b) significant wave height in front of the dike. Wind speed is the mean hourly wind speed during the peak of the storm surge water levels measured in the study, obtained from the KNMI (Royal Netherlands Meteorological Institute). Variability in water level and wave height for each storm data is due to differences between locations (e.g. marsh vs mudflats).

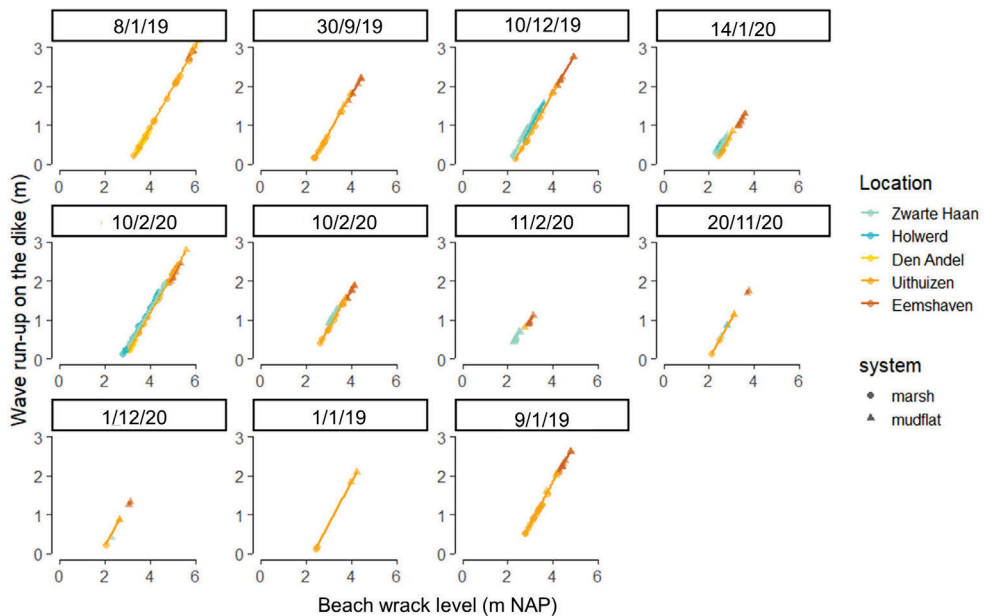


Fig. S8. Correlation between wave run-up on the dike (m) and beach wrack levels (m, NAP). Beach wrack levels and wave runoff were very closely correlated and the slopes were different between the west (Zwarte Haan and Holwerd) and the east (Den Andel, Uithuizen, Eemshaven) (i.e. for the same run-up value, the east area had higher beach wrack levels than the west). Within each area, the locations with the highest wave run-up also had the highest beach wrack levels.

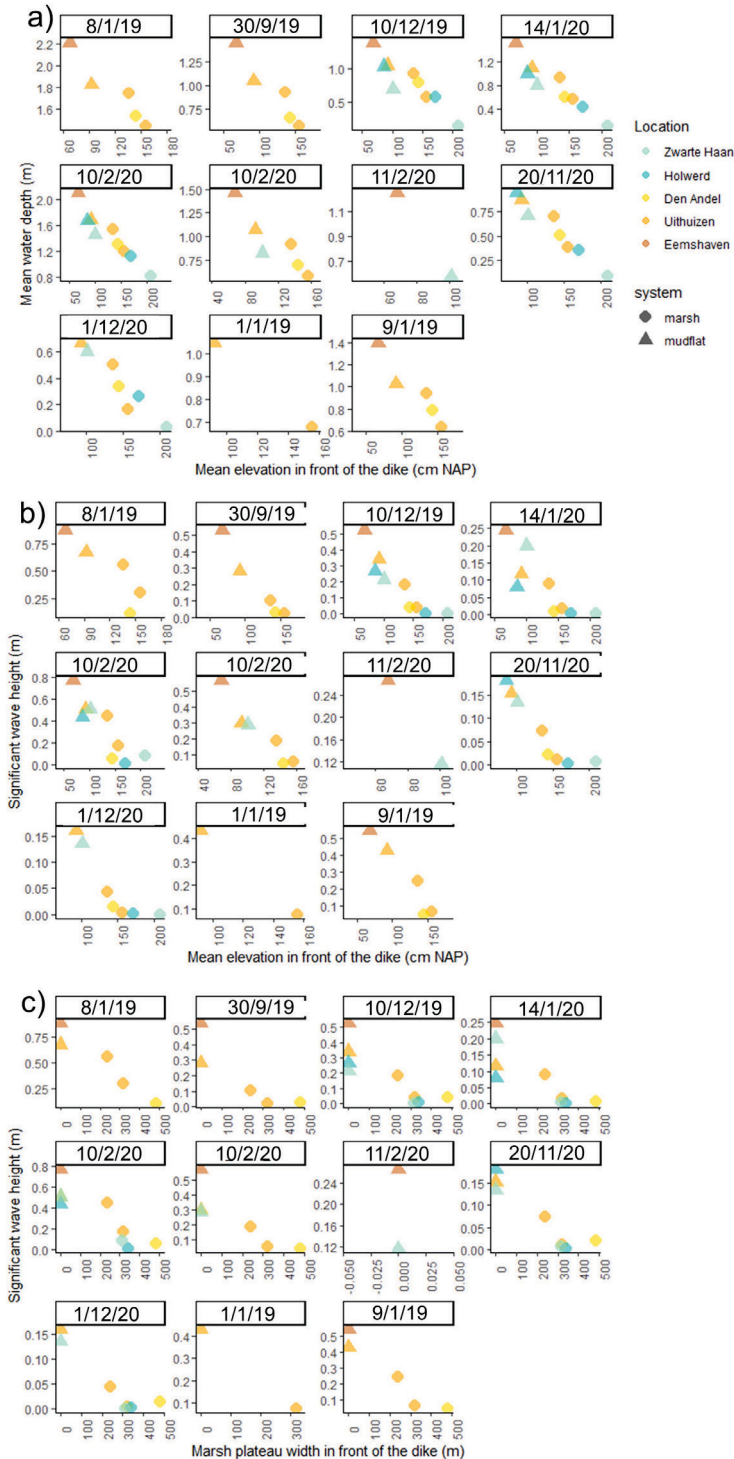


Fig. S9. Relationships separated by dates between a) soil elevation and water depth; b) marsh elevation and wave height and c) marsh width and wave height. Colours indicate the locations (west: Zwarte Haan and Holwerd; east: Den Aniel, Uithuizen and Eemshaven) and shape indicates the ecosystem fronting the dike.

MARSHES AND RUN-UP

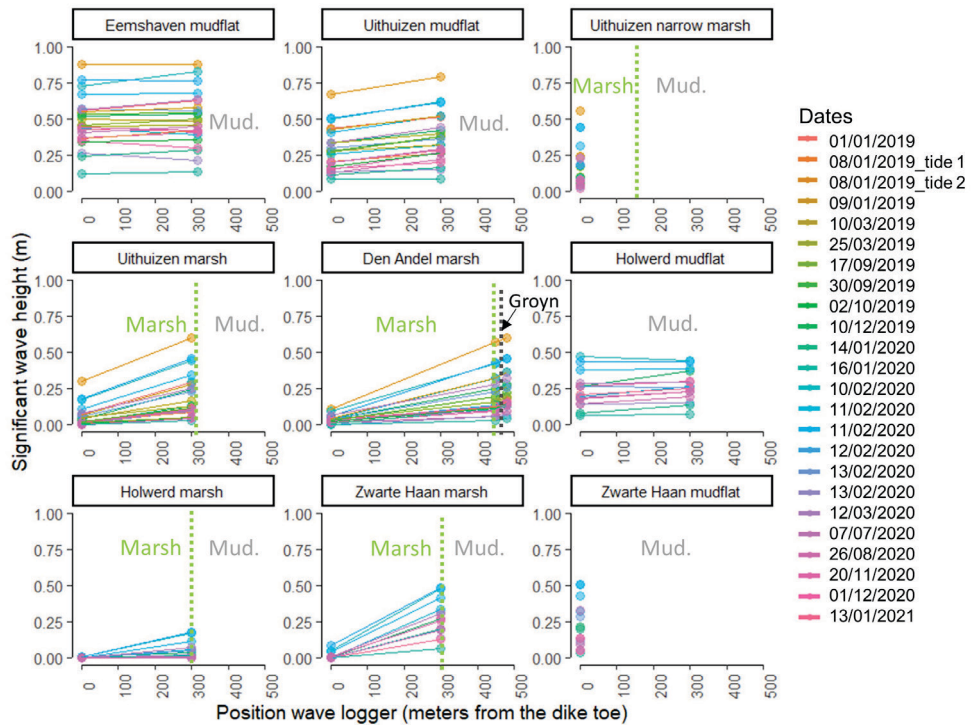


Fig. S10. Effect of different foreshore types on wave attenuation during 24 high tides measured during the monitoring period, including the dates with run-up on the dikes.

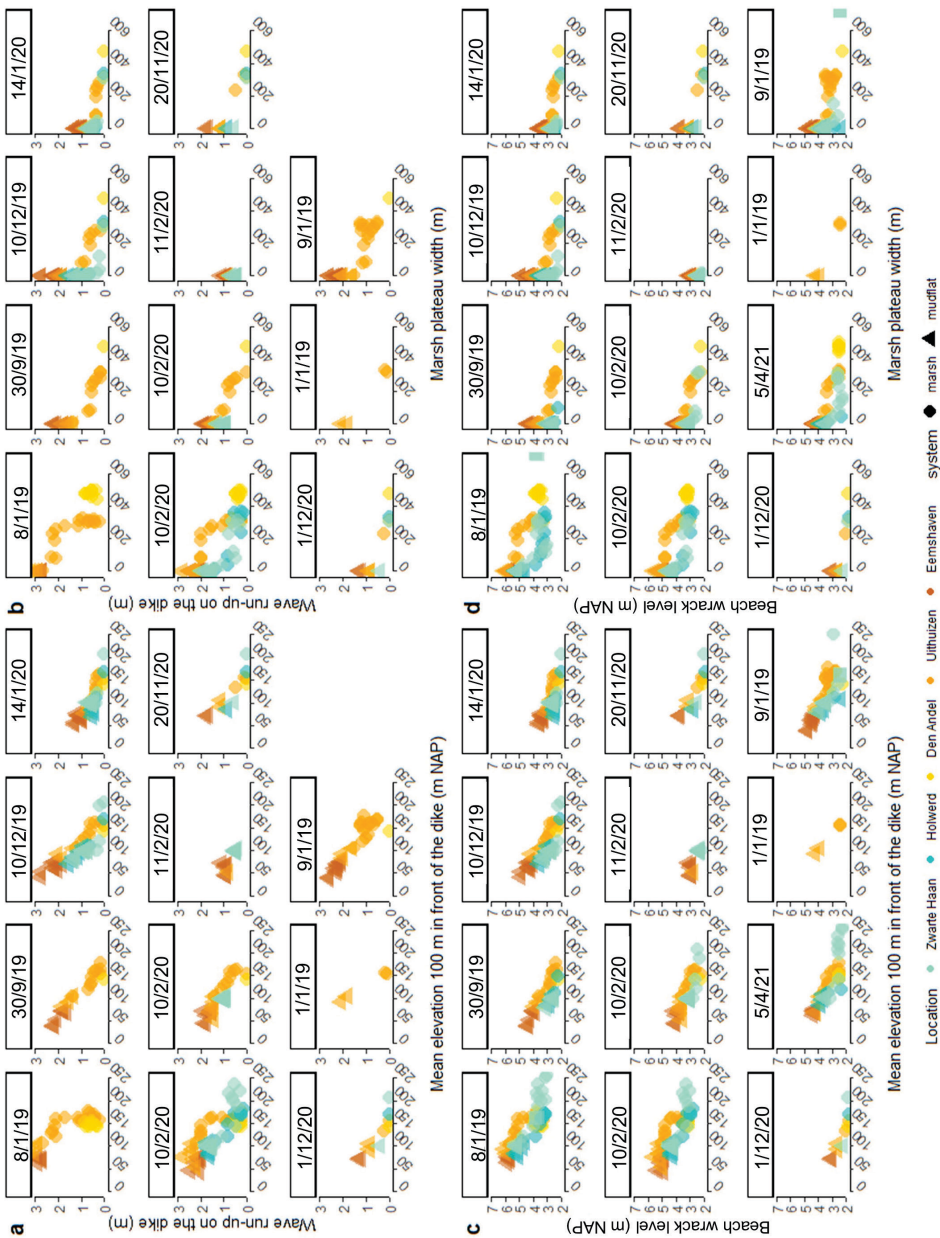


Fig. S11. Correlations between run-up and beach wrack levels on the dike with marsh elevation and marsh width for all the measured dates. It can be observed that although each date had a different wind directions, the patterns remain similar (i.e. higher beach wrack and run-up in the east than in the west). Colours indicate the locations (west: Zwarte Haan and Holwerd; east: Den Aniel, Uithuizen and Eemshaven) and shape indicates the ecosystem fronting the dike.



Chapter 3

The importance of marshes providing
soil stabilization to resist fast-flow
erosion in case of a dike breach

Beatriz Marin-Diaz, Laura L. Govers, Daphne van der Wal, Han Olff,
Tjeerd J. Bouma

Ecological Applications e2622 (2022)

ABSTRACT

Salt marshes provide valuable ecosystem services including coastal protection by reducing wave loading on dikes and seawalls. If the topsoil is erosion-resistant to fast flowing water, it may also reduce breach depth if a dike fails. In this experiment we quantified the topsoil erosion resistance from marshes and bare tidal flats with different soil types to understand the extent to which they can help reduce breach depth. Intact soil samples were collected from eleven locations in the Netherlands at different tidal elevations and then exposed for three hours to 2.3 m s^{-1} currents. To the samples that remained stable after flow exposure, an artificial crack was made to test their stability following soil disturbance. All samples from the tidal flats were completely eroded, regardless of sediment type. In contrast, all samples from well-established marsh plateaus were stable as long as no disturbances were made, including those with sandy subsoils. After creating artificial cracks, samples with a thin cohesive top layer on top of sandy subsoil collapsed, while marshes with silty subsoils remained stable. Pioneer marshes on sandy substrate without a cohesive top layer were the only vegetated soils that completely eroded. The lower erosion of marshes with either sandy or silty soils compared to bare tidal flats, was best explained by the presence of a top layer with belowground biomass, high organic content, high water content and low bulk density. When analysing the erodibility of marshes only, fine root density was the best predictor of erosion resistance. This study demonstrates the importance of preserving, restoring or creating salt marshes, to obtain a topsoil that is erosion-resistant under fast flowing water, which helps reducing breach dimensions if a dike fails. The probability of topsoil erosion in established marshes with sandy subsoil is higher than in silty marshes. A silty layer of cohesive sediment on top of the sand provides extra erosion resistance as long as it does not break. Pioneer marshes that have not developed a cohesive top layer are erosion sensitive, especially in sandy soils. For future marsh creations, using fine grained sediments or a mixture of sand with silt or clay is recommended.

INTRODUCTION

Many coastal communities are facing flood risks due to accelerating sea level rise, land subsidence and intensifying storms, which will probably further increase with climate change (Syvitski et al. 2009; IPCC 2014). As a result, increasing investment in coastal defence structures is needed worldwide (Temmerman et al. 2013). Combining 'green' infrastructure, such as salt marshes or mangroves, with conventional 'grey' infrastructures like sea-walls and dikes, can improve the coastal protection in addition to be a more sustainable solution by preserving natural ecosystems and its related ecosystem services (Shepard et al. 2011; Temmerman et al. 2013; Morris et al. 2018; Schoonees et al. 2019). Furthermore, nature-based flood defences may be capable of recovering from storm disturbances (Feagin et al. 2015; Gijsman et al. 2021) and be resilient against sea-level rise (Kirwan et al. 2016; Fagherazzi et al. 2020; Morris et al. 2020). Ecosystems higher in the intertidal zone like marshes, mangroves or dunes will have more direct effects on coastal protection (Bouma et al. 2014). For example, salt marshes can effectively reduce waves even under storm surge conditions (Möller et al. 2014; Willemsen et al. 2020) and lower the wave run-up on the dikes compared to dikes with bare tidal flat in front (Vuijk et al. 2016; Zhu et al. 2020). As a result, it can be shown that the presence of marshes reduce the likelihood of a dike breach during historic storm floods (Zhu et al. 2020). Moreover historic analyses revealed that the presence of a marsh in front of a dike reduced the breach depth by providing an elevated stable soil layer, thereby saving many lives during a flooding (Zhu et al. 2020). As this latter effect is becoming increasingly important when having dikes protecting people living in low-lying areas faced with sea level rise (Zhu et al. 2020), there is urgent need to gain in-depth understanding of the erosion resistance of foreshores fronting dikes against fast flow running over the soil surface.

Salt marsh soil stability has mainly been tested regarding lateral or cliff erosion (Fig. 1a), as related to marsh retreat (Brooks et al., 2020 and references therein). Fine-grained soils, higher organic content and/or high belowground biomass have been correlated to less lateral erosion (Feagin et al. 2009; Ford et al. 2016; Wang et al. 2017). More specifically, higher root density has been linked to lower lateral erosion, which becomes increasingly important for sandier soils (Lo et al. 2017; De Battisti et al. 2019). Higher soil salinity has been related to higher belowground biomass (Alldred et al. 2017) and less marsh retreat during hurricanes (Howes et al. 2010). Additionally, large grazers such as livestock can modify the soil properties and belowground biomass, thereby increasing the resistance to lateral erosion (Davidson et al. 2017; Pagés et al. 2018; chapter 6). The effect of salt marshes on topsoil (surface) erosion resistance (Fig. 1a), has to the best of our knowledge only rarely been studied under controlled conditions. Specifically, there have been few experiments focusing on the effect of belowground biomass after the removal of aboveground vegetation. Measurements under strong wave conditions after clipping the aboveground vegetation showed that marsh soil with belowground vegetation is highly erosion-resistant (Spencer et al. 2016). Coops et al. (1996) also found reduced surface erosion under wave exposure in reed species growing on sandy soils compared

to bare soils. Furthermore, the effect of the belowground biomass under wave conditions occurs even with the vegetation in winter state (Paul and Kerpen 2021). However, in pioneer marsh vegetation, which can be sparse and grow in patches, tidal current can induce surface erosion on sandy substrates due to scouring around stiff stems (Bouma et al. 2009b; a).

To better understand how marshes can reduce the breach depth during a dike failure (Fig. 1b), which is a different process to the previous erosion experiments done with foreshore ecosystems (Fig. 1a), we need to gain more insight into which factors control the resistance of foreshores against topsoil erosion under fast flow conditions. In terrestrial ecosystems, top soil erosion by runoff was reduced with increasing root density compared to bare soils, especially with high fine root density (below 1 or 0.5 mm Ø, depending on the author) (Li et al. 1991; Baets et al. 2006, 2007; Burylo et al. 2012). For vegetation that grows on dikes, it was shown that topsoil erosion was also reduced with increased root density together with clay sediments and with higher plant species diversity (Scheres and Schüttrumpf 2019, 2020 and references therein). However, to our knowledge it has not yet been studied which factors control the resistance of foreshores soils against topsoil erosion under fast water flow conditions.

To further our understanding of the extent to which foreshores, and marshes in particular, can help reducing breach depth, we investigated the topsoil erosion resistance of salt marshes and tidal flats under conditions of fast water flow (2.3 m s^{-1}) (Fig. 1a). More specifically, we focused on the effect of soil and belowground vegetation properties reducing the top erosion. We excluded aboveground vegetation as they might break off, and to get insight into the erosion resistance under the most erosion-sensitive setting. For this, soil samples of tidal flats and salt marshes representing a wide range of vegetation and sediment types were obtained from elevational transects at 11 intertidal areas around the Netherlands. Erosion was measured following three hours of exposure to fast water flow in a flow flume. Subsequently, artificial cracks were applied to samples that remained stable to test their stability following soil damage like could happen if debris hit the soil or tension cracks develop during a dike breach.

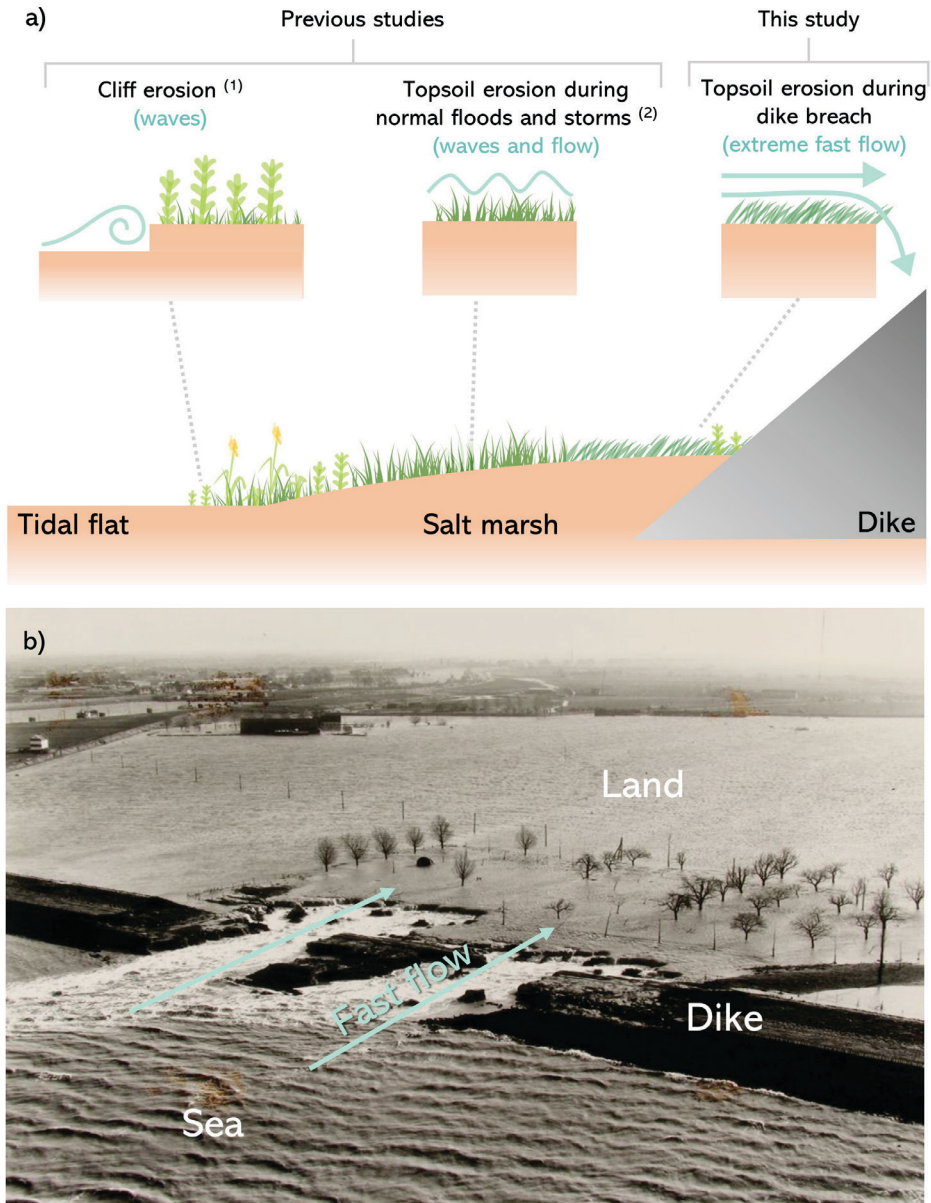


Fig. 1. a) Diagram depicting the types of marsh erosion processes previously studied under controlled conditions: (1) cliff erosion c.f. Feagin et al. 2009, Ford et al. 2016, Lo et al. 2017, Wang et al. 2017 and De Battisti et al. 2019; and (2) topsoil erosion during normal floods and storms c.f. Coops et al. 1996, Bouma et al. 2009a, Spencer et al. 2016 and Paul and Kerpen 2021. In this study we focus on a different type of marsh topsoil erosion which can occur during a dike breach: fast-flow topsoil erosion. b) Example of fast flow following a dike breach after the winter storm of 1953 in Nieuw-Neuzenpolder, Zeeuws-Vlaanderen, Westerschelde Estuary. Photo credit: ZB, Beeldbank Zeeland.

METHODS

Study sites

Soil samples were collected in salt marshes and tidal flats from 11 locations in the Netherlands to include a wide range of biological and physical conditions (Fig. 2). Six locations were located in the Wadden Sea, which is a meso-tidal zone with a tidal range between 2 and 3 m (RWS 2013) in the North of the Netherlands (Fig. 2). The Wadden Sea sampling areas (Table S1) included four locations along the Dutch mainland coast (Dollard Bay, Uithuizen, Holwerd and Zwarte Haan), one barrier island (Schiermonnikoog) and one fetch-limited barrier island (Griend). The remaining five locations were located along the Westerschelde, the estuary of the Scheldt river with a meso to macro-tidal range between four to five m (RWS 2013) in the South-West of the Netherlands (Fig. 2). This Westerschelde sampling area (Table S1) consisted of both relatively exposed (Waarde, Rilland and Zuidgors) and relatively sheltered (Paulina Polder and Ritthem) marshes (Van der Wal et al. 2008; Callaghan et al. 2010).

Experimental set up

The samples were collected along elevation transects to obtain a range of different soil and vegetation types. The transects started in front of the dikes, and went through the different vegetation types, ending in the pioneer marsh and the tidal flat (Fig. 2, Table S1). The samples were classified into six habitat types i) silty established marshes, understanding “established” as the marsh plateau, ii) silty pioneer marshes, found on the edge of the silty mature marshes, iii) silty tidal flats, iv) sandy established marshes, with a sand with peat cohesive top layer and sandy subsoil, v) sandy pioneer marshes, without cohesive top layer and vi) sandy tidal flats (Fig. 2). Samples were also classified by grazing status of large herbivores like cows and sheep (grazed or ungrazed) and type of surface (cohesive, with thick detritus layer, with cracks due to a summer drought, or with soft mud) (Table S1).

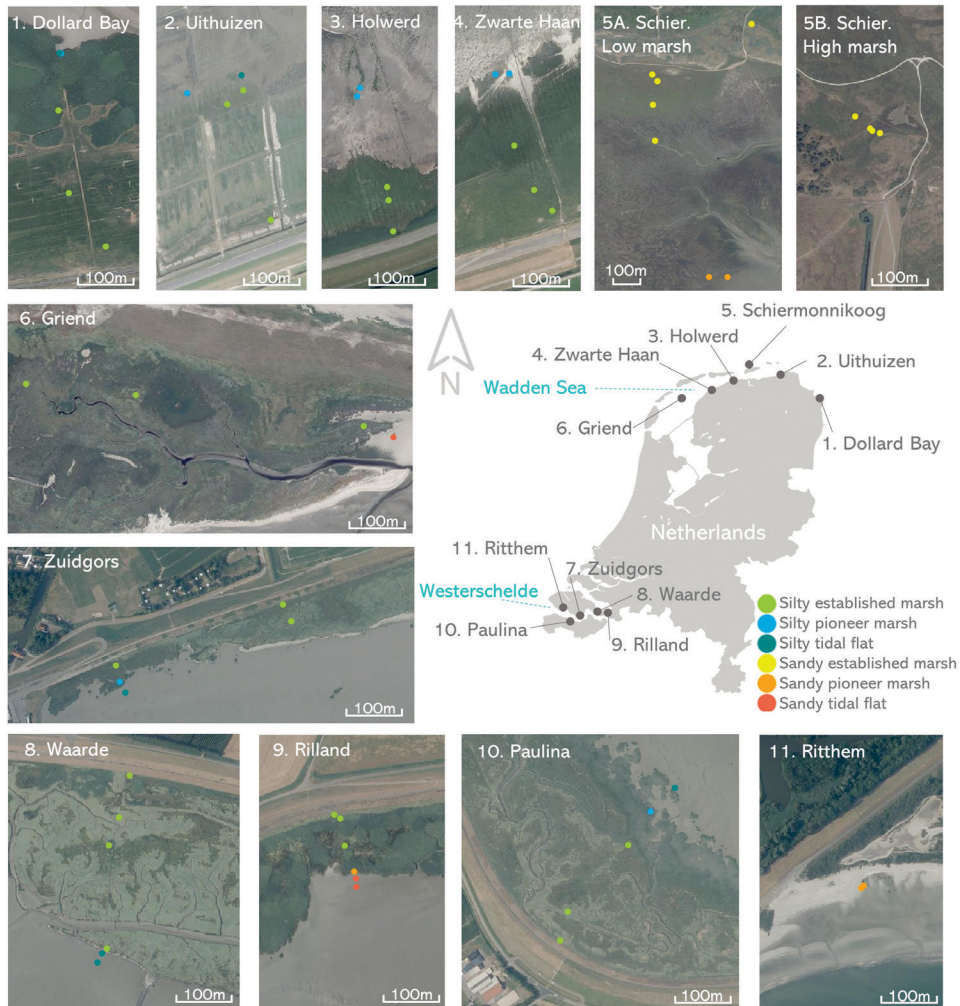


Fig. 2. Sampling locations in the Wadden Sea and the Westerschelde estuary. Colour points indicate the habitat type, with silty soils in cool colours and sandy soils in warm colours. Photographs were obtained from PDOK (Public Geodata Portal in The Netherlands) and all are oriented with the north pointing up.

Top erosion

Rectangular soil cores of 40 cm long x 20 cm high x 13 cm width were collected in all the study sites during October and November of 2018. The cores were extracted with a custom-made steel box-core with sharp edges which was inserted in the soil and carefully dug out, placing a board below the bottom to keep the sample intact (Fig. S1). The soil sample was then carefully placed into a custom-made wooden box which fits in the flow flume. To prevent cohesive soil samples from getting stuck to the walls of the steel frame, the frame was sprayed inside with a thin layer of oil. The oil did not interfere with the erosion experiment because the parts exposed to the erosion were never in contact with the oil. The wooden boxes had nails in the bottom to

TOPSOIL EROSION UNDER FAST WATER FLOW

prevent the complete sample from dislodging with the water flow. From each rectangular soil core, 8 cm from the total 40 cm length were cut off from one of the sides to analyse the vegetation belowground, leaving a soil sample of 32 x 20 x 13 cm for the erosion test (Fig. S2). The samples were transported to the Royal Netherlands Institute for Sea Research (NIOZ) in Yerseke and stored in tanks with seawater to keep the sediment wet until the erosion test. Muddy samples were covered with a plastic film in the field to prevent drying out during the transport. The elevation from each sampling site was measured with a dGPS (Leica GS12).

Top erosion was determined in a fast flow flume developed in the NIOZ (Fig. 3). The flume consisted of a water tank filled at a constant flow rate of 247 L min⁻¹. The tank had an opening of 2.4 cm high and 11 cm width in the bottom of one corner from where the water was flowing at a constant velocity of 2.3 m s⁻¹ with an estimated bottom shear stress of ~ 27 N m⁻² (Eq. S1). Due to the formation of a supercritical sheet flow, bottom shear stress calculations may not be strictly valid but can serve as an estimation. The flow velocity was based on the scenario of a dike breach (Kamrath et al. 2006; Albers 2014). The samples were placed on the other side of the opening, exposing the top layer of the samples to continuous water flow (Fig. S2). The outflowing water was disposed of. Before each erosion test, the aboveground vegetation was clipped to the soil surface level to remove any erosion-protective effects of the canopy. Two wooden walls were installed on each side of the test section to avoid water infiltration through the sides of the sample, leaving an exposed area of 32 cm long x 11 cm wide. Top erosion was determined after 10 min, 1 h, 2 h and 3 h by measuring the average change in elevation with a pin-profiler adapted from the sedimentation erosion bar method (Nolte et al. 2013) and similarly used in (Scheres and Schüttrumpf 2019). Two lines of measurements were done at 3 cm intervals along the axis parallel to the flow and 3.7 cm spacing on the cross-stream axis. The vertical resolution was 1 mm. Samples were classified into stable (mean erosion up to ~ 2 cm depth) and non-stable (completely eroded). The erosion after 10 min was subtracted from the total mean erosion after 3h in stable marsh samples to avoid a bias in the results because it was mainly loose debris.

After the top erosion tests, artificial cracks were made to 17 samples that had remained stable to mimic damage in the soil like could occur during a dike breach (e.g. by debris hitting the ground or development of tension cracks). Samples with sandy bottoms and different cohesive layer thickness were included. Two types of cracks were made in the centre of the soil samples (Fig. 3). The first crack type was 4 cm deep x 2 cm wide and samples were exposed to the water flow for one hour. If the sample did not collapse, a crack of 8 cm deep x 2 cm wide was made and exposed for another hour. To test if the soil would remain stable after a longer time exposure, six of the samples were exposed to the fast flow for 16 h (Fig. S3). The cracks were always oriented with a 45° angle (Fig. 3).

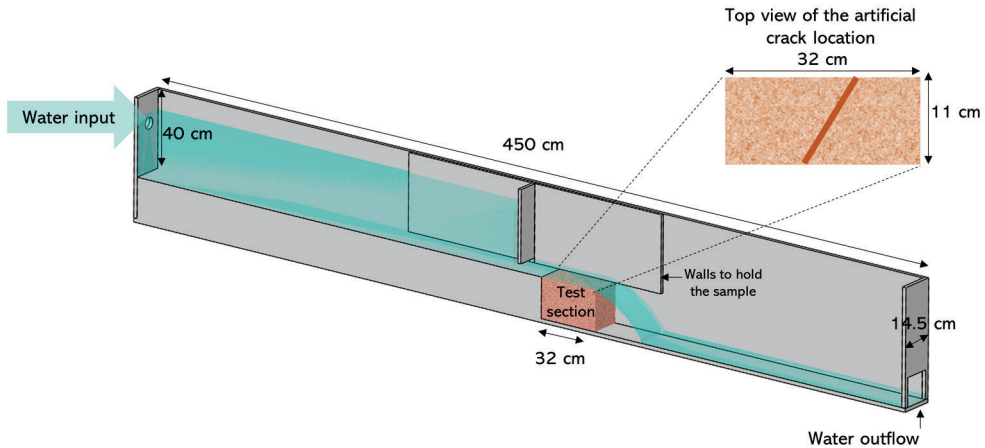


Fig. 3. Schematic cross-section of the fast flow flume developed and built at the NIOZ. In the top right, a diagram of the location in a sample of the artificial cracks made for the second part of the experiment. Water flow reached 2.3 m s^{-1} .

Belowground vegetation properties

Belowground vegetation properties were determined from a $8 \times 20 \times 13 \text{ cm}$ subsample of the same soil samples collected for the erosion test. The belowground biomass was cleaned and separated into roots and rhizomes. Representative subsamples of rhizomes, coarse roots ($> 0.5 \text{ mm } \varnothing$) and fine roots ($< 0.5 \text{ mm } \varnothing$) including fine dead root material that could not be distinguished and removed (cf. De Battisti et al., 2019) were separated from each sample to calculate the respective proportions. This separation was done to disentangle the effect of each root compartment on topsoil erosion. The samples and subsamples were dried at 60°C until constant weight to obtain the biomass. Densities of each compartment were calculated as the respective biomass divided by the volume of the soil sample (g cm^{-3}) (Baets et al. 2006; De Battisti et al. 2019).

Soil properties

Additional small cores of $2.2 \text{ cm } \varnothing$ and 20 cm depth were collected next to each rectangular core to determine the soil properties. The core was split from 0 to 5 cm and 5 to 20 cm depth. In the case of sandy bottoms, the soil was split from 0 cm to the start of the sand layer, and from there to 20 cm . The sediment samples were freeze dried for four days. From these samples, we calculated the bulk density as the dry weight in a known volume (g cm^{-3}) and the percentage of soil water content as the difference between wet and dry weight (Wang et al. 2017). To determine the soil organic content, first the coarse roots, rhizomes and large detritus were removed from the sediment to take into account only the particulate organic matter. The sediment was then burned for six hours at 450°C (Craft et al. 1991). Sediment grain size was determined with a Malvern® Mastersizer 2000. Clay-silt fraction ($< 63 \mu\text{m}$), hereafter called silt content, has been previously related to clay content and soil cohesion in our marine region (Van Ledden et al. 2004) and for reproducibility it was used in this study instead of the clay

fraction alone (e.g. Ford et al. 2016; Lo et al. 2017). For more information on the other soil fractions obtained see Table S2. Additional deep soil profiles up to 1.5 m depth were extracted to visually explore the presence of deeper sandy layers. Finally, a simple and fast field-applicable method adapted from Howison et al. (2015) and hereafter referred to as dynamic soil deformation test, was measured to study if it could be used as a proxy for soil erodibility. This method consisted of releasing a 5 kg metal weight of 10 cm Ø 10 times from 1.5 m height through a guiding PVC pipe. The distance between the soil surface and the bottom of the compacted soil (cm) was used as the dynamic soil deformation value.

Statistical analysis

Data was first analysed including all the samples (the ones that completely eroded and the ones that barely eroded). Soil properties from the top layer (0 to 5 cm depth) were used for the analysis. To visually analyse the non-linear relationships among environmental variables and their effect on erosion, non-metric multidimensional scaling (NMDS) analysis based on Bray-Curtis similarities (a non-parametric multidimensional analysis) and Spearman correlation matrices were used. Stress values reported with the NMDS indicate the accuracy of the representation (Stress < 0.05 indicates perfect representation, < 0.2 should be interpreted with caution and > 0.3 indicates arbitrary ordination) (Clarke 1993). Because the probability of complete erosion including all the samples was binary (completely eroded or not eroded, Fig. S4), correlations between the environmental variables and complete erosion probability were modelled with logistic generalized linear models (GLM) with binomial distribution. To find the best combination of environmental variables explaining the complete probability of erosion, an initial logistic GLM was built including only the total belowground biomass, rhizome density, soil organic content, silt %, mean grain size and dynamic soil deformation. The initial variables were selected based on the NMDS and correlation matrices to avoid collinearity. For instance, total root density, total belowground biomass and fine root density were strongly correlated (Fig. S5). Soil water content, organic content and bulk density were also strongly correlated (Fig. S5). The final model selection was based on stepwise regression and the lowest Akaike's information criterion (AIC). The significance of the models was tested using Type II Wald Chi-square test. Additionally, simple logistic regressions were fitted to each individual variable to visualize their correlation with the complete erosion probability. A limitation from these simple logistic regressions was that the significant trend in silt and mean grain size seemed to be due to the higher number of silty vegetated samples. To study the variability in erosion among stable samples, a second analysis was done using only the samples that remained stable, now using the erosion-depth (cm) as continuous variable. Because of the non-linear relationships among variables, the same procedure of NMDS ordination based on Bray-Curtis similarities and Spearman correlation matrices were used to visually analyse the relationships among environmental variables and their effect on erosion. Gamma with link "log" GLM were fitted to each environmental variable and erosion depth to assess the possible correlations within stable samples. The erosion with artificial cracks was modelled fitting a logistic GLM with binomial distribution, using the binary erosion (collapse or not collapse) as the response variable and the ratio of cohesive layer depth to crack depth as the independent variable. All statistical

analyses were performed using R 3.5.0 (R Development Core Team 2018). The *vegan* package was utilised for the NMDS ordinations (Oksanen et al. 2018).

RESULTS

Top erosion in different habitat types

After three hours of flow exposure, samples were found to be either completely eroded or not eroded (up to 2 cm), hereafter called stable samples (Fig. S4, S6 and S7). The probability of being completely eroded could be differentiated between habitat types (Fig. 4). Silty established marshes, silty pioneer marshes and sandy established marshes were stable, with the exception of one silty pioneer sample which completely eroded (Fig. 4, S4 and S6). Tidal flats, either silty or sandy, and sandy pioneer marsh samples were all completely eroded (Fig. 4, S4 and S6).

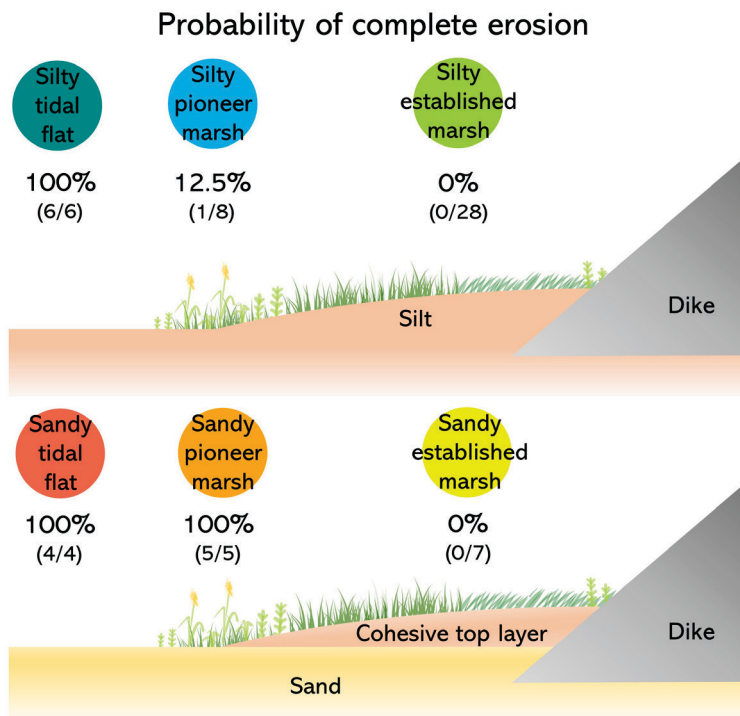


Fig. 4. Graphic representation of the habitat types and the probability of complete erosion in samples from each of these habitats. Numbers in brackets indicate the number of samples completely eroded by the total number of samples for each habitat type.

Relationships between environmental factors and erosion comparing all the samples

The NMDS analysis resulted in clear differences between habitat types and erosion types based on the biotic and abiotic factors measured (stress value = 0.09) (Fig. 5a). Erosion was explained mainly by the belowground vegetation variables (i.e., first NMDS axis) in combination with the soil properties (i.e., second NMDS axis; Fig. 5a). In summary, bare tidal flats were completely eroded independently of whether they were silty or sandy (Fig. 5ab). Stable silty soils with vegetation (established and pioneer marsh) had roots and higher organic content in some of the samples compared to silty tidal flats, with the exception of one pioneer sample with very sparse *Salicornia* (Fig. 5ab). In this case, soil water content and bulk density did not strongly differ compared to silty tidal flats (Fig. 5ab). Stable sandy soils with vegetation (established marsh) had higher organic content, lower bulk density and higher water content on the top layer compared to sandy pioneer marsh and tidal flats (Fig. 5ab). In contrast, sandy pioneer marshes (completely eroded) had low belowground biomass in combination with very low organic content, high bulk density and low water content, similarly to the sandy tidal flats (Fig. 5ab).

The most parsimonious model explaining erosion included total belowground biomass and mean grain size, without significant interaction (GLM: $X^2(2) = 56.7$, $p < 0.001$). Although not selected in the model, there was a significant correlation between lower organic content, higher bulk density and lower water content with higher erosion, but mainly driven by the sandy samples (Fig. 5b). Additionally, we assumed that silt content and mean grain size alone appeared significantly correlated to erosion because of the higher number of silty established marsh samples, rather than because the silt or grain size alone decreased erosion (Fig. 5b). Dynamic soil deformation and rhizome density were not correlated to erosion (logistic regressions both not significant) (Fig. 5b).

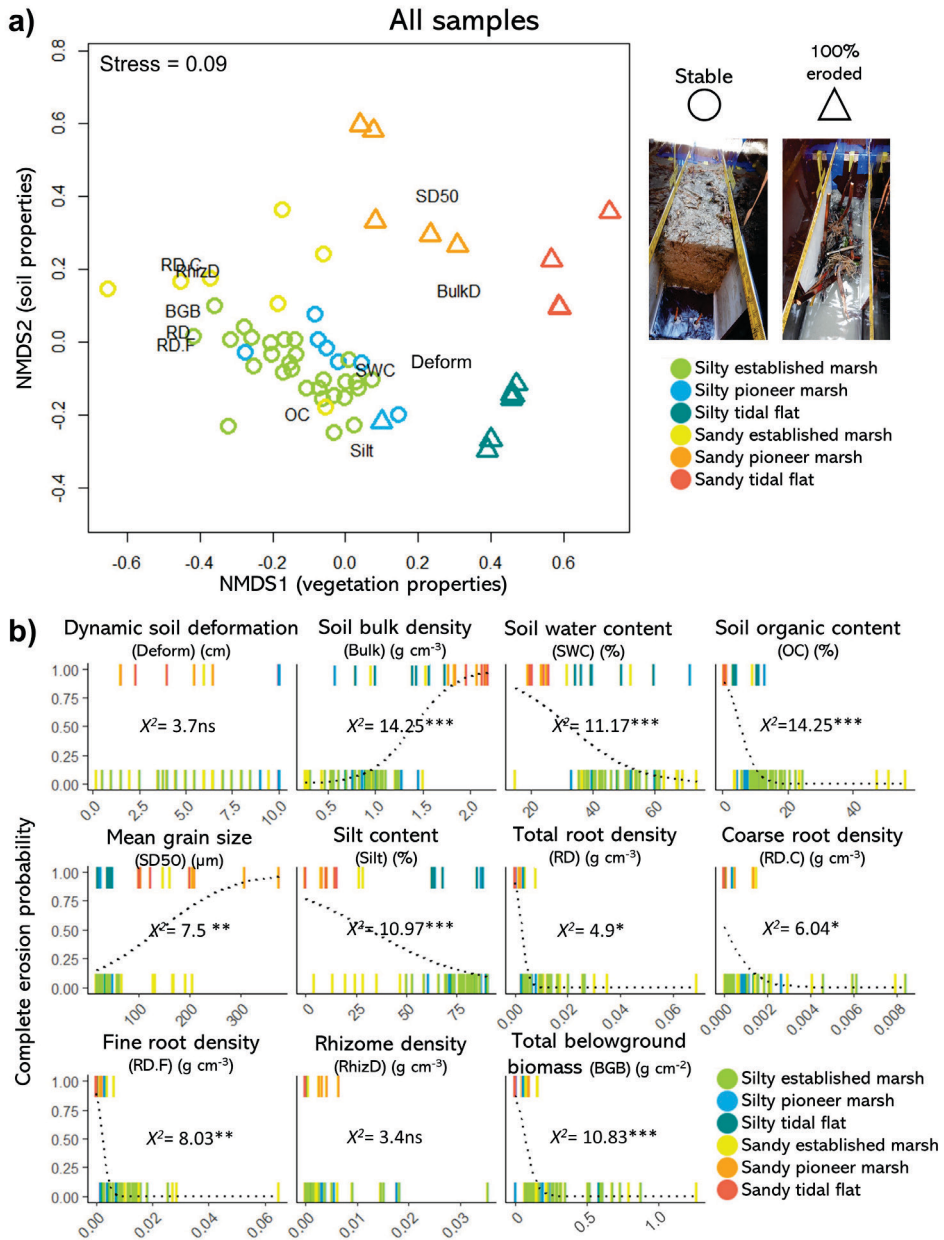


Fig. 5. a) NMDS ordination depicting the environmental variables, habitat types and erosion, including samples that completely eroded and stable samples. Erosion is expressed as binary in the shapes of the points. Stress value = 0.09; and b) Simple logistic regressions between the environmental variables and binary erosion (stable = 0 vs completely eroded = 1) including all the samples. Points are represented as lines for better visualization due to points overlapping. Significance codes refer to $p < 0.001$ (***), $p < 0.001$ (**), $p < 0.01$ (*), $p > 0.05$ (ns).

Relationships between environmental factors and erosion comparing only stable samples

Comparing only stable samples, the NMDS analysis did not result in a clear separation of the mean erosion depth (cm). Nevertheless, a relationship between root density, dynamic soil deformation and erosion was observed along the first NMDS axis (Fig. 6a). Higher fine root density, followed by higher total root density (strongly correlated to fine root density), higher belowground biomass and lower dynamic soil deformation were significantly correlated to less erosion (Fig. 6b). The combination of low root density and higher dynamic soil deformation led to the highest erosion, and was found in soft muddy pioneer samples and swampy areas. Additionally, higher erosion was also found in samples with natural cracks due to the summer drought (not captured by the continuous variables measured) (Fig. S8, Table S1) and samples with thick detritus layer containing *E. atherica* (captured by the dynamic soil deformation test) (Table S1). Rhizome density, coarse root density and any of the soil properties besides dynamic soil deformation were not significantly correlated to the erosion (Fig. 6b).

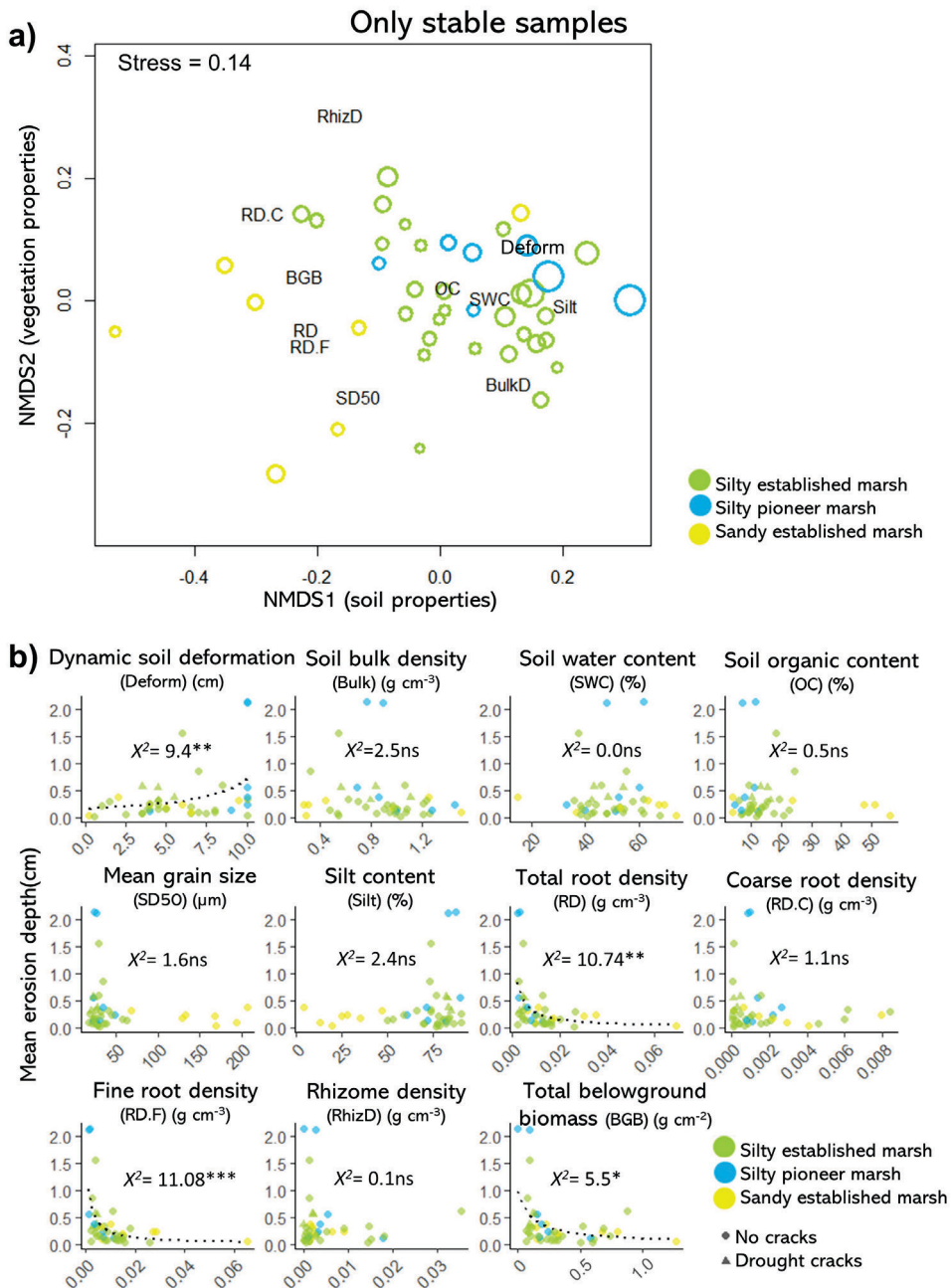


Fig. 6. a) NMDS ordination depicting the environmental variables, habitat types and erosion, using only the stable samples. Stress value = 0.14. Erosion is expressed as the size of the points. b) Simple gamma regressions between the environmental variables and erosion as a continuous variable, with only stable samples. Significance codes refer to $p < 0.001$ (***), $p < 0.001$ (**), $p < 0.01$ (*), $p > 0.05$ (ns).

Stability of stable marsh samples when artificial cracks were created

Established marshes with thin cohesive layers (< 20 cm, less than the sample depth) and sandy subsoils, were stable when no cracks were present (Fig. 3). Nevertheless, when a physical disturbance was artificially created and reached the sandy bottom, they would collapse (Fig. 7). With the specific cracks created (4 and 8 cm depth), only the samples with cohesive layers thicker than 8 cm were stable (Fig. 7). This process was modelled as the collapse probability explained by the ratio of the cohesive layer depth to the crack depth (GLM: $\chi^2(1) = 13.3$, $p < 0.001$). When the crack reached the sandy subsoil (ratios ≤ 1) the samples collapsed, while with ratios above 1, where the crack did not reach the sand, samples were stable (Fig. 7).

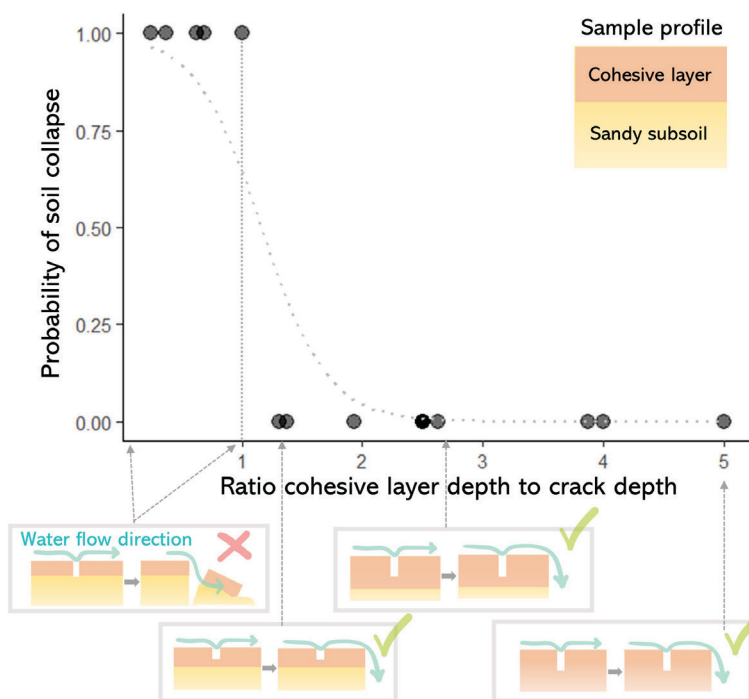


Fig. 7. Soil stability in marsh stable samples when creating artificial cracks. Cracks were either 4 or 8 cm depth. Ratios below 1 represent cracks that reached the sandy subsoil, therefore representing samples with i) cohesive layers thinner than 4 cm and cracks of 4 cm or ii) cohesive layers thinner than 8 cm and cracks of 8 cm.

DISCUSSION

Understanding the stability of salt marshes is crucial for being able to integrate them into coastal defence schemes (Bouma et al. 2014). Most erosion experiments on marshes have focussed on the erodibility of cliffs to understand marsh width (e.g., see Feagin et al. 2009; Ford et al. 2016; Lo et al. 2017; Wang et al. 2017; Battisti et al. 2019), while only few studies have focussed on the erodibility of surface / topsoil under wave forcing (Coops et al. 1996; Spencer et al. 2016; Paul and Kerpen 2021) (Fig. 1a). To gain more insight into which marsh types can help reduce breach depth in case of a dike failure, we investigated the factors determining marsh erodibility under fast water flow as can occur during a dike failure (Kamrath et al. 2006; Albers 2014). We found that established salt marshes even with sandy subsoils were resistant to fast water flow (2.3 m s^{-1}), compared to tidal flats, which completely eroded, independently of their sediment properties. Pioneer sandy marshes were the only marsh type that were completely eroded. Silty pioneer marshes were mostly stable, with exception of sparse *Salicornia* with very low root density (which could be classified as pre-pioneer). Some of the established marshes had a thick root-mat and erodible sandy subsoil as described by Allen (1989). These samples were stable if the cohesive top layer was intact, but collapsed as soon as an (artificial) crack reached the sandy subsoil.

Effect of belowground vegetation and soil properties on top soil erosion

Interestingly, although silty and sandy established salt marshes had different soil properties, both were equally stable compared to bare tidal flats. This indicates that on the bigger picture, established marsh vegetation is what made the foreshores stable in the first place, although the underlying processes varied among habitat types. We did not find any correlation between the soil type and vegetation species, as all the species were found in both sandy and silty marshes, with the exception of *Juncus maritimus* (only sampled in Schiermonnikoog, which was sandy) and *Phragmites australis* (only found in silty locations) (Table S1). Overall, the factors controlling topsoil erosion in bare versus vegetated soils were similar to the findings on lateral erosion, where the roots and organic content reduce erosion and sand content increases erosion (Feagin et al. 2009; Lo et al. 2017; De Battisti et al. 2019). However, in our study, a high percentage of sand increased erosion only in pioneer vegetation, and not in established marshes. In the sandy pioneer marshes, which although being vegetated, were completely eroded, the cohesive top layer of fine roots, organic matter and/or silt, found in the stable marshes, was missing. These samples were differentiated by having higher bulk density and lower water content than the stable marsh samples, due to the coarse grain size and very low organic content present (Bartholdy et al. 2010). Lower erosion in established sandy marshes was correlated to higher belowground biomass, lower bulk density, higher organic content, and higher water content in the top layer, and in some cases, silt content was slightly higher than in the bare sandy soils. Hence, in the sandy vegetated samples with less than 25% silt, similar in bare sand samples, higher organic content together with the belowground biomass may have played the biggest role reducing erosion, similarly to Feagin et al. (2009). In the samples with higher silt percentage in the top layer compared to the sandy tidal flats, which in our study

region is correlated to the clay content and therefore sediment cohesion (Houwing 1999; Van Ledden et al. 2004), may have also reduced erosion together with the belowground biomass and organic content. In contrast, vegetated silty soils (either pioneer or established marsh) had similar physical properties to silty tidal flats with slightly higher organic content only in some vegetated samples but not in all. Therefore, the primary factor reducing erosion in silty soils may be the belowground biomass and secondarily the organic matter, similar to Lo et al. (2017). The dynamic soil deformation test used in this study was not a good proxy for erosion when including all the habitat types such as tidal flats and sandy marshes without cohesive top layers.

When analysing the differences of erosion within samples that remained stable (up to 2 cm of total mean erosion), we found the fine root density (< 0.5 mm Ø) as the most important factor, independent of the grain size. This is in agreement with terrestrial experiments on top erosion both in silty (Li et al. 1991; Baets et al. 2007; Burylo et al. 2012) and sandy soils (Vannoppen et al. 2017). This means that a high density of fine roots would be more effective at reducing erosion than few coarse roots. However, we have to take into account that coarse roots in this study (maximum 1.6 mm Ø), are still considered fine roots in other studies, where the threshold is at < 1 mm Ø (e.g. Li et al. 1991; Baets et al. 2007). In contrast, Battisti et al. (2019) found the coarse roots and rhizomes in *Spartina* as the root compartments explaining most of the lateral erosion. This might be explained by the species studied (*Spartina* and *Atriplex*), which have more coarse biomass than other marsh species, so that the belowground biomass will be mainly explained by rhizomes and/or coarse roots. In this experiment, fine root density explained most of the total root density, which includes fine and coarse roots ($r = 0.99$, $p < 0.001$). Therefore, total root density would also be a good indicator of susceptibility to top erosion, similarly to lateral erosion (chapter 6). Previous topsoil erosion experiments show similar root densities at which erosion starts to be reduced (~ 5 kg m⁻³) (e.g. Baets et al. 2006, 2007; Scheres and Schüttrumpf 2019). However, one should be careful with attributing the effect to this specific root density because soil properties and erosion tests were different between studies. Total belowground biomass may not be as good of a predictor for top erosion because it includes the weight of the rhizomes, which were not correlated to erosion. For example, soil with high total belowground biomass due to thicker rhizomes but low root density may have higher erosion than a sample with lower total belowground biomass but higher root density. Nevertheless, total belowground biomass is still a significant indicator in this study and in previous lateral erosion experiments (Ford et al. 2016; Lo et al. 2017; Wang et al. 2017).

Higher dynamic soil deformation was also significantly correlated to higher erosion in stable samples. This was driven by few samples with thick detritus layers, found with *Elytrigia atherica*, and in muddy samples on the silty marsh edge (silty pioneer marsh) or swampy areas, all having higher dynamic soil deformation. Additionally, livestock grazing may contribute to lower erosion by compacting the soil (Elschot et al. 2013; Pagés et al. 2018; Keshta et al. 2020, chapter 6). However in this study, grazing does not seem essential to further reduce surface erosion because similar low erosion values were obtained both in grazed and ungrazed marshes (Table

S1). Lastly, future research could investigate the critical flow velocities at which stable marshes start to have high erosion.

Effect of artificial cracks and deeper cohesive soil layers on soil stability

Although in this experiment all the established marshes were resistant to gradual particle-by-particle erosion, during a dike breach deeper soil layers may be also exposed to waterflow (Zhu et al. 2020). Our small-scale test with artificial cracks led to block failure in samples with sandy bottoms. This only occurred for marshes with thin cohesive top layers over sandy subsoils, when the artificial crack penetrated to the sandy subsoil. The cohesive layer depth in marshes can increase with age, productivity, sediment availability and flooding frequency (e.g. Olff et al. 1997; Elschot et al. 2013; Esselink et al. 2021). Furthermore, grazing can also affect soil accretion, making this process very context dependent (Elschot et al. 2013; Koppenaal et al. 2021). Cracks in the field may be bigger and deeper, therefore even with thicker cohesive layers the marsh could collapse if the sandy subsoil is eroded. This indicates that in case of a dike breach, marshes with sandy subsoils may not be as stable as silty marshes. Similar processes have been reported in the field, due to wave undercutting of the sandy bottoms (Allen 1989). Nevertheless, even in case of a sandy bottom, the remaining cohesive top layer could still provide more protection than a bare tidal flat. Similarly, previous studies show that tension cracks on the edge of silty soils can lead to bank failure (Allen 1989; Francalanci et al. 2013). Therefore, although in our study the silty marshes were stable even with artificial cracks, this effect may vary dependent on the crack size. In addition, soil profiles of up to 1.5 m depth from this study indicate that sandy layers can also be found below silty soils, together with a decrease in the amount of roots with increasing depth (Brooks et al. 2020 and references therein) (Fig. S9). Therefore we expect the effect of soil disturbances to vary depending on the size of the crack and the depth and type of the exposed soil. Overall, in case of a dike breach, marshes should provide more stability than tidal flats, and silty marshes more than sandy marshes.

Potential effect of climate change on top erosion: natural drying cracks

Cracks in marsh soils can occur naturally during summer due to soil shrinkage after low rain periods or lower summer spring tides (Brooks et al. 2020 and references therein). Four silty samples in this experiment had natural cracks due to soil shrinkage after an unusually dry summer in The Netherlands. The cracks were ~ 4 cm deep and led to higher erosion in the form of blocks compared to soils with similar properties but without cracks. The increased erosion only occurred on the surface of the soil, and not in the layers deeper than the crack depth. Similar processes on a larger scale have been described in the context of cliff erosion formation where tension cracks after soil shrinkage appear in silty marsh edges leading to bank failure (Allen 1989). In the case of a dike breach, small cracks due to soil shrinkage in the upper marsh like those found in our study may not be very important because they were shallow and only the top layer eroded faster. However, if droughts or heat waves followed by storms become more frequent due to climate change (IPCC 2014; Voudoukas et al. 2018; Perkins-Kirkpatrick and Lewis 2020), marshes may become less resilient and more fragmented (Silliman

et al. 2005; Cahoon et al. 2011; Derksen-Hooijberg et al. 2019), and the enhanced erodibility seen in this experiment could contribute to marsh degradation.

Management implications for coastal protection

Overall, to protect the dikes and hinterland, we should aim to conserve existing marshes, even if they are sandy, as far as they have a cohesive top layer. This is not only offering protection by providing increased soil stability, but also wave and flow attenuation (Möller et al. 2014; Leonardi et al. 2018; Zhu et al. 2020). The growth of pioneer marshes should be promoted to become more stable and wider. The creation of new marshes would be the next step, although this is only possible in locations with suitable conditions for marsh establishment (van Loon-Steensma 2015). The establishment of new marshes or the expansion of already established marshes can be promoted with the use of groynes and sedimentation fields to increase the soil elevation (Bakker 2014) or by sediment disposal from dredging activities (Baptist et al. 2019). New restoration approaches using biodegradable artificial structures may also facilitate marsh establishment by reducing physical stresses such as hydrodynamics (Temmink et al. 2020). If the aim is to have a stable soil in case of a dike breach, we discourage the use of sand to create marshes, because sandy marshes will probably take longer to become stable as they need to grow developed roots, accumulate decayed organic matter and accrete a silty top layer to become stable. Therefore, we recommend that the input of sediment should have a fine grain-size to provide a stable marsh bottom. In sandy marshes, the placement of a thin layer of fine-grained sediment amendments to increase soil stability could be investigated. However the potential ecological implications should also be considered (e.g. species composition). Additionally, vegetation with dense root networks could be transplanted to enhance soil stability. A combination of species may be the best option to promote high root biomass (Ford et al. 2016).

Conclusions

Overall we conclude that marshes are much more resistant to topsoil erosion compared to bare tidal flats. This translates into better protection by soil stabilization in the case of a dike breach, preventing the breach from becoming wider. Within the different types of marshes, silty mature marshes will be the most stable. It is not recommended to rely on narrow pioneer marshes, especially with sandy soils, due to the less cohesive sediment and their higher probability of erosion. We should also not rely on mature marshes with sandy subsoils because they could easily erode if the water reaches deeper layers. Nevertheless, in this latter case, the cohesive mat of roots on top of the sand could still provide more protection to the dike than a bare tidal flat. That said, to relate these results to less extreme situations, it should be taken into account that i) the fast flow velocities used in this experiment do not normally occur in natural conditions (Le Hir et al. 2000; Bouma et al. 2005a; Van der Wal et al. 2008; Callaghan et al. 2010) and therefore any type of continuous marsh will likely provide protection against top erosion during normal flooding conditions compared to bare tidal flats, and ii) the aboveground vegetation that was removed in our experiment in order to study the most erosion-sensitive setting, will normally

provide extra erosion protection by flow and wave attenuation (Nepf 2012). Finally, when creating marshes artificially, we encourage the use of fine sediment inputs rather than erodible sand.

ACKNOWLEDGMENTS

This work is part of the Perspectief Research Programme “All-Risk”, project number P15-21 B1, which is co-financed by NWO Domain Applied and Engineering Sciences, in collaboration with: the Dutch Ministry of Infrastructure and Water Management (RWS), Deltares, STOWA, the regional water authority Noorderzijlvest, the regional water authority Vechtstromen, it Fryske Gea, HKV consultants, Natuurmonumenten and the waterboard HHNK. In addition, we would like to thank Rens Riggers, Rebecca Christiaanse, Anne Bauw and Pol Martinez Garcia for field and flume-work assistance. We are also thankful to Lennart van IJzerloo from the Nioz for technical assistance and Sarah Paulson for her help in checking the grammar. The authors declare no conflict of interest.

SUPPORTING INFORMATION

Eq. S1. Calculation of the bottom shear stress and flow velocity applied to the samples during the erosion tests. It should be taken into account that the uncertainty in the bed roughness is not possible to measure and that we are dealing with a supercritical sheet flow, for which shear stress calculations may not be strictly valid. Therefore with this calculation we aimed to provide an indication of the shear stress.

Shear stress (N m^{-2}) was calculated as

$$\tau_b = \rho g \left(\frac{u^2}{C^2} \right)$$

Where ρ is water density (1025 kg m^{-3}), g is gravitational acceleration (9.81 m s^{-2}), u is flow velocity and C is the Chézy coefficient ($\text{m}^{0.5} \text{ s}^{-1}$).

Flow velocity was calculated as

$$u = \frac{d}{h_2}$$

Where d is the discharge, calculated as

$$d = h_0 h_2 \left(\frac{2g}{h_2 + h_0} \right)^{0.5}$$

Where h_0 is the water depth of the basin (0.3 m), and h_2 is the minimum water depth behind the gate (i.e., where velocity is highest), calculated as

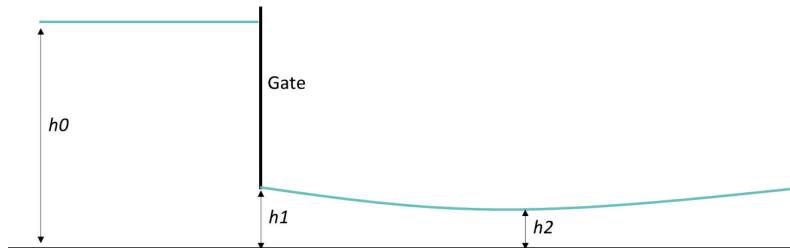
$$h_2 = \frac{h_1}{\text{contract}}$$

h_1 is the opening height (0.024 m) and contract is the contraction constant (0.6).

The Chézy roughness coefficient, which can be approximated for hydraulic rough flow as (van Rijn 2019), was calculated as

$$C = 18 \log_{10} \left(\frac{12 h_2}{k_s} \right)$$

Where k_s is bed roughness (0.0005 m).



Reference:

van Rijn, L. C. 2019. Erodibility of Mud–Sand Bed Mixtures. J. Hydraul. Eng. 146: 04019050. doi:10.1061/(asce)hy.1943-7900.0001677

Table S1Part I. Sites and properties of the sampling locations. Dollard Bay, Holwerd, Paulina Ritthem, Schiermonnikoog,

	Code sample	Habitat type	Elevation (NAP)	Dominant vegetation	Large grazers	Orchestia presence	Cohesive layer depth core (cm)	Top layer from stable samples
Dollard Bay	do1	Silty established marsh	1.931	Festuca	cows	0	20	cohesive
	do2	Silty established marsh	1.898	Puccinellia	cows	0	20	cohesive
	do3	Silty established marsh	1.99	Phragmites	cows	1	20	cohesive
	do4	Silty pioneer marsh	1.396	Phragmites	ungrazed	1	20	cohesive
	do5	Silty tidal flat	0.986	\	ungrazed	0	20	\
Holwerd	ho1	Silty established marsh	1.546	Phragmites	ungrazed	1	20	cohesive
	ho2	Silty established marsh	1.638	Atriplex prostrata	ungrazed	1	20	cracks
	ho3	Silty established marsh	1.571	Atriplex prostrata	ungrazed	1	20	cohesive
	ho4	Silty pioneer marsh	1.149	Spartina	ungrazed	1	20	pioneer (mud)
	ho5	Silty pioneer marsh	1.141	Salicornia	ungrazed	0	20	pioneer (mud)
Paulina	pau1	Silty established marsh	2.413	Elytrigia atherica	ungrazed	0	20	cracks
	pau2	Silty established marsh	2.398	Elytrigia atherica	ungrazed	1	20	cracks
	pau3	Silty established marsh	2.338	A. portulacoides	ungrazed	0	20	cohesive
	pau4	Silty pioneer marsh	1.282	Spartina	ungrazed	0	20	cohesive
	pau5	Silty tidal flat	0.626	\	ungrazed	0	20	\
Ritthem	rit1	Sandy pioneer marsh	2.019	Spartina	ungrazed	0	0	\
	rit2	Sandy pioneer marsh	1.933	Spartina	ungrazed	0	0	\
Schiermonnikoog	schi1	Sandy established marsh	2.222	Elytrigia atherica	ungrazed	1	0	cohesive
	schi10	Sandy established marsh	1.342	Aster	ungrazed	1	5	cohesive
	schi11	Sandy pioneer marsh	0.988	Salicornia	ungrazed	0	0	\
	schi12	Sandy tidal flat	0.857	\	ungrazed	0	0	\
	schi2	Sandy established marsh	1.801	Juncus maritimus	sheep	1	14.5	cohesive
	schi3	Sandy established marsh	1.834	Juncus maritimus	sheep	1	16	cohesive
	schi4	Sandy established marsh	1.866	Juncus gerardi	sheep	0	12.5	cohesive
	schi5	Sandy established marsh	1.521	Juncus maritimus	ungrazed	1	2	cohesive
	schi6	Sandy established marsh	1.147	Suaeda,Puccinellia	ungrazed	1	5	\
	schi7	Sandy pioneer marsh	1.129	Spartina	ungrazed	0	0	\
	schi8	Sandy established marsh	1.697	Elytrigia	ungrazed	1	10.5	cohesive
	schi9	Sandy established marsh	1.591	Juncus	ungrazed	1	6	\

TOPSOIL EROSION UNDER FAST WATER FLOW

Table S1 Part II. Sites and properties of the sampling locations Griend, Uithuizen and Zwarte Haan belong to the Dutch Wadden Sea area., Rilland, Waarde and Zuidgors belong to the Westerschelde area in the South of the Netherlands.

	Code sample	Habitat type	Elevation (NAP)	Dominant vegetation	Large grazers	Orchestia presence	Cohesive layer depth core (cm)	Top layer from stable samples
Uithuizen	uit1	Silty established marsh	3.544	Festuca	sheep	0	20	cohesive
	uit2	Silty established marsh	3.587	Elytrigia atherica	sheep	0	20	cohesive
	uit3	Silty established marsh	3.322	Salicornia	sheep	0	20	cohesive
	uit4	Silty pioneer marsh	3.236	Salicornia	ungrazed	0	20	cohesive
	uit5	Silty tidal flat	3.143	\	ungrazed	0	20	\
Waarde	waa1	Silty established marsh	2.853	Limonium	ungrazed	1	20	cohesive
	waa2	Silty established marsh	2.891	Elytrigia atherica	ungrazed	1	20	detritus/lose
	waa3	Silty established marsh	2.848	Scirpus	ungrazed	1	20	cohesive
	waa4	Silty established marsh	2.983	Elytrigia atherica	ungrazed	1	20	cohesive
	waa5	Silty tidal flat	1.701	\	ungrazed	0	20	\
	waa6	Silty tidal flat	1.657	\	ungrazed	0	20	\
Zuidgors	zui1	Silty established marsh	2.374	Atriplex	ungrazed	1	20	cohesive
	zui2	Silty established marsh	2.602	Elytrigia atherica	ungrazed	1	20	cohesive
	zui3	Silty established marsh	2.441	Aster	ungrazed	0	20	cohesive
	zui4	Silty pioneer marsh	2	Spartina	ungrazed	0	20	pioneer (mud)
	zui5	Silty tidal flat	1.742	\	ungrazed	0	20	\
Zwarte Haan	zwa1	Silty established marsh	2.199	Festuca	cows	0	20	cohesive
	zwa2	Silty established marsh	1.925	Festuca	cows	0	20	cohesive
	zwa3	Silty established marsh	1.49	Suaeda	cows	1	20	cracks
	zwa4	Silty pioneer marsh	1.132	Spartina	ungrazed	0	20	pioneer (mud)
	zwa5	Silty pioneer marsh	1.145	\	ungrazed	0	20	\
Griend	gri1	Silty established marsh	1.381	Elytrigia	ungrazed	1	5.5	cohesive
	gri2	Silty established marsh	1.041	Atriplex	ungrazed	1	5	cohesive
	gri3	Silty established marsh	1.263	Aster	ungrazed	1	2.5	cohesive
	gri4	Sandy tidal flat	1.096	\	ungrazed	0	0	\
Rilland	ri1	Silty established marsh	3.406	Elytrigia atherica	ungrazed	0	20	detritus/lose
	ri2	Silty established marsh	3.004	Phragmites	ungrazed	0	20	pioneer (mud)
	ri3	Silty established marsh	3.042	Scirpus	ungrazed	1	20	pioneer (mud)
	ri4	Sandy pioneer marsh	2.738	Scirpus	ungrazed	1	0	\
	ri5	Sandy tidal flat	2.494	\	ungrazed	1	0	\
	ri6	Sandy tidal flat	2.304	\	ungrazed	1	0	\

Table S2 part I. Grain sizes from the top layer of the samples (0-5cm depth) determined with Malvern® Mastersizer 2000. SD50MUM = Median grainsize D50 in μm , SD50PHIM = Median grainsize D50 in PHI, SMODE = Modus grainsize in μm , SCOARSE% = Coarse sand fraction PHI 0-1, 500-1000 μm , SMEDIUM% = Medium sand fraction PHI 1-2, 250-500 μm , SFINES% = Fine sand fraction PHI 2-3, 125-250 μm , SVFINES%_2 = Very Fine sand fraction PHI 3-4, 62.5-125 μm , SSILT63 = Silt fraction < 63 μm

Code	SD50MUM (μm)	SD50PHIM (phi)	SMODE (μm)	SCOARSE% (%)	SMEDIUM% (%)	SFINES% (%)	SVFINES% (%)	SSILT63 (%)
ri1	29.2	5.1	47.1	1	2.4	6.3	16.6	73.9
ri2	27.4	5.2	33.7	2.8	4.7	6.2	12.3	74.2
ri3	30	5.1	44.8	0.4	0.9	4	18	77
ri4	104.8	3.3	108.2	0	0.1	30.5	59	10.7
ri5	102.6	3.3	107.3	0	0.2	30.4	55.4	14.2
ri6	100.6	3.3	105.5	0	0.2	28.9	55.6	15.6
waa1	44.7	4.5	38.7	0.6	9.4	15.9	15.3	59
waa2	34.7	4.9	54	0.6	1.3	4.8	20.6	73
waa3	32.3	5	46.7	1.9	1.4	5	18.1	73.9
waa4	40.7	4.6	64.6	1.4	1	7.8	23.7	66.3
waa5	39.1	4.7	65.8	0	0.1	7.2	24.8	68.3
waa6	43.1	4.5	78.2	0	0.1	9.4	27.2	63.6
pau1	23.4	5.4	32.8	0.1	1.1	4	12.7	82.3
pau2	21	5.6	32.2	0.1	0.9	2.4	11.6	85.2
pau3	28.4	5.1	36.5	4.2	1.6	3.5	13.4	77.7
pau4	49	4.4	59.3	0.1	3.2	10.8	25.2	61
pau5	46.7	4.4	65.1	0.2	0.7	6.1	28.9	64.5
zui1	18.7	5.7	26.7	0	0.9	1.5	7.2	90.6
zui2	24.7	5.3	37.2	0	0.8	2.7	13.4	83.5
zui3	21.3	5.6	28.7	0	1.2	2.7	9.7	86.6
zui4	27.1	5.2	36.9	0.2	1.1	2.1	13.6	83.3
zui5	48.1	4.4	67.5	0.2	0.3	6.9	30.1	63
sch1	205.9	2.3	209.6	0	28	63.1	4.7	4.2
sch2	167.1	2.6	171.8	21	17	20.8	16.4	25
sch3	132.7	2.9	123.4	15.1	16.4	20.3	19.9	28.4
sch4	169.6	2.6	137.1	17.9	19.9	22.6	19.8	20
sch5	193.6	2.4	216	0.4	29.4	46.7	10	13.6
sch6	161.8	2.6	212.9	0.1	23	38.2	9.9	28.8
sch7	205.6	2.3	211.9	0	26.8	62.5	2.8	7.9
sch8	67.8	3.9	74.7	1.2	8.9	18.9	23.9	47.4

TOPSOIL EROSION UNDER FAST WATER FLOW

Table S2 Part II. Grain sizes from the top layer of the samples (0-5cm depth) determined with Malvern® Mastersizer 2000. SD50MUM = Median grainsize D50 in μm , SD50PHIM = Median grainsize D50 in PHI, SMODE = Modus grainsize in μm , SCOARSE% = Coarse sand fraction PHI 0-1, 500-1000 μm , SMEDIUM% = Medium sand fraction PHI 1-2, 250-500 μm , SFINES% = Fine sand fraction PHI 2-3, 125-250 μm , SVFINES%_2 = Very Fine sand fraction PHI 3-4, 62.5-125 μm , SSILT63 = Silt fraction < 63 μm

Code	SD50MUM (μm)	SD50PHIM (phi)	SMODE (μm)	SCOARSE% (%)	SMEDIUM% (%)	SFINES% (%)	SVFINES% (%)	SSILT63 (%)
sch19	148.8	2.8	216.3	2.6	22.3	31.7	16.9	26.8
sch10	129.4	3	224.8	3.4	20.8	26.8	13.7	35.5
sch11	209.2	2.3	215.8	0	30	59.2	3.3	7.6
sch12	199.6	2.3	198.4	0	23.9	70.1	6	0
rit1	308.4	1.7	307.9	10.2	60	29.6	0.2	0
rit2	374.6	1.4	376.3	22.2	63.7	14.1	0	0
Do1	25.2	5.3	33.4	0.4	2.3	4.4	12.8	80.4
Do2	23.6	5.4	28.3	2.7	1.8	3.4	11.1	81.2
Do3	18	5.8	24.1	0.5	0.9	1.5	6.6	90.7
Do4	23.1	5.4	29.1	1	2.3	3.8	10.6	82.5
Do5	20.5	5.6	29.6	0.8	1.4	2.3	10.1	85.5
Uit1	25.8	5.3	32.5	0.4	1.6	3.6	12.6	82
Uit2	28.4	5.1	44.2	1.1	1.1	3.6	16.9	77.6
Uit3	38.5	4.7	55.8	0.8	1.6	5	22.4	70.5
Uit4	31	5	37.1	1.7	1.2	7	18	72.3
Uit5	23.5	5.4	28.6	0.1	0.4	1.6	10	88.2
Ho1	28.8	5.1	39.1	0.9	1.8	3.7	15	78.9
Ho2	23.6	5.4	30.9	1.5	1.5	3	11.3	82.9
Ho3	24.7	5.3	33.1	0.5	1.2	2.5	11.9	84.3
Ho4	23	5.4	30.3	0	0.2	0.7	9.4	89.8
Ho5	24.4	5.4	31.5	0.1	0.5	1.4	10.9	87.3
Zwa1	32.2	5	42.2	0.2	1.6	3.5	17	78.1
Zwa2	30.7	5	39.1	2	2	4	15.6	76.7
Zwa3	27.8	5.2	36.1	0.2	1.3	2.3	12.9	83.6
Zwa4	34.7	4.9	39.8	3.4	4.2	5.1	16.1	71.4
Zwa5	24.8	5.3	32.3	0.1	0.8	1.5	10.7	87.1
gri3	58	4.1	70.9	5	6.3	12.6	23.4	53
gri2	36.3	4.8	47.1	1.1	3.7	7.7	18.3	69.5
gri1	62.5	4	78.4	5.1	7.9	15.9	21.1	50.2
gri4	123	3	129	0	3.2	45.3	41.3	10.3



Fig. S1. Images from the method used to collect the rectangular soil samples for the erosion experiment.

TOPSOIL EROSION UNDER FAST WATER FLOW

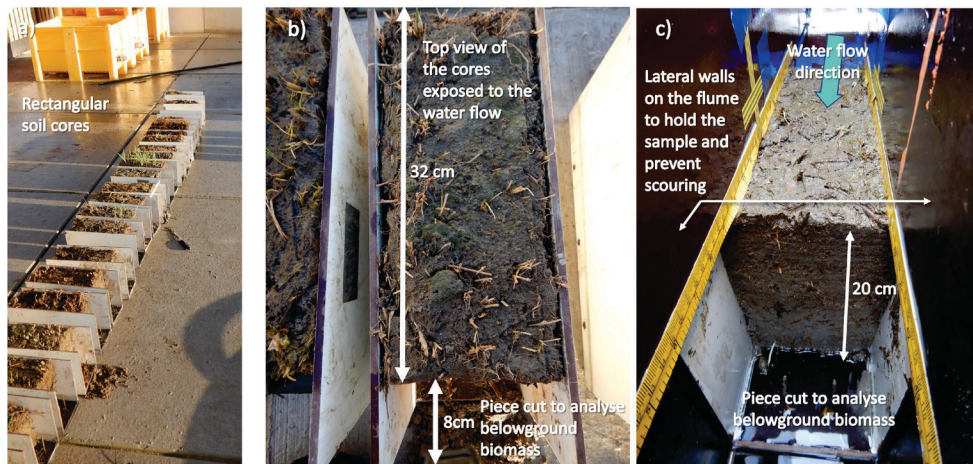


Fig. S2. a) Custom-made wooden boxes which fit in the flow flume with the soil samples inside, b) top view of a sample outside the flume. From each sample, 8 cm were cut off prior to the erosion test to analyse the vegetation belowground biomass and c) example of a sample inside the flume. An extra "wall" was installed in each side of the flume walls and on top of the sample edges to hold the samples and shield the small gap between the sample and the wooden box in order to prevent soil scouring in the margins of the sample. The extra walls were removed after each erosion test and installed again for every sample.

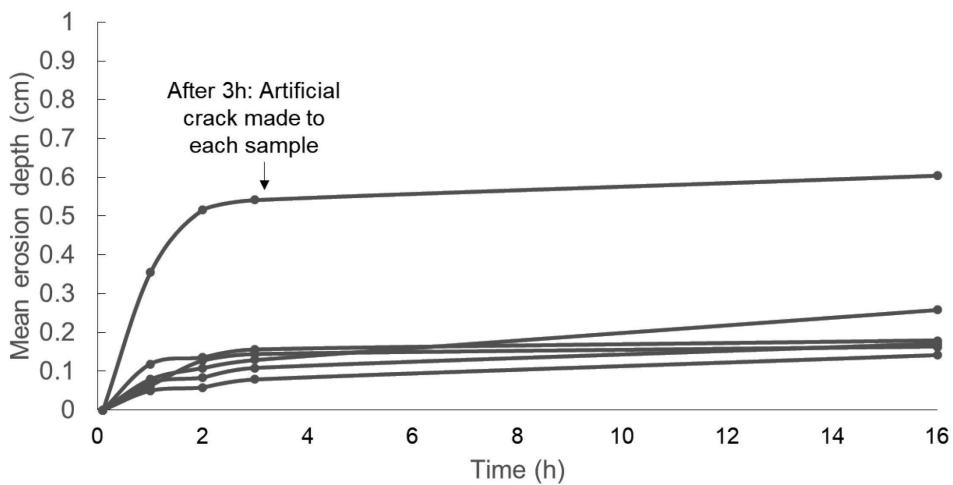


Fig. S3. Mean erosion depth over time from a subset of samples to test their stability during a prolonged period of time (16h) exposed to fast water flow. All these samples had an artificial crack made after 3h of flow exposure.

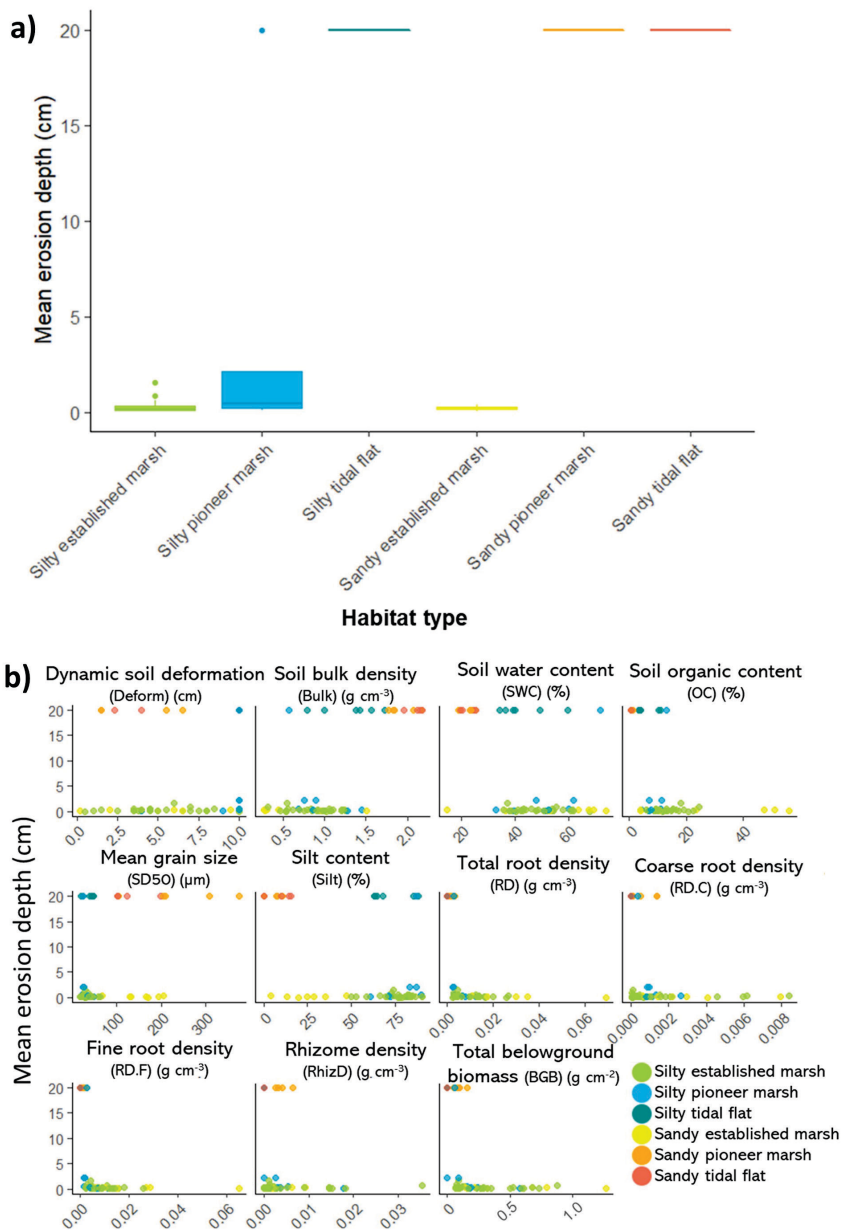


Fig. S4. Erosion data including all the samples, were it can be observed the binary response (completely eroded or not eroded). a) shows a boxplot of the mean top erosion, measured as erosion depth (cm), at the end of the experiment after 3 hours of flow exposure, separated by habitat types. The cores were 20 cm depth, therefore, erosion of 20 cm indicates complete erosion; b) shows the erosion depth (cm) in relation to the environmental variables measured.

TOPSOIL EROSION UNDER FAST WATER FLOW

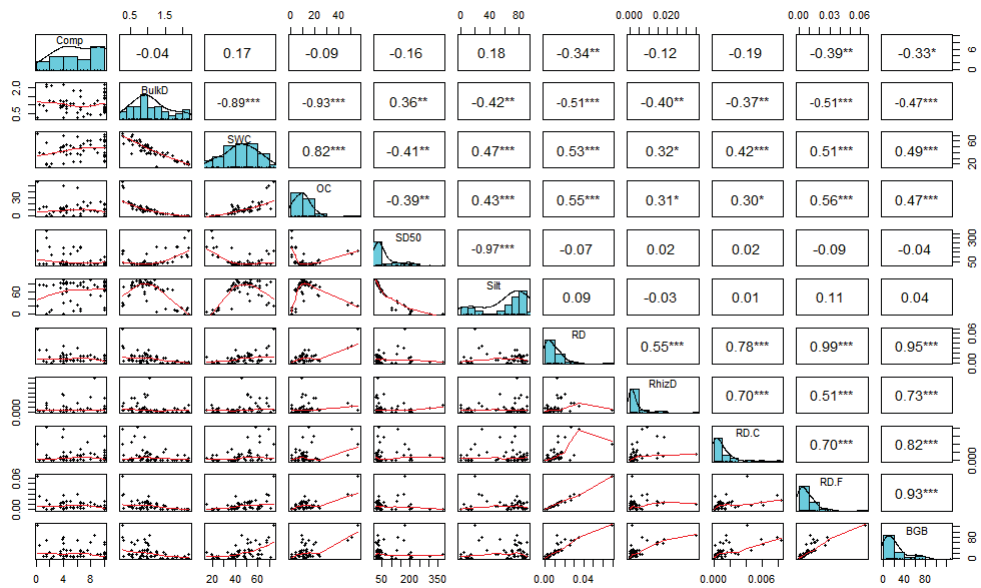


Fig. S5. Spearman correlation matrix showing the relationships among the environmental variables. Comp = dynamic soil deformation (cm), BulkD = Bulk density (g cm^{-3}), SWC = Soil water content (%), OC = Soil organic content (%), SD50 = mean grain size (μm), Silt = silt %, RD = total root density (g cm^{-3}), RhizD = Rhizome density (g cm^{-3}), RD.C = coarse root density (g cm^{-3}), RD.F = fine root density (g cm^{-3}), BGB = belowground biomass (roots + rhizomes) (g).

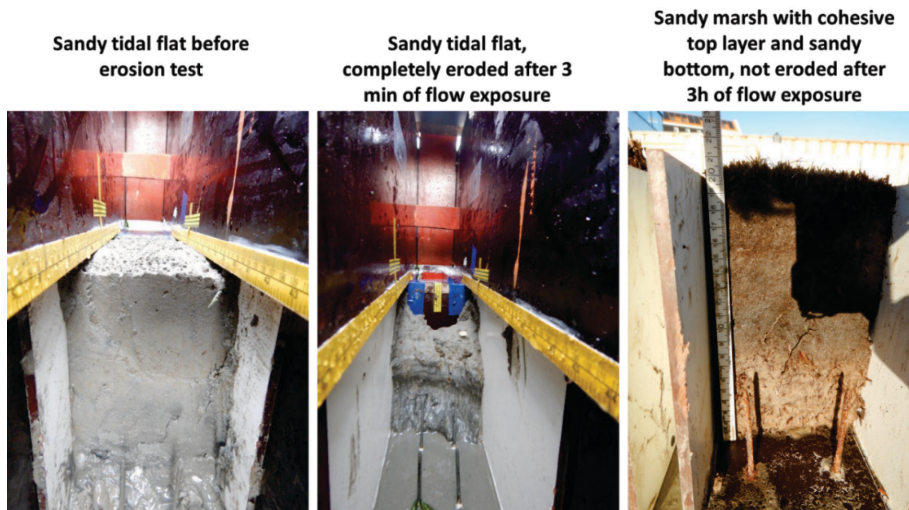


Fig. S6. Front view from a sandy tidal flat sample before and after 3 minutes of flow exposure, where it completely eroded; and from a sandy marsh with cohesive top layer, which did not erode after 3 hours of flow exposure.

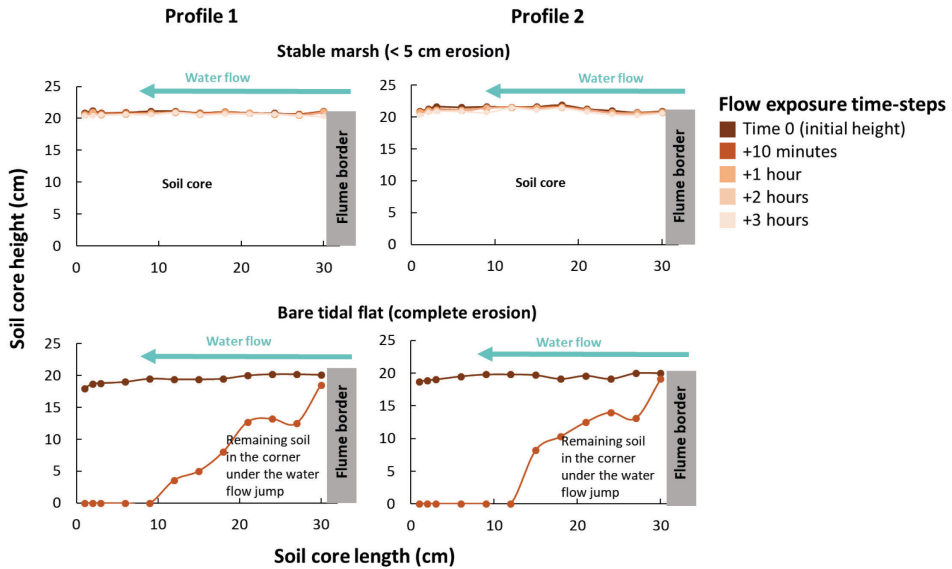


Fig. S7. Example of the erosion profiles measured with the erosion pins in a stable marsh sample and a bare tidal flat sample (not stable), for the two profiles done per sample.

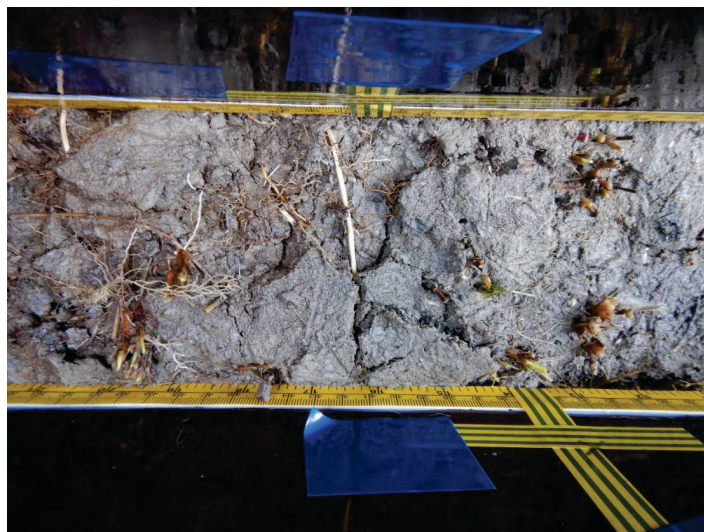


Fig. S8. Example of the erosion in form of blocks in samples with natural cracks due to a summer drought (top view of the sample).

TOPSOIL EROSION UNDER FAST WATER FLOW

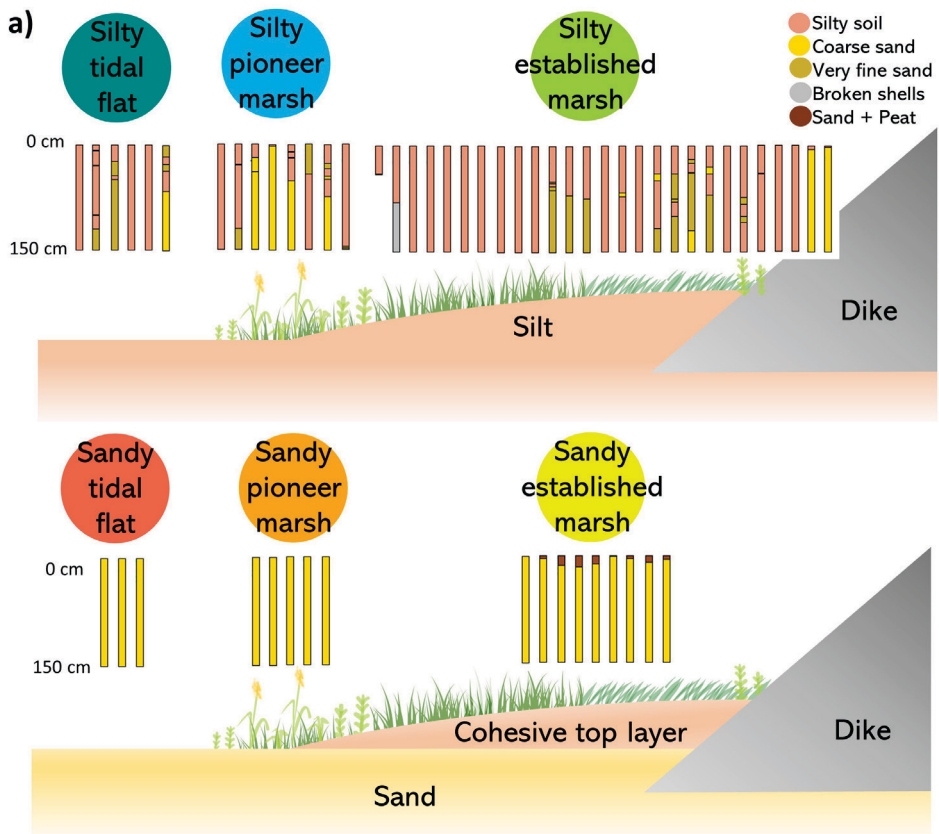


Fig. S9. a) Overview of the deep soil profiles up to 1.5 m depth found in the different habitat types from all the locations studied. Each bar corresponds to one sampling location. Silty and sand + peat top layers in the profiles are the ones considered cohesive top layers. It can be observed that it is common to find an alternation between silty and sandy layers.

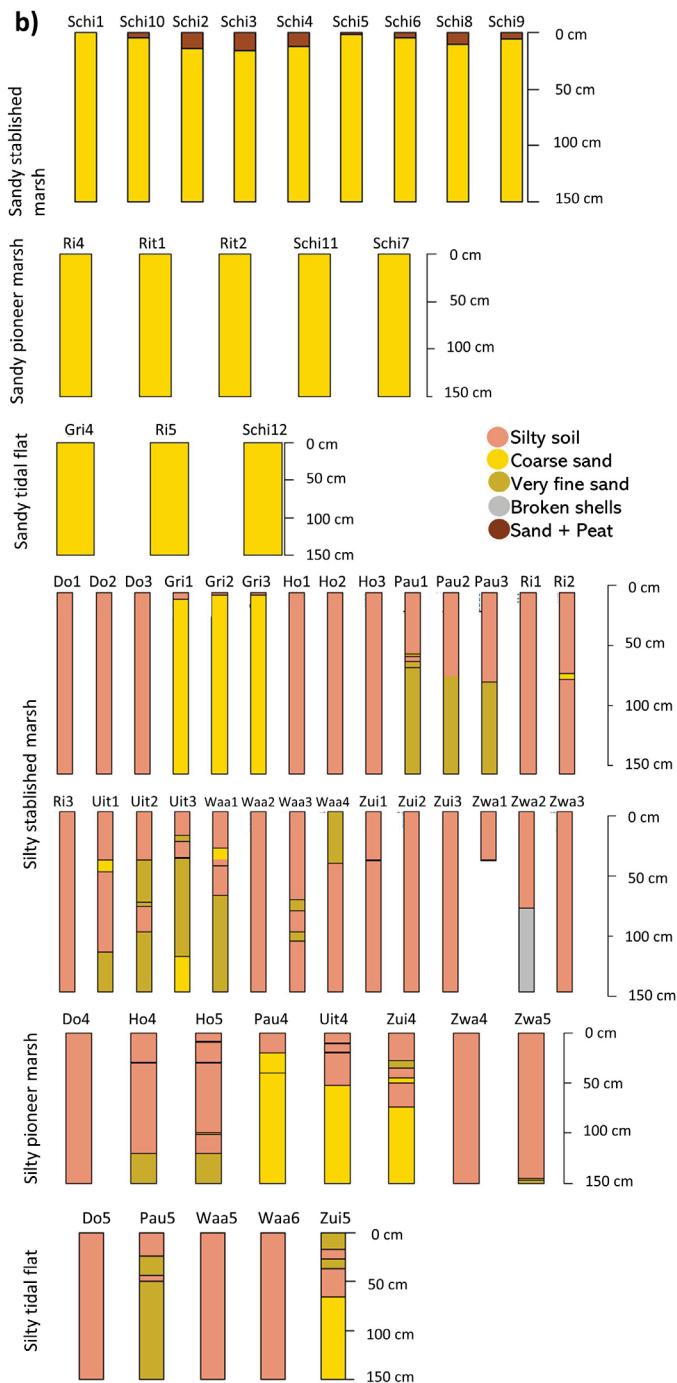


Fig. S9 b) Deep profiles separated by habitat and location

(Schi=Schiermonnikoog, ri=Riland, rit = Ritthem, Gri=Griend, do=Dollard Bay, ho = Holwerd, Pau= Paulina, Uit= Uithuizen, Waa = Waarde, Zui= Zuidgors, Zwa = Zwarte Haan). More details from each location can be found in Table S1.



Chapter 4

Quantifying the resistance to cliff and sheet erosion across vegetation zones in a sandy back-barrier island

Beatriz Marin-Diaz, Valérie C. Reijers, Linda Meijers, Daphne van der Wal,
Han Olff, Tjeerd J. Bouma, Laura L. Govers

Pending submission

ABSTRACT

Small soft-sediment barrier islands are dynamic coastal landscapes that consists of sandy dune barriers at the sea side with silty back-barrier marshes in their wake, and are often of key ecological importance in estuarine landscapes, such as for breeding colonies of seabirds. During storm surges, part of the island may accrete through overwash, while other parts may diminish due to sheet erosion (i.e., erosion of the top surface) and/or cliff retreat (i.e., lateral erosion). Sediment stabilization by dune and saltmarsh vegetation may greatly reduce both erosional processes, and thereby be an important factor for predicting soft-sediment islands resistance to storm surges and thus their long-term persistence. In this study we quantified the erosion resistance to hydraulic forces of a sandy back-barrier island by i) correlating the top and lateral soil erosion resistance to sediment and vegetation properties and ii) relating these properties to the past management and development of the island. Testing soil cores taken over the biogeomorphic gradient from (1) barrier dune-ridge, (2) back-barrier salt marshes to (3) unvegetated tidal flat edges revealed that only the salt marsh was erosion resistant, and that this erosion resistance was different between lateral and topsoil erosion. All marsh samples had a cohesive top layer (due to finer grained sediment, high root density and organic content) that was resistant to top erosion. The resistance to lateral erosion depended on the thickness of this cohesive top layer: thin cohesive layers (< 10 cm) collapsed when the sandy bottom underneath was eroded. Overall, coastal engineering increased the island's soil resistance to erosion, through creating a sand ridge and subsequently sheltered conditions for marsh development. The thickness of the cohesive top layer was related to the historic coastal engineering and island development duration, with the thickest layers found in old marshes that established at low elevations (~ 1.1 m NAP) near the island creek system.

INTRODUCTION

Barrier islands are migrating and dynamic soft-sediment coastal landscapes that accommodate both sandy dune barriers and silty back-barrier marshes in their wake (Oertel 1985). Situated parallel to the mainland coast, these barrier islands can protect the shore from ocean waves and storms, therefore being an important part of flood defences (Cooper et al. 2007; Otvos 2020). These barrier islands are subject to changes during storms and changes in sediment dynamics, sediment supply and sea level rise (Timmons et al. 2010; Conery et al. 2018; Otvos 2020). Main morphological processes during storm surges involve both accretion through overwash, supplying sediments; and erosion, which can be both top and laterally, especially around the island edges (Timmons et al. 2010; Castagno et al. 2018; Conery et al. 2018; Otvos 2020) (Fig. 1). Extreme events are expected to be more common (IPCC 2014). For this reason, barrier islands are becoming increasingly important to protect shorelines from ocean waves, but also becoming increasingly vulnerable in that they may erode and disappear if there is lack of recovery time in between storms (Durán Vinent and Moore 2015; Vinent et al. 2021).

Back-barrier islands or fetch-limited barrier islands are a type of smaller sandy islands that can be found behind the ocean barrier islands, in estuaries or bays (Cooper et al. 2007). In contrast to the ocean barrier islands, back-barrier islands do not often form dunes through aeolian sand transport (Pilkey et al. 2009). Instead, beach or a chenier ridge form on the exposed side during strong storm events depositing shells and beach wrack (Neal et al. 2002; McBride et al. 2007; Pilkey et al. 2009). Their sediment supply is not constant but depends on sediment and coarse materials transported during storms (Nordstrom and Jackson 2012; Castagno et al. 2018) (Fig. 1). Due to the lower exposure to wave energy, the shape and location of back-barrier islands is not only dependent on storms but also on the vegetation growing on them (Cooper et al. 2007; Pilkey et al. 2009). Vegetation may play a key role in stabilizing back-barrier islands by attenuating waves, winds and currents and hence preventing erosion (Pilkey et al. 2009). Coastal vegetation in addition can trap fine sediment, accumulate organic matter and produce belowground biomass (i.e. roots and rhizomes) (e.g. Redfield et al. 1972; Allen 2000; Morris et al. 2002; Cahoon 2006; Marani et al. 2013). In turn, all this properties can make the sediment more cohesive and resistant to erosion (Brown et al. 1995; Gailani et al. 2001; Grabowski et al. 2011). Therefore, soil stability provided by the coastal vegetation (e.g. Coops et al. 1996; Spencer et al. 2016; Lo et al. 2017; Paul and Kerpen 2021, chapter 6) may be an important factor for predicting soft-sediment islands development and resistance to storm surges.

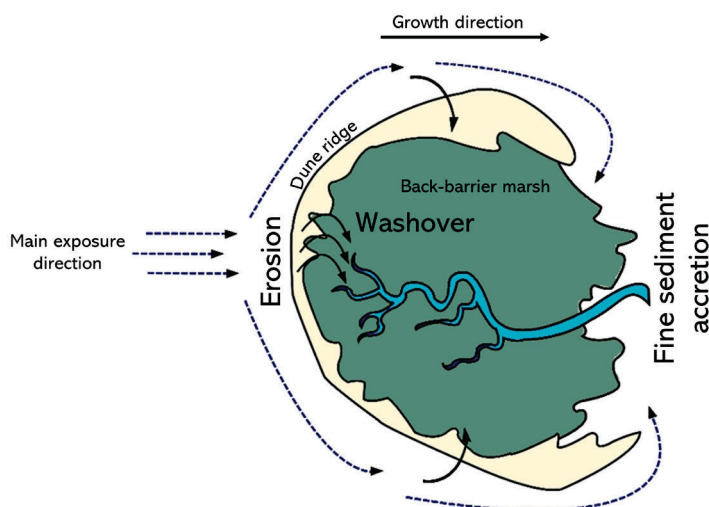


Fig. 1. Processes important for the formation and dynamics of small back-barrier islands. Barrier ridge is eroded during storms on the exposed side while the back-barrier marsh grows during calmer storm conditions. Dashed arrows indicate directions of sediment transport. Illustration modified from Govers and Reijers (2021).

Coastal management measures can affect the development of these islands and hence their stability. For example, sand nourishment strategies on the dune part may also induce marsh formation by creating more sheltered conditions on the wake of the island (Govers and Reijers 2021). This type of management may increase the overall stability of the island ecosystem by promoting the development of sediment-stabilizing marsh vegetation (e.g. Coops et al. 1996; Spencer et al. 2016; Lo et al. 2017; chapter 6). In some cases, this may be a desired effect, as the island ecosystem might otherwise be eroded away altogether which may be undesirable from the perspective of human use or key biodiversity values, such as breeding bird colonies (Piersma et al. 1993; Loonstra et al. 2016). On the other hand, the migration of these type of back-barrier islands is a natural process, in which the dynamics lead to a high habitat heterogeneity. Reducing morphological dynamics due to denser or more stable vegetation may thus affect their ecosystem functioning (Osswald et al. 2019), thereby presenting an enigma for nature management. It is thus important to better understand how different vegetation types affects the stability of these sandy systems, to better understand how to manage them for nature value and being able to potentially integrate them as part of sustainable flood defences.

Several studies on soil erosion resistance to hydrodynamics (i.e. waves and currents) of coastal systems have been carried out with flumes under controlled conditions and in the field (e.g. references in Brooks et al., 2020 and Infantes, Smit, Tamarit, & Bouma, 2021). However, to our knowledge, a simultaneous comparison of lateral and topsoil erosion by water in the sandy systems of barrier islands has not yet been conducted. Sheet erosion (i.e topsoil erosion)

can occur due to increased bed shear stress by currents or waves during storms (Van Rijn 1984a; b; Brown et al. 1995; Ganthy et al. 2015). This process may be important in sandy islands during storm surges or overwash situations (Fig. 1). Lateral erosion, also called cliff erosion, can occur in form of gradual detachment of soil particles from the sediment due to hydraulic pressure from waves or currents at the edge of a cliff (e.g. Feagin et al. 2009; Wang et al. 2017, chapter 6). Lateral erosion can also occur at a larger scale in form of blocks or "mass failure", which can be due to undercutting, normally by wave swash, and the creation of tension cracks (Schwimmer et al. 2001; Francalanci et al. 2013; Priestas et al. 2015). Undercutting occurs at marsh cliffs when the sediment below the cohesive top layer of the marsh starts to erode, and the top layer with roots overhangs until it breaks off and collapses. Lateral erosion may be important during storm surges in zones laterally exposed to waves as in the island margins (Leonardi et al. 2018). Investigating top and lateral erosion simultaneously is important because soil properties can change with depth. This is especially important for sandy marshes, where cohesive top layers can form on initially unstable sand flats during marsh development (Olf et al. 1997, chapter 6). These marshes will have sandy subsoils which are typically non-cohesive and therefore less resistant to erosion than fine-grained soils (Brown et al. 1995). The thickness of these cohesive top layers may depend on both marsh age and elevation. At intermediate/low elevations, the marsh platform is more frequently flooded which facilitates the formation of a thicker cohesive layer (Olf et al. 1997; Van de Koppel et al. 2005). Similarly, thicker cohesive layers can be found in older marshes which had longer time to develop and accrete organic matter and sediment.

Previous top erosion experiments have shown that soils with belowground biomass of dune vegetation, as compared to bare sandy soils, can reduce soil erosion under wave run-up conditions (De Battisti et al. 2020). Similarly, seagrass with dense root mats are able to reduce top erosion even with a very sparse, grazed aboveground canopy (Christianen et al. 2013, chapter 5). In marshes, fine-grained soils, higher organic content and/or high belowground biomass make the soil more resistant to both lateral (Feagin et al. 2009; Ford et al. 2016; Wang et al. 2017, chapter 6) and top erosion (Coops et al. 1996; Spencer et al. 2016, chapter 3), even with the vegetation in winter state (Paul and Kerpen 2021). Moreover higher root density is especially important to reduce erosion in sandy soils, both laterally (Lo et al. 2017; Wang et al. 2017; De Battisti et al. 2019, chapter 6) and in the topsoil, compared to bare tidal flats (chapter 3).

To further understand the relation between factors governing lateral and top erosion by water on managed sandy back-barrier islands, in this study we aimed to *i)* correlate top and lateral erosion resistance to sediment and vegetation properties of different soft-sediment ecosystems of a typical back-barrier sandy island and *ii)* relate this properties to the past management and development of the island.

METHODS

Description of the study site and past management

The study was conducted in Griend, an uninhabited back-barrier island in the Dutch Wadden Sea (53°14'24.97"N, 5°14'53.56"E) (Fig. 2a). The normal tidal range in this area is ~ 190 cm, with spring high water level of ~ 93 cm NAP (Dutch Ordnance level, which is about mean sea level) (RWS 2013). Back-barrier islands are mobile but can disappear due to changes in hydrodynamics and sediment dynamics in the tidal basin (Govers and Reijers 2021). In 1930 a nearby estuary was closed off, resulting in a tidal amplitude change in the surroundings of Griend causing a trend towards gradual disappearance (Brouwer, G et al. 1950). To prevent the complete disappearance of the island, and the consequent loss of its ecosystem functioning, including breeding and roosting habitat for shore birds (Piersma et al. 1993; Loonstra et al. 2016) and pupping ground for grey seals (Brasseur et al. 2015), several large-scale management interventions including various types of breakwaters and dikes took place in the since 1925 (Govers and Reijers 2021). In the 1980s (1985-1988), a 2.5 km long sand dike with a hook shape was constructed on the west and north side of the island (900,000 m³ sand) to prevent erosion. Subsequently, this measure led to marsh development in the sheltered region between the dune ridges which continues growing towards the east (Fig. 2b and S1). In 2016, the western side of the dike had almost disappeared, and a large (200 000 m³) sand nourishment on the western side of the island was carried out, together with the construction of shell ridges (20 000 m³), sod removal to set back vegetation development on the dike/dune and a washover to mimic the natural inundation dynamics of the island (Govers and Reijers 2021). These interventions led to the present island shape with a relatively young marsh (Fig. 2bc and S1).

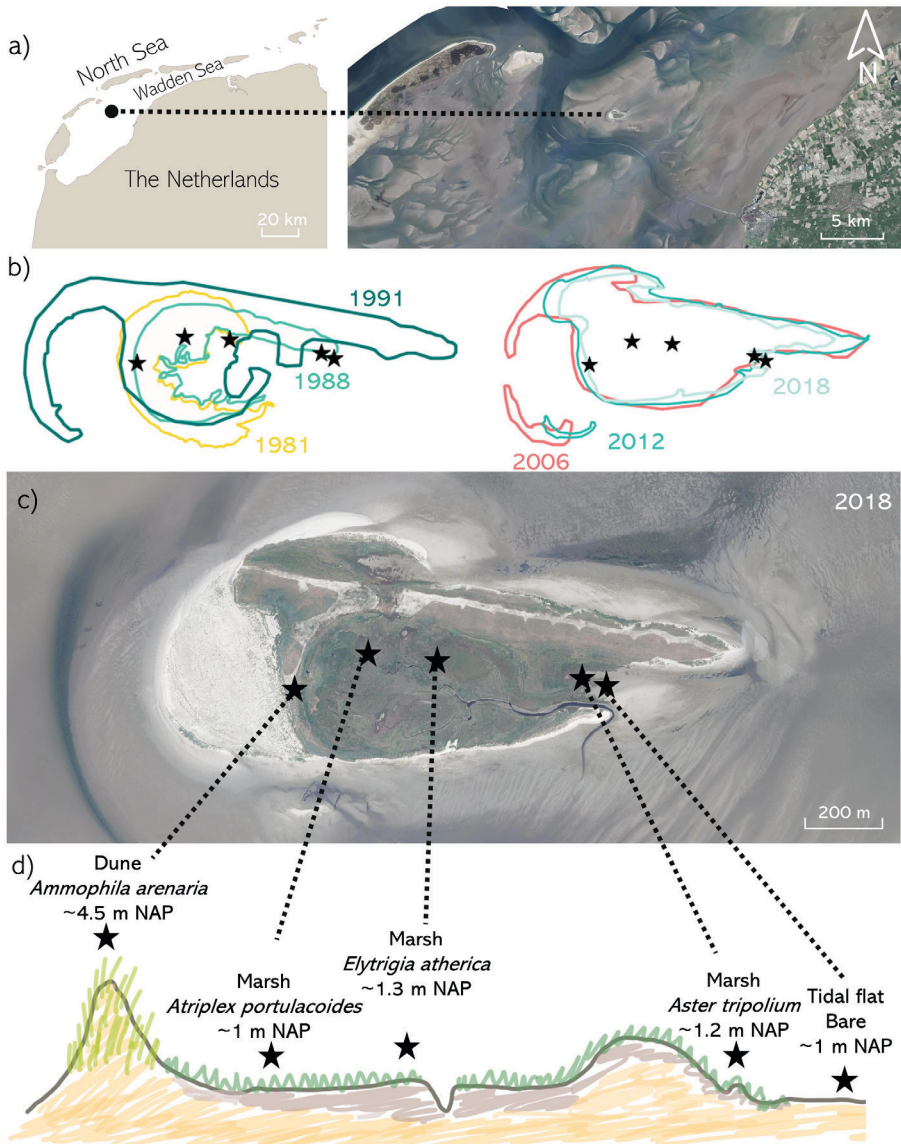


Fig. 2. a) Location of the fetch-limited back-barrier island of Griend, in the Netherlands; b) development of the island after different management actions since 1981, when the salt marsh started to develop. Stars indicate the field locations from this experiment in panel b-d; c) Locations of the sampling sites in Griend and d) Schematic representation of the island profile and the elevation of the sampling sites (NAP is Dutch Ordnance level, which is about mean sea level). Photographs were obtained from PDOK (Public Geodata Portal in The Netherlands).

Top and lateral erosion

Soil cores were collected in five locations along a cross section of the island to test the lateral and top erosion with different vegetation and soil types. From west to east, three replicates for

SOIL EROSION OF A BACK-BARRIER ISLAND

top erosion and three replicates for the lateral erosion were collected on each sampling location (Fig. 2): in the dunes dominated by *Ammophila arenaria* (~ 4.5 m NAP) followed by the oldest marsh dominated by *Atriplex portulacoides* (~ 1 m NAP), marsh dominated by *Elytrigia atherica* (~ 1.3 m NAP), marsh dominated by *Aster tripolium* (~ 1.2 m NAP) and finally, bare tidal flat (~ 1 m NAP). The elevation of each sampling site was measured with an rtk-dGPS (Leica GS12). All soil cores were transported to the Royal Netherlands Institute for Sea Research (NIOZ) in Yerseke and stored in tanks with seawater from the Oosterschelde estuary until the erosion test during one week.

Samples for the top erosion consisted of rectangular soil cores of 40 cm long x 20 cm high x 12 cm width, as in (chapter 3). The cores were extracted with a custom-made steel box core and placed into a customized wooden box which fitted in the flow flume. The soil cores were then cut to 32 cm long, and the remaining part was utilised to analyse the belowground vegetation properties. Aboveground vegetation was clipped before the erosion test. Top erosion was determined by exposing the top soil of the cores to water flows of 2.3 m s^{-1} in a fast flow flume as in (chapter 3). Top erosion was determined after 10 minutes, 1h, 2h and 3h as the average change in elevation measured with a calibrated stick in a spatial grid of 3 cm in the axis parallel to the flow and 3.7 cm in the axis cross-stream, with a 1 mm vertical resolution. The erosion after 10 minutes was subtracted from the total mean erosion after 3h in the samples that remained stable to avoid bias in the results due to differences in the vegetal debris surface layer, which differed between cores.

Cores for the lateral erosion measurements were collected next to each top erosion core. These samples consisted of round soil cores of 15 cm diameter and 20 cm depth collected by inserting PVC pipes in the soil and carefully digging them out as in chapter 6. Lateral erosion was determined in four wave flumes of 360 cm long x 90 cm high x 82 cm wide as in Lo et al. (2017), Wang et al. (2017) and chapter 6. The same settings of ~ 8 cm wave height with swash intersecting the whole core were used as in Lo et al. (2017) and chapter 6. The cores were transferred into metal cores with 12 cm width opening in the longitudinal side. The exposed side was cleanly sliced and adjusted to 15 cm height. Lateral erosion was determined after 10 min, 1, 2, 4, 8, 24, 32 and 45 h of wave exposure. Cores with readily erodible sandy bottom collapsed after the 10 minutes, and only oldest marsh cores dominated by *Atriplex* resisted for the entire 45 h. Erosion (% of volume eroded) was determined by photogrammetry (structure from motion) technique developed by (Nieuwhof et al. 2015) and applied by Lo et al. (2017), Wang et al. (2017) and chapter 6.

Belowground vegetation properties

Belowground biomass from the 8 x 20 x 10 cm subsample of the top soil erosion core was cleaned over a 1 mm sieve and separated into roots and rhizomes as in chapter 6. This biomass was representative for both top and lateral core samples. A representative subsample of rhizomes, coarse roots (> 0.5 mm Ø) and fine roots (< 0.5 mm Ø) were separated from each sample to extrapolate the biomass of each compartment to the whole sample. Fine roots

included some fine dead root material that could not be distinguished and removed (cf. De Battisti; chapter 6). Biomass was obtained by drying the samples and subsamples at 60 °C until constant weight. Densities for each compartment were calculated as the biomass by the volume of the soil sample (g cm^{-3}).

Sediment properties

Soil properties were obtained by taking additional smaller cores of 2.2 cm Ø and 20 cm depth next to each set of erosion cores. In the case of marshes, a cohesive topsoil layer is present in top of sandy subsoils. The thickness of this cohesive topsoil layer was measured up to 20 cm. Soil samples were obtained from the 5 first cm of soil and from the sandy bottom up to 20 cm. For marsh cores with cohesive layer thickness thinner than 5 cm, the soil sample was collected until the start of the sandy layer to obtain the properties of the cohesive top layer separated from the sandy subsoil. The sediment samples were weighed and freeze dried during four days. Water content was calculated as the difference between wet and dry weight. Bulk density was calculated as the dry weight in a known volume (g cm^{-3}). Soil organic content was measured by loss on ignition method after burning the sediment for 6 h at 450 °C. Thick rhizomes were previously removed to avoid biases in the soil organic content. Sediment grain size was determined using a Malvern ® Mastersizer 2000. Lastly, a simple and fast field-applicable method adapted from Howison et al. (2015) and hereafter referred to as dynamic soil deformation test was measured as in chapter 3. This method consisted of releasing a 5 kg metal weight of 10 cm Ø 10 times from 1.5 m height through a guiding PVC pipe and gives an idea of the porosity and ease of deformability of the soil. The distance between the soil surface and the bottom of the compacted soil (cm) was used as the dynamic soil deformation value. To further explore the depth of the cohesive top layer on the island, thickness of the cohesive topsoil layer was measured at 10 extra locations along the cross section of the island, and 4 perpendicular to the main transect.

Statistical analysis

We used one-way ANOVA to test the differences of top erosion between soil cores that resist to the flow exposure followed by a Tukey's HSD post hoc test. Assumptions of normality of residuals and homogeneity of variance were tested. The dependence of the probability of complete top erosion and complete lateral erosion on vegetation and soil properties were modelled using a logistic regression, performed with bayesian GLMs with binomial distribution, using the package *arm*. Bayesian GLM was performed to deal with the complete separation in the logistic regressions, which can occur when the predictor is perfectly predictive of the outcome (Gelman et al. 2008). Dependence of mean top erosion depth on vegetation and soil properties were modelled with GLMs assuming a gamma distribution as the response variable contained only positive continuous values. All statistical analyses were performed using R 3.5.0 (R Development Core Team 2018).

RESULTS

Top and lateral erosion

All marsh locations (marsh- *Atriplex*, *-Elytrigia*, *-Aster*) were resistant to top erosion, independently of the cohesive top layer thickness (Fig. 3a). Top erosion resistance did not differ significantly among locations (one-way ANOVA: $F_{2,6} = 0.14$, $p > 0.05$) (Fig. 3b). However, when a physical disturbance was artificially created that reached into the sandy bottom of the cores, even resistant cores collapsed. In contrast, both dunes and mudflats were completely eroded in the first 5 minutes (Fig. S2).

Regarding lateral erosion, only the marsh *-Atriplex* site, with the thickest cohesive layer (> 15 cm) resisted, with 1 – 18 % of erosion after 45 h of wave exposure (Fig. 3c). Marsh with *Elytrigia* and *Aster*, with thinner cohesive layers (< 10 cm), collapsed when the sand below was eroded, although the cohesive top layer remained resistant to erosion when left under the wave exposure. Similar to top-erosion, dune and mudflat cores were completely eroded in the first 5 minutes after exposure to waves in the flume.

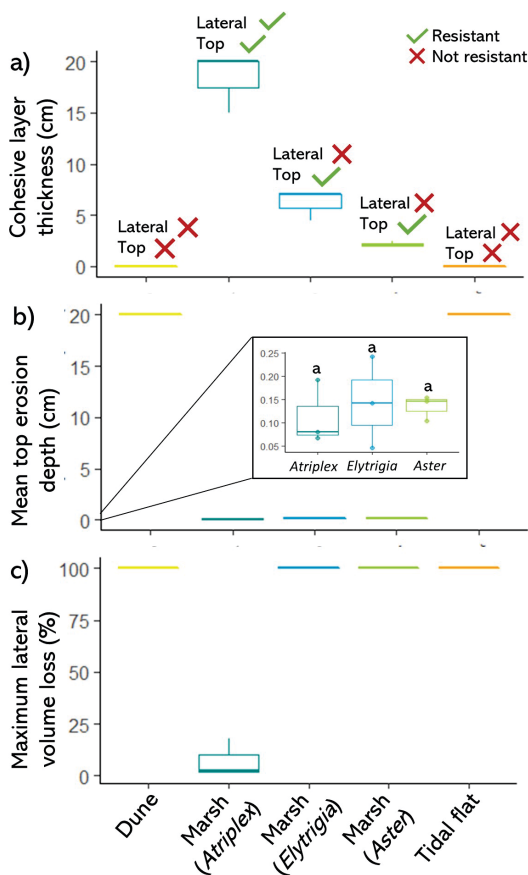


Fig. 3. a) Cohesive layer thickness at the different locations and its relation with top and lateral erosion. Not resistant refers to the collapse of the cohesive top layer in marsh samples after the erosion of the sandy subsoil or due to the 100 % soil erosion in dune and tidal flat cores; b) top erosion measured as the mean erosion depth, where 20 cm is complete erosion. In the subplot, letters depict non-significant differences between resistant locations (Tukey HSD, $p > 0.05$) and c) lateral erosion quantified as the percentage of volume loss.

Soil and vegetation properties in relation to island morphology

Marsh cores were characterized by a cohesive layer on top of a sandy bottom layer, compared to the dune and the bare tidal flat, where the complete profile was sandy (Fig. 3a and 4). Cohesive layer thickness varied across the island, being the thickest (up to 20 cm) in the oldest marsh (> 56 yr old) with *Atriplex* (Fig. 4). The thickness could be related to the elevation and age of each zone. Older and lower elevated (~ 1.1 m NAP) areas connected to the channel, like in the western and oldest part of the marsh, had the thickest cohesive sediment layer (~ 20 cm) (Fig. 4). More elevated areas (~ 1.4 to 1.9 m NAP) towards the east, had thinner cohesive layers (~ 7 to 2 cm). Finally, young marshes in the east (~ 28 yr), not connected to creeks and near the tidal flat had thin cohesive layers (~ 2 cm) although being low elevated (~ 1.1 m) (Fig. 4).

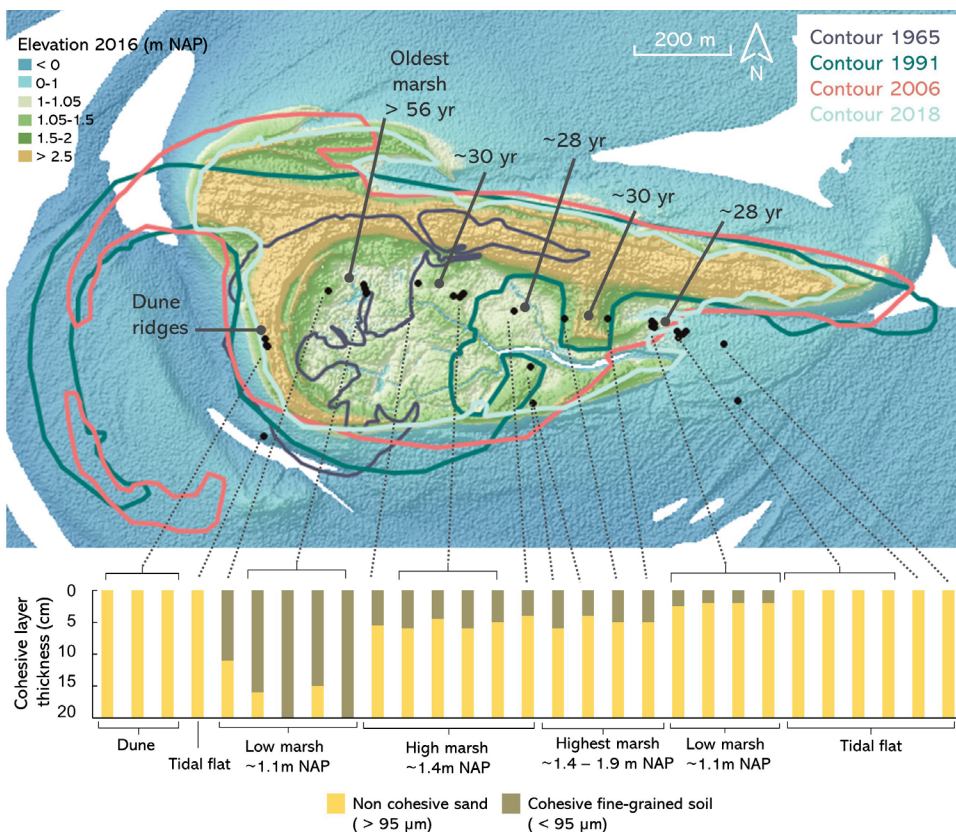


Fig. 4. Map showing the elevation of the island in 2016, with the newest elevation map to date (source Rijkswaterstaat, 2 m resolution). The bar plot below indicates the soil profile up to 20 cm depth and the thickness of the cohesive top layer (cm, in brown) measured at different locations across the island (indicated by black dots in the map). Contour lines of the island from 1965, 1991, 2006 and 2018 are shown as a reference for the indicated age of the marsh areas.

SOIL EROSION OF A BACK-BARRIER ISLAND

The cohesive layer consisted of smaller grain size ($< 95 \mu\text{m}$), higher organic content ($> 10\%$), higher soil water content ($> 40\%$) and lower bulk density ($< 1 \text{ g m}^{-3}$) than the sandy soils found in the bottom layer and in the dune and tidal flat locations (Fig. 5a and S3). Belowground biomass was higher ($> 0.1 \text{ g cm}^{-2}$) in the marsh cores compared to the dune cores, especially the marsh area dominated by *Aster*, followed by *Atriplex* and lastly *Elytrigia* (Fig. 5a and S3). Dune cores with *Ammophila* were characterized by lower belowground biomass ($< 0.1 \text{ g cm}^{-2}$), organic ($\sim 0.1\%$) and water content ($\sim 4\%$) compared to the marsh cores. Tidal flat cores did not have any vegetation at all.

Relationships between environmental factors, top erosion and lateral erosion

Resistance to top erosion was correlated to both the biotic and abiotic properties of the top layer (from 0 to 5 cm depth) (Fig. 5a). Finer sediment ($< 95 \mu\text{m}$), higher total belowground biomass ($> 0.1 \text{ g cm}^{-2}$), higher root density ($> 0.005 \text{ g cm}^{-3}$), especially fine root density ($> 0.005 \text{ g cm}^{-3}$), higher organic content ($> 10\%$) and lower bulk density ($< 1 \text{ g cm}^{-3}$) were correlated to higher top erosion resistance. Moreover, many of these variables were strongly correlated (Fig. S4). Coarse root density and soil dynamic deformation were the only variables not correlated to erosion. Within the resistant marsh cores, none of the vegetation nor soil properties significantly explained the small differences in top erosion between cores (Fig. 3b and S5).

Lateral erosion was also explained by the same explanatory variables as top erosion (Fig. 5b). However, we could not explore correlations between lateral erosion and soil and vegetation properties due to low sample sizes ($n=3$). In contrast to top erosion, cohesive sediment layer thickness was the most important driver for lateral erosion resistance (Fig. 3a).

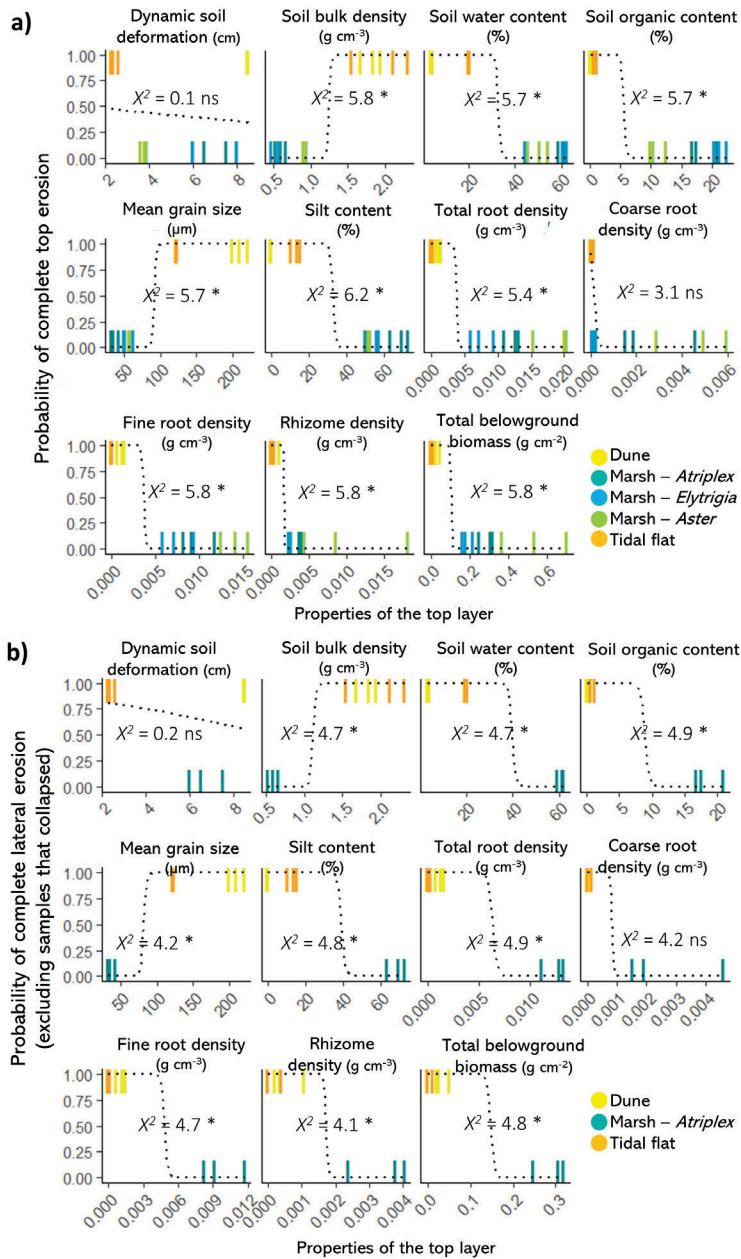


Fig. 5. Relationships between a) top erosion and soil and vegetation properties, with erosion treated as binomial (resistant core or completely eroded) and b) lateral erosion and soil and vegetation properties including cores that either completely eroded (dune and tidal flat) or resisted (marsh with *Atriplex*), but excluding cores that collapsed due to thin cohesive layers. Coefficients correspond to logistic regressions. Significance codes refer to $p < 0.01$ (*) and $p > 0.05$ (ns).

DISCUSSION

Soft-sediment island systems may be threatened by increasing storm surges and sea level rise as a result of climate change. We therefore studied how erosion resistance to hydraulic forces of sandy island habitats (dunes, 3 marsh habitats and tidal flats) was i) affected by sediment and vegetation properties and ii) linked to past management and island development. By assessing top and lateral soil erosion resistance simultaneously, we found that erosion resistance is mainly determined by the thickness of the cohesive sediment layer that is accreted by marsh vegetation. Furthermore, the accretion of this cohesive sediment layer was linked to past and present management interventions on the island.

Erodibility of soft-sediment systems in a managed back-barrier island

We found that marshes were the most resistant system due to the cohesive top layer accreted and composed of higher belowground biomass ($> 0.1 \text{ g cm}^{-2}$), more specifically fine root density ($> 0.005 \text{ g cm}^{-3}$), higher organic content ($> 10 \%$), lower bulk density ($< 1 \text{ g cm}^{-3}$) and higher silt content ($> 40 \%$) compared to the easily erodible sandy soils in the dune and tidal flat (Brown et al. 1995; Gailani et al. 2001; Grabowski et al. 2011). These properties have been previously related to increase the erosion resistance of marsh soils, both top (Coops et al. 1996; Spencer et al. 2016; Paul and Kerpen 2021, chapter 3) and laterally (Feagin et al. 2009; Ford et al. 2016; Wang et al. 2017; De Battisti et al. 2019; chapter 6). Although the percentage of lateral erosion was not measured for marsh *-Elytrigia* and marsh *-Aster* cores due to the collapse, we speculate that the cohesive layer, with similar properties than marsh *-Atriplex* (Fig. 5a), would have also been erosion resistant (Lo et al. 2017; Wang et al. 2017; chapter 6).

Regarding the grain size, our results show that more resistance to erosion is related to finer sediments ($< 95 \mu\text{m}$), and vice versa, coarse sediment to more erosion. However, in a previous study we found that grain size alone it is not a good erosion indicator because there are marshes with coarse sandy soils which are resistant to top erosion as a result of having high belowground biomass and organic content (chapter 3). Therefore, we argue that the main drivers that could be used in the field as a proxy of the erosion resistance are the belowground biomass, specially the fine roots, the soil organic content and more importantly, the thickness of this cohesive layer (chapter 3 and 6).

Battisti et al. (2020) show that belowground biomass from dune vegetation reduced the erosion compared to bare sand, while in our study we did not find any effect of dune vegetation on erosion resistance. This difference may be explained by a much longer exposure time in our study. While Battisti et al. (2020) exposed samples to 6 consecutive swashes, in our study we exposed the cores for minimum 10 minutes (> 150 swashes). Nevertheless, although not quantified, we also observed a resistance to erosion with *Ammophila* roots during the first swashes compared to the bare tidal flat. During a storm surge we expect that sandy soil with

low root density would likely be eroded and deposited in other areas (Cooper et al. 2007; Engelstad et al. 2018; Vinent et al. 2021). However, the role of dune vegetation may be more important on reducing aeolian erosion (Feagin et al. 2015), a factor that we did not study here. The resistance to lateral erosion may be more important in the marsh area as marshes may act as an anchor for the sand ridges or dunes of the island (Cooper 2013).

Back-barrier island development and management implications

Our results show that through soft-structure coastal engineering, such as the suppletion of sand to prevent dune erosion and simultaneously creating sheltered conditions for facilitating marsh development, fetch-limited back-barrier islands like Griend can indeed be stabilised. This stabilisation occurred thanks to the accretion of a cohesive erosion-resistant top layer by the marsh vegetation. Management measures can interfere with the natural development of these type of islands, which are known to be migratory. However, if the island is predicted to be eroded like Griend, such measures may guarantee its persistence and therefore the persistence of its linked ecosystem services including habitat for several endangered bird species and breeding areas for seals (Piersma et al. 1993; Brasseur et al. 2015; Govers and Reijers 2021).

The variability in cohesive layer thickness in the back-barrier island of Griend was (very likely) linked to marsh age and inundation time (bathymetry). With increasing marsh age, marshes had more time to trap fine sediment and accumulate more belowground biomass and organic content (Olf et al. 1997; Van de Koppel et al. 2005). Similarly, if marshes establish at intermediate elevation (~ 1.1 m NAP in our study site), they will be more frequently flooded and therefore have more opportunities to trap sediment than marsh vegetation that establish at higher elevations (> 1.4 m NAP in our study site). In agreement with Van de Koppel et al. (2005), our results also show that if elevation gets too low near the tidal flats, this sedimentation process is lower again. Furthermore, the thickness of the cohesive layer may vary depending on if the marsh is well drained and has enough sediment input (Reed et al. 1999; Koppenaar et al. 2021). For instance, in our study, the lower elevated areas connected to flood plains from a creek (i.e. marsh – *Atriplex*) have been related to deeper cohesive layers. If a marsh loses the natural creeks and no drainage arrives to the back, sediment supply may be reduced and thus the cohesive layers may not become as thick as in a more frequently flooded area.

The future marsh accretion will also depend on if there is enough sediment supply to keep pace with sea level rise (e.g. Timmons et al. 2010; Kirwan et al. 2016; Ladd et al. 2019; Hu et al. 2021). Furthermore, in case of extreme storms, the dunes or chenier ridges could also migrate on top of the marsh transported by hydraulic forces (Cooper 2013). Therefore, enough sediment supply and having windows of opportunity for new marsh establishment (Hu et al. 2015, 2021) become even more important for the marsh to keep up with the dune migration and sea level rise. Constructing areas with lower elevations in the dune or sand ridge to promote washovers and prevent the complete reduction of the island dynamics, may also be an important management to improve the sediment input during storm surges (Timmons et al.

2010). Finally, if erosion caused by wave action during storm surges occurs too frequently for the vegetation and soil to recover and develop, island erosion will be fast and extensive as the recovery time will be too short (Timmons et al. 2010; Cooper 2013; Durán Vinent and Moore 2015; Vinent et al. 2021). Therefore, management strategies that increase this recovery time by fortifying the dune barrier may enhance soil stability in the back barrier marsh thereby reducing island erosion. Simultaneously, complete dune and/or island fixation should be avoided as it may make the island less able to adapt to sea level rise as well as having negative impacts on biodiversity (Arens et al. 2013; Osswald et al. 2019).

Overall, sand-island management aimed at enhancing soil stability provided by coastal vegetation may be important to support future-proof, storm-surge resistant sandy islands and their associated ecological communities. However, this study also highlights the importance of taking into account both lateral and top erosion in sandy systems. While marshes may be resistant to top erosion, which could be important for example during overwash, they may be vulnerable to wave attack in the island edges if the cohesive top layer is thin. Finally, in addition to creating more erosion resistant soils, further protection is also expected to be provided by the wave or current attenuating effect of the vegetation canopy (Bouma et al. 2014; Leonardi et al. 2018; Feagin et al. 2019; Türker et al. 2019).

ACKNOWLEDGEMENTS

This work is part of the Perspectief research programme All-Risk with project number P15-21 project B1 which is (partly) financed by NWO Domain Applied and Engineering Sciences, in collaboration with the following private and public partners: the Dutch Ministry of Infrastructure and Water Management (RWS), Deltares, STOWA, the regional water authority Noorderzijlvest, the regional water authority Vechtstromen, it Fryske Gea, HKV consultants, Natuurmonumenten, waterboard HHNK. LLG was funded by NWO VENI grant 016.Veni.181.087. In addition, we would like to thank Lennart van IJzerloo from the NIOZ for technical assistance, Jantsje van Loon-Steensma from the University of Wageningen for supporting L.M. and to Sien and Saar Niermeijer and Jouke van der Meilen who have hosted us on the Ambulant. The authors declare no conflict of interest.

SUPPORTING INFORMATION

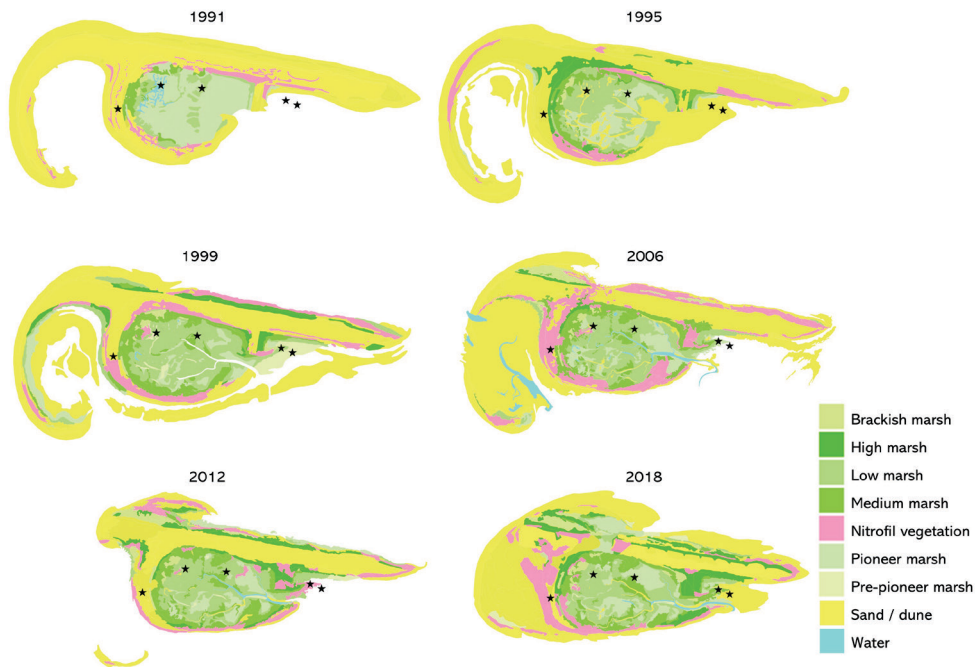


Fig. S1. Island and habitats evolution over the years in Griend. Stars indicate the sampling locations. Polygon maps were obtained from Rijkswaterstaat.

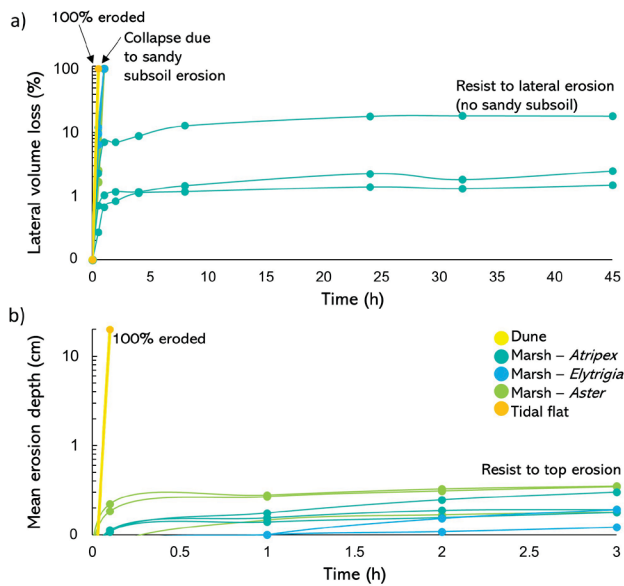


Fig. S2. a) Lateral erosion under wave exposure over time, quantified as volume loss (%); and b) Top erosion under fast water flow exposure over time, quantified as erosion depth (cm).

SOIL EROSION OF A BACK-BARRIER ISLAND

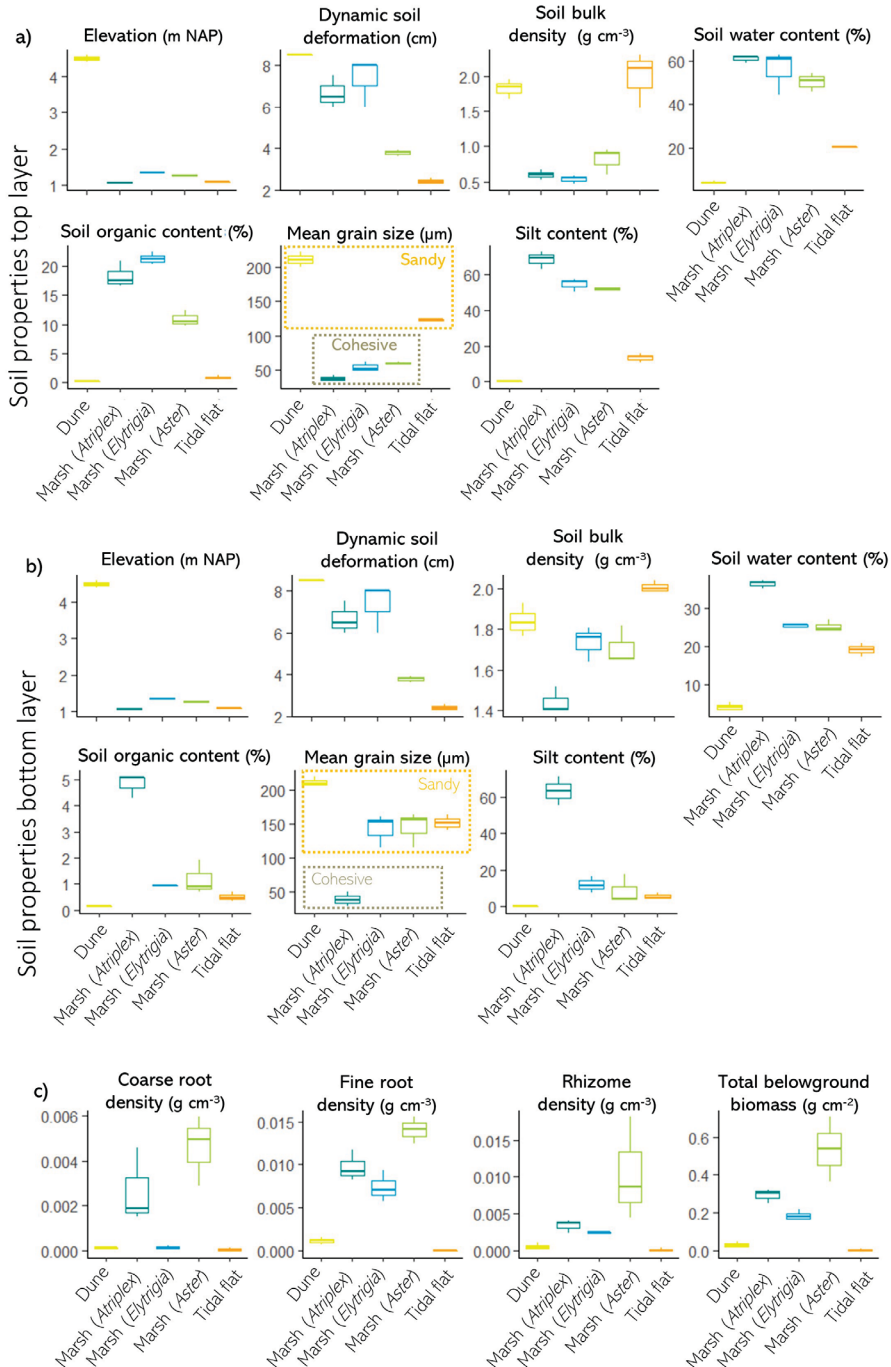
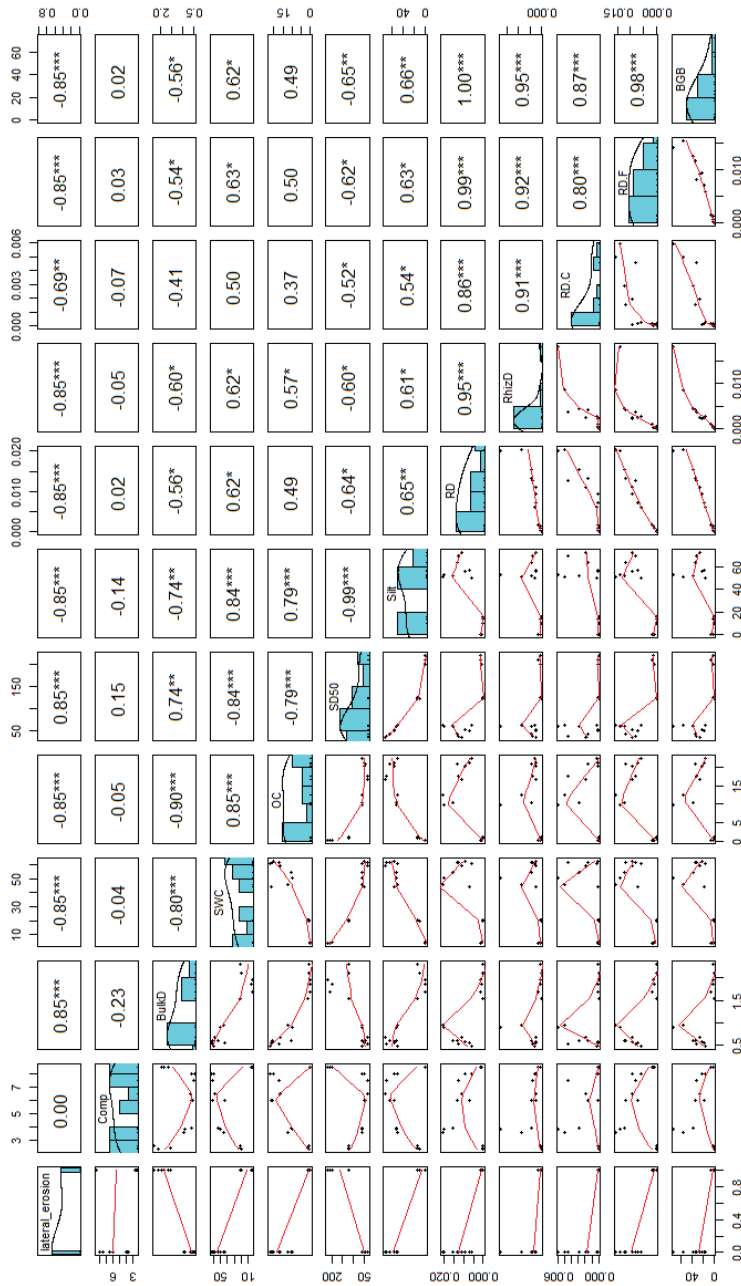


Fig. S3. a) Soil properties from the top layer for each location (0-5 cm depth, or to the start of the sandy subsoil in marsh-Aster (~2 cm); b) soil properties from the bottom layer; and c) vegetation belowground properties from soil samples until 20 cm depth.

Fig. S4. Spearman correlation matrix showing the relationships among the environmental variables. Comp = dynamic soil deformation (cm), BulkD = Bulk density (g cm⁻³), SWC = Soil water content (%), OC = Soil organic content (%), SD50 = mean grain size (μm), Silt = silt %, RD = total root density (g cm⁻³), RhizD = Rhizome density (g cm⁻³), RD.C = coarse root density (g cm⁻³), RD.F = fine root density (g cm⁻³), BGB = belowground biomass (roots + rhizomes) (g).



SOIL EROSION OF A BACK-BARRIER ISLAND

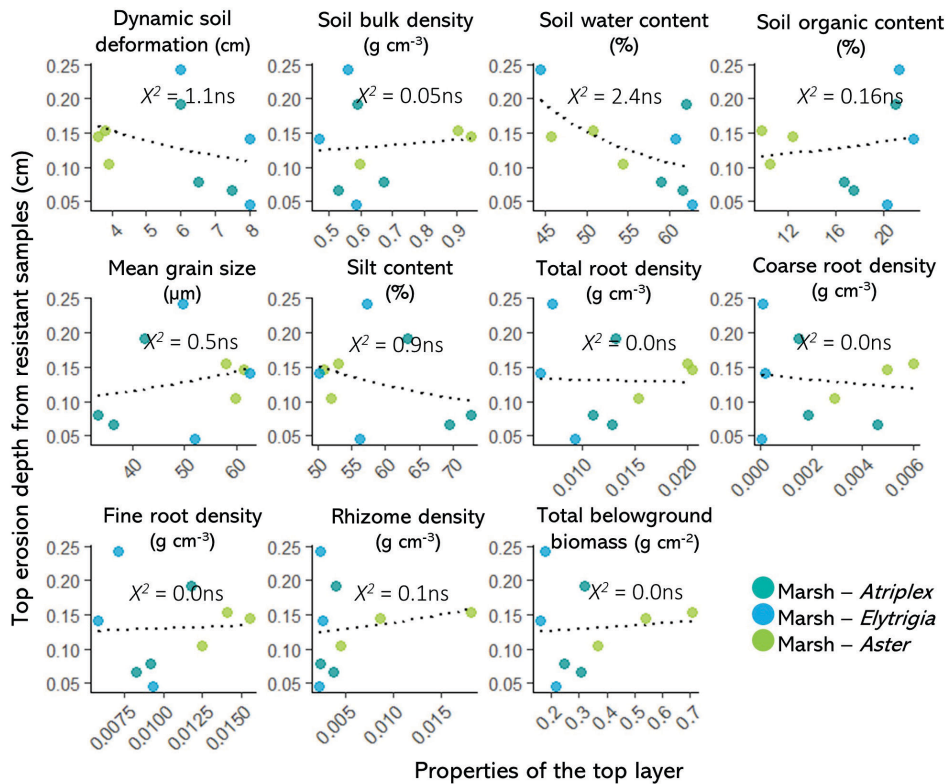


Fig. S5. Relationships between top erosion and soil and vegetation properties only including cores that resisted the waterflow exposure (marsh with *Atriplex*, *Elytrigia* and *Aster*). Coefficients correspond to gamma correlations. Significance codes refer to $p > 0.05$ (ns).



Chapter 5

Role of eelgrass on bed-load transport and sediment resuspension under oscillatory flow

Beatriz Marin-Diaz, Tjeerd J. Bouma, Eduardo Infantes

Limnology and Oceanography (2020) 65(2): 426-436

ABSTRACT

Coastal vegetation is widely attributed to stabilize sediment. While most studies focused on how canopy causes flow reduction and thereby affect sediment dynamics, the role of roots and rhizomes on stabilizing the surface sediment has been less well studied. This study aims to quantify interactions between above and belowground biomass of eelgrass (i.e. living *Zostera marina* plants and mimics) with surface sediment erosion (i.e. bedload and suspended load), under different hydrodynamic forcing that was created using a wave flume. Belowground biomass played an important role preventing bedload erosion, by roughly halving the amount of sediment transported after being exposed to maximal orbital velocities of 27 cm s^{-1} , with and without canopy. Surprisingly, for suspended sediment transport, we found opposite effects. In the presence of eelgrass, the critical erosion threshold started at lower velocities than on bare sediment, including sand and mud treatments. Moreover, in muddy systems, such resuspension reduced the light level below the minimum requirement of *Z. marina*. This surprising result for sediment resuspension was ascribed to a too small eelgrass patch for reducing waves but rather showing enhanced turbulence and scouring at meadow edges. Overall, we conclude that the conservation of the existent eelgrass meadows with developed roots and rhizomes is important for the sediment stabilization and the meadow scale should be taken into account to decrease sediment resuspension.

INTRODUCTION

Coastal vegetation provide a broad range of ecosystem services such as nutrient cycling, support for global fisheries, improvement of the water quality and carbon sequestration (Orth et al. 2006; Gedan et al. 2009; McLeod et al. 2011). In the face of global change, there is a growing interest in the role of mangroves, salt marshes and seagrass meadows in coastal protection (Temmerman et al. 2013; Bouma et al. 2014; Narayan et al. 2016). Coastal protection by vegetation is provided either by the standing biomass and/or by a reduction of the sediment erosion leading to an enhancement of higher foreshores, both related to wave attenuation (Bouma et al. 2014; Möller et al. 2014; Gracia et al. 2018). In this context, an in depth mechanistic understanding of the role of coastal vegetation on reducing sediment erosion is pivotal for making predictions in the future, where the frequency and magnitude of extreme sea levels is predicted to increase (Menéndez and Woodworth 2010; Vousdoukas et al. 2018).

Sediment erosion from the surface layer can be caused by the initiation of horizontal sediment transport (i.e., bedload) or by sediment resuspension (i.e., suspended load) (Einstein et al. 1940; Brown et al. 1995). Bedload occurs when sediment particles move along the bottom horizontally by rolling whereas sediment resuspension occurs when the sediment particles are lifted vertically into the water column creating turbidity and reducing the light (Einstein et al. 1940; Brown et al. 1995). Erosion of sediment with grain size smaller than 62.5 μm (mud) can be quantified as turbidity because these sediment particles are carried directly to the suspended load (Aberle et al. 2004). In contrast, sediment with particles larger than 62.5 μm (sand) will have bedload phase and should not be quantified only as turbidity (Aberle et al. 2004).

Several studies indicate that coastal vegetation may reduce erosion both on bed load form and resuspension (Ward et al. 1984; Christianen et al. 2013; Spencer et al. 2016), which is normally attributed to a reduction of the hydrodynamics within the canopy (Bos et al. 2007; Infantes et al. 2012; Möller et al. 2014). The reduction of the sediment erosion is important to maintain the water clarity, necessary for seagrass development (Dennison 1987; Duarte 1991), and to retain the sediment in coastal areas (Christianen et al. 2013; Ganthly et al. 2015; Spencer et al. 2016). Whereas a lot of work has focussed on the aboveground plant-flow interactions, the effect of belowground biomass (rhizomes and roots) on the sediment stabilization is still relatively poorly studied. The latter is especially true for seagrasses, despite of them being present in many coastal systems.

Reduction of erosion by belowground biomass has been previously assessed in terrestrial and saltmarsh plants (Baets et al. 2007; Feagin et al. 2009; Wang et al. 2017). For example, two types of erosion are common in coastal ecosystems: *i*) lateral cliff-erosion, which occur at the front of the (cliffed) saltmarsh, or in the edges of vegetation patches, and leads to narrowing of the marsh (Bouma et al. 2009b; Lo et al. 2017; Wang et al. 2017), and *ii*) horizontal surface-erosion, which is the gradual erosion of sediment particles from the surface layer in

between the plants, caused by the bed shear stress (Brown et al. 1995; Ganthly et al. 2015). Lateral cliff-erosion of saltmarshes seems to be controlled by the sediment type and root biomass at small scale (Feagin et al. 2009; Wang et al. 2017), and is outside the scope of the present study, as we focus on horizontal surface-erosion. In the case of seagrass, rhizomes and roots seem to play a major role in sediment stability (Christianen et al. 2013), but to the best of our knowledge, there are no mechanistic studies that directly quantify the effect of belowground biomass on surface-erosion. Similar to saltmarsh vegetation, we expect the effect of the seagrass belowground biomass on sediment stabilization to interact with other factors as the sediment properties and wave energy (Widdows et al. 2008; Feagin et al. 2009; Wang et al. 2017).

This study aims to *i*) quantify how much surface-erosion in the form of both suspended load and bedload transport are affected by the presence of eelgrass and *ii*) quantify the relative effect of aboveground and belowground biomass, sediment type and wave conditions on surface-erosion. To answer these questions, we carried out a flume experiment in which we used both artificial and natural eelgrass on muddy and sandy sediment, by applying a range of wave orbital velocities.

METHODS

Eelgrass and sediment collection

Eelgrass samples with intact sediment were collected from the field to keep the sediment properties, above-ground and below-ground biomass undisturbed. Samples were collected in Bokevik bay in the Gullmars Fjord, Sweden (58°14'N, 11°26'E). Sediment with eelgrass was collected between 1.5 – 10 m depth to cover a range of sediment types, eelgrass densities and morphologies. Samples from 3-10 m depth were taken with a 0.35 x 0.35 m box-core from a vessel and placed into custom-made trays of 0.35 x 0.35 m (Dahl et al. 2018). The trays with the sediment were transported in PVC boxes to protect the sediment from tilting. Samples from shallow sites (1.5 m) were taken with cores of 12 cm diameter using scuba or snorkelling because the vessel with the box-core could not reach the shallow waters. The sediment thickness collected varied from 5 to 10 cm depending on the sediment compactness. To maintain the plants in optimal conditions until the hydrodynamic experiments, the sediment trays and cores were stored in shallow-water flow-through 1500 L outdoor tanks at the Sven Lovén Centre for Marine Infrastructure, Kristineberg.

Wave flume

The study was conducted in a hydraulic wave flume developed and constructed at the Netherlands Institute for Sea Research (NIOZ) and located at Kristineberg Marine Research Station (Fig. 1a). The wave flume was 3.5 m long, 0.6 m wide and 0.8 m high (Fig. 1b). Waves were generated with a pneumatic piston and damped with a wave absorber made of synthetic

fibre with a slope of 20°. The test section was composed of a PVC box of 0.35 x 0.35 x 0.15 m (length x width x height). The sediment trays were carefully inserted in the test section and adjusted in order to be at the same level as the flume bottom (Fig. 1a). In the case of the samples from shallow sites, 5 cores were carefully inserted together to fill the test section and one additional core was sliced to fill any remaining gap, producing a continuous bed of minimal disturbed sediment. The flume was filled with seawater until 25 cm depth. For each sediment sample, orbital flow velocities were increased stepwise from 2 to 27 cm s⁻¹, with each time step maintained during 8 min (56 minutes of wave exposure in total) (Table S1). These conditions represent similar wave exposures in shallow bays where eelgrass is present in the Swedish west coast (Infantes, unpublished data). Waves were measured next to the sample box with a pressure sensor (Druck, PT1830) and sampling rate of 25 Hz. Wave height (H) was calculated from the pressure data as,

$$H = 2 * \sqrt{\frac{\sum_{i=0}^n P_i^2}{n}} * \sqrt{2} \quad [1]$$

where P is the pressure data.

Flow velocities were measured with an acoustic Doppler velocimeter, ADV (Nortek, Vectrino) at 10 cm above the bottom and 5 cm in front of the test section to not interfere with the canopy. The sampling rate was 25 Hz, sampling volume of 7 mm, and velocity range of 0.3 m s⁻¹. Mean orbital velocities (U_{rms} , cm s⁻¹) were calculated as,

$$U_{rms} = \sqrt{\frac{1}{N} \sum_{i=1}^n (u_i^2)} \quad [2]$$

where u is the horizontal flow velocity during n measurement points.

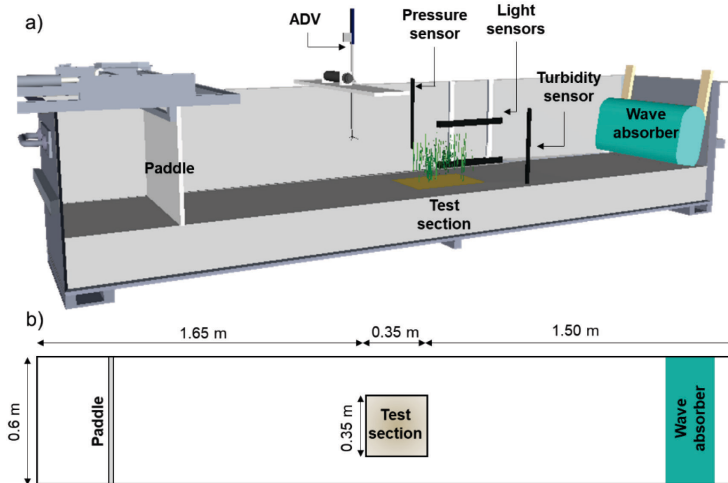


Fig. 1. a) Diagram of the hydraulic wave flume and sensors. The wave flume is a further elaboration of the wave mesocosms used by La Nafie *et al.* (2012) and the wave tanks used by Wang *et al.* (2017) and (Lo *et al.* 2017). b) diagram of the top view of the wave flume. The total length of the flume is 3.5 m, 0.6 m wide and 0.8 m high.

Suspended load and critical erosion thresholds

Erosion as suspended load and the critical erosion threshold per treatment were assessed by measuring the turbidity and light reduction of the water column. Since sediment type and eelgrass densities varied widely in the field, a first trial with mimic plants aimed to assess the effect of both the absence/presence of shoots, and shoot density on sediment resuspension using the same sediment across treatments. These trials were performed both with muddy and sandy sediment and three treatments (Fig. 2a, b): 1) bare sediment, 2) 40 shoots of mimics in the test section, equivalent to 333 shoots m^{-2} , considered low density and 3) 90 shoots of mimics in the test section, equivalent to 750 shoots m^{-2} , considered high density (Lefebvre et al. 2010). Mimic shoots were made from four polyethylene blades of 25 cm length, 2 mm width and 1 mm of thickness attached to a wooden dowel with a 4 cm plastic straw of 0.4 cm of diameter (see González-Ortiz et al. 2014). Muddy and sandy sediment was prepared by homogeneously mixing sediment from the field that was previously sieved (2 mm) to remove shells and debris (Table 1).

To quantify the effect of above and belowground vegetation in sediment resuspension in different sediment types, three treatments were made with muddy and sandy intact sediment from the field: 1) eelgrass with both the aboveground and belowground biomass being present, 2) eelgrass from which only the rhizomes and roots were present, by cutting the aboveground leaves and 3) bare sediment without eelgrass (Fig. 2c, d). Treatment 2 was made only with sandy samples, since pilot trials showed similar results in muddy sediment with eelgrass and only-rhizomes. Three to seven replicates of each treatment were carried out. Hence, our treatments consisted of the test section filled with homogeneous sediment in which we also placed two densities of eelgrass mimics with a random distribution (333 vs. 750 shoots m^{-2}), and natural sediment with either intact eelgrass plants, with eelgrass roots and rhizomes only, and without any eelgrass (Fig. 2).

Water turbidity and the percentage of surface light reaching the bottom were measured during the last 2 min of each time step in all experiments. Water turbidity was measured with a turbidity meter (Campbell, OBS), located 10 cm after the sample box to be in line with the light sensors (Fig. 1a) and 5 cm above the bottom, at a sampling frequency of 25 Hz. At the moment of the measurements, the turbidity was homogeneous in the whole flume. Voltage data from the turbidity meter was calibrated to $mg\ L^{-1}$ of suspended particles by filtering 0.5 L of water at different concentrations on pre-weighed filters and calculating the weight difference after drying for 48 h at 60 °C. Photosynthetic active radiation (PAR) was measured using two Apogee light meters separated 14 cm for later calculation of the light attenuation coefficients (K_d) and percentage of incident radiation at the bottom (Fig. 1a). Light was generated using two Sirio 2070, 500 W lamps placed 1.1 m above the water surface level. The height of the lamps was chosen in order to provide enough light to the light meter in the bottom. K_d was calculated as,

$$K_d = \frac{\ln(I_{z2}/I_{z1})}{Z_2 - Z_1} \quad [3]$$

where I_{z1} is the PAR irradiance at depth Z_1 and I_{z2} at the deeper depth, Z_2 (Beer et al. 2014). The % of light at the bottom was calculated as (Beer et al. 2014),

$$\% \text{ light at the bottom} = \frac{I_{z2}}{I_{z1}} * 100 \quad [4]$$

The critical erosion threshold was determined as a measurement of sediment stability. Two erosion phases can be distinguished accordingly to Amos *et al.* (1992, 1997): a first slow lineal increase of the resuspension with increasing orbital velocities (erosion Type I), and a second rapid increase of resuspension with increasing orbital velocities (erosion Type II). The first phase may correspond to the resuspension of the organic “fluff” layer (Amos et al. 1992, 1997; Bale et al. 2006). The critical erosions thresholds were determined as the start of the Type II erosion from scattegrams of turbidity plotted against the orbital velocities. The Type II erosion was fitted to an exponential regression where turbidity values below 9.5 mg L⁻¹ (ambient concentration) were not accounted.

Bedload erosion with eelgrass plants

To quantify the role of eelgrass on horizontal sandy sediment transport, bedload erosion was assessed in sandy samples after the exposition to the 7 different wave settings ranging from 0 to 27 cm s⁻¹ (Table S1). This experiment was performed with the three sandy treatments (Fig. 2c): 1) eelgrass aboveground and belowground biomass, 2) rhizomes and roots only and 3) bare sediment without eelgrass. We defined bedload erosion as the sediment transported outside of the test-section box. After the trials, the water of the flume was emptied, while the sandy sediment remained on the flume bottom. Then, the sediment deposited on the flume bottom outside of the test-section was collected with a window wiper and a dustpan. The sediment was then dried at 60°C for one week and weighed.

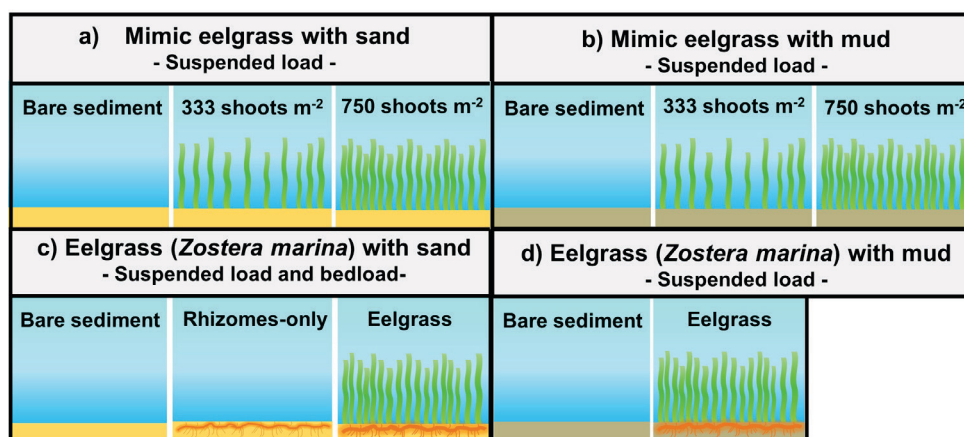


Fig. 2. Experimental design where it was quantified a) suspended load with mimic plants and sandy sediment b) suspended load with mimic plants and muddy sediment, c) suspended load and bedload with eelgrass and sandy sediment and d) suspended load with eelgrass and muddy sediment. Treatment "Rhizomes-only" include root and rhizomes biomass.

Sediment and vegetation properties

Sediment bulk density, organic content, water content and grain size of the 1-2 cm top layer were determined for each sample. Bulk density was calculated as sediment dry weight in a volume of 20 ml. Water content was calculated as the difference of wet and dry weight. Organic content was determined by loss on ignition (LoI) method after burning the sediment sample for 5h at 450°C. The sediment grain size was analyzed using a Malvern® Mastersizer 2000. Sediment samples with mean grain size above 62.5 µm were classified as sandy, while grain sizes below 62.5 µm were classified as muddy.

Plant morphologies were measured at the end of the experiment for each sample. The length and thickness of the leaves and rhizomes were measured. The *total root length* per sample was extrapolated from the total root biomass of the sample and the dry weight of three subsamples of 15 to 20 random roots selected from the sample, which were previously measured and then dried at 60°C for 48h. Then, the diameter of the roots was measured in the subsamples. The *root length density* was calculated using the *total root length per volume of sediment* (see Baets et al. 2007). Above-ground and below-ground biomass was calculated by drying separately the leaves, roots and rhizomes at 60°C for 48h.

Statistical analysis

One-way ANOVA's were used to analyze significant differences in sediment properties, bedload erosion and turbidity between the treatments followed by a Tukey HSD post hoc test. Two-way ANOVA was used to analyze the effect of eelgrass presence and sediment type on turbidity. Differences at P values of 0.05 were considered significant. Turbidity values at 25 cm s⁻¹ for each sample were used for the analysis. Spearman correlation coefficients (r_s) and principal

component analysis (PCA) (Fig. S1) were done with all the treatments to assess possible correlations between i) turbidity and plant/sediment characteristics and ii) bedload erosion and plant/sediment characteristics. Data was standardized for the PCA.

RESULTS

Suspended load and critical erosion thresholds

Sediment resuspension increased at higher densities of eelgrass mimics for both sandy and muddy sediments (Fig. 3a, b). The increase of resuspension was linear during the erosion Type I and exponential during the erosion Type II. After the exposure to all the wave settings, the highest mimic density (750 shoots m^{-2}) reached a maximum turbidity of 58 mg L^{-1} in sandy sediment, while in muddy sediment the turbidity was five times larger, 290 mg L^{-1} . The critical erosion threshold (increase of turbidity and reduction of K_d) started at orbital velocities above 12 cm s^{-1} in sand with eelgrass mimics and at 13.7 cm s^{-1} for bare sand (Fig. 3a). In contrast, the critical erosion threshold started with orbital velocities above 5 cm s^{-1} with 750 shoots m^{-2} and 9 cm s^{-1} with 333 shoots m^{-2} in mud with eelgrass mimics (Fig. 3b). The critical erosion threshold in bare mud was lower than with mimics (5 cm s^{-1}), and contrary to the treatments with mimics, turbidity increased linearly at orbital flow velocities above 9 cm s^{-1} (Fig. 3b). The increase in turbidity showed a significant correlation with the light attenuation coefficient (K_d) ($R^2=0.97$, $p<0.001$). The maximum K_d , $\sim 3.8 \text{ m}^{-1}$ and $\sim 25 \text{ m}^{-1}$ were obtained with sandy and muddy sediment respectively at orbital velocities between 21-29 cm s^{-1} .

Sediment resuspension in natural samples followed a lineal increase during the erosion Type I and an exponential increase during the erosion Type II in all the treatments (Fig. 3c, d). Critical erosion threshold started at orbital flow velocities around 9.4 cm s^{-1} in sandy sediment with eelgrass, 10.5 cm s^{-1} with rhizomes-only and at 14.4 cm s^{-1} in bare sediment (Fig. 3c). In contrast, the critical erosion threshold in muddy sediment started at velocities of 5.1 cm s^{-1} in eelgrass samples and 7.6 cm s^{-1} in bare sediment (Fig. 3d). Turbidity and K_d were lower in sandy sediments than in muddy (Fig. 3). K_d reached maximum values of $\sim 3.6 \text{ m}^{-1}$ and $\sim 21.4 \text{ m}^{-1}$ in sand and mud respectively at orbital velocities between 22-29 cm s^{-1} . In the muddy trials, rhizomes and roots started to be uprooted around 15 cm s^{-1} , which was not the case in the sandy trials. In addition, the turbulent kinetic energy (TKE) was calculated from the ADV data as a measurement of turbulence, which was correlated to the U_{rms} . Calculations of the TKE and plots of the turbidity with TKE can be found in the supplementary information Fig. S2.

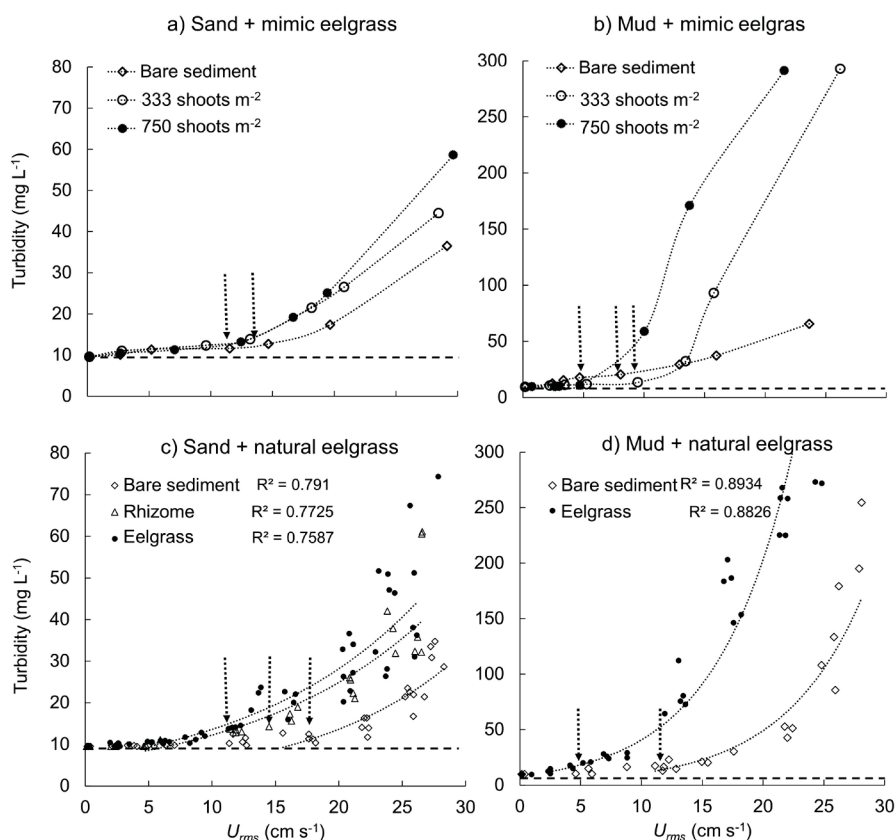


Fig. 3. Orbital flow velocities (U_{rms} , cm s⁻¹) and turbidity (mg L⁻¹) for a) mimic eelgrass with sandy sediment, b) mimic eelgrass with muddy sediment, c) natural eelgrass with sandy sediment and d) natural eelgrass with muddy sediment. The dashed horizontal line represents the ambient concentration (9.5 mg L⁻¹). The dashed vertical arrows represent the observed critical erosion threshold for eelgrass with sand (12 cm s⁻¹), rhizomes-only with sand (14 cm s⁻¹), bare sand (17.5 cm s⁻¹), eelgrass with mud (4 cm s⁻¹) and bare mud (11 cm s⁻¹) respectively. Each point represents a single measurement. Turbidity against the TKE can be found in Fig. S2.

Eelgrass presence was correlated with higher turbidity in both sandy (Spearman, $r_s = 0.61$, $p < 0.01$) and muddy sediment (Spearman, $r_s = 0.81$, $p < 0.01$). ANOVA and Tukey HSD tested for the turbidity reached at 21 and 25 cm s⁻¹, showed significant differences between all the treatments except between rhizomes-only and eelgrass with sand (One-way ANOVA: 21 cm s⁻¹: $F_{2,13} = 14.91$, $p < 0.001$; 25 cm s⁻¹: $F_{2,13} = 11.81$, $p < 0.001$). Given a flume water depth of 25 cm, only the muddy trials reduced the light below the minimum light-requirement for *Z. marina* (20% of surface light) for both mimics and natural eelgrass (Fig. 4). In contrast, none of the sandy trials with or without eelgrass reached the minimum light-requirement threshold. In the eelgrass mimics experiment, the light threshold was reached at 10 cm s⁻¹ and 15 cm s⁻¹ with 750 shoots m⁻² and 333 shoots m⁻² respectively. In natural eelgrass with muddy sediment,

the light threshold was reached at orbital velocities of 15 cm s^{-1} with eelgrass and 25 cm s^{-1} with bare sediment (Fig. 4).

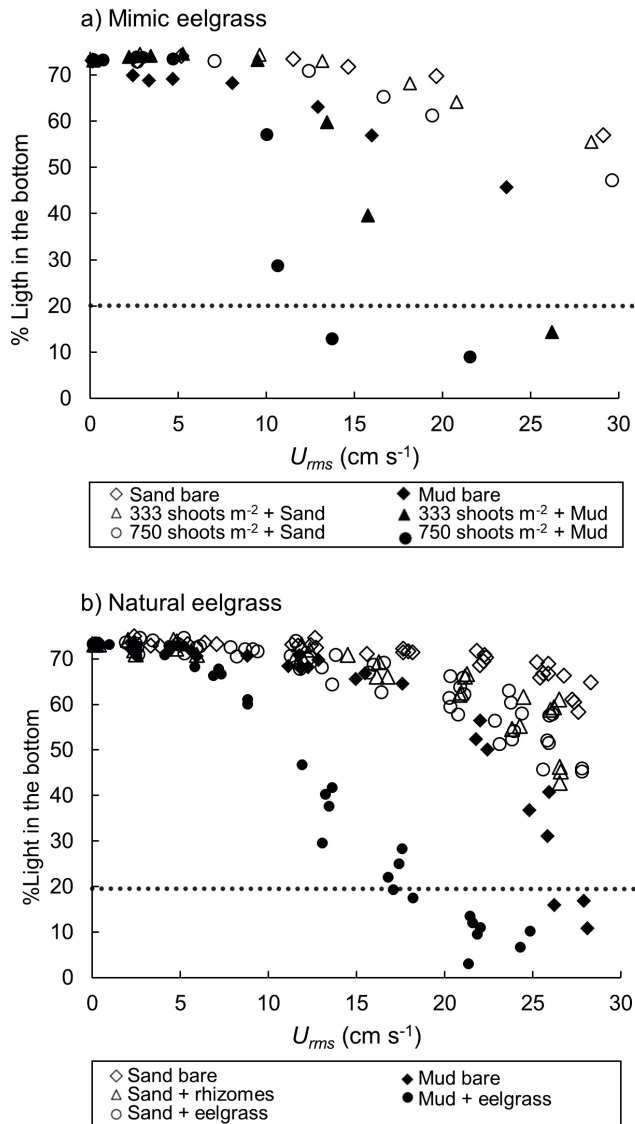


Fig. 4. Percentage of surface light reaching the bottom with increasing flow orbital velocities (U_{rms} , cm s^{-1}) for a) mimic eelgrass and b) natural eelgrass. The dot line indicates the minimum light requirement for eelgrass growth (20 %).

Bedload erosion

Sediment erosion in the form of bedload transport was significantly lower in the presence of eelgrass and rhizomes-only, when compared to bare sediment (One-way ANOVA: $F_{2,7} = 24.21$, $p < 0.05$) (Fig. 5). The total erosion after one hour of wave exposure was similar for vegetated sandy sediment, vegetated muddy sediment and bare muddy sediment, although erosion in sandy trials was mainly as bedload while in muddy trials was mainly as suspended load (Fig. 5). In contrast, bare sandy sediment had a predominance of bedload transport compared to the other treatments (Fig. 5).

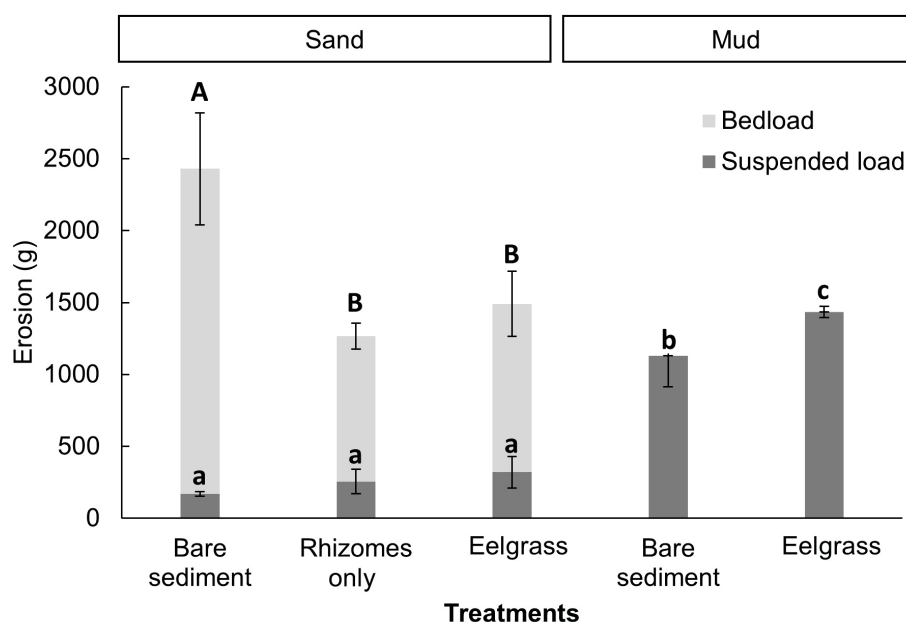


Fig. 5. Total erosion (g) in the form of bedload and suspended load for sandy and muddy trials after 56 min of wave exposure (Mean \pm SD). Significant differences in the bedload of sandy treatments are indicated by upper case letters and differences in the suspended load between all the treatments are indicated by lower case letters (Tukey HSD, $p < 0.05$). Bedload erosion in muddy sediment is negligible. Total erosion as suspended load (g) was extrapolated from the turbidity (mg L^{-1}) at the end of the trials to the volume of water contained in the flume, assuming that the turbidity was homogeneous in the whole flume.

Sediment and vegetation properties

Sediment and vegetation properties are summarized in Table 1. The sediment water content and organic content were significantly higher in the muddy sediment, whereas the bulk density was significantly higher in sandy sediment (One-way ANOVA: SWC: $F_{4,19} = 164.6$, $p < 0.001$, OC: $F_{4,19} = 46.8$, $p < 0.001$, Bulk density: $F_{4,19} = 82.09$, $p < 0.001$). No significant differences were found in bulk density, water content or organic content comparing within the sandy or muddy trials separately.

Eelgrass morphology varied between the samples present in sand and mud (Table 1). Leaves were shorter (< 30 cm) and thinner (0.3 cm), rhizomes were thinner (0.25 cm) and root diameter was thinner (0.05 cm) in sandy samples. In contrast, leaves were longer (> 30 cm) and wider (0.7 cm), rhizomes were thicker (0.5 cm) and root diameter was larger (0.07 cm) in muddy samples. In contrast to muddy samples, eelgrass in sandy sediment formed a dense network of roots and rhizomes which aggregated and retained the sediment.

Table 1. Vegetation and sediment properties. Mean (Std. Err).

		Mimic eelgrass		Natural eelgrass			
		Sand	Mud	Sand		Mud	
Seagrass morphology	n° of shoots	-	-	67.1 (8.1)		8.6 (2.4)	
	Root diameter (cm)	-	-	0.05 (0.0)		0.07 (0.0)	
	Total rhiz length (m)	-	-	6.7 (0.7)		1.4 (0.4)	
	Total root length (m)	-	-	71.8 (5.2)		21.1 (5.7)	
	Root length density (cm cm ⁻³)	-	-	0.8 (0.06)		0.003 (0)	
Biomass	DW leaves (g)	-	-	6.1 (1.0)		1.4 (0.1)	
	DW Rhiz+roots (g)	-	-	11.1 (0.8)		3.7 (0.8)	
Sediment properties	Water content (%)	19.9	59.6	24.1 (0.4)		64.9 (1.94)	
	Organic content (%)	0.4	5.5	0.6 (0.05)		7.4 (0.68)	
	Bulk density (g cm ⁻³)	1.7	0.6	1.6 (0.03)		0.5 (0.03)	
	Sand >62.5 µm (%)	86.2	3.7	75.8 (3.8)		17.0 (2.2)	
	Mud <62.5 µm (silt + clay) (%)	14.1	96.4	24.2 (3.8)		83.3 (2.2)	
	SD50 (µm)	256.1	42.1	183.2 (10.9)		53.1 (4.1)	

*DW =dry weight

Water content, organic content and the percentage of mud were significantly correlated to higher turbidity, comparing all the samples (mud and sand) (Fig. 6). Bulk density, the percentage of sand and the median grain size (SD₅₀) were correlated to lower turbidity (Fig. 6). No significant correlations with plant morphology and turbidity were found. There was a significant interaction between sediment type (mud or sand) and eelgrass presence (Two-way ANOVA: $F_{1,19}=173$, $p<0.001$), which led to the maximum rates of turbidity and lower critical erosion thresholds in the mud with eelgrass treatments (Fig. 3).

ROLE OF EELGRASS ON TOPSOIL EROSION

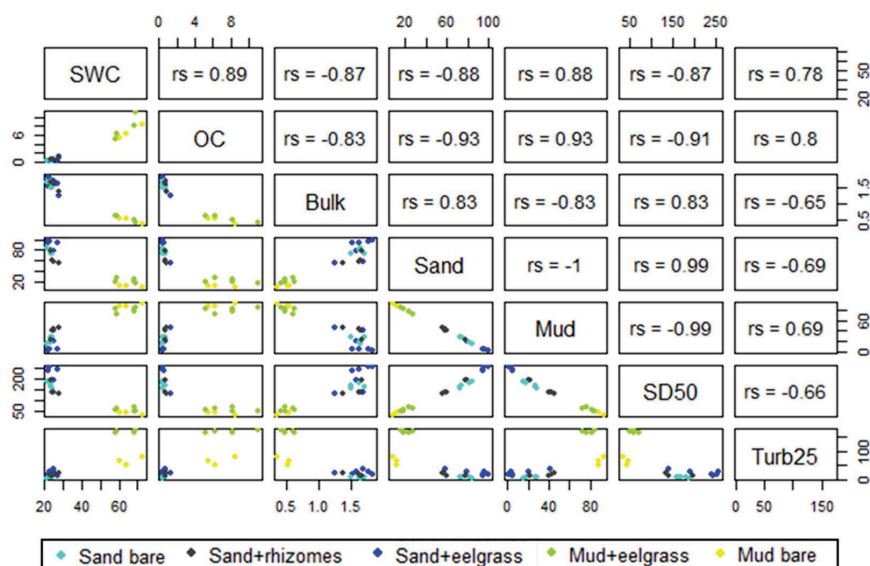


Fig. 6. Matrix plot of the variables significantly correlated with the turbidity. All the Spearman correlation coefficients (r_s) are significant ($p < 0.001$). SWC = sediment water content (%), OC = organic content (%), Bulk = bulk density (g cm^{-3}), Sand (%), Mud (%), SD50 = median grain size (μm), Turb25 = turbidity (mg L^{-1}) reached at orbital velocities around 25 cm s^{-1} .

Belowground biomass was the only variable significantly correlated with less bedload erosion in sandy sediment (Spearman, $r_s = -0.68$, $p < 0.001$) (Fig. 7a). None of the morphologic traits were significantly correlated with bedload erosion. Eelgrass with lower percentage of mud seems to reduce less the bedload erosion compared to eelgrass with higher percentage of mud, although the correlation was not significant (Fig. 7b).

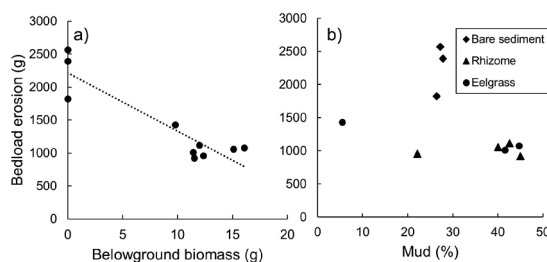


Fig. 7. a) Correlation between belowground biomass (g) and bedload erosion (g), Spearman correlation = -0.68 , $p < 0.001$. b) Scattergram between mud content and bedload erosion (g). Eelgrass and only-rhizome trials, even with variable mud content, had lower bedload erosion than bare sediment trials.

DISCUSSION

This study showed that the bedload erosion was reduced in sandy trials with eelgrass (either with leaves or only rhizomes and roots) compared with bare sediment, even at the highest wave velocities ($\sim 27 \text{ cm s}^{-1}$). Nevertheless, turbidity increased in the presence of natural eelgrass or mimics compared to bare sediment at orbital velocities above 5 and 10 cm s^{-1} in both muddy and sandy sediments respectively. Sediment properties showed key differences in the maximum turbidity reached with mud ($\sim 272 \text{ mg L}^{-1}$) and with sand ($\sim 74 \text{ mg L}^{-1}$) and the type of erosion (i.e., suspended load with mud vs. bedload with sand).

Eelgrass presence on sediment resuspension

Previous studies show that seagrass can reduce sediment resuspension by a reduction of the water flow and the shear stress compared to the unvegetated areas, either with currents (Gambi et al. 1990; Widdows et al. 2008) or waves (Ward et al. 1984; Hansen and Reidenbach 2012; Infantes et al. 2012; Ros et al. 2014). Nevertheless, the results of this study showed that eelgrass did enhanced the resuspension of the sediment and lowered the critical erosion threshold both in sandy and muddy trials. Hydrodynamics inside the eelgrass patch could not be measured due to the small size (0.12 m^2 , $35 \times 35 \text{ cm}$). Other experiments with patches ranging from 2.2 m to 0.3 m width have shown to increase the sediment dynamics created by the turbulence generated by the shoots or by the meadow edges under both currents (Bouma et al. 2007, Fonseca and Koehl 2006, Chen et al. 2012) and waves (Granata et al. 2001). Low plant densities could also increase the turbulence and scouring around shoots as flow moves through the sparse canopy (Bouma et al. 2009; Lefebvre et al. 2010). This increase in turbulence and scouring by the eelgrass presence suggests the observed increase in sediment resuspension and turbidity in all trials.

Sediment characteristics on turbidity and light attenuation

The comparison between muddy and sandy trials indicate that the critical erosion threshold and the subsequent increase in turbidity and light attenuation (K_d) are dependent on the sediment properties, in accordance with Bale et al. (2006), together with the interaction with eelgrass presence. In our experimental set up with a water depth of 25 cm, only the muddy sediment reduced the light below the minimum 20%, assessed for *Z. marina* (Dennison et al. 1993). Sandy treatments led to a major part of erosion in the form of bedload (from 2567 to 918 g) and a small part as suspended load (from 154 to 329 g), not causing high turbidity nor light reduction, in agreement with Houwing (1999). In contrast, muddy sediment with mean grain size smaller than $62.5 \mu\text{m}$, passed directly to suspended load with negligible bedload phase, causing higher turbidity and light reduction (Widdows et al. 2008; Grabowski et al. 2011). The response was similar for mimic treatments, although mimics needed less wave velocities to reduce the percentage of light than natural eelgrass (10 cm s^{-1} and 15 cm s^{-1} respectively).

Mimic shoots were slightly stiffer than natural eelgrass, which is related with more scouring and turbulences around the shoots (Bouma et al. 2009a; Ros et al. 2014).

Importance of the belowground biomass: Applications for conservation and restoration

Bedload erosion of sandy sediment was reduced in treatments with eelgrass compared to bare sediment. Furthermore, there were no differences between the treatments of full canopy eelgrass (above- and belowground biomass), and only roots and rhizomes (only belowground biomass), suggesting that the effect of sediment stabilization is mediated by the belowground biomass rather than the canopy. These results are important and in line with earlier findings from Christianen et al. (2013), which increases the still limited available literature on this topic. In this study, eelgrass present in sandy sediment had a dense network of roots and rhizomes with root length densities of 0.8 cm cm^{-3} . In terrestrial plants, a high density of roots with less than 1 mm of diameter are related with less erosion (Baets et al. 2007). In contrast, eelgrass in muddy sediment with root length density of 0.003 cm cm^{-3} led to less aggregation and retention of the sediment, as found by Widdows et al. (2008). In addition, the sediment properties of sandy eelgrass samples with higher percentage mud ($>20 \%$), might have increased the sediment cohesiveness reducing even more the erodibility (Brown et al. 1995; Gailani et al. 2001) (Fig. 7b). Nevertheless, eelgrass samples with less mud ($< 5 \%$) still had less bedload erosion than the bare sediment (with higher % of mud) (Fig. 7b), suggesting again that belowground biomass may play a major role reducing bedload erosion.

This study underlines the importance of the conservation of the existent eelgrass meadows with developed belowground biomass to reduce the sediment erosion by bedload transport. The data obtained in this study confirms that an eelgrass patch of 0.12 m^2 with developed belowground biomass has a stabilizing effect of the sediment, reducing bedload transport. On the other hand, such a small patch will not have any effect preventing resuspension of the sediment. This experiment provides more evidence that the fragmentation of the meadows due to anthropogenic causes could increase the turbidity by exposing more edges of the meadow to hydrodynamics which increases the sediment resuspension (Allaoui et al. 2016).

Sediment characteristics as bulk density and grain size, exposure to hydrodynamics and patch size are important factors to consider during eelgrass restoration. Our results suggest that in sites with sediment median grain size smaller than $75 \mu\text{m}$ and exposure to orbital velocities above 10 cm s^{-1} , sediment resuspension may be a problem in the restorations (Van Der Heide et al. 2007; Moksnes et al. 2018), and larger patches than 0.12 m^2 might be needed to reduce sediment resuspension (Silliman et al. 2015; van Katwijk et al. 2016). On the other hand, in sandy sediments with mean grain size larger than $130 \mu\text{m}$ and exposed to orbital velocities up to 30 cm s^{-1} , sediment resuspension might not reduce the light below the 20% in shallow waters (Adams et al. 2016). Bedload erosion might however be the cause of restoration failure due to the lack of a developed network of roots and rhizomes and uprooting of the initial plant

units. In this case, to start a self-reinforcing feedback with sediment stabilization and low bedload erosion, wave barriers (Maxwell et al. 2017) or biodegradable geotextiles (Zanuttigh et al. 2015) could be implemented to reduce hydrodynamics and stabilize the sediment at the restoration site until the seagrass patches develop a dense root and rhizome network.

ACKNOWLEDGMENTS

B. Marin would like to thank to Erasmus + and MOBINT grants and to the University of Gothenburg. E. Infantes will like to thank FORMAS grant Dnr. 231-2014-735. Thanks to the staff of Sven Lovén Center, Kristineberg Station for providing their great facilities. Funds for this work were also provided by the Wilhelm and Martina Lundgrens Foundation and the Royal Society of Arts and Sciences in Gothenburg.

SUPPORTING INFORMATION

Table S1. Wave settings generated with the hydraulic flume.

	SETTING	0	1	2	3	4	5	67	
Wave conditions	Wave height (cm)	0	1.6	2.1	3	4.3	5	5.8	7.3
	Wave period (s)	0	5.8	5.1	4.1	4.1	4.1	4.1	3.3
	Wave length (m)	0	7.8	6.8	5.4	5.4	5.4	5.4	4.4
Flow	U_{rms} (cm s ⁻¹)	0	2	5	11	17	22	25	27

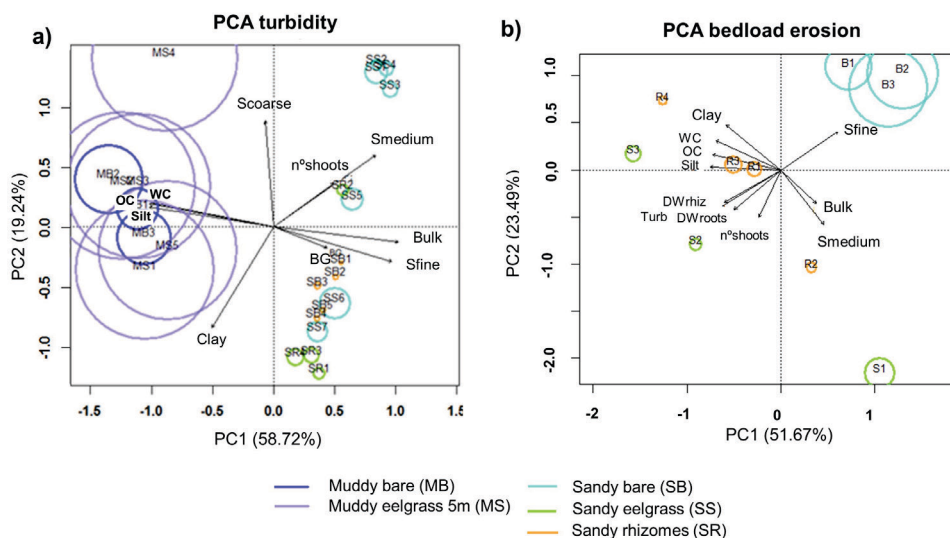


Fig. S1. PCA of the two principal component (PC) indicating the more explanatory variables related to the a) turbidity and b) bedload erosion, separated per treatments. The size of the colour circles is a rescale of the quantity of turbidity/bedload erosion in each sample. BG=belowground biomass; DW= dry wheight; OC=organic content; WC=Water content; Bulk= bulk density; S=sand; Rhiz=rhizomes

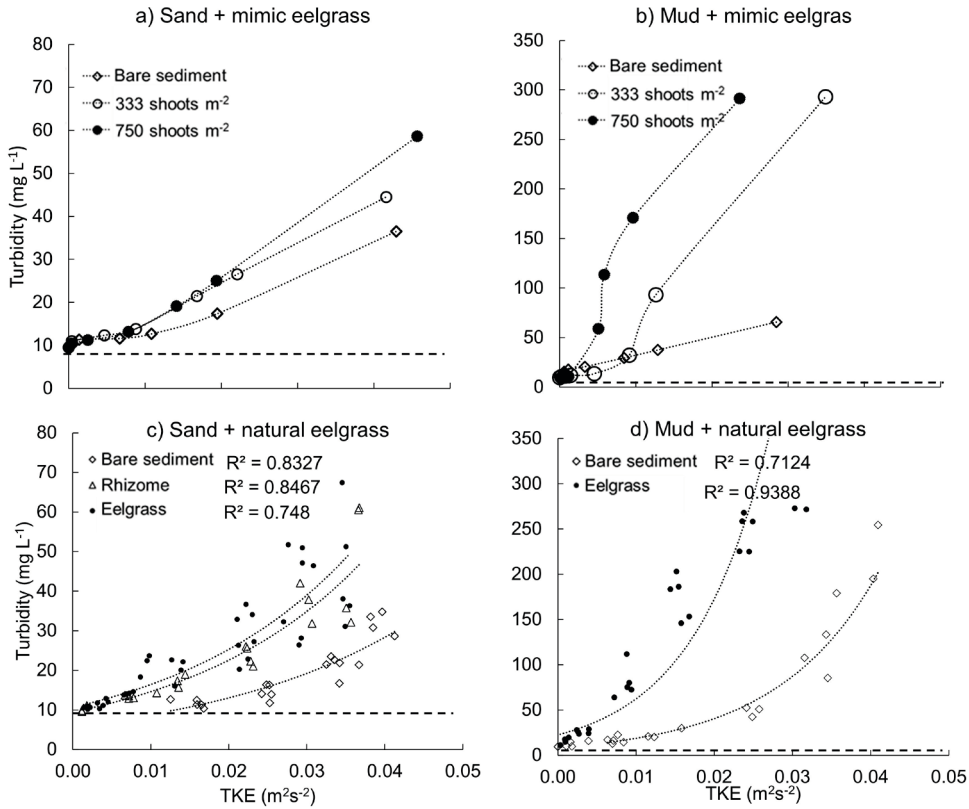


Fig. S2. Turbulent kinetic energy (TKE, m²s⁻²) and turbidity (mg L⁻¹) for a) mimic eelgrass with sandy sediment, b) mimic eelgrass with muddy sediment, c) natural eelgrass with sandy sediment and d) natural eelgrass with muddy sediment. The dashed horizontal line represents the ambient concentration (9.5 mg L⁻¹). Each point represents a single measurement. TKE was calculated from the ADV data as $\frac{1}{2}(\overline{u'^2} + \overline{v'^2} + \overline{w'^2})$, in m² s⁻², as a measurement of turbulent fluctuation. u , v , and w are the velocities in x, y and z direction respectively. u' , v' and w' are the components of turbulent velocity, calculated as:

$$u'(t) = u(t) - \bar{u},$$

$$v'(t) = v(t) - \bar{v},$$

$$z'(t) = z - \bar{z}$$



NL7559
5363

NL7559
1203
Stellondo

Chapter 6

How grazing management can maximize erosion resistance of salt marshes

Beatriz Marin-Diaz, Laura L. Govers, Daphne van der Wal, Han Olff,
Tjeerd J. Bouma

Journal of Applied Ecology (2021) 58(7): 1533-1544

ABSTRACT

Combining natural saltmarsh habitats with conventional barriers can provide a sustainable and cost-effective alternative for fully-engineered flood protection, provided that a minimal salt marsh width can be guaranteed for a long period. Hence, it is essential to understand both the key factors and management options driving the lateral erodibility / stability of salt marshes. We aimed to determine how salt marsh management (i.e., grazing by large vs. small grazers vs. artificial mowing), marsh elevation and marsh age affect soil stability (i.e., soil-collapse) and intrinsic lateral erodibility of salt marshes (i.e., particle-by-particle detachment). Soil cores were collected in high and low marshes (above and below 0.5 m MHWL respectively) of different ages. At these locations, we compared cores from grazed areas to cores inside grazer enclosures, with and without artificial mowing. All cores were exposed to waves in flumes to test their stability and lateral erodibility. All soil cores were characterized by a stable fine-grained layer deposited on top of readily erodible sand. The thickness of the fine-grained layer was a key parameter in reducing salt marsh instability (cliff-collapse). This layer-thickness increased with marsh age and at lower elevations, but decreased with cattle grazing due to compaction. The erosion-resistance of the fine-grained layer increased with *i)* large grazers that compacted the soil by trampling, *ii)* mowing that excluded soil-bioturbating species, and *iii)* grazing by small grazers that promoted vegetation types with higher root density. Overall, marshes with thinner cohesive and/or fine-grained top layers are more sensitive to lateral erosion than marshes with deep cohesive soils, independently of the management. Grazing and artificial mowing can reduce the erodibility of fine-grained soils, making salt marshes more resilient to lateral erosion. However, compaction by large grazers simultaneously leads to thinner fine-grained layers and lower elevation, potentially leading to more inundation under sea level rise. Hence, to effectively manage salt marshes to enhance their contribution to coastal protection we recommend *i)* moderate/rotational livestock grazing, avoiding high intensity grazing in sediment-poor systems sensitive to sea level rise and *ii)* investigating measures to preserve small grazers.

INTRODUCTION

Many countries around the world are currently facing the challenge of flood risk due to sea level rise, land subsidence and frequent storm surges (Syvitski et al. 2009; IPCC 2014; Voudoukas et al. 2018). The adoption of hard engineering solutions is associated with the destruction of the coastal ecosystems, and related loss of the ecosystem services (e.g., Lai et al. 2015). Ecosystem-based coastal defence may offer a more sustainable approach towards coastal protection, by combining hard engineering with natural coastal ecosystems into hybrid designs (Temmerman et al. 2013; Schoonees et al. 2019). A recent analysis of historic flood-disasters revealed that salt marshes in front of a dike reduce both the chance of a dike breaching as well as the impact of a dike breach (Zhu et al. 2020). Despite being increasingly recognized for their coastal protection services (Gedan et al. 2009; Shepard et al. 2011; Temmerman et al. 2013), implementing the use of salt marshes into hybrid ecosystem-based flood-designs is hampered by the lack of in-depth understanding of their long-term dynamics (Bouma et al. 2014).

Salt marshes are dynamic ecosystems that vary in width in time, either due to intrinsic biogeomorphic and ecological processes, or by changes in physical factors such as storms and sea level rise (Phillips 1986; Van de Koppel et al. 2005). With climate change, the frequency and intensity of storms and storm surges is expected to increase (IPCC 2014). Extreme storms may induce the formation of a marsh cliff (Bouma et al. 2016), where after especially frequently occurring moderate (winter) storms determine the rate of lateral retreat (Leonardi et al. 2016). Landward migration of marshes, e.g. to keep pace with sea level rise, is often prevented due to human land use. This may eventually result in the complete loss of a marsh by coastal squeeze (Doody 2013). Hence, understanding the susceptibility of salt marshes to this type of edge erosion (i.e., known as cliff erosion, scarp erosion or lateral erosion, also found in marsh creeks: Eerd 1985; Sharma et al. 2016; Pagés et al. 2018), is of key importance for being able to integrate marshes as sustainable flood defence strategies.

The susceptibility of marsh edges to lateral erosion can be divided into soil stability and lateral erodibility. Soil stability refers to marsh-edge collapse due to undercutting by wave erosion (Schwimmer et al. 2001; Francalanci et al. 2013; Priestas et al. 2015). Lateral erodibility refers to the gradual detachment of soil particles from the sediment due to hydraulic pressure (Bouma et al. 2009b; Feagin et al. 2009). Previous studies showed that sandy soils erode faster than fine-grained soils (Feagin et al. 2009; Lo et al. 2017; De Battisti et al. 2019). Belowground plant structures (roots and rhizomes) also were found to decrease erodibility (Ford et al. 2016; Wang et al. 2017; De Battisti et al. 2019), with the strongest effects found in sandy soils (Lo et al. 2017; De Battisti et al. 2019). Coarse detritus including roots and decaying plant parts seem to promote erosion while fine-grained detritus may reduce erosion (Feagin et al. 2009).

Grazing is often used for managing biodiversity in salt marshes (Bakker 1989; Davidson et al. 2017), but is known to affect marsh properties in many ways. For example, trampling by large grazers increases soil bulk density and root density by soil compaction (Elschot et al. 2013, 2015; Schrama et al. 2013; Howison et al. 2015). A study by Pagés et al. (2018) using an overshot-weir flume related the higher compaction of the trampled soil by cattle with less lateral erosion. On the other hand, ungrazed soils may be colonized by tall plant communities and *Orchestia sp.* (Olf et al. 1997; Friese et al. 2018), a bioturbator that has been related to higher soil porosity (Howison et al. 2015), which in return could increase erodibility. In addition, small grazers have also shown to structure salt marsh vegetation communities (Kuijper and Bakker 2005; Chen et al. 2019) although previous studies show no significant effect on soil properties (Elschot et al. 2013). On sandy barrier islands, older marshes and low marshes (below mean high water level) may have deeper fine-grained soil layers due to increased accretion (Olf et al. 1997; Elschot et al. 2013), which may increase salt marsh erosion-resistance and stability. An integrated view on how grazing-management in combination with abiotic factors like marsh age, marsh elevation and sediment layering, affect the susceptibility of marsh edges to lateral erosion remains however lacking.

In order to facilitate the use of salt marshes as part of a nature-based flood protection, we aimed to enhance the understanding on how soil stability and erodibility processes are affected by management in relation to the physical setting of a marsh. The aims of this study hence are *i)* to assess how salt marsh management (including grazing by small and large grazers and artificial mowing), elevation and age affect relevant biotic and abiotic factors related to sediment erosion, *ii)* how these changes affect the lateral erosion in the studied system and *iii)* discuss the implications of the results on the management of the salt marshes for coastal protection.

METHODS

Study area

The study sites were located in the back-barrier marsh of the island of Schiermonnikoog (the Netherlands) (Fig. 1a, 53°29'N 6°14'E). This island is expanding to the east, creating a salt marsh chronosequence (Olf et al. 1997). The western and oldest marsh has been grazed by large grazers (cattle) until 1958, ungrazed between 1958 to 1972 and grazed again thereafter (Bakker and de Vries 1992). The eastern younger marshes have been only grazed by small grazers (hare and geese) but never by cattle (Fig. 1a) (Kuijper and Bakker 2005). The tidal range is approximately 2.5 m and mean high tide (MHT) is 1 m.

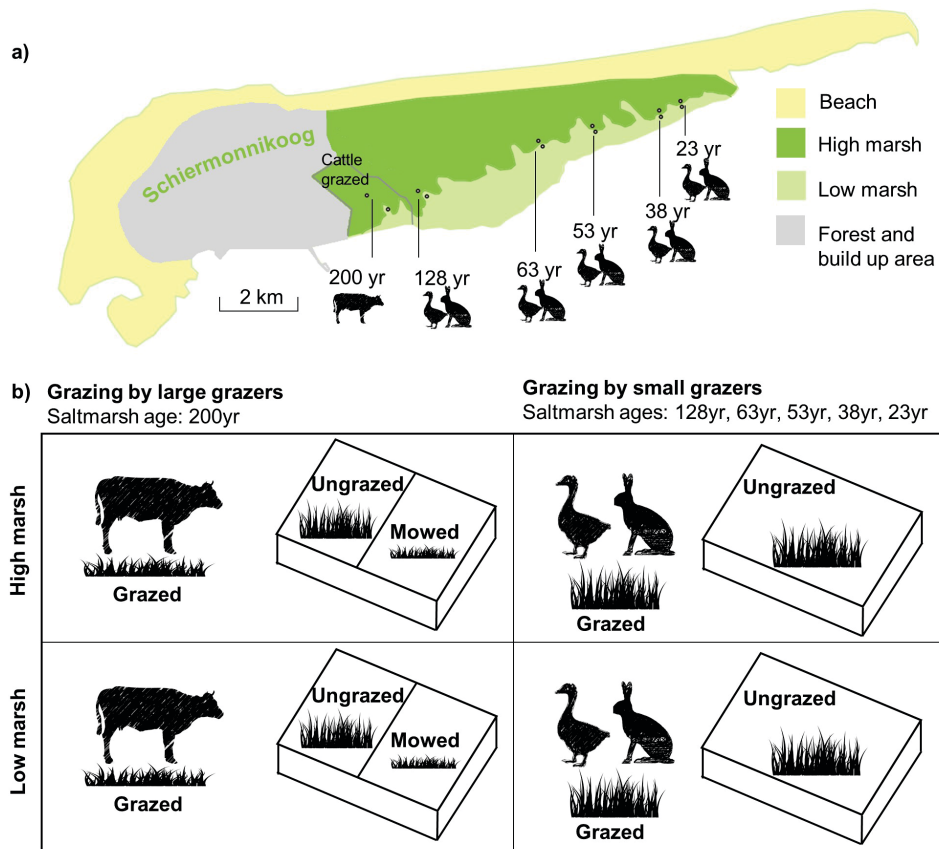


Fig. 1. (a) Locations of the sampling sites in the island of Schiermonnikoog (b) Experimental treatments in the different salt marsh ages and elevations.

Experimental set-up

To study the effect of management, salt marsh age and salt marsh elevation on soil properties and how this is related to marsh stability and lateral erodibility, soil samples were collected from six locations along the back-barrier marsh of Schiermonnikoog (Fig. 1a). Because this salt marsh is a well-protected National Park, human impact is not expected to have an effect on the marsh, neither close nor far from build-up area. In 2018, the ages of each study site were approximately 23, 38, 53, 63, 128 and 200 yr (Olf et al. 1997). In 1972, large grazer enclosures (8 m x 42 m) were deployed in the high (above 0.5 m + MHWL) and low (below 0.5 m + MHWL) 200 yr old salt marsh, excluding large grazers but not small grazers (Bos et al. 2002). Artificial mowing treatments were established inside the enclosures to test the effect of grazing (aboveground removal) without trampling (Veeneklaas et al. 2011). The vegetation was mown twice annually (June/July and August/September) (Chen et al. 2020). One enclosure in the high marsh and one in the low marsh were sampled inside in the non-mowed area, with dominant *Elytrigia atherica*; inside in the mowed area, with *E. atherica* mixed with other species

like *Festuca rubra* and *Plantago maritima*, hereafter called mixed *E. atherica*; and outside in the trampled soil with *Juncus gerardii*.

In 1994, small grazer enclosures (7 m x 7 m) were deployed in the low and high marsh in each of the five youngest stages, not grazed by cattle (further details in Kuijper and Bakker 2005). Samples were collected in the high marsh outside and inside of the enclosure, both dominated by *E. atherica*; in the low marsh outside the enclosures with mixed species with predominance of *Atriplex portulacoides*, hereafter called mixed *A. portulacoides*; and inside the enclosure with *E. atherica* (excluding stages 23 and 63 with mixed *A. portulacoides*). Therefore, the treatments consisted of soil samples from high and low marshes grazed and ungrazed by small grazers at the stages 23-, 38-, 53-, 63- and 128-year-old; and high and low marsh grazed, ungrazed and mowed at the stage 200-year-old from the cattle grazed area (Fig. 1b).

Salt marsh soil stability and lateral erodibility

Soil samples were collected during April 2018. A total of 78 sediment cores of 15 cm diameter and 20 cm depth were extracted from the 6 locations (Fig. 1ab), with 3 replicates per treatment, by inserting PVC pipes in the soil and carefully digging them out. The roots sticking out of the bottom of the core were cleanly cut and a plastic lid was placed below to keep the sediment intact. Following the protocol of Lo et al. (2017), sediment cores were transported to the wave mesocosms installations in the Royal Netherlands Institute for Sea Research (NIOZ) in Yerseke, the Netherlands, and stored in tanks with seawater from the Oosterschelde estuary until the erosion experiments. The elevation of each plot was determined with DGPS measuring 5 to 8 paired points inside and outside the enclosures.

Soil stability and lateral erodibility was determined in four wave flumes of 360 cm long x 90 cm high x 82 cm wide at the Royal Netherlands Institute of Sea Research with the same set-up as Lo et al. (2017) and Wang et al. (2017) (Fig. 2a). The same wave settings as in Lo et al. (2017) were utilised, with wave heights of ~ 8 cm in front of the cores, and the swash intersecting the whole sample. The sediment cores taken in the field were transferred into the metal cores which had an opening of 12 cm width in the longitudinal side. The exposed lateral side was cleanly sliced into a flat surface in the opening of the metal core and adjusted to 15cm high (Fig. 2b). Lateral erodibility from the fine-grained layer was measured after 1 h, 2h, 4h, 8h, 16h, 24h, 32h and 38h of wave exposure. Soil stability was measured as the time when the fine-grained layer collapsed forward or slid to the bottom after the erosion of the sand layer (Fig. 2c). Sediment collapsing was considered an artefact for the volume loss calculation and this data was excluded from the lateral erodibility analyses. The volume eroded was assessed by photogrammetry (structure from motion) technique as developed in Nieuwhof et al. (2015), and applied by Lo et al. (2017) and Wang et al. (2017). Some samples with sand layer on the bottom did not collapse even with the sand eroded, and the window to calculate the volume loss was adjusted to the fine-grained layer.

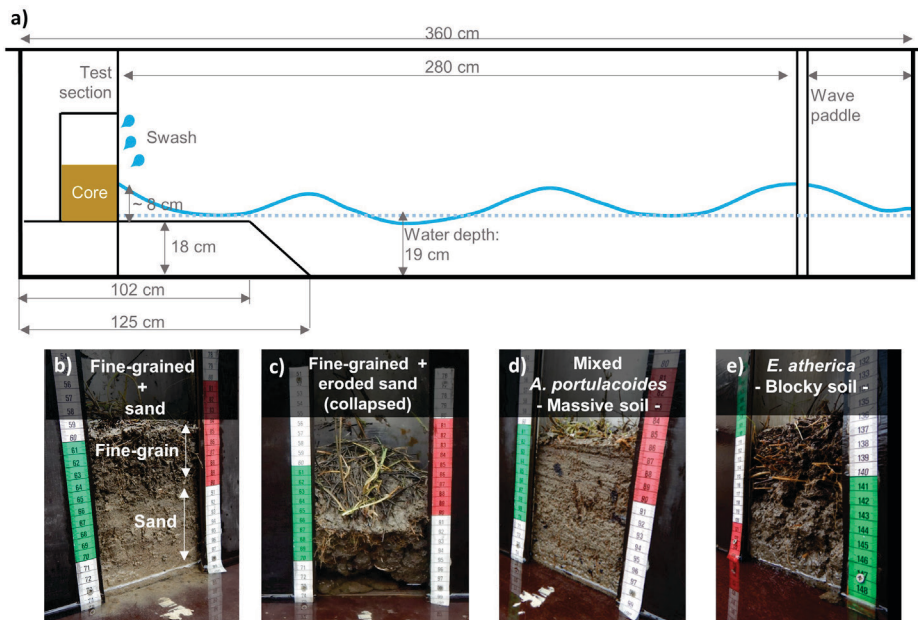


Fig. 2. a) Schematic side view of the wave mesocosms, b) sample with fine-grained layer on top of sandy layer, c) collapsed sample after the sand layer eroded, d) soil structure with mixed *Atriplex portulacoides* and e) soil structure with *Elytrigia atherica*.

Belowground vegetation properties

Belowground biomass was cleaned over a 1 mm sieve after the wave exposure and the roots and rhizomes were separated. After sieving the sediment, we soaked the remaining roots in a bucket with water and poured the floating roots into another bucket, while the small sediment aggregates remained in the bottom and were discarded. A representative subsample of i) rhizomes, ii) coarse roots (diameters between 0.5 to 2 mm for the plant species of this experiment) and iii) fine roots (diameters < 0.5 mm), which include some fine dead root material that could not be distinguished and removed (cf. De Battisti et al. 2019), was separated from each sample. The subsamples of rhizomes and coarse roots were displayed in a calibrated red tray and photographed with a compact camera (model Nikon Coolpix W300). The subsamples and the rest of the sample were dried at 60 °C until constant weight to obtain the biomass (g). The biomass of coarse roots and fine roots was extrapolated from the dry weights of the subsamples and the dry weight of the whole sample. Diameters of the rhizomes and coarse roots were measured from the images of the subsamples with the software Imagem (Schneider et al. 2012). Total root density, coarse roots density, fine roots density and rhizome density were calculated as in Table S1.

Soil properties

Soil properties were determined from small cores of 2.2 cm Ø and 20 cm depth collected next to each 15 cm Ø sediment cores taken for the erosion experiment. After measuring the length of the fine-grained layer depth, the small cores were sliced separating the fine-grained layer from the sand layer to determine the properties of each layer separately. Sediment samples were weighed and freeze dried during four days. Bulk density was calculated as the sediment dry weight in a known volume (g cm^{-3}). Water content was calculated as the difference of wet and dry weight. Organic content was determined by lost on ignition method after burning the sediment sample for 6 h at 450 °C. The sediment grain size was analysed using a Malvern® Mastersizer 2000. Soil strength at 5 cm depth (Mpa) was measured in the field with an Eijkelkamp Penetrologger with a 1 cm Ø cone. Deeper measurements of soil strength were not utilised because the intersection with the sand layer biased the results. Soil structure was determined visually from the soil cores and categorized into granular, blocky, massive or single grained, based on the Soil Survey Manual (Soil Science Division Staff 2017).

Bioturbators

Presence and absence of the bioturbator *Orchestia gammarellus* was noted in all the sampling locations by superficial inspection of the area where the cores were extracted and within the core.

Statistical analysis

The lateral erodibility of the fine-grained layer was only studied for the samples that did not collapse (all the samples from the large-grazers area, the low marsh samples from the small-grazers area and the high marsh samples from stage 53). Estimates of the possible maximum volume loss over time (E_{max}) were calculated fitting a saturating-type function (Appendix S1). Full factorial, well-replicated design was limited by the layout of successional stages and long-term grazing treatments in the field. For this reason, data was analysed separately for the large-grazers and small-grazers. In addition, because vegetation communities varied between successional stages in unreplicated way, belowground biomass properties were primarily utilised as variables to relate to erosion. Principal component analysis (PCA) without rotation and Pearson correlation matrices were performed to find relationships between E_{max} , vegetation and soil properties. All the variables were log transformed to account for non-linear relationships. Because of high correlation among vegetation and soil variables, bulk density, soil structure and total root density were used in the further analysis as representative of the soil and vegetation properties. For the cattle-grazed area, we used a full factorial two-way ANOVA to test the effect of management and elevation on a set of response variables: the fine-grained layer depth (cm), maximum volume loss (%), bulk density and root density. For the small-grazers area, the analysis was done for high and low marsh separately. We first used a two-way ANOVA to test the effect of grazing by small-grazers and age on the set of response variables (the fine-grained layer depth (cm), maximum volume loss (%), bulk density and root density). Because the interaction of grazing and age was not significant, and to obtain an overall effect of grazing on

the set of response variables, we followed the analysis with a linear mixed model (LMM) to test the effect of management (as fixed factor) on the set of response variables with age as random factor. One-way ANOVAs were used to test the effect of age on the small-grazers area on the set of response variables. The same analysis for large and small herbivores separately were done to test the effect of soil structure on the maximum volume loss (%) as response variable. In addition, for the large-grazers area, two-way ANOVA was used to test the effect of i) soil texture and elevation on bulk density (response variable) and ii) vegetation type and elevation on root density (response variable). Similarly, for the small-grazers area we used one-way ANOVA to test the effect of i) soil texture on bulk density and ii) vegetation type on root density. Where necessary, the response variables were log-transformed to meet normality and homogeneity assumptions. To test differences in soil elevation between treatments, T-test were performed among the large grazer treatments, and Paired Wilcoxon signed rank test was performed between the small grazer treatments due to intrinsic variability of the topography. Statistical analyses were performed using R 3.5.0 (R Development Core Team 2018). The *drc* (Ritz et al. 2015) package was used for the saturating-type function.

RESULTS

Lateral stability and fine-grained layer erodibility across different managements, elevations and ages

All the samples from high marsh with a fine-grained sediment layer less than 12.5 cm (i.e., all but stage 63 yr and the 200 yrs large-grazers area) collapsed within 2 hours of wave exposure, when the sand below was completely eroded (Fig. 3a). We did not observe collapse in any of the other locations, further indicating that the collapse threshold indeed occurred around with a fine-grained layer less than 12.5 cm (Fig. 3ab). The properties of the fine-grained layer and sand layer can be found in the Table S2 and S3. Sandy soils eroded with any type of vegetation and management. In contrast, the fine-grained layer only eroded up to 9.4% during the experimental period. In the large-grazers area, erodibility was significantly lower in the grazed treatment ($\sim 0\%$), followed by the mowed, compared to the ungrazed (up to 9.4%) ($F_{2,12} = 61.7$, $p < 0.001$), without effect nor interaction of marsh elevation ($F_{2,12} = 0.2$, $p > 0.05$ and $F_{2,12} = 0.3$, $p > 0.05$ respectively) (Fig. 3c, S2a). Fine-grained layer erodibility in the small-grazers area was significantly lower in the grazed ($\sim 1\%$) than ungrazed (up to 6%) ($\chi^2(1) = 12.28$, $p < 0.001$), although we can observe the exceptions at stage 23 and 63 yr (Fig. 3c, S2b). Erodiability differed significantly among locations but not in relation to age ($F_{5,29} = 10.7$, $p < 0.001$).

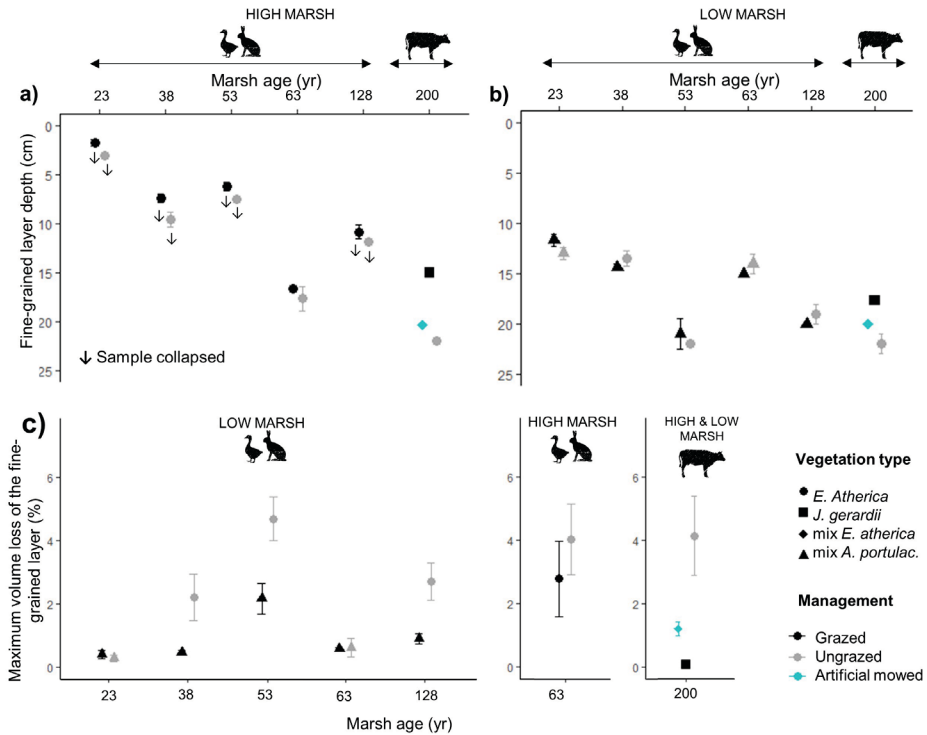


Fig. 3. Fine-grained layer depth for each treatment in the a) high marsh and b) low marsh. c) Maximum volume loss of the fine-grained layer for each treatment. Error bars represent standard errors.

Effect of soil properties and vegetation characteristics on the fine-grained layer erodibility

Both in the large and small-grazers area, fine-grained layer erodibility was significantly reduced by soils with higher bulk density, higher soil strength and higher belowground biomass (Fig. 4, 5, S3 and S4). Additionally, lower silt % and soil water content in the large grazers area and higher soil water content in the small herbivores area were also associated with less erosion (Fig. 4, 5, S3 and S4). Organic content for both areas and rhizome density and silt % in the small-grazers area were the only variables not correlated to erosion (Fig. 4 and 5). Erodibility also differed significantly between massive and both granular and blocky soil structure, but not between the latter two (large-grazers area: $F_{2,12} = 61.7$, $p < 0.001$, small-grazers area: $\chi^2 (2) = 73$, $p < 0.001$) (Fig. 4 and 5). Massive structure appeared with *J. gerardii* and mixed *A. portulacoides*; platy structure with mixed *E. atherica* and blocky structure with *E. atherica*. Granular structure was the exception, present with both mixed *A. portulacoides* and *E. atherica* at stage 53 yr. Belowground biomass was mainly explained by the root density, specifically by the compartment of the fine roots, and less by the rhizomes or coarse roots (Table S4 and S6). For the sake of simplicity, bulk density, soil structure and total root density were used in the further analysis as representative of highly correlated soil and vegetation properties. Therefore, similar relations are expected for all these variables. Total root density was higher in *J. gerardii*

(trampled by cattle) and mixed *A. portulacoides* compared to *E. atherica* (large-grazers area: $F_{2,12} = 132$, $p < 0.001$; small-grazers area: $F_{1,3} = 95.2$, $p < 0.001$ respectively) (Fig. 4 and 5). Bulk density was significantly higher in massive soils (Fig. 2d) compared to platy, granular (Fig. S1) and blocky soil structure (Fig. 2e), but did not differ between the latter two (large-grazers area: $F_{2,12} = 44.9$, $p < 0.001$; small-grazers area: $F_{2,31} = 16.2$, $p < 0.001$) (Fig. 4 and 5). Granular structure from stage 63 yr, explained the high erodibility even with mixed vegetation, which can not be explained by any other variable (Fig. 5).

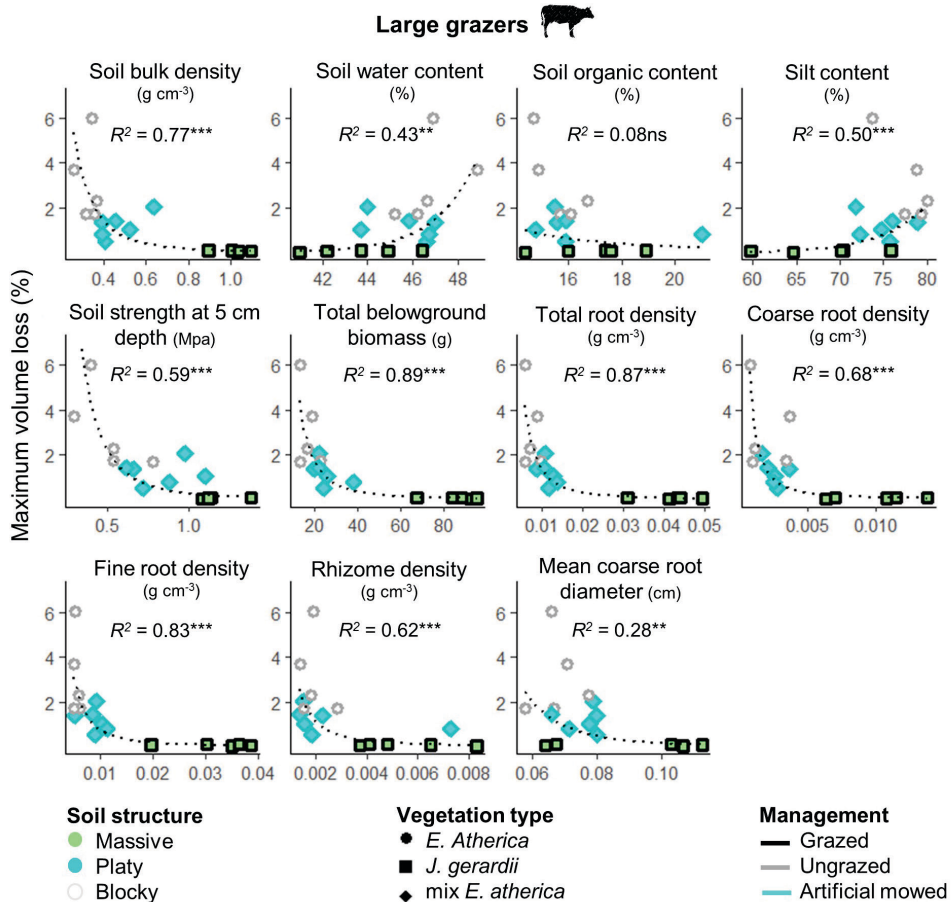


Fig. 4. Relationships between maximum volume loss (%) and the soil and vegetation variables in the large- grazers area. R^2 and significance values were obtained from power- law regressions ($y = ax^b$). Significance codes refer to $p < 0.001$ (***), $p < 0.001$ (**), $p > 0.05$ (ns).

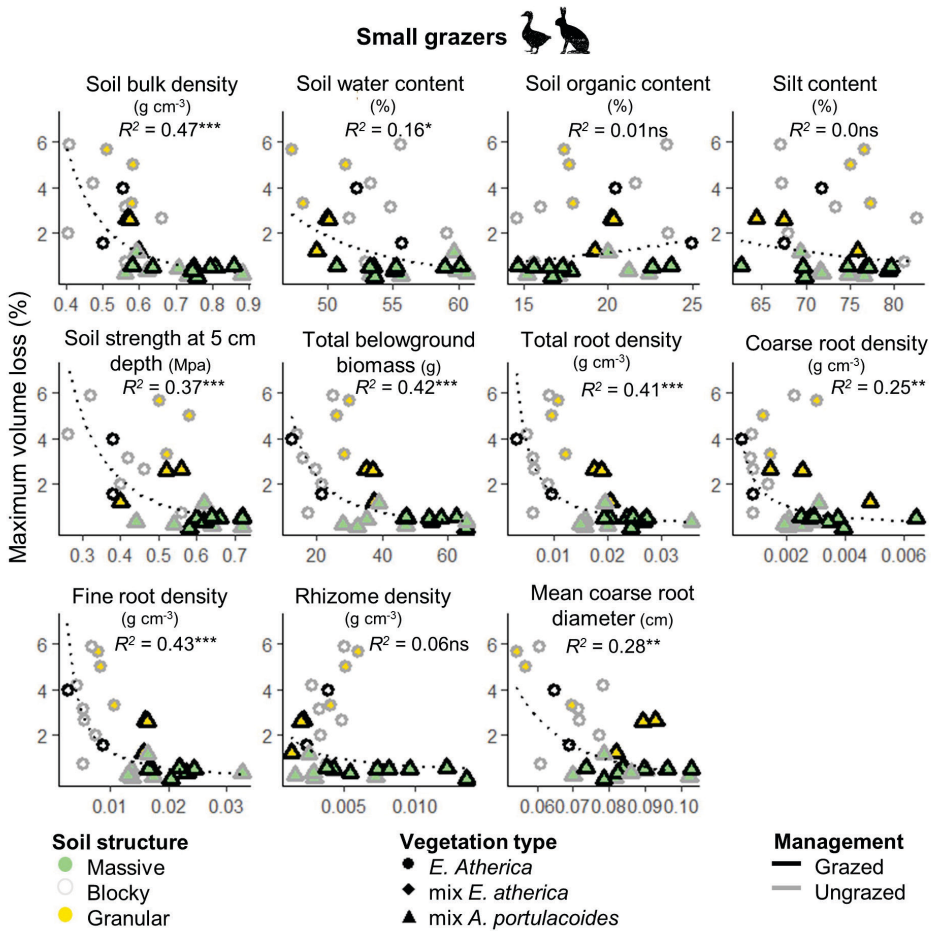


Fig. 5. Relationships between maximum volume loss (%) and the soil and vegetation variables in the small-grazers area. R^2 and significance values were obtained from power-law regressions ($y = ax^b$). Significance codes refer to $p < 0.001$ (***), $p < 0.001$ (**), $p < 0.01$ (*), $p > 0.05$ (ns).

Effects of management, elevation and age on soil properties, vegetation characteristics and bioturbators

The effect of management, elevation and age on fine-grained layer depth was investigated in relation to the lateral stability. Grazing by large grazers reduced the fine-grained layer depth followed by the mowed treatment, compared to the ungrazed ($F_{2,12} = 102.6$, $p < 0.01$), being ~ 2 cm deeper in the low marsh ($F_{2,12} = 10.7$, $p < 0.01$) (Fig. 3ab). In the small grazers area, the fine-grained layer was up to 15 cm deeper in the low marsh and tended to increase with age, however these changes were not completely linear along the age gradient (high marsh: $F_{4,25} = 129$, $p < 0.001$; low marsh: $F_{4,25} = 54.6$, $p < 0.001$) (Fig. 3ab). The fine-grained-layer depth was overall significantly thinner in the small herbivores grazed treatment in the high marsh ($\chi^2(1) = 15.9$, $p < 0.001$), but not in the low marsh ($\chi^2(1) = 0.03$, $p > 0.05$) (Fig. 3ab).

The compaction of the fine-grained layer by large grazers was related to lower soil elevation, with grazed soils in average 5 cm lower than ungrazed in the high marsh and 2 cm in the low marsh ($t_{17} = 5.1$, $p < 0.01$ and $t_{21} = 2.7$, $p < 0.05$ respectively) and up to 7 cm lower than the artificial mowed in the high marsh and 2 cm in the low marsh ($t_2 = 12$, $p < 0.01$ and $t_6 = 1.3$, $p > 0.05$ respectively). Small grazers only reduced the elevation significantly in the low marsh at stage 23 yr by on average 1.3 cm ($Z = 3$, $p < 0.05$).

The effect of management, elevation and age on soil structure, soil bulk density, total root density and bioturbators, as representative soil and vegetation variables, was investigated in relation to the fine-grained layer erodibility. Large grazers led to the highest bulk density and root density with massive soil structure, followed by the mowing treatment with platy structure, compared to the ungrazed with *E. atherica* and blocky structure ($F_{2,12} = 44.9$, $p < 0.001$, $F_{2,12} = 132$, $p < 0.001$ respectively) (Fig. 4). Grazing by small herbivores indirectly affected the root density, bulk density and soil structure by suppressing *E. atherica* with exception of stage 23 and 63 yr with mixed *A. portulacoides* inside the enclosure, and stage 53 yr with granular structure (Fig. 5, Table S2). In the large-grazers area, bulk density and root density did not differ between the high and low marsh ($F_{1,12} = 2.5$, $p > 0.05$ and $F_{1,12} = 0.8$, $p > 0.05$ respectively). In the small-grazers area, bulk density differed significantly among locations, but not in relation to age ($F_{4,30} = 10.3$, $p < 0.001$) and root density was not affected by age ($F_{4,30} = 0.6$, $p > 0.05$). Lastly, large grazers and mowing suppressed the presence of bioturbators, except for one mowed sample, and it may be related to the differences in bulk density and soil structure in the large-grazers area (Table S5). In the small-grazers area, bioturbators did not have an effect on erosion as they were found both in grazed and ungrazed sites (Table S5).

DISCUSSION

Ecosystem-based coastal defence, combining traditional hard engineering with natural coastal ecosystems such as salt marshes, may offer a more sustainable approach towards future flood risk prevention (Temmerman et al. 2013). Hence, it is essential to understand key factors driving the lateral erodibility and stability of salt marshes to optimize their coastal protection management. We here investigated how salt marsh management can be used to optimize the erosion-resistance of salt marshes and how it interacts with marsh age and elevation. In this study, we found that erosion-resistance of fine-grained soils can be increased by management that enhances *i*) large grazers, which compact the soil by trampling, *ii*) mowing, which excludes soil-bioturbating arthropods, and *iii*) small grazers (hares, geese) which promotes vegetation types with higher belowground biomass, mostly explained by higher root density. More specifically, we observed faster erodibility for fine-grained soils with low bulk density ($< 0.6 \text{ g cm}^{-3}$), in combination with blocky or granular soil structure and low root density ($< 0.015 \text{ g cm}^{-3}$), as typical for *E. atherica* vegetation zones. However, bulk density should be used with caution as a proxy for erodibility, because soils with the same bulk density can have different grain size and soil structure, and therefore different erodibility. Furthermore, the stability of the fine-grained soils depended on the thickness of the fine-grained layer, which generally increased

GRAZING AND LATERAL SOIL EROSION

in sandy barrier islands with marsh successional age and at lower elevations, but decreased with cattle grazing. Sandy marshes with thin cohesive layers will still provide coastal protection (e.g. wave attenuation) (Shepard et al. 2011), but their lateral erosion rate may be higher than in marshes with deeper cohesive soils. These results can be used to formulate recommendations to optimize the management of salt marshes for ecosystem-based-coastal-protection (Fig. 6).

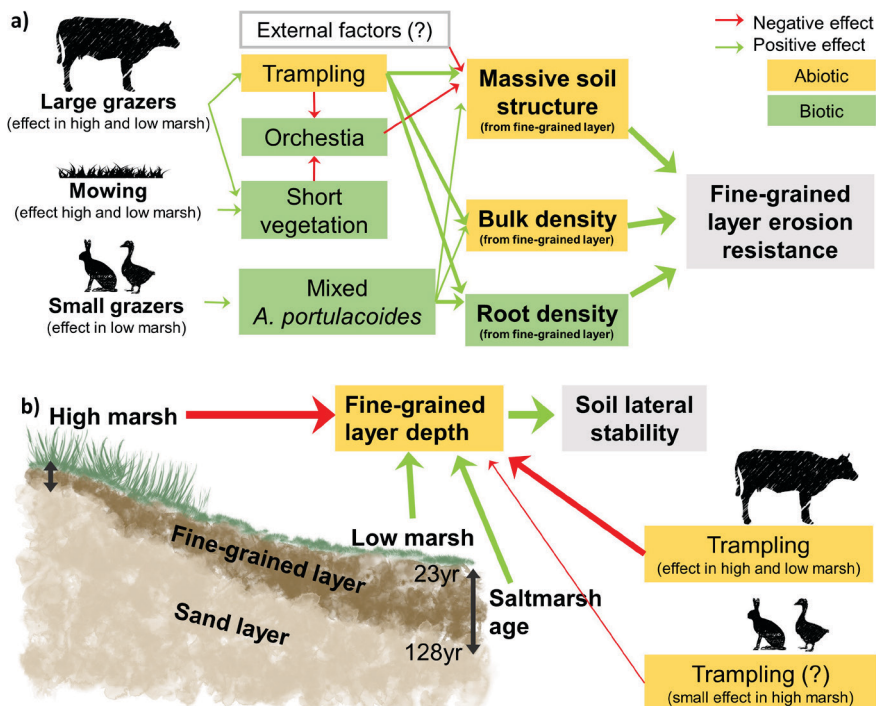


Fig. 6. Conceptual model of the variables analysed in this study that can affect a) the fine-grained layer erodibility (i.e. gradual erosion) and b) lateral soil stability (i.e. cliff collapse) of salt marshes on sandy barrier islands and spits.

Ecosystem services provided by grazing management: increased soil resistance by livestock grazing as a new management application

Livestock grazing has been traditionally used as a management tool for preserving plant biodiversity in grasslands and salt marshes worldwide (Olf and Ritchie 1998; Davidson et al. 2017). In this study area, grazing has increased the plant diversity in the long term by suppressing *E. atherica* dominance (Kuijper and Bakker 2005; Chen et al. 2020). Furthermore, our experiment shows that the effect of suppressing *E. atherica*, together with the compaction of the soil and exclusion of bioturbators, can reduce the fine-grained soil erodibility. In the case of mowing for promoting plant diversity, the reduction on erodibility may be explained by the platy soil structure from past grazing, which has not yet been converted to blocky as in the ungrazed treatment, which is likely due to the low abundance of bioturbators in the mowed areas (Howison et al. 2015, 2017; Schrama et al. 2015).

Surprising positive effect by small grazers on soil resistance

Hares and geese grazing can also suppress the dominance of *E. atherica*, but only in the low marsh (Kuijper and Bakker 2005; Chen et al. 2019). This study shows that the shift from *E. atherica* to vegetation with higher belowground biomass, higher bulk density and massive soil structure can reduce the erodibility of the fine-grained layer on the low marsh. The importance of high belowground biomass is in accordance with previous salt marsh studies (Brooks et al. 2020 and references therein). More specifically, the importance of fine root density (<1 or 0.5 mm Ø, depending on the author), is in accordance with previous terrestrial system studies (e.g. Li et al. 1991; Baets et al. 2006, 2007). For these small grazers, we can not attribute the higher erodibility to bioturbators effects, because they were found in both grazed and ungrazed treatments. The 53-year stage was an exception compared to stages 23, 38, 63 and 128 yr, in that it had a more granular soil structure and a higher erodibility. We hypothesize that this was due to the presence of more large detritus (dead belowground biomass), which we observed but did not quantify. However, the presence of more large detritus has been previously related to increase the soil erodibility (Feagin et al. 2009). In contrast to the cattle grazing, small grazers overall did not cause soil compaction and thus did not reduce the fine-grained layer depth nor soil elevation.

Grazing management under global change

Livestock grazing as a management tool for coastal protection should be taken cautiously because it can reduce soil elevation by compaction, as shown in this study and others (Elschot et al. 2013; Bakker et al. 2020). This could promote marsh vegetation mortality in face of sea level rise, although livestock grazing may only enhance this problem in sediment-poor systems with low accretion rates (Kirwan et al. 2016; Törnqvist et al. 2020). Low sediment input can occur due to changes in the sediment supply (Ladd et al. 2019) or in microtidal and/or organogenic marshes (e.g. found in the U.S.), where the accretion is mainly due to decay of organic material (Kearney and Turner 2016). In contrast, accretion rates of minerogenic marshes (common in Europe and south-east U.S.) is higher and depends on suspended sediment levels in the tidal input (Bakker et al. 2015). Additionally, too high livestock grazing can have negative effects in other trophic levels or soil carbon content in organogenic marshes (Davidson et al. 2017, 2020). Moderate intensity grazing and rotational grazing may be the best solution for reducing soil erodibility without excessive soil compaction as well as maintaining biodiversity at different trophic levels (Bouchard et al. 2003; van Klink et al. 2016; Bakker et al. 2020). Low marshes with low sediment input will benefit from being grazed by natural occurring small grazers (hares or geese) preventing the expansion of *Elytrigia spp.* without decreasing the elevation. However, small grazers like geese increasingly prefer higher fertilized agricultural grasslands over nearby natural salt marshes (Dokter et al. 2018), therefore we recommend management at the landscape scale to recover small grazers abundance in the natural marshes.

Relevance to other coastal regions

Livestock grazing in coastal marshes occurs worldwide, especially in European marshes, Asia and South America while less commonly in North America (Davidson et al. 2017). Using cattle grazing for soil stabilization in organogenic marshes as found in North America needs to be further studied because in addition to be sediment-poor systems, the effect of trampling could reduce even more the elevation and speed up soil decomposition (Nolte et al. 2013; Davidson et al. 2017). The effect of small herbivores through limiting the expansion of *E. atherica* can be applied to other low marshes with dominant *Elytrigia sp.* as found in Europe but may be different in other regions, like America, where the marshes are commonly dominated by taller, less palatable species as *Spartina spp.* (Davidson et al. 2017).

ACKNOWLEDGMENTS

This work is part of the Perspectief Research Programme “All-Risk”, project number P15-21 B1, which is co-financed by NWO Domain Applied and Engineering Sciences, in collaboration with: the Dutch Ministry of Infrastructure and Water Management (RWS), Deltares, STOWA, the regional water authority Noorderzijlvest, the regional water authority Vechtstromen, it Fryske Gea, HKV consultants, Natuurmonumenten and the waterboard HHNK. LLG was supported by NWO-VENI grant 016.VENI.181.087. In addition, we would like to thank Marc Santasusagna for field and flume-work assistance and Fee Smulders, Hacen M. El-Hacen, Arne van Eerden and Tessel H. Lagerwerf for field assistance. We are also thankful to Tjalf van Minnen and Geert-Jan Sieperda for helping analysing root samples; Lennart van IJzerloo and Bert Sinke from the Nioz for technical assistance; Nelly Eck for laboratory assistance; and Dr Matty Berg for discussions on bioturbators.

SUPPORTING INFORMATION

Appendix 1. Maximum volume loss calculation.

Estimates of the possible maximum volume loss over time (E_{max}) were calculated fitting a saturating-type function as,

$$E = \frac{E_{max}t}{E_m + t}$$

where E is the volume eroded, E_{max} is the possible maximum volume lost over time, t is time and E_m is the time when half of E_{max} is eroded, which is an approximation of how fast the sediment is eroded. Maximum volume lost, E_{max} , was used to describe the relationships between soil properties, vegetation properties and clay lateral erosion.

Supplementary Table 1. Calculation of the vegetation belowground properties

Total root density (coarse roots + fine roots) (g cm ⁻³)	Total root biomass (coarse roots + fine roots) / core volume
Coarse roots density (g cm ⁻³)	Coarse roots biomass / core volume
Fine roots density (g cm ⁻³)	Biomass of fine roots / core volume
Rhizomes density (g cm ⁻³)	Rhizome biomass / core volume

GRAZING AND LATERAL SOIL EROSION

Supplementary Table 2 (part I). Abiotic properties of the fine-grained layer (means \pm SD). Note that the top 10 cm of the stage 23 in high marsh include sand.

	Treatment	Age	Classified elevation	Vegetation type	Soil structure	Mean soil elevation NAP (cm)	
Small herbivores	Ungrazed	23	H	<i>E. atherica</i>	single grained	168	\pm 15
	Grazed		H	<i>E. atherica</i>	single grained	165	\pm 17
	Ungrazed		L	Mixed spp.	massive	136	\pm 1
	Grazed		L	Mixed spp.	massive	135	\pm 1
	Ungrazed	38	H	<i>E. atherica</i>	blocky	164	\pm 9
	Grazed		H	<i>E. atherica</i>	blocky	164	\pm 10
	Ungrazed		L	<i>E. atherica</i>	blocky	145	\pm 2
	Grazed		L	Mixed spp.	massive	142	\pm 6
	Ungrazed	53	H	<i>E. atherica</i>	granular	177	\pm 5
	Grazed		H	<i>E. atherica</i>	granular	175	\pm 9
	Ungrazed		L	<i>E. atherica</i>	granular	149	\pm 2
	Grazed		L	Mixed spp.	granular	150	\pm 5
	Ungrazed	63	H	<i>E. atherica</i>	blocky	169	\pm 11
	Grazed		H	<i>E. atherica</i>	blocky	173	\pm 16
	Ungrazed		L	Mixed spp.	massive	134	\pm 2
	Grazed		L	Mixed spp.	massive	135	\pm 3
	Ungrazed	128	H	<i>E. atherica</i>	blocky	164	\pm 2
	Grazed		H	<i>E. atherica</i>	blocky	166	\pm 6
	Ungrazed		L	<i>E. atherica</i>	blocky	141	\pm 1
	Grazed		L	Mixed spp.	massive	140	\pm 5
Large herbivores	Mowed	200	H	Mixed spp.	platy	159	\pm 1
	Ungrazed		H	<i>E. atherica</i>	blocky	152	\pm 2
	Grazed		H	<i>J. gerardii</i>	massive	147	\pm 3
	Mowed	200	L	Mixed spp.	platy	155	\pm 2
	Ungrazed		L	<i>E. atherica</i>	blocky	159	\pm 2
	Grazed		L	<i>J. gerardii</i>	massive	157	\pm 2

Supplementary Table 2 (part II). Abiotic properties of the fine-grained layer (means \pm SD). Note that the top 10 cm of the stage 23 in high marsh include sand.

	Treatment	Age	Elev.	Fine-grained layer depth depth (cm)			Soil water Content (%)			Bulk density (g/cm ³)		
Small herbivores	Ungrazed	23	H	3.0	\pm	0.0	12.3	\pm	2.2	1.1	\pm	0.1
	Grazed		H	1.7	\pm	0.6	9.4	\pm	2.1	1.1	\pm	0.1
	Ungrazed		L	13.0	\pm	1.0	55.9	\pm	1.7	0.8	\pm	0.1
	Grazed		L	11.7	\pm	1.0	54.3	\pm	2.5	0.8	\pm	0.1
	Ungrazed	38	H	9.5	\pm	1.3	37.1	\pm	2.4	0.8	\pm	0.0
	Grazed		H	7.3	\pm	0.8	36.8	\pm	7.1	0.8	\pm	0.1
	Ungrazed		L	13.5	\pm	1.3	54.1	\pm	3.2	0.6	\pm	0.1
	Grazed		L	14.3	\pm	0.6	56.8	\pm	0.4	0.8	\pm	0.0
	Ungrazed	53	H	7.5	\pm	0.5	45.4	\pm	1.3	0.6	\pm	0.1
	Grazed		H	6.2	\pm	0.8	36.2	\pm	4.0	0.6	\pm	0.1
	Ungrazed		L	22.0	\pm	0.0	48.4	\pm	3.2	0.6	\pm	0.0
	Grazed		L	21.0	\pm	2.6	49.0	\pm	2.1	0.6	\pm	0.0
	Ungrazed	63	H	17.7	\pm	2.1	55.5	\pm	3.9	0.4	\pm	0.0
	Grazed		H	16.7	\pm	0.6	53.2	\pm	3.8	0.5	\pm	0.1
	Ungrazed		L	14.0	\pm	1.7	58.5	\pm	0.8	0.6	\pm	0.0
	Grazed		L	15.0	\pm	0.0	59.4	\pm	4.7	0.6	\pm	0.1
	Ungrazed	128	H	11.8	\pm	0.3	47.0	\pm	2.8	0.7	\pm	0.2
	Grazed		H	10.8	\pm	1.3	46.4	\pm	4.5	0.5	\pm	0.2
	Ungrazed		L	19.0	\pm	1.7	50.2	\pm	1.7	0.5	\pm	0.0
	Grazed		L	20.0	\pm	0.0	55.8	\pm	1.9	0.7	\pm	0.1
Large herbivores	Mowed	200	H	20.3	\pm	0.6	43.9	\pm	2.0	0.5	\pm	0.1
	Ungrazed		H	22.0	\pm	0.0	45.0	\pm	2.4	0.4	\pm	0.0
	Grazed		H	15.0	\pm	0.0	38.3	\pm	8.2	0.9	\pm	0.2
	Mowed	200	L	20.0	\pm	0.0	43.6	\pm	1.5	0.5	\pm	0.1
	Ungrazed		L	22.0	\pm	1.7	42.5	\pm	2.1	0.3	\pm	0.0
	Grazed		L	17.7	\pm	0.6	42.1	\pm	1.4	1.0	\pm	0.1

GRAZING AND LATERAL SOIL EROSION

Supplementary Table 2 (part III). Abiotic properties of the fine-grained layer (means \pm SD). Note that the top 10 cm of the stage 23 in high marsh include sand.

	Treatment	Age	Elev.	Organic content (%)			Sand content (%)			SD50 (μ m)			Resistance to penetration at 5cm depth (MPa)		
Small herbivores	Ungrazed	23	H	3.9	\pm	1.1	85.4	\pm	3.9	178.9	\pm	7.9	0.6	\pm	0.1
	Grazed		H	3.8	\pm	1.8	68.7	\pm	24.9	176.9	\pm	5.1	0.5	\pm	0.0
	Ungrazed		L	16.6	\pm	1.2	24.2	\pm	1.0	28.6	\pm	0.9	0.7	\pm	0.1
	Grazed		L	16.0	\pm	1.1	26.4	\pm	3.6	29.4	\pm	1.9	0.6	\pm	0.1
	Ungrazed	38	H	14.4	\pm	0.8	53.2	\pm	14.7	72.2	\pm	15.7	0.6	\pm	0.1
	Grazed		H	14.0	\pm	1.3	43.9	\pm	4.4	62.0	\pm	24.9	0.6	\pm	0.0
	Ungrazed		L	15.4	\pm	0.7	21.3	\pm	4.9	25.7	\pm	3.6	0.5	\pm	0.1
	Grazed		L	16.9	\pm	1.2	21.6	\pm	1.4	25.5	\pm	0.9	0.7	\pm	0.1
	Ungrazed	53	H	17.0	\pm	2.1	41.2	\pm	9.2	47.0	\pm	13.0	0.4	\pm	0.0
	Grazed		H	11.5	\pm	0.5	53.4	\pm	3.6	74.8	\pm	11.3	0.4	\pm	0.0
	Ungrazed		L	17.7	\pm	0.3	24.0	\pm	1.2	27.0	\pm	1.0	0.5	\pm	0.0
	Grazed		L	19.9	\pm	0.6	31.0	\pm	5.9	33.0	\pm	5.2	0.5	\pm	0.1
	Ungrazed	63	H	22.8	\pm	1.1	32.9	\pm	0.5	36.7	\pm	0.6	0.3	\pm	0.1
	Grazed		H	23.3	\pm	2.5	31.4	\pm	2.6	34.6	\pm	4.3	0.4	\pm	0.0
	Ungrazed		L	21.2	\pm	1.2	29.3	\pm	1.3	33.3	\pm	0.8	0.5	\pm	0.1
	Grazed		L	25.9	\pm	4.8	35.0	\pm	3.8	38.6	\pm	5.0	0.6	\pm	0.1
	Ungrazed	128	H	20.3	\pm	1.7	34.3	\pm	4.1	39.5	\pm	4.6	0.4	\pm	0.1
	Grazed		H	28.4	\pm	7.9	46.2	\pm	1.2	57.2	\pm	1.8	0.5	\pm	0.2
	Ungrazed		L	17.5	\pm	0.8	26.3	\pm	4.6	29.0	\pm	3.7	0.5	\pm	0.1
	Grazed		L	17.9	\pm	1.1	24.3	\pm	2.3	27.1	\pm	1.3	0.6	\pm	0.1
Large herbivores	Mowed	200	H	15.7	\pm	0.2	24.7	\pm	3.5	28.0	\pm	2.5	0.8	\pm	0.2
	Ungrazed		H	17.3	\pm	2.0	23.8	\pm	5.8	28.0	\pm	4.1	0.6	\pm	0.0
	Grazed		H	18.1	\pm	5.0	36.3	\pm	3.8	37.7	\pm	3.8	1.1	\pm	0.1
	Mowed	200	L	17.2	\pm	3.3	25.9	\pm	1.8	29.9	\pm	1.7	0.9	\pm	0.2
	Ungrazed		L	15.3	\pm	0.8	23.6	\pm	2.7	28.3	\pm	1.7	0.5	\pm	0.3
	Grazed		L	17.9	\pm	0.8	28.1	\pm	3.3	31.1	\pm	2.4	1.2	\pm	0.1

Supplementary Table 3. Abiotic properties of the sand layer (means \pm SD) (Part I). In grey, samples that did not include sandy subsoil (fine-grained top layer thicker than 15 cm).

	Treatment	Age	Elevation	Vegetation type	Water Soil Content (%)			Bulk density (g/cm ³)		
Small herbivores	Ungrazed		H	<i>E. atherica</i>	8.3	\pm	1.8	1.8	\pm	0.1
	Grazed	23	H	<i>E. atherica</i>	7.7	\pm	0.6	1.7	\pm	0.1
	Ungrazed		L	Mixed spp.	16.6	\pm	0.8	1.9	\pm	0.1
	Grazed		L	Mixed spp.	20.7	\pm	0.3	2.1	\pm	0.2
	Ungrazed		H	<i>E. atherica</i>	16.1	\pm	4.5	1.8	\pm	0.2
	Grazed	38	H	<i>E. atherica</i>	20.3	\pm	4.6	1.6	\pm	0.1
	Ungrazed		L	<i>E. atherica</i>	20.8	\pm	0.0	2.0	\pm	0.0
	Grazed		L	Mixed spp.						
	Ungrazed		H	<i>E. atherica</i>	18.5	\pm	1.7	1.9	\pm	0.1
	Grazed	53	H	<i>E. atherica</i>	20.9	\pm	13.3	1.8	\pm	0.4
	Ungrazed		L	<i>E. atherica</i>						
	Grazed		L	Mixed spp.						
	Ungrazed		H	<i>E. atherica</i>						
	Grazed	63	H	<i>E. atherica</i>						
	Ungrazed		L	Mixed spp.						
	Grazed		L	Mixed spp.						
	Ungrazed		H	<i>E. atherica</i>	17.7	\pm	4.7	1.9	\pm	0.1
	Grazed	128	H	<i>E. atherica</i>	22.5	\pm	6.5	1.6	\pm	0.2
	Ungrazed		L	<i>E. atherica</i>						
	Grazed		L	Mixed spp.						
Large herbivores	Mowed		H	Mixed spp.						
	Ungrazed	200	H	<i>E. atherica</i>						
	Grazed		H	<i>J. gerardii</i>						
	Mowed		L	Mixed spp.						
	Ungrazed	200	L	<i>E. atherica</i>						
	Grazed		L	<i>J. gerardii</i>						

GRAZING AND LATERAL SOIL EROSION

Supplementary Table 3. Abiotic properties of the sand layer (means \pm SD) (Part II). In grey, samples that did not include sandy subsoil (fine-grained top layer thicker than 15 cm).

	Treatment	Age	Elev.	Organic content (%)		Sand content (%)		SD50 (μ m)		Soil structure
Small herbivores	Ungrazed		H	1.	0.	88.		184.		single grained
				1 \pm 3		7 \pm 1.5		8 \pm 2.5		
	Grazed	23	H	0.	0.	78.		186.		single grained
				8 \pm 1		2 \pm 2.1		0 \pm 1.5		
	Ungrazed		L	0.	0.	96.		208.		single grained
				7 \pm 1		3 \pm 2.9		6 \pm 1.9		
	Grazed		L	0.	0.	98.		203.		single grained
				8 \pm 2		0 \pm 3.1		1 \pm 4.9		
	Ungrazed		H	2.	1.	91.		190.		single grained
				1 \pm 2		8 \pm 4.0		8 \pm 4.2		
	Grazed	38	H	3.	2.	88.		195.		single grained
				5 \pm 0		6 \pm 5.5		8 \pm 9.5		
	Ungrazed		L	1.	0.	83.		189.		single grained
				4 \pm 0		9 \pm 0.0		3 \pm 0.0		
	Grazed		L							
	Ungrazed		H	1.	0.	95.		193.		single grained
				2 \pm 2		0 \pm 1.9		3 \pm 7.0		
	Grazed	53	H	1.	0.	94.		184.		single grained
				0 \pm 2		8 \pm 1.6		2 \pm 5.1		
	Ungrazed		L							
	Grazed		L							
Large herbivores	Ungrazed		H							
	Grazed	63	H							
	Ungrazed		L							
	Grazed		L							
	Ungrazed		H	2.	1.	83.	14.	166.		single grained
				0 \pm 1		1 \pm 7		3 \pm 28.1		
	Grazed	12	H	4.	2.	77.	10.	155.		single grained
		8		0 \pm 0		3 \pm 5		4 \pm 19.2		
	Ungrazed		L							
	Grazed		L							
	Mowed	20	H							
	Ungrazed	0	H							
	Grazed		H							
	Mowed	20	L							
	Ungrazed	0	L							
	Grazed		L							

Supplementary Table 4. Pearson correlations of the soil and vegetation variables and erosion (d_{max_lost}) in the large grazers area. Bold font indicates significant correlations ($p < 0.05$). All the variables were log transformed. RootDiam = root diameter (cm), RD.C = coarse root density (g cm⁻³), RD.F = fine root density (g cm⁻³), RhizD = Rhizome density (g cm⁻³), RDtot = total root density (g cm⁻³), Bulk = Bulk density (g cm⁻³), OC = Soil organic content (%), SWC = Soil water content (%), PenResist = soil resistance to penetration at 5 cm depth (Mpa), Silt = silt %, TotalBiom = total belowground biomass (roots + rhizomes) (g).

	TotalBiom	RootDiam	RD.C	RD.F	RhizD	RDtot	Bulk	OC	SWC	PenResist	Silt
RootDiam	0.53										
RD.C	0.89	0.57									
RD.F	0.97	0.45	0.78								
RhizD	0.81	0.55	0.71	0.69							
RDtot	0.99	0.51	0.89	0.98	0.73						
Bulk	0.91	0.6	0.77	0.93	0.65	0.93					
OC	0.44	-0.03	0.39	0.33	0.61	0.37	0.22				
SWC	-0.29	-0.45	0.13	-0.4	-0.08	-0.33	-0.5	0.56			
PenResist	0.76	0.4	0.59	0.79	0.6	0.76	0.83	0.45	0.34		
Silt	-0.69	-0.71	0.59	0.65	-0.72	-0.67	0.77	-0.18	0.42	-0.6	
d_{max_lost}	-0.95	-0.58	0.84	0.92	-0.8	-0.94	0.89	-0.38	0.31	-0.79	0.73

GRAZING AND LATERAL SOIL EROSION

Supplementary Table 5. Biotic properties of the fine-grained layer (means \pm SD) (Part I).

	Treatment	Age	Elev.	Vegetation type	Root Diameter (mm)		
Small herbivores	Ungrazed	23	H	<i>E. atherica</i>	0.08	\pm	0.01
	Grazed		H	<i>E. atherica</i>	0.06	\pm	0.02
	Ungrazed		L	Mixed spp.	0.09	\pm	0.01
	Grazed		L	Mixed spp.	0.08	\pm	0.00
	Ungrazed	38	H	<i>E. atherica</i>	0.07	\pm	0.00
	Grazed		H	<i>E. atherica</i>	0.07	\pm	0.01
	Ungrazed		L	<i>E. atherica</i>	0.07	\pm	0.01
	Grazed		L	Mixed spp.	0.09	\pm	0.01
	Ungrazed	53	H	<i>E. atherica</i>	0.10	\pm	0.03
	Grazed		H	<i>E. atherica</i>	0.06	\pm	0.01
	Ungrazed		L	<i>E. atherica</i>	0.06	\pm	0.01
	Grazed		L	Mixed spp.	0.09	\pm	0.01
	Ungrazed	63	H	<i>E. atherica</i>	0.07	\pm	0.01
	Grazed		H	<i>E. atherica</i>	0.07	\pm	0.01
	Ungrazed		L	Mixed spp.	0.08	\pm	0.01
	Grazed		L	Mixed spp.	0.08	\pm	0.01
	Ungrazed	128	H	<i>E. atherica</i>	0.08	\pm	0.01
	Grazed		H	<i>E. atherica</i>	0.08	\pm	0.01
	Ungrazed		L	<i>E. atherica</i>	0.07	\pm	0.01
	Grazed		L	Mixed spp.	0.09	\pm	0.01
Large herbivores	Mowed	200	H	Mixed spp.	0.08	\pm	0.00
	Ungrazed		H	<i>E. atherica</i>	0.07	\pm	0.01
	Grazed		H	<i>J. gerardii</i>	0.10	\pm	0.01
	Mowed	200	L	Mixed spp.	0.07	\pm	0.01
	Ungrazed		L	<i>E. atherica</i>	0.06	\pm	0.01
	Grazed		L	<i>J. gerardii</i>	0.08	\pm	0.02

Supplementary Table 5. Biotic properties of the fine-grained layer (means \pm SD) (Part II).

	Treatment	Age	Elev.	Root density (RDtot) (g/cm ³)		Coarse root density (RD.C) (g/cm ³)	
Small herbivores	Ungrazed	23	H	3.67	\pm 1.05	1.32	\pm 0.43
	Grazed		H	3.49	\pm 0.76	1.18	\pm 0.57
	Ungrazed		L	17.13	\pm 2.46	2.22	\pm 0.29
	Grazed		L	22.99	\pm 2.32	3.38	\pm 0.79
	Ungrazed	38	H	6.25	\pm 0.22	1.30	\pm 0.51
	Grazed		H	7.77	\pm 1.02	1.90	\pm 1.05
	Ungrazed		L	6.02	\pm 0.09	0.79	\pm 0.06
	Grazed		L	23.10	\pm 3.62	4.20	\pm 1.93
	Ungrazed	53	H	5.11	\pm 1.93	1.05	\pm 0.17
	Grazed		H	4.94	\pm 0.33	1.09	\pm 0.15
	Ungrazed		L	10.69	\pm 1.25	1.87	\pm 1.01
	Grazed		L	18.92	\pm 1.53	2.93	\pm 1.74
	Ungrazed	63	H	7.54	\pm 2.30	1.46	\pm 0.72
	Grazed		H	6.36	\pm 3.24	0.72	\pm 0.25
	Ungrazed		L	23.30	\pm 10.86	2.62	\pm 0.63
	Grazed		L	28.09	\pm 3.92	2.76	\pm 0.18
	Ungrazed	128	H	8.84	\pm 1.11	1.28	\pm 0.45
	Grazed		H	8.85	\pm 1.77	1.45	\pm 0.45
	Ungrazed		L	8.50	\pm 1.41	1.55	\pm 0.28
	Grazed		L	28.01	\pm 12.31	3.04	\pm 1.30
Large herbivores	Mowed	200	H	10.36	\pm 1.50	2.66	\pm 1.03
	Ungrazed		H	8.96	\pm 1.79	2.38	\pm 1.15
	Grazed		H	32.96	\pm 7.57	9.65	\pm 2.88
	Mowed	200	L	12.36	\pm 1.56	2.35	\pm 0.27
	Ungrazed		L	6.74	\pm 1.66	1.76	\pm 1.66
	Grazed		L	45.58	\pm 3.34	10.55	\pm 3.43

GRAZING AND LATERAL SOIL EROSION

Supplementary Table 5. Biotic properties of the fine-grained layer (means \pm SD) (Part III).

	Treatment	Age	Elev.	Fine root density (RD.F) (g/cm ³)		Total biomass (roots + rhizomes) (g)	
Small herbivores	Ungrazed	23	H	2.35	\pm 0.78	11.6	\pm 3.2
	Grazed		H	2.32	\pm 0.76	8.8	\pm 0.8
	Ungrazed		L	14.90	\pm 2.17	38.2	\pm 7.8
	Grazed		L	19.61	\pm 2.74	58.6	\pm 9.6
	Ungrazed	38	H	4.95	\pm 0.73	14.5	\pm 1.1
	Grazed		H	5.88	\pm 1.62	17.5	\pm 2.6
	Ungrazed		L	5.23	\pm 0.08	17.5	\pm 1.9
	Grazed		L	18.90	\pm 3.66	53.3	\pm 5.7
	Ungrazed	53	H	4.05	\pm 1.77	14.3	\pm 4.8
	Grazed		H	3.85	\pm 0.34	11.2	\pm 0.4
	Ungrazed		L	8.82	\pm 1.52	28.0	\pm 1.9
	Grazed		L	15.99	\pm 0.33	36.6	\pm 1.4
	Ungrazed	63	H	6.08	\pm 1.76	20.1	\pm 5.6
	Grazed		H	5.64	\pm 3.03	16.8	\pm 4.4
	Ungrazed		L	20.68	\pm 10.53	44.3	\pm 19.5
	Grazed		L	25.34	\pm 4.09	58.6	\pm 14.0
	Ungrazed	128	H	7.56	\pm 0.79	22.2	\pm 3.4
	Grazed		H	7.40	\pm 1.86	19.9	\pm 2.0
	Ungrazed		L	6.95	\pm 1.31	23.1	\pm 4.2
	Grazed		L	24.97	\pm 11.07	56.9	\pm 25.6
Large herbivores	Mowed	200	H	7.69	\pm 2.30	22.0	\pm 2.2
	Ungrazed		H	6.58	\pm 1.05	20.0	\pm 3.3
	Grazed		H	23.31	\pm 10.32	75.5	\pm 14.3
	Mowed	200	L	10.01	\pm 1.31	28.6	\pm 8.3
	Ungrazed		L	4.97	\pm 0.04	14.8	\pm 3.1
	Grazed		L	35.03	\pm 4.35	88.9	\pm 5.8

Supplementary Table 5. Biotic properties of the fine-grained layer (means \pm SD) (Part IV).

	Treatment	Age	Elev.	Rhizome density (RD.R) (g/cm ³)		Orchestia presence
Small herbivores	Ungrazed	23	H	2.97	\pm 0.79	yes
	Grazed		H	1.48	\pm 0.22	yes
	Ungrazed		L	4.87	\pm 2.18	yes
	Grazed		L	11.11	\pm 3.30	yes
	Ungrazed	38	H	2.01	\pm 0.43	yes
	Grazed		H	2.18	\pm 0.45	yes
	Ungrazed		L	3.99	\pm 0.79	yes
	Grazed		L	7.78	\pm 2.12	yes
	Ungrazed	53	H	3.05	\pm 0.93	yes
	Grazed		H	1.34	\pm 0.52	yes
	Ungrazed		L	5.08	\pm 0.98	yes
	Grazed		L	1.89	\pm 0.44	yes
	Ungrazed	63	H	3.72	\pm 1.20	yes
	Grazed		H	3.03	\pm 0.80	yes
	Ungrazed		L	2.37	\pm 0.68	yes
	Grazed		L	5.86	\pm 3.11	yes
	Ungrazed	128	H	3.37	\pm 0.80	yes
	Grazed		H	2.37	\pm 0.41	yes
	Ungrazed		L	4.54	\pm 1.01	yes
	Grazed		L	5.37	\pm 4.47	yes
Large herbivores	Mowed	200	H	1.90	\pm 0.37	1 sample only
	Ungrazed		H	1.92	\pm 0.87	yes
	Grazed		H	8.23	\pm 1.66	no
	Mowed	200	L	3.41	\pm 3.37	no
	Ungrazed		L	1.61	\pm 0.27	yes
	Grazed		L	4.23	\pm 0.56	no

GRAZING AND LATERAL SOIL EROSION

Supplementary Table 6. Pearson correlations of the soil and vegetation variables and erosion (d_{max_lost}) in the small grazers area. Bold font indicates significant correlations ($p < 0.05$). All the variables were log transformed. RootDiam = root diameter (cm), RD.C = coarse root density (g cm⁻³), RD.F = fine root density (g cm⁻³), RhizD = Rhizome density (g cm⁻³), RDtot = total root density (g cm⁻³), Bulk = Bulk density (g cm⁻³), OC = Soil organic content (%), SWC = Soil water content (%), PenResist = soil resistance to penetration at 5 cm depth (Mpa), Silt = silt %, TotalBiom = total belowground biomass (roots + rhizomes) (g).

	<i>d_{max} lost</i>	<i>Silt</i>	<i>PenRes</i>	<i>SWC</i>	<i>OC</i>	<i>Bulk</i>	<i>RDtot</i>	<i>RhizD</i>	<i>RD.F</i>	<i>RD.C</i>	<i>RootDiam</i>	<i>Total Biom</i>
	-0.66	0.04	0.67	0.16	-0.17	0.66	0.97	0.42	0.96	0.88	0.59	
	-0.56	-0.04	0.42	0.18	-0.12	0.6	0.62	0.1	0.64	0.45		
	-0.53	0.08	0.51	0.12	-0.11	0.47	0.87	0.29	0.82			
	-0.68	-0.07	0.65	0.27	-0.02	0.57	0.99	0.17				
	-0.27	0.36	0.43	-0.16	-0.58	0.56	0.2					
	-0.66	-0.05	0.63	0.24	-0.03	0.56						
	-0.7	0.51	0.76	-0.09	-0.7							
	0.23	-0.79	-0.47	0.47								
	-0.45	-0.34	0.07									
	-0.63	0.33										
	-0.19											



Fig. S1. Granular soil structure found at stage 53 yr, which led to higher erosion rates.

GRAZING AND LATERAL SOIL EROSION

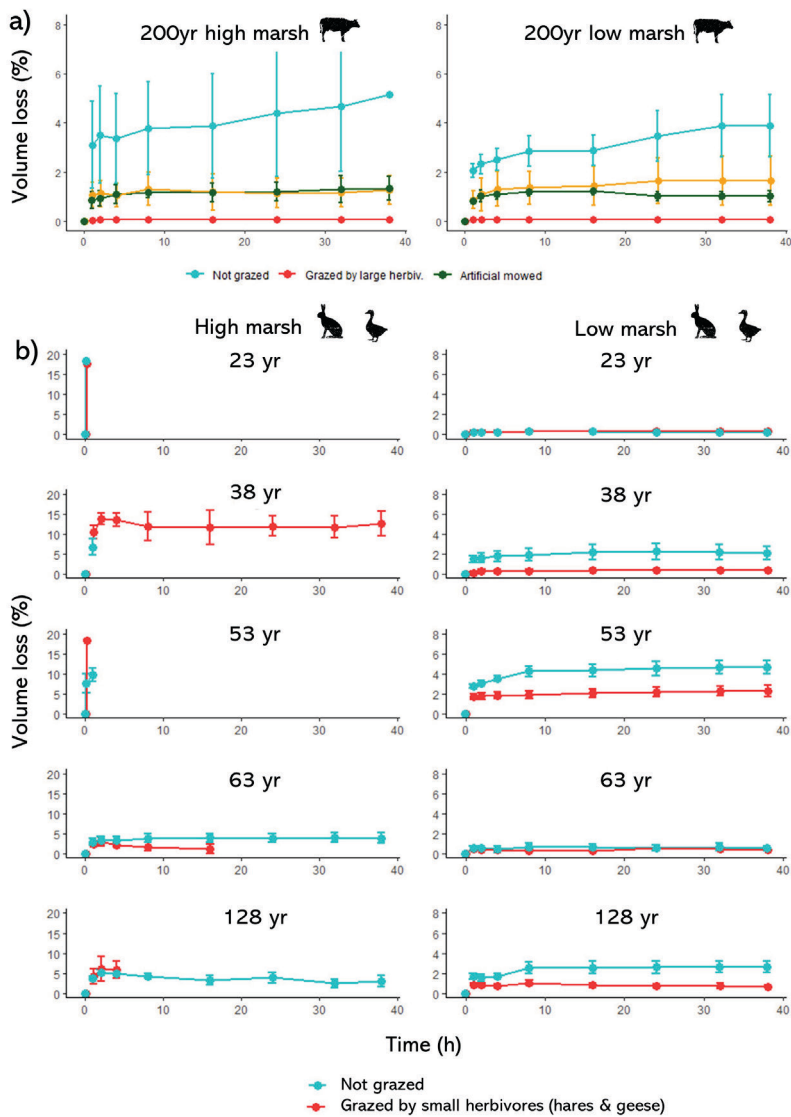


Fig. S2. Soil volume loss (%) over time for a) large grazers area and b) small grazers area.

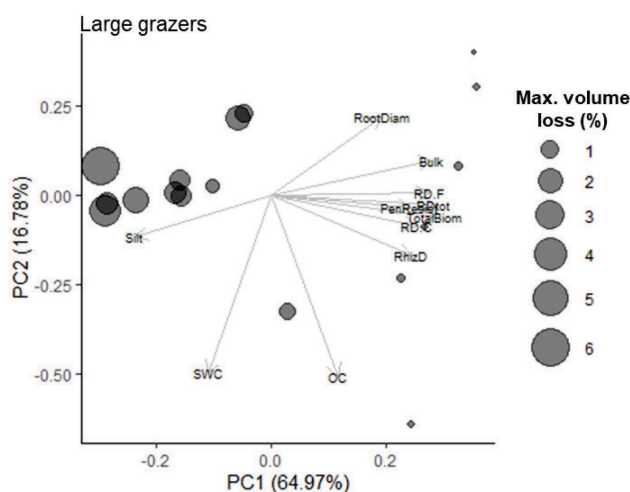


Fig. S3. Principal component analysis of the biotic and abiotic variables from the large grazers area. Size of the points indicate the maximum volume loss (%). RootDiam = root diameter (cm), RD.C = coarse root density (g cm⁻³), RD.F = fine root density (g cm⁻³), RhizD = Rhizome density (g cm⁻³), RDtot = total root density (g cm⁻³), Bulk = Bulk density (g cm⁻³), OC = Soil organic content (%), SWC = Soil water content (%), PenResist = soil resistance to penetration at 5 cm depth (Mpa), Silt = silt %, TotalBiom = total belowground biomass (roots + rhizomes) (g).

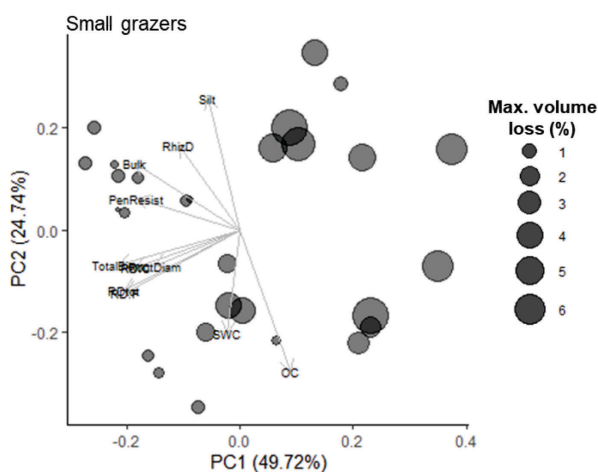


Fig. S4. Principal component analysis of the biotic and abiotic variables from the small grazers area. Size of the points indicate the maximum volume loss (%). RootDiam = root diameter (cm), RD.C = coarse root density (g cm⁻³), RD.F = fine root density (g cm⁻³), RhizD = Rhizome density (g cm⁻³), RDtot = total root density (g cm⁻³), Bulk = Bulk density (g cm⁻³), OC = Soil organic content (%), SWC = Soil water content (%), PenResist = soil resistance to penetration at 5 cm depth (Mpa), Silt = silt %, TotalBiom = total belowground biomass (roots + rhizomes) (g).



Chapter 7

On the use of large-scale biodegradable artificial reefs for intertidal foreshore stabilization

Beatriz Marin-Diaz, Gregory S. Fivash, Janne Nauta, Ralph J.M. Temmink,
Nadia Hijner, Valérie C. Reijers, Peter P.M.J.M. Cruijsen, Karin Didderen, Jannes
H.T. Heusinkveld, Emma Penning, Gabriela Maldonado-Garcia, Jim van Belzen,
Jaco C. de Smit, Marjolijn J.A. Christianen, Tjisse van der Heide,
Daphne van der Wal, Han Olf, Tjeerd J. Bouma, Laura L. Govers

Ecological Engineering (2021) 170: 106354

ABSTRACT

Combining foreshore ecosystems like saltmarshes and mangroves with traditional hard engineering structures may offer a more sustainable solution to coastal protection than engineering structures alone. However, foreshore ecosystems, are rapidly degrading on a global scale due to human activities and climate change. Marsh-edges could be protected by using connected ecosystems, such as shellfish reefs and seagrass beds, which can trap and stabilize sediments, thereby reducing hydrodynamics loads on the saltmarsh edge. In our study, we aimed to test the effect of large-scale biodegradable artificial reefs on tidal flat accretion and/or stabilization. We hypothesized that the structures would attenuate waves and trap sediment. For this, a large-scale experiment was conducted on the tidal flats of the Dutch Wadden Sea, by installing biodegradable artificial reefs along 630 m. Waves, sediment dynamics and sediment properties around the structures were monitored over three years. Our results demonstrate that intact structures attenuated circa 30 % of the wave height with water levels below 0.5 m. Variability in wave-attenuation increased when the wind direction was parallel to the structures/foreshore. Sediment dynamics were variable due to the exposed nature of the location and environmental heterogeneity because of the landscape-scale set-up. We observed local sediment accretion up to 11 cm. However, the effect did not expand beyond 10 m from the landward edge of the structures and up to 10 cm scouring was also found. Additionally, near sediment properties were not affected by the presence of the artificial reefs. Long-term effects could not be assessed due to the degradation of the structures during the experimental period. In general, we conclude that artificial reefs have the potential to attenuate waves and trap sediment on tidal flats. However, to benefit connected foreshore ecosystems like salt marshes, an even larger implementation scale and the use of more resistant structures in exposed sites is needed to affect long-term tidal flat morphology.

INTRODUCTION

Combining natural ecosystems, such as saltmarshes and mangroves, with hard engineering structures, such as sea walls and dikes, may enhance coastal flood protection compared to hard engineering alone, while simultaneously improving the foreshore ecosystem and its linked services (Temmerman et al. 2013; Schoonees et al. 2019). These foreshore ecosystems are able to attenuate waves (Barbier et al. 2011; Shepard et al. 2011), even under extreme storm surge conditions (Möller et al. 2014; Willemsen et al. 2020). Moreover, historic data demonstrated that marshes in front of a dike both reduce the chance of dike breaching during extreme events, and the size of dike breaches when dikes fails (Zhu et al. 2020). To be able to rely on natural ecosystems, such as saltmarshes and mangroves, for flood defence, their width must be persistent and predictable over time (Bouma et al. 2014). Ecosystems located in the lower intertidal, such as mussel beds or seagrass meadows, may facilitate the stability of protective natural ecosystems, such as salt marshes and mangroves (Gillis et al. 2014; van de Koppel et al. 2015). However, as these ecosystems located lower in the intertidal zone attenuate waves less effectively than upper intertidal salt marshes and mangroves (Bouma et al. 2014), they are often neglected.

The morphology of tidal flats is important for the stability of the edges of marshes and mangrove forests. Several recent studies show that higher, wider, convex and gentler sloping tidal flat profiles may attenuate waves more efficiently. This leads to reduced erosion in the pioneer vegetation zone of a salt marsh (Mariotti and Fagherazzi 2013; Hu et al. 2015; Bouma et al. 2016; Willemsen et al. 2017). In this context, oyster and mussels beds that occur much lower in the intertidal than salt marshes, may be efficient in protecting the marsh edge from eroding by attenuating waves and inducing accreting conditions (Meyer et al. 1997; Borsje et al. 2011; Donker et al. 2013; Walles et al. 2015). Seagrass beds can also attenuate waves and stabilize the sediment, and may therefore also improve stability and morphology of tidal flats (Fonseca and Cahalan 1992; Bos et al. 2007; Christianen et al. 2013, chapter 5).

To date, many natural foreshore ecosystems are degrading due to sea level rise, changes in sediment supply, eutrophication, overexploitation and ocean sprawl among others (Bishop et al. 2017; Ladd et al. 2019; Murray et al. 2019). Additionally, landward migration of foreshore ecosystems to keep pace with sea level rise is often prevented due to the presence of dikes and sea walls (Doody 2013). As a result, coastal ecosystems are steepening, thereby making protective natural ecosystems, such as salt marshes and mangroves more prone to edge erosion, and lowering benefits from physical facilitation by lower intertidal ecosystems. In such situations, foreshore erosion is typically reduced by using hard-engineered coastal structures such as groynes and breakwaters (Schoonees et al. 2019; Siemes et al. 2020), stone dams (Van Loon-steensma and Slim 2013) or concrete reefs (Chowdhury et al. 2019). Trials of more environmentally friendly options, such as the restoration of biogenic reefs (e.g. dominated by oysters or mussels) at a large scale and at exposed sites remain scarce (Bouma et al. 2014;

Morris et al. 2018), and their success is often negatively affected by the strong hydrodynamics (Paoli et al. 2015; Schotanus et al. 2020).

BESE-biodegradable artificial reef-structures (<https://www.bese-products.com>), have been shown to be suitable for restoring mussel beds, seagrass and marsh vegetation at small scales (Fivash et al. 2020; Temmink 2020; Temmink et al. 2020). In addition having such hard structures in the tidal flat could change the tidal flat morphology, which ultimately could be beneficial for adjacent saltmarsh stability. In this study, we aimed to test how the use of these biodegradable artificial reef-structures at a larger scale would 1) attenuate waves, 2) change tidal flat morphology, and 3) affect the near surrounding sediment properties. We hypothesized that artificial reef structures would promote sediment accretion, but that long-term morphological effect of these structures would depend on their structural integrity. For this, we set up a large-scale experiment on the tidal flats of the Dutch Wadden Sea, consisting of BESE-biodegradable artificial reef-structures along 630 m, which also provided hard substrate for mussel settlement (Temmink et al. 2020).

METHODS

Study site

The Wadden Sea is a very extensive intertidal flat system listed as UNESCO World Heritage since 2009 and part of the Natura 2000 protected areas in Europe. This shallow inland sea stretches for ~500 km along the coast of the Netherlands, Germany and Denmark. Natural reefs of blue mussel (*Mytilus edulis*), which declined in the 1990 due to overfishing and are slowly recovering, and Pacific oyster (*Crassostrea gigas*), which was introduced in 1960, do occur in this area (Christianen et al. 2017a; Folmer et al. 2017). The field experiment was conducted on an exposed intertidal area south of Griend, a fetch-limited island in the Dutch Wadden Sea (53°14'24.97"N, 5°14'53.56"E) (Fig. 1a). The tidal flat is sandy and long straight bedforms of approximately 2 to 6 cm high and 10 to 30 m width can be observed on the flat (Fig. 1b and A. 3). In this area, the normal tidal range is ~190 cm (RWS 2013). Wind direction and wind speed during the experimental period were obtained from the Royal Dutch Meteorological Institute (KNMI), recorded in the weather station of Vlieland, at ~11 km from Griend (53°17'49.4"N 5°05'27.6"E).

Study design and deployment of the artificial-reef structures

The experimental set-up consisted of sixteen plots installed perpendicular to the nearest gully at a mean elevation of -0.32 ± 0.003 m NAP (Dutch ordinance level, close to the Dutch mean sea level) and a mean inundation frequency of 65% (Fig. 1b). Plots were grouped in blocks (n=4 blocks) with plots randomly assigned to either i) unmodified control (from here on called 'Control') or ii) artificial reef treatment (from here on called 'Reef'). Each artificial reef plot consisted of ten bands of 5 m long, each one made of 5 modules which consisted of 8 layers

of stacked biodegradable BESE-sheets of 91.5x45.5x2 cm (L x W x H) (Fig. 1c). The BESE is made from biodegradable potato-waste derived Solanyl C1104M (Rodenburg Biopolymers, Oosterhout, the Netherlands). Each module was braided with 70 m of coir rope and placed on anti-erosion coir mats (~ 4 cm thick) and secured with 1.5 m long L-shaped anchors. Once the modules were installed, the height of the artificial reefs was ~ 20 cm above the bed level. In total, the plots measured 20 x 10 m (Fig. 1c). Control plots were completely bare and unmodified (Fig. 1d). The reef structures were deployed in March of 2017 and monitoring was conducted in May 2017, August 2017, August 2018 and August 2019 (Fig. 1e).

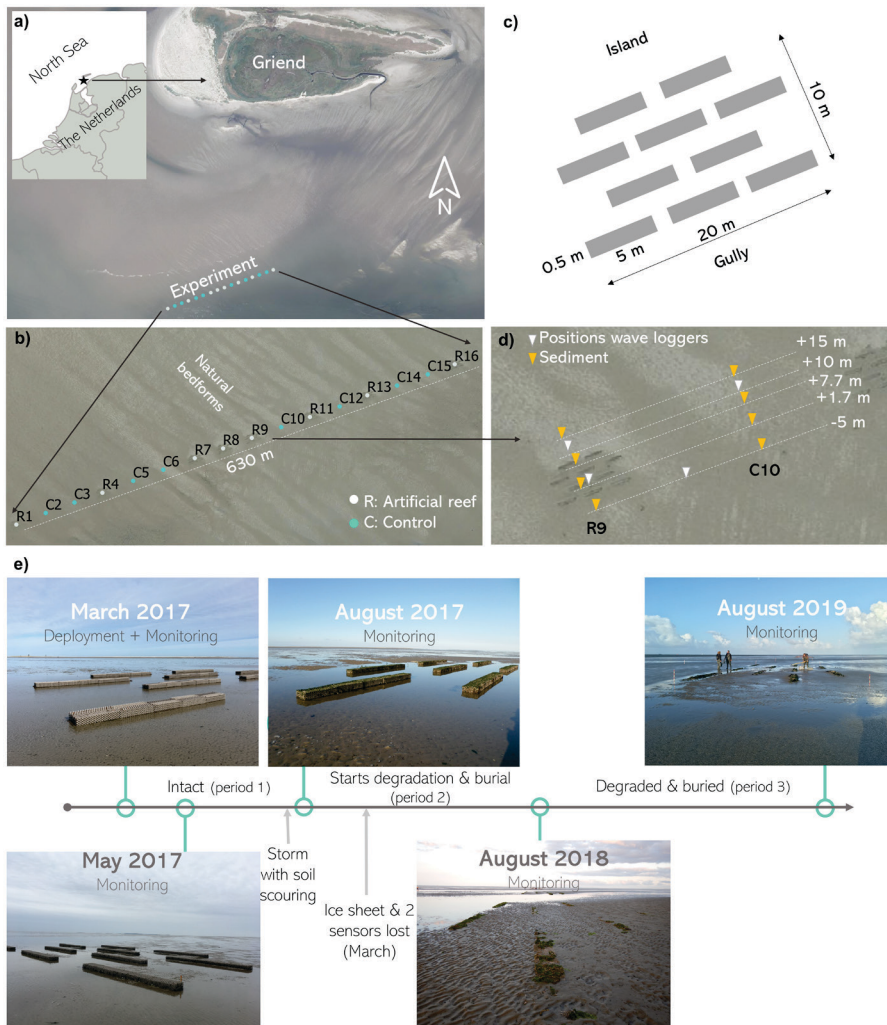


Fig. 1. a) location of the experiment in the southern tidal flat of Griend, b) plots of the experiment and view of the large bedforms in 2017, c) set-up of an artificial reef plot consisting of 10 bands, d) position of the wave loggers in plot number 9 (artificial reef) and plot number 10 (control) and the distances where sediment samples were collected; and e) timeline of the experiment and degradation of the structures.

Wave measurements and data analyses

Four pressure sensors (wave loggers, OSS1-10-003C) were deployed 10 cm above the bed level in the artificial reef plot R9 and the control plot C10, which were randomly selected, to monitor the effect of the artificial reef on wave dampening. We assumed similar effects for the other reefs, which were all located in the same orientation (340°) and tidal elevation. The reference sensor was located -5 m seaward between the plot R9 and C10 (Fig. 1d). Two other sensors were located in the plot R9 in between the artificial reef (+1.7 m) and +10 m landward from the artificial reef and one sensor in the control C10 at the same distance as the sensor at +10 m from the artificial reef. Data was recorded between March 2017 to August 2017 (period 1), September 2017 to January 2018 (period 2) and January 2019 to March 2019 (period 3) (Fig. 1e). These periods were categorized based on the wave logger deployment and measurements of the degradation of the structures. Unfortunately, the sensor in the control plot got lost as a result of ice-sheet formation on the tidal flat in March 2018. Therefore, the analysis of period 2 and 3 only include the sensors in the artificial reef plot.

Data was recorded with a 7-minute interval every 15 minutes with a measuring frequency of 10 Hz. For every sensor, significant wave height (H_s) was determined through spectral analysis of the wave time series after correcting for air pressure (Appendix R script). To reduce stochasticity in the wave attenuation analysis, records with $H_s < 0.05$ m (too small), $H_s/h < 0.2$ (waves too small relative to the water level) and $H_s/h > 0.4$ (higher probability of breaking waves) were excluded (Kroon 1994; Donker et al. 2013). H_s was then split into tidal cycles and categorized into rising or falling tide. H_s and mean water depth during the highest point of the tides, considered stable sea state, were used to relate to wind conditions. Wave attenuation was calculated as the percentage of H_s reduction between the reference sensor and the sensors in the artificial reef R9 and control C10.

Bed level change and reef degradation

Tidal flat elevation was monitored along 5 evenly-spaced transects of 105 m long in each plot via rtk-dGPS. The transect started -5 m seaward from the artificial reefs and finished 100 m landwards of the reefs. The vertical resolution was 1 mm. Horizontally, the interval of measurements was 10 m at the large scale and 1 m at the local scale. These measurements were taken in March 2017 (only the central transect per plot), May 2017, August 2017 (not all the plots completed), August 2018 and August 2019. Digital elevation models (DEM) were created with a grid cell of 10 cm for each time-step by interpolating the dGPS points using the natural neighbour method from QGIS software. Elevation change was calculated at a large scale (plots of 20 x 105 m) and at local scale (reef section of 20 x 10 m) by subtracting each time-step DEM from the initial DEM from March 2017. Estimation of the artificial reef height degradation over time was calculated as the difference in the reef elevation for each time-step compared to March 2017. The artificial reef elevation was measured in the central transect of each plot by placing the dGPS on the top of the artificial reef.

Sediment properties

To investigate the effect of the artificial reefs on the edaphic conditions over time, sediment properties were determined across the central transect at positions -5, +1.7, +7.7 and +15 m in the 12 most westward plots (1 to 12, $n=6$ for each treatment) (Fig. 1d). Sediment properties were determined from samples of the top 5 cm of sediment, collected with a 3 cm \varnothing core. Sediment samples were freeze dried during four days and sieved with a 0.8 mm mesh. Grain size was determined for all time steps using a Malvern® Mastersizer 2000. Organic matter content was determined by weight loss on ignition (LOI, 4h at 550°C) during all monitoring campaign until August 2018.

Statistical analyses

Relationships between wave attenuation and water depth were explored with Spearman's rank correlations. Two-way ANCOVAs were used to test differences on slopes of wave attenuation between i) the control plot and artificial reef plot (inside the reef and + 10 m landward from the reef) and ii) rising and dropping tide, with mean water depth as a covariate (i.e. slopes were considered different when the interaction between treatment and water depth was significant). To further test the effect of wave attenuation by the reef at different water depths during period 1, the water depth was categorized into 3 groups (from 0.15 to 0.3, 0.3 to 45 and 0.45 to 0.6 m water depth). Two-way ANOVAs were performed with treatment and water level as factors and wave attenuation as response variable, followed by Tukey post hoc test for i) data including all the wind directions to have an overall effect, ii) data only including wind directions coming perpendicular to the set-up to avoid possible confounding effects due to the wind direction (i.e. both control and reef were subjected to the same waves coming offshore). Differences in i) maximum sediment accretion per plot and ii) maximum erosion per plot, iii) standard deviation of the accretion per plot and iv) net sediment accretion per plot, between control and artificial reef plots were analysed with a 3-way ANOVA including block and time. Tukey HSD post-hoc tests were used to distinguish significant differences between groups. Linear mixed models were used to study the main and interactive effects of the artificial reefs, time and position on the transect on sediment grain size and sediment organic content, with block as random effect. The significance of the fixed factors was tested with the Type II Wald Chi-square test. Assumptions of normality and homogeneity of variance were analysed with histograms and residual plots. Wave attenuation, when including all the wind directions, contained several outliers and was cube root transformed, and in addition to the two-way ANOVA, Kruskal-Wallis non-parametric tests were performed to confirm the results. All statistical analyses were performed using R 3.5.0 (R Development Core Team 2018). The lme4 package (Bates et al. 2014) was used for the linear mixed models.

RESULTS

Wave attenuation and reef height reduction over time

The artificial reef structures were still intact in May 2017 and August 2017. The differences in the SD likely came from measurement error in the field. In August 2018, after a winter with heavy storms and abrasion by ice sheet formation, the artificial reefs lost around 12 cm of height. This was around 50% of the initial elevation. In August 2019, the artificial reefs lost another 2 cm, which left a reef of circa 6 cm height (Table 1, Fig. 2e).

Table 1. Mean cumulative degradation of the artificial reefs height over time (\pm SD), with respect to the initial installed height (~ 20 cm).

	May 2017 (n=16)	August 2017 (n=16)	August 2018 (n=16)	August 2019 (n=16)
Mean cumulative artificial reef height degradation (cm)	0.0 \pm 2.4	0.0 \pm 2.2	-12.6 \pm 2.5	-14 \pm 1.9
Remaining reef height (cm)	~ 20 (intact)	~ 20 (intact)	~ 8 (degraded)	~ 6 (degraded)

From March 2017 to August 2017, the artificial reef, either inside and + 10 m landward, attenuated significant wave heights on average by 30 %, reaching a maximum of 60 %, when compared to the bare plot, including all the wind directions (Fig. 2a). The amount of wave attenuation was dependent on the water depth (ANCOVA for period 1: $F_{2,519} = 7.1$, $p < 0.001$) (Fig. 2a). There were no significant effects in attenuation during the rising or dropping tide (ANCOVA for period 1: $F_{1,519} = 0.8$, $p = 0.3$). Including all wind directions, attenuation by the reefs was significantly higher compared to the control with water levels below 0.5 m, but not with higher water levels (two-way ANOVA: $F_{2,1719} = 283.4$, $p < 0.001$ [effect of the treatment]) (Fig. S1 and S2a). When analysing the wave attenuation data from only days with winds perpendicular to the set-up (130 to 190 degrees, therefore reef and control subjected to the same waves coming offshore), the results were the same but the variability was reduced, confirming the effect of the reef (two-way ANOVA: $F_{2,132} = 28.9$, $p < 0.001$ [effect of the treatment]) (Fig. S2b). The highest variability in wave attenuation therefore occurred during tides with winds coming from directions not perpendicular to the set-up, primarily from the south west (200 - 300 degrees), which were lateral to the experimental set-up (Fig. 3). In addition, these south west winds had the highest wind speeds and were related to higher mean water depth and significant wave height, therefore, related to less wave attenuation by the artificial reefs (Fig. S3).

The mean attenuation by the artificial reef started to decrease below 30 % after September 2017 due to the reef degradation and was absent from September 2017 onwards (ANCOVA for period 2: $F_{1,310} = 0.7$, $p = 0.37$; and period 3: $F_{1,208} = 0.03$, $p = 0.84$) (Fig. 2b,c).

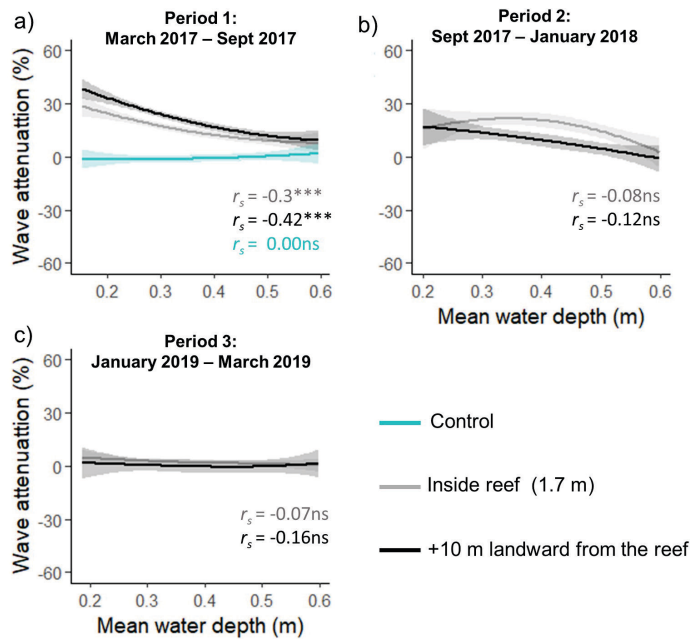


Fig. 2. Wave attenuation by the artificial reef compared to the bare tidal flat (control) including all the wind directions during a) March 2017 to August 2017, with intact reef, b) September 2017 to January 2018, with the reef starting to degrade and the control sensor lost, and c) January 2019 to March 2019, with degraded and buried reef and control sensor lost. The mean water depth is only shown until 0.6 m, where the effect of the reefs was negligible. Significant codes refer to $p < 0.001$ (***) and $p > 0.05$ (ns).

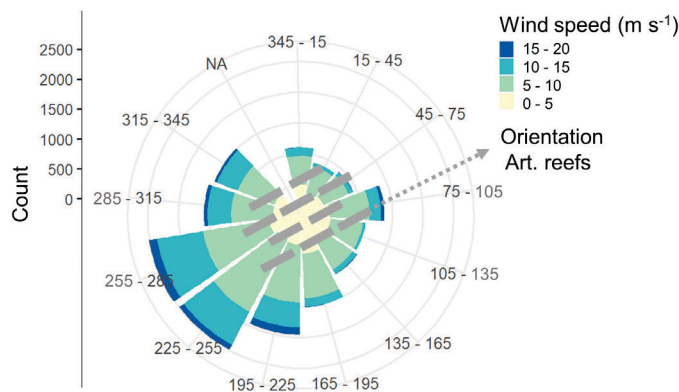


Fig. 3. Wind speed and wind directions during the experimental period. The grey blocks indicate the position of the artificial reef modules with respect to the north and how they were parallelly exposed to the predominant wind direction (200-300 degrees). Frequency of each wind type (combination of wind direction and wind speed) are represented as count in the length of the bins.

Effect of the artificial reefs on sediment dynamics

Due to the high exposure of the study site and the migrating large bedforms, there were strong and complex large-scale sediment dynamics in the experimental area (Fig. 4). The effect of the artificial reefs on sediment dynamics did not expand beyond 10 m from the landward edge of the structures and varied between plots. The migration of natural bedforms, unrelated to the experiment, interfered with the measurement of changes in bed level caused by the artificial structures, however, the effect of the reefs was still visible (Fig. S4). The magnitude of these effects can best be seen in the changes in bed level in the control plots. Satellite images of these migrating bedforms between 2017 and 2019 can be found in Fig. S5.

At the local scale (plots of 20 x 10 m, Fig. 1), both sediment trapping and scouring often occurred simultaneously within a single plot (Fig. 4 and 5a,b,c). Overall, most of the reefs significantly increased the maximum elevation locally up to 11 cm compared to the controls, independently of time and block (3-way ANOVA: $F_{1,30} = 27.86$, $p < 0.001$). However, the first two reef plots always accreted less due to the large bedforms unrelated to the experiment (Fig. 4 and 5b). At the same time, some reefs also induced higher scouring than the control plots (3-way ANOVA: $F_{1,30} = 9.1$, $p = 0.004$) (Fig. 5b,c), leading to more variable elevation within each reef plot (3-way ANOVA: $F_{1,30} = 28.6$, $p < 0.001$) (Fig. 5d). Due to the balance between eroding and accreting zones within each single plot and the first two reefs which had more erosion, the overall effect of the reefs on the net accretion at the local scale during all the experimental period did not significantly differ from the controls (3-way ANOVA: $F_{1,30} = 1.89$, $p = 0.17$) (Fig. 5e).

In May 2017, the maximum accretion within reefs was 6 cm compared to the 3 cm in the control plots, while the net accretion was ~ 0 cm for both treatments. In August 2017, the net sedimentation was negative (~ -4 to ~ -2 cm), while the maximum accretion within the reefs was 5 cm and 4 cm in the controls. In August 2018, mean net accretion was around 0 cm, and although the structures started to degrade, sediment was still trapped by the reefs up to 11 cm, with the highest sediment accretion occurring in the five centre-most reef plots. The sedimentation pattern of the artificial reefs was related to the migrating bedforms, with higher sediment deposition in the areas where the crest of the bedforms encountered a reef (Fig. 4, Fig. S4 and S5). Lastly, in August 2019, when the artificial reefs were in their most degraded state, mean net accretion was around 0 cm in the reefs and - 3 cm in the controls. However, sediment accretion up to 6 cm was still present in the five centre-most reef plots, compared to a maximum of 3 cm in the controls (Fig. 4, 5b, and Fig. S4).

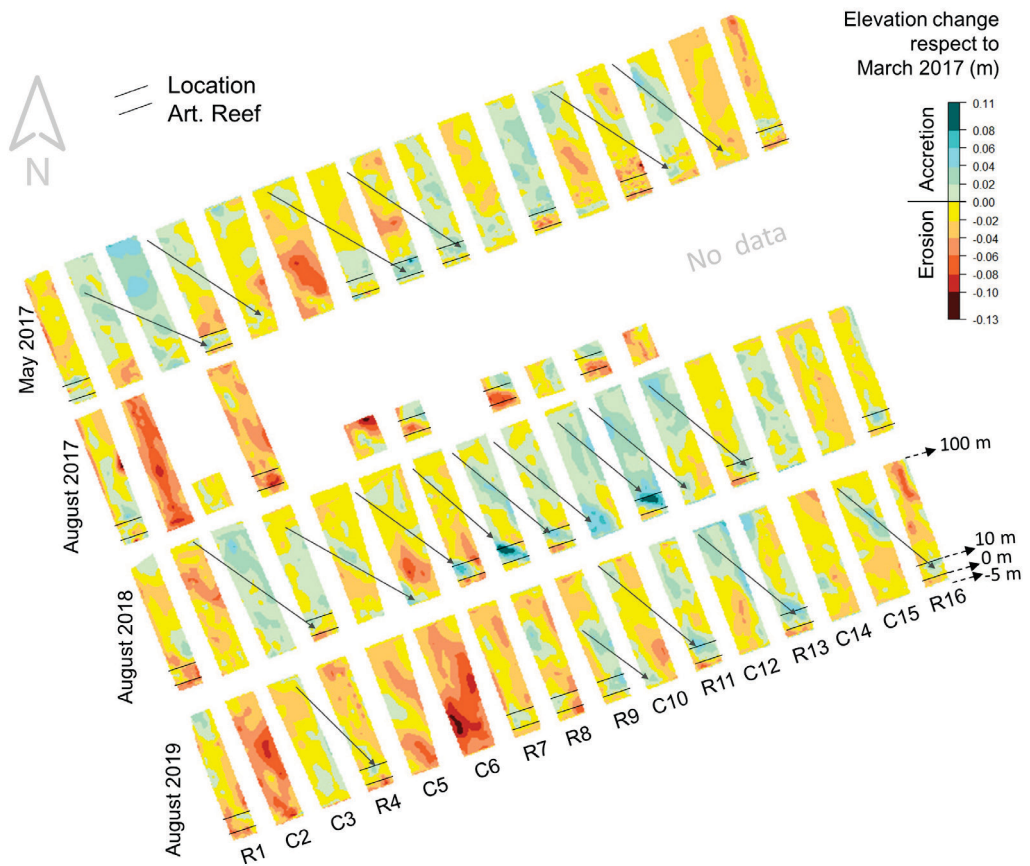


Fig. 4. Digital elevation models (DEM) of the 105 m transects showing the elevation changes for each time period compared to the initial elevation in March 2017. Arrows indicate the direction of the crest of some of the large bedforms and black lines the location of the artificial reefs. During the whole experimental period, there were areas with up to 13 cm of erosion (dark red areas) and areas with up to 11 cm accretion (dark green areas).

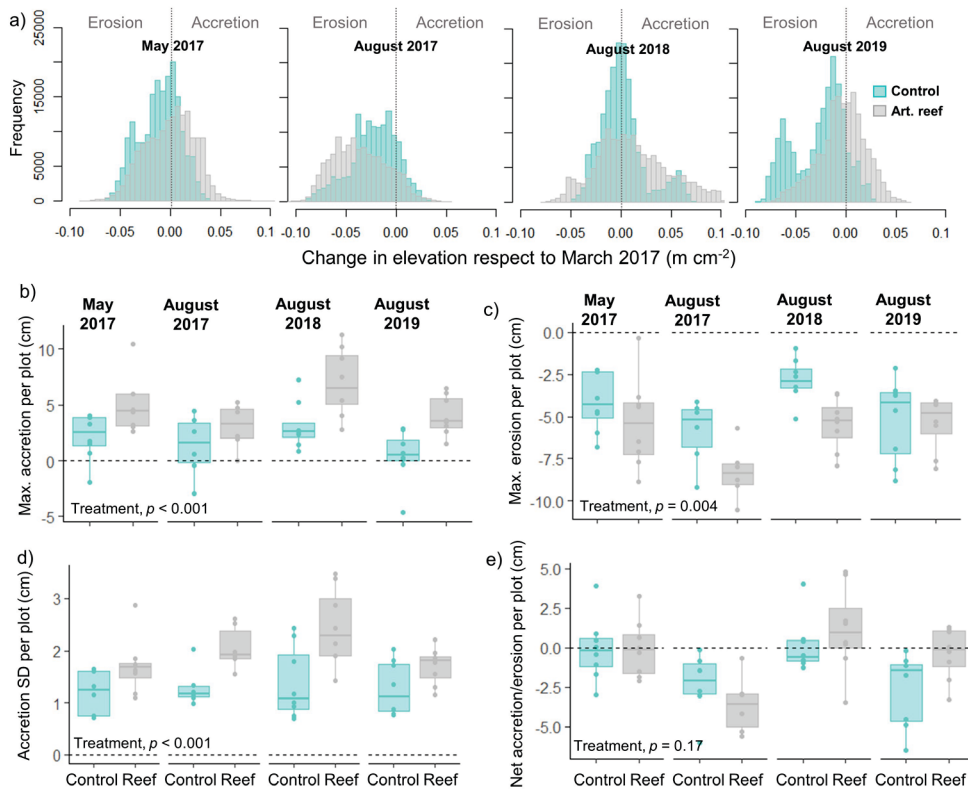


Fig. 5. a) Distributions of the elevation changes (m) per pixel (1 cm²) in control and artificial reefs plots at a local scale (plot of 1.0 x 20 m); and boxplots of the b) maximum accretion per plot (cm), c) maximum erosion per plot (cm), d) standard deviation of the accretion per plot (cm) and e) net accretion/erosion per plot (cm), all at a local scale and separated by treatment and time-step. *P* values correspond to 3-way ANOVAs.

Effect of artificial reefs on sediment properties

Overall, sediment properties did not significantly differ between control and artificial reef plots [$\chi^2(1) = 0.003$, $p = 0.95$ (mean grain size), $\chi^2(1) = 0.21$, $p = 0.64$ (silt %), $\chi^2(1) = 1.57$, $p = 0.21$ (organic matter %)] (Fig. S6). Variability in these properties was mainly found over time. Mean grain size ranged from 180 to 240 μm and overall smaller grain sizes were found in August 2017 ($\chi^2(3) = 38.74$, $p < 0.001$). Silt % ranged from 0 to 6.5 %, being lower in August 2017 ($\chi^2(3) = 53.22$, $p < 0.001$). Organic matter ranged from 0.6 to 1.18 % and was significantly lower in August 2017 ($\chi^2(3) = 153.01$, $p < 0.001$).

DISCUSSION

Ecosystem-based or nature-based coastal defence provides a promising coastal protection framework (Temmerman et al. 2013; Schoonees et al. 2019). Hence, there is need for understanding how we can use low-intertidal tidal flat ecosystems to stabilize wave-attenuating high intertidal coastal systems, by making use of cross-habitat connectivity. Our study is the first of its kind to experimentally test the potential of biodegradable artificial reefs for foreshore coastal protection through tidal flat stabilization. In this study, we tested the use of a 630 m long biodegradable artificial reefs for attenuating waves and stabilizing and accreting sediment on a tidal flat, as alternative to hard engineering structures typically used for this purpose (Schoonees et al. 2019). We showed that the artificial reefs could reduce wave heights up to 60 % and on average 30%, compared to the adjacent bare tidal flat, despite being placed in a highly exposed area. Interestingly, we discovered that artificial reef effects on local sediment dynamics interfered with migrating bedforms, as result of the scale of our experiment. However, it was still clear that biodegradable reefs were able to accrete sediment at a local scale, depending on the time the ephemeral reefs persisted. In addition, surrounding sediment properties were not affected by the presences of the structures. The use of biodegradable artificial reefs looks promising for local and temporal tidal flat stabilization due to wave attenuation and sediment trapping, but promoting large-scale connectivity between tidal flats and high intertidal systems such as salt marsh would require a much larger spatial scale than our current experiment.

Wave attenuation by biodegradable artificial reefs and interaction with wind conditions

The ratio of water depth to structure height is an important variable for wave attenuation. The higher the water levels relative to the structure height, the less attenuation will occur (Möller et al. 1999; Ysebaert et al. 2011; Yang et al. 2012; Chowdhury et al. 2019). In our experiment, waves were attenuated mainly during the first measurement period (March 2017 to August 2017) when artificial reefs were still ~20 cm high and only when water levels were below 0.5 m. Wave attenuation by vegetation or reefs also depends on the relative wave height (significant wave height relative to the water depth, H_s/h) (Möller 2006; Ysebaert et al. 2011; Yang et al. 2012; Donker et al. 2013). In our study, small values of H_s/h (< 0.2) led to less attenuation because either the water was too deep or the waves too small to interact with the reefs. In contrast, high values of H_s/h (> 0.4) which can lead to wave breaking were also less attenuated (Kroon 1994; Donker et al. 2013). Lastly, in our study, an increase in attenuation variability appeared when strong winds were coming from the south west, which led to higher water levels and wave heights. In addition, these winds were parallel to the set-up; instead of perpendicular, which obviously greatly reduce the efficiency of wave attenuation. Overall, this indicates that the orientation of the structures relative to the wind direction may determine their wave attenuating and thus stabilizing effects. However, as our experiment was near an island, the wind conditions

pushing waves over the reef can vary much more widely compared to a much wider mainland foreshore.

Effect of the biodegradable artificial reefs on tidal flat sediment dynamics

The installation of stiff structures in a tidal flat can lead to sediment erosion and accretion patterns within the structures and in the near surroundings (Bouma et al. 2007, 2009b; Walles et al. 2015). In our study, the installation of artificial reefs in the tidal flat also led to both erosion (up to -11 cm) and accretion (up to $+11$ cm) at the local scale (~ 10 m landwards from the reef). Interestingly, the sedimentation pattern of the artificial reefs was related to the migrating large bedforms, with higher sediment deposition in the areas where the crest of the bedforms encountered a reef (Fig. S4 and S5). This accretion was more evident in August 2018 and mainly in the landward side of the structures. In contrast, in August 2017, when the structures were still intact, more sediment scouring and erosion was observed. This suggests that whereas higher structures can lead to higher wave attenuation, it can also lead to higher sediment scouring due to enhanced turbulences.

Migrating bedforms have been found in different areas of upper tidal flats in the Wadden Sea, and are influenced by the tidal dynamics (Donker et al. 2013; Adolph et al. 2018). These migrating bedforms led to values of sediment accretion in control plots in this study. However, the maximum sedimentation in the reefs plots was still higher compared to controls, confirming their effect on sediment accretion. This sedimentation in the field can be visualized in the Figure S4. Nevertheless, the net accretion, taking into account all areas that eroded and accreted, was always similar in reef and control plots. Sediment could be trapped due to the wave attenuation effect, but likely due to flow attenuation (Bouma et al. 2007, 2009b; Donadi et al. 2013; Colden et al. 2016) as observed in August 2019 when the reefs were degraded thus not attenuating waves but still accreting sediment compared to the control plots. This indicates that although ~ 6 cm high reefs did not affect wave attenuation, they likely affected the sediment dynamics by attenuating the water flow. Flow attenuation and subsequent sediment trapping by this type of artificial reefs has been demonstrated in a flow flume experiment, where flow velocities were attenuated by an order of magnitude compared to a bare treatment (from 8.5, 14.5, and 23 cm/s to 0.7, 1.6, and 2.5 cm/s) over the first 50 cm of a 6 cm high BESE structure (Fivash et al. 2021).

Effect of the biodegradable artificial reefs on sediment properties

Natural shellfish reefs can change their environmental surrounding, both biotic and abiotically by creating calm conditions and/or by their faeces and pseudo-faeces (Donadi et al. 2013, 2015; Salvador de Paiva et al. 2018). By installing artificial reefs, we were expecting an increase in organic matter or fine sediments by the creation of calmer conditions and by the possible mussel establishment on the reefs which could produce faeces and pseudo-faeces (Donadi et al. 2015; Chowdhury et al. 2019). However, although sedimentation was observed and mussel establishment occurred (Temmink 2020), the artificial reefs did not have an overall significant

effect on sediment properties compared to the control plots. This may be due to the high exposure of the site, which did not let to settle changes in the sediment properties or because higher mussel densities during a longer period were needed to observe a significant effect (Temmink 2020).

Application of biodegradable artificial reefs for coastal protection

The results of this study on the effect of biodegradable artificial reefs on tidal flat stabilization together with the mussel establishment observed (Temmink 2020), emphasizes the importance of distinguishing the application of these structures depending on the aim: ecological (i. e. mussel bed restoration) or engineering (i. e. stabilization of the tidal flat) as previously pointed out by Morris et al. (2019). Mussel bed restoration is sensitive to strong hydrodynamics (Paoli et al. 2015; Schotanus et al. 2020), and often it is exactly at these locations where management for coastal protection is needed. In addition, the effect of the artificial reefs on trapping sediment, which is desired for coastal protection, may counteract the mussel establishment (Walles et al. 2016b; Temmink 2020).

Overall, our set-up was not sufficiently resistant to persist long term, or to sustain a stable mussel reef which would overtake the effect of the artificial reefs on trapping sediment. Moreover, the set-up was not large enough to have a significant large scale effect in the tidal flat morphology. If the aim is solely to restore mussel beds using biodegradable artificial reefs, a more sheltered location may be preferred (Piazza et al. 2005). In the other hand, if the aim is to integrate ecosystem restoration as part of a coastal protection scheme, aimed at long-term tidal flat stabilization at an exposed location, it would be recommended to use a large set-up with more resistant material. For example, one should build wider and longer structures as well as dispose the blocks along the foreshore but also across the foreshore. This would help to attenuate hydrodynamics in a bigger area and therefore have a larger effect on sediment stabilization (Walles et al. 2015). The width of the bedforms occurring at the tidal flat could be a good starting point to design the length of each reef plot. For example, in our system this could be between 10 to 30 m, which is similar to the length of the natural bed-forms. Also, the installation of more bands of reefs going landwards and perpendicular to the bedforms or flow direction could create sedimentation in a larger area (Colden et al. 2016). The orientation facing the tidal flow direction may be the most effective for sediment trapping because as seen in this study, even when not reducing waves due to the degradation of the structures height, they could still trap sediment likely due to flow attenuation. If using higher structures, a test of the resistance of the material and effect on sediment dynamics should be done because this could increase scouring. Lastly, installing the reefs higher in the tidal flat could have a greater impact on the marsh, but the feasibility of it on developing on a mussel bed will depend on the tidal range and flood frequency of the location for the biogenic reef establishment and survival (Walles et al. 2016a).

ACKNOWLEDGEMENTS

This work is part of the Perspectief research programme All-Risk with project number P15-21 project B1 which is (partly) financed by NWO Domain Applied and Engineering Sciences, in collaboration with the following private and public partners: the Dutch Ministry of Infrastructure and Water Management (RWS), Deltares, STOWA, the regional water authority Noorderzijlvest, the regional water authority Vechtstromen, it Fryske Gea, HKV consultants, Natuurmonumenten, waterboard HHNK. LLG was supported by NWO-VENI grant 016.VENI.181.087. H.O., E.P and L.L.G were funded by Waddenfonds and Rijkswaterstaat, for the project 'dynamic Griend'. T.v.d.H, L.L.G and V.C.R. were additionally funded by OBN. R.J.M.T., G.S.F. and K.D. were funded by NWO/TTW-OTP grant 14424, in collaboration with private and public partners: Natuurmonumenten, STOWA, Rijkswaterstaat, Van Oord, Bureau Waardenburg, Enexio and Rodenburg Biopolymers. T.v.d.H. was funded by NWO/TTW-Vidi grant 16588. In addition, we would like to thank the anonymous reviewers for their constructive comments in the previous version of this manuscript, to all volunteers who helped with setting up and monitoring the experiments, to Sien, Saar and Jouke who have hosted us on the Ambulant and to the crew of the Asterias from the 'Wadden Unit' for enabling transport to and from the experiment. The authors declare no conflict of interest.

SUPPORTING INFORMATION

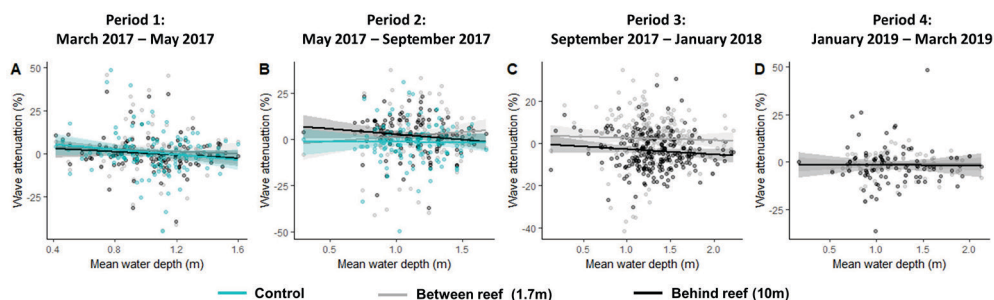


Fig. S1. Significant wave height attenuation during high tide comparing reef and control plot. It can be observed that with high water levels the attenuation by the reef is not existent.

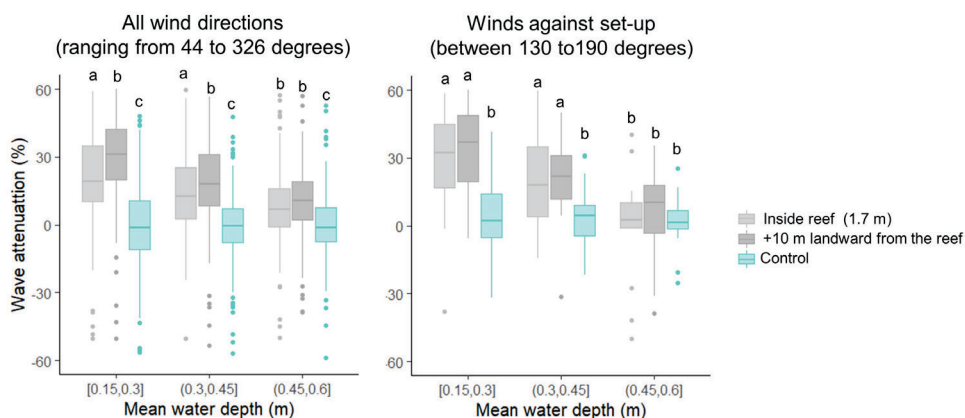


Fig. S2. Differences between wave attenuation by the control plot and reef plot for a range of water depths with a) all wind conditions and b) only winds perpendicular the set-up, to avoid possible confounding effects due to the wind direction (i.e. both control and reef were subjected to the same waves coming offshore and not parallel to the setup). Letters depict significant differences of wave attenuation obtained from the Tukey Post Hoc tests ($p < 0.05$).

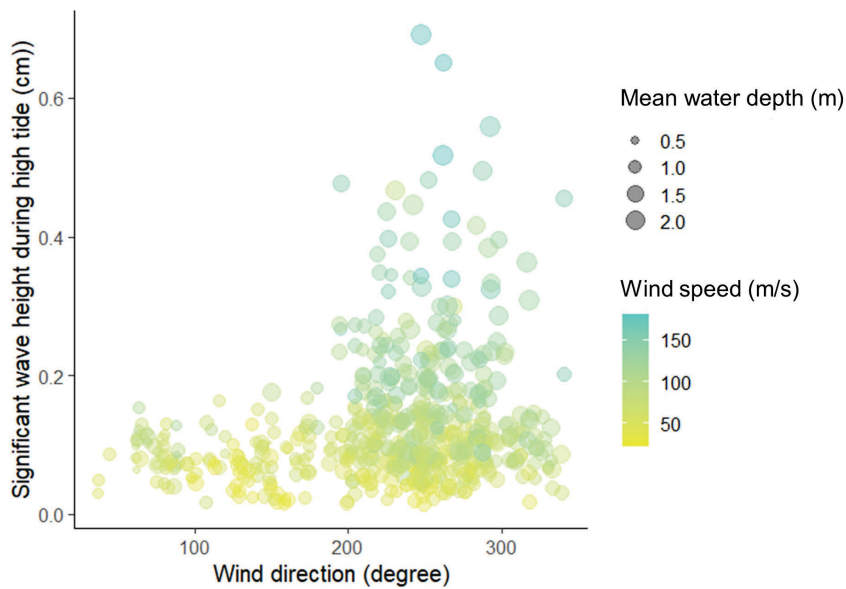


Fig. S3. Relation of the wind conditions and water level during the experimental period. The highest wind speeds came from the south-west and led to higher water levels and wave heights.



Fig. S4. Images of the experiment in August 2018 and August 2019, where sediment dynamics can be observed.

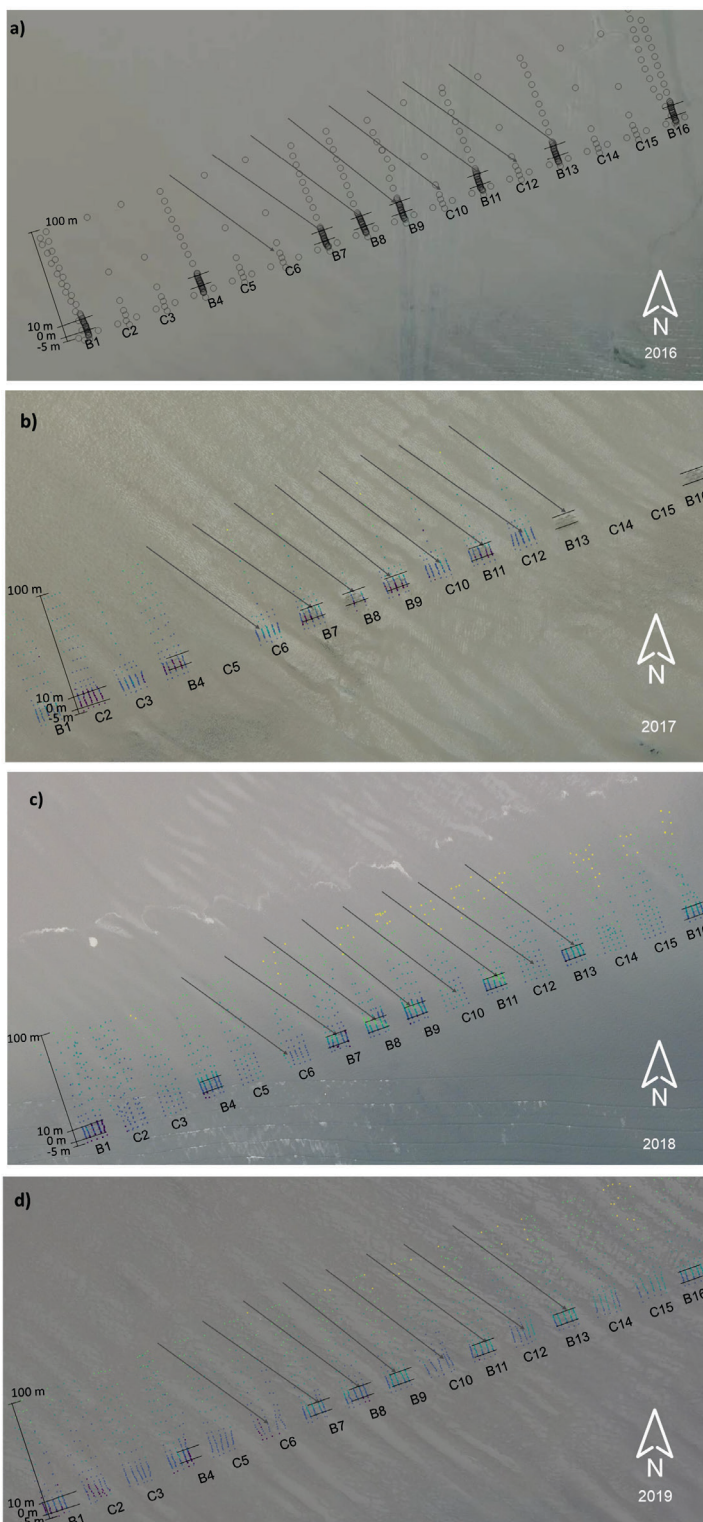


Fig. S5. Satellite images of the field plots and large bed forms for a) 2016, in which no bed forms can be observed, b) 2017, c) 2018 and d) 2019.

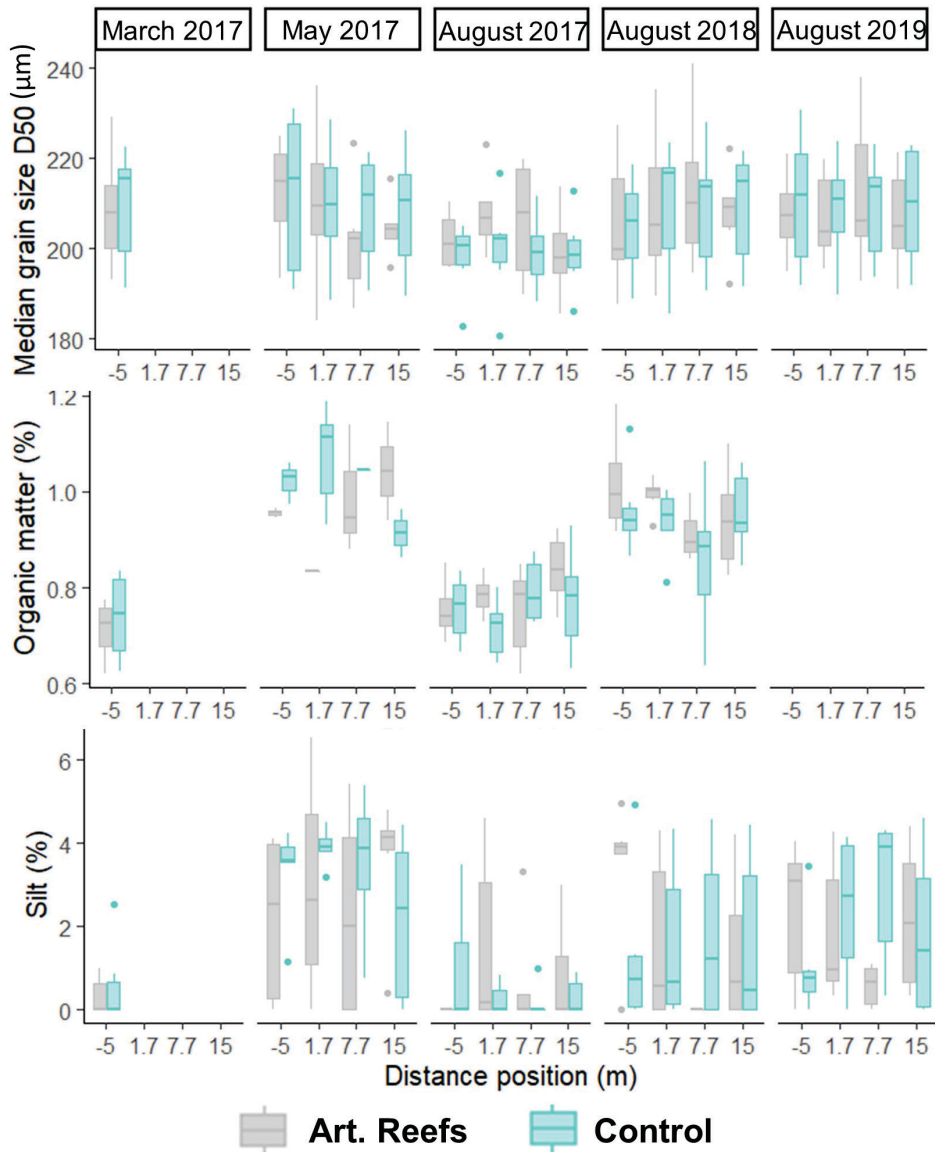


Fig. S6. Soil properties over time and at different positions in the transect. Position -5 refers to the seaside of the reef and the following positions are in landwards direction.



Chapter 8

Synthesis

Coastal protection is becoming increasingly important worldwide because many coastal communities are currently facing flood risks due to accelerating sea level rise (IPCC 2014), land subsidence (Syvitski et al. 2009; Weston 2014) and extreme events such as storms surges (Kiesel et al. 2021), which will probably become more frequent with climate change (Menéndez and Woodworth 2010; IPCC 2014; Voudoukas et al. 2018). Hard engineering structures such as dikes, sea walls, breakwaters and storm surge barriers, also known as 'grey' solutions, are commonly used for coastal protection. Nevertheless, these measures are often associated with negative impacts on coastal ecosystems and the loss of their ecosystem services (e.g. Lai et al. 2015). Furthermore, because conventional hard engineering is static, it can be increasingly challenged by climate change and the maintenance may become highly costly (Temmerman et al. 2013; Bouma et al. 2014; Morris et al. 2020). Alternatively, hybrid ecosystem-based coastal defence, or 'green' solutions, which combines conventional hard engineered barriers with coastal ecosystems, can be a more sustainable, ecologically valuable and cost-effective alternative to hard engineering alone (Shepard et al. 2011; Temmerman et al. 2013; Morris et al. 2018; Schoonees et al. 2019; Vuik et al. 2019). Natural ecosystems such as sand dunes, marshes, mangroves, seagrass, kelp forest, coral and shellfish reefs are able to attenuate waves and currents and stabilise the soil (Shepard et al. 2011; Bouma et al. 2014). Furthermore, ecosystems are capable of recovering from storm disturbances and be resilient against sea-level rise (Feagin et al. 2015; Kirwan et al. 2016; Fagherazzi et al. 2020; Morris et al. 2020). In addition to coastal protection, they provide a broad range of other ecosystem services including biodiversity conservation, nutrient cycling, support for fisheries and carbon sequestration (Orth et al. 2006; Gedan et al. 2009; Barbier et al. 2011; Duarte et al. 2013).

However, uncertainties about the actual effectiveness of these ecosystem-based measures still hampers the practical implementation. To safely implement natural ecosystems as part of the coastal protection programmes, we need to further address specific knowledge gaps regarding their functioning (i.e. coastal ecosystem dynamics in space and time), as well as providing thorough understanding of management effects on the safety value, ecological status and ecosystem behaviour (long-term dynamics), across connected habitat types.

In this thesis, I provided field evidence that supports the effectivity of foreshore ecosystems for coastal protection as well as the importance of the connectivity between ecosystems (Fig. 1). More specifically I investigated *i)* the importance of elevation and width of both tidal flats and marshes for wave run-up onto the dikes (chapter 2), *ii)* the importance of tidal flat elevation (changes) on the long-term marsh development (chapter 2), *iii)* topsoil and lateral erosion resistance across foreshore ecosystems, location, age and management type (chapters 3, 4, 5 and 6) and *iv)* the use of 'green' management measures to stabilise tidal flats and thereby facilitate marsh expansion (chapter 7). The first part of this chapter integrates the key findings of this thesis, unravelling knowledge gaps about coastal ecosystems dynamics and its management in relation to coastal protection. To conclude, I will discuss management implications and applications within the Dutch Flood Protection Program (HWBP).

Chapter 2: Marshes effectively reduce run-up but do not occur where most needed. Marsh expansion is related to tidal flat accretion

Chapter 3: Most of the marshes resist to fast water flow topsoil erosion, in contrast to the tidal flats. Only pioneer sandy marshes without cohesive topsoil layers are vulnerable

Chapter 4: Management of sandy islands by creating sheltered conditions for marsh development can lead to more stable soils

Chapter 5: Seagrass roots and rhizomes reduce bedload (top) erosion

Chapter 6: Grazing by small and large herbivores makes the soil more resistant to lateral erosion

Chapter 7: Biodegradable artificial reefs have the potential to stabilize tidal flats. However, reefs should be larger and the materials should match the hydrodynamic exposure

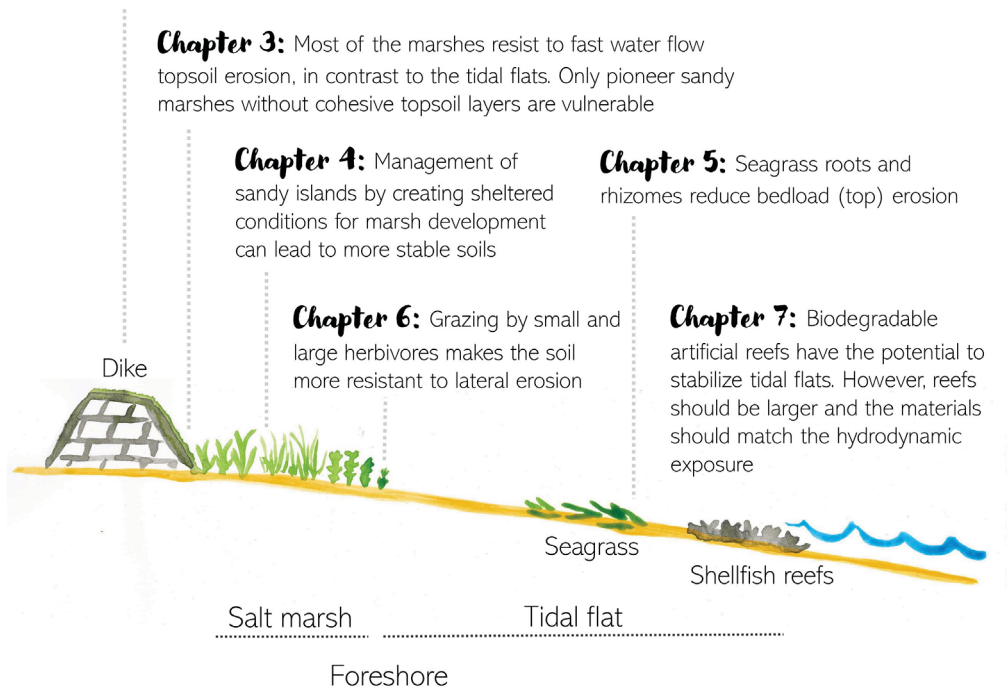


Fig 1. Illustration of the main results of this thesis.

INTEGRATION OF MAIN FINDINGS

Marshes effectively reduce wave run-up on the dikes but are hard to get where most needed

In this thesis we show that the morphology of the foreshore is important for both i) run-up reduction by wave attenuation (reducing dike failure risk) and ii) marsh development (i.e. low wave exposure and minimum elevation for specific flooding regime necessary for the vegetation to stablish) (chapter 2). Our field measurements show that foreshore sites with salt marshes reduced wave heights and halved wave run-up on the dikes during our monitoring period (2019 - 2021), even when the marshes had shorter and less dense vegetation during winter (Fig. 2). Differences of wave run-up between locations was mainly attributed to differences in elevational profile (i.e. higher elevation and/or marsh width). This is in accordance with previous studies that describe increased wave attenuation in wider and higher vegetated foreshores, even during severe storms (Vuik et al. 2016; Willemsen et al. 2020). Furthermore, locations with higher tidal ranges led to higher high-tide water levels causing higher wave run-up. Interestingly, wind direction and fetch length differences did not significantly explain differences in run-up between

SYNTHESIS

locations, so it was mainly driven by the topography. We expect that vegetation friction would also explain part of this attenuation (Vuik et al. 2016; Willemsen et al. 2020; Keimer et al. 2021). However, this was not disentangled in our model due to the high variability of vegetation parameters in time and space, which made it impossible to create a single vegetation variable to fit the statistics. Although vegetation was represented as marsh width in our models, future research could investigate the integration of these vegetation parameters that vary in time and space into a model to disentangle the real vegetation effect on run-up separated from the bathymetry.

Through analysis of vegetation and bathymetry maps we showed that the more vulnerable areas to wave run-up due to lower elevated tidal flats (< 0.5 m above mean sea level in the Dutch Wadden Sea) are also the areas where marshes are not able to develop (chapter 2). In these low elevated locations, the establishment of vegetation is challenging due to too high flooding frequencies and higher wave exposure, which also translates into higher run-up onto the dikes (Fig. 2). Furthermore, we show that marsh retreat in the past decade was related to the erosion of the tidal flats in front of the marsh. In contrast, accretion of tidal flats was correlated to an expansion of the marsh edge. This catch-22 problem implies that engineering measures will always be needed in the vulnerable areas: *either* to strengthen exposed dikes or to stimulate tidal flat accretion to induce marsh development at those exposed places where marshes cannot develop without our help. It also calls for better understanding of the erosion and sedimentation dynamics of the higher tidal flats, as this can ultimately promote the formation of salt marshes. Furthermore, it should be noted that although the effect of the marshes on wave attenuation in our field study was large, the effect may be lower during storms with higher water levels, as higher water levels are related to lower wave attenuation capacity (Vuik et al. 2016; Willemsen et al. 2020). Therefore, continuing the monitoring of run-up and wave attenuation until there is a storm with higher water levels would be a next step to quantify the effectiveness of the marshes in the field under extreme conditions.

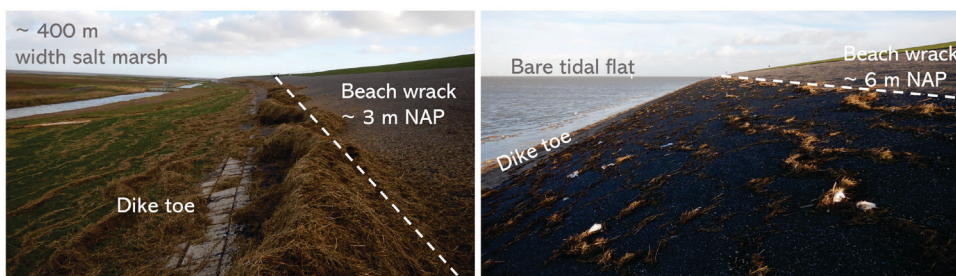


Fig. 2. Comparison of the elevation of the highest beach wracks on the dikes (wave run-up height) after the storm of the 8th of January 2019 between a wide marsh in Uithuizen (~400 m width) and bare tidal flat in Eemshaven: run-up is higher when the marsh is absent. NAP is the Dutch ordinance level, which is similar to the local mean sea level.

Soil stability of foreshore ecosystems

In line with chapter 2, soil stability of coastal ecosystems is of key importance for maintaining the high elevation of the foreshore which in turn is beneficial for coastal protection (Le Hir et al. 2000; Hu et al. 2015; Zhu et al. 2020). Although it is known that coastal vegetation stabilises the soil (e.g. Coops et al. 1996; Christianen et al. 2013; Lo et al. 2017; Wang et al. 2017) there were prior to this thesis still knowledge gaps regarding how different ecosystems can stabilize the soil and how it is affected by their physical and biological properties as well as by their management. Furthermore, sediment stabilization is not only important in communities higher in the intertidal zone, such as marshes, which have more wave attenuating capacity (Bouma et al. 2014). The presence and development of such communities higher in the intertidal zone is related to the elevation of the adjacent tidal flats (Hu et al. 2015, chapter 2). Therefore it was also important to understand the role of lower lying communities, such as bare tidal flats and seagrass, on sediment stabilization.

We demonstrated that almost all types of saltmarshes, including marshes with sandy subsoil, were resistant to topsoil erosion under fast water flow (2.3 m s^{-1}), which could occur during a dike breach (chapter 3). This is important to reduce the chance of dike breaching during extreme events, and to reduce the size of dike breaches when dikes fails (Zhu et al. 2020). Resistance to erosion occurred as long as the marshes had a cohesive top layer of high root density and organic content. Saltmarshes trap sediment, organic content and belowground biomass through time, and this cohesive, fine-grained top layer is the most erosion resistant. This biogenic cohesive top layer is especially visible in soil profiles of marshes that developed from sandy intertidal flats, like in Griend (chapter 2 and 4) and Schiermonnikoog (chapter 2 and 6) (Fig. 3 and 4). Pioneer marshes with sandy soil and low organic content were the only marshes that completely eroded because were not cohesive. Furthermore, not a single tidal flat soil was erosion resistant. Contrary to the expected, grazing was not related to less topsoil erosion. If an artificial crack reaching the sandy subsoil (easily erodible) was created in resistant marsh samples, mimicking what could occur during a dike breach due to tension cracks or debris hitting the soil, the soil would collapse. Overall, chapter 3 highlights the importance of preserving and/or restoring saltmarshes in front of the dikes to decrease the size of the dike breach and increase the evacuation time. However, sandy marshes may be more vulnerable. Nevertheless they could still reduce the wave energy impacting the dike (chapter 2).

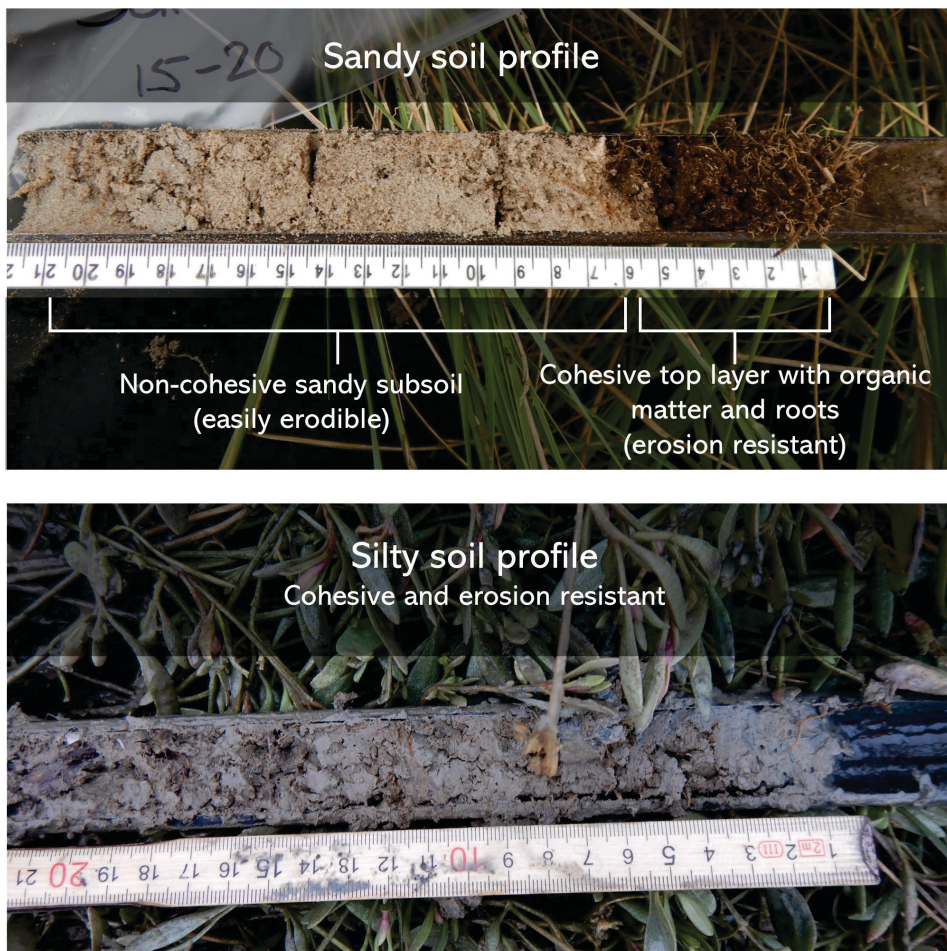


Fig. 3. Example of a sandy marsh soil profile (top), with easy erodible sand below the cohesive top layer of organic content, roots and fine sediment, and a silty marsh soil profile (bottom), which is erosion resistant.

In addition to the main findings in chapter 3, we also found a slight increase in topsoil erosion due to cracks formed in the sediment at four of the sampling locations during an unusually dry summer. These drought cracks were shallow (~4 cm depth), and led to a faster sediment erosion in form of small blocks of the surface layer. Nevertheless, the marsh was still stable. Therefore, in the case of a dike failure, this faster erosion of the most surface layer due to soil shrinkage may not be very important. However, if droughts or heat waves followed by storms become more frequent due to climate change (IPCC 2014; Voudoukas et al. 2018; Perkins-Kirkpatrick and Lewis 2020), marshes may become less resilient and more fragmented (Silliman et al. 2005; Cahoon et al. 2011; Derksen-Hooijberg et al. 2019). In this case, the enhanced erosion seen in this experiment could contribute to marsh degradation. For this reason, future research could focus on the effect of increased drought periods on marsh degradability.

In chapter 4 we studied top and lateral soil erosion resistance at Griend, a back-barrier island, which is a sandy system consisting of low dunes with shells and beach wrack deposited by storms, sheltering a salt marsh (Cooper et al. 2007; Pilkey et al. 2009) (Fig. 4). Barrier islands and back-barrier islands are an important part of coastal protection in shallow soft-bottom coasts like the Wadden Sea because they are the first barrier attenuating waves coming towards the coast from the open seas, resulting in fetch limitation (Otvos 2020). These islands are sometimes managed by coastal engineering to prevent their complete erosion, like in the case of Griend (Govers and Reijers 2021). The past management of Griend through sand enforcement of the initial chenier barrier, which are the current dunes, led to a shelter area at the wake of the island suitable for marsh development. As expected, neither higher dune soil nor the bare tidal flat soil were resistant to lateral or top erosion due to the lack of cohesive sediment with organic matter and dense belowground biomass. Nevertheless, a salt marsh formed in the sheltered side, creating a cohesive erosion-resistant top soil layer through the accumulation of fine sediment, organic matter and roots by the marsh vegetation. Lateral soil stability increased when the marsh established nearer to a creek and at low elevations, due to more fine sediment deposition and thus thicker cohesive layers; and decreased near to the dunes or at higher elevations due to mostly sandy soil profiles (Fig. 3). Therefore, soil erosion resistance due to the presence of thicker cohesive top layers seems to be related to the topography and presence of creeks which enhances sediment input and drainage of the island, as seen in mainland marshes (Reed et al. 1999; Koppenaal et al. 2021).



Fig. 4. Study sites in the Netherlands (top), including the Wadden Sea and the Scheldt Estuary. Numbers indicate which chapters took part at each location. Aerial image of a part of the Wadden Sea (bottom) indicating examples of barrier islands, back-barrier islands, mainland marshes, back-barrier marshes and tidal flats. The dotted line indicates the mainland dike. It can be observed that some stretches of the dike are fronted by marshes and others by bare tidal flats. The aerial photograph was obtained from PDOK (Public Geodata Portal in The Netherlands).

Finally, we showed that eelgrass (*Zostera marina*) with developed roots and rhizomes (i.e. root-mat forming seagrass) can reduce top erosion by roughly halving the horizontal sediment transport compared to bare sediment samples (Chapter 5, Fig. 5). In contrast, turbidity within the eelgrass samples was higher than in the bare sediment. We attributed this to enhanced turbulence and scouring at meadow edges enhancing the resuspension of the most fine sediment particles ($< 62.5 \mu\text{m}$). Nonetheless, the overall effect was that belowground biomass of eelgrass with high root density reduce top erosion. Although eelgrass can provide stabilization to the foreshores it has declined worldwide due to human impact, and its restoration is challenging due to diverse factors such as hydrodynamic exposure and poor water quality (e.g. van Katwijk et al. 2016). Therefore future research effort should focus on conservation and restoration of these communities.



Fig. 5. Underwater photo of *Zostera marina*, commonly known as eelgrass. The mat of roots and rhizomes that *Z. marina* can create can be observed in the sides of a hole from where a soil sample was extracted.

In general, a clear message from our chapters is that belowground biomass of vegetation with high root density and organic content can increase sediment top and lateral erosion resistance even under strong hydrodynamic conditions. The most erosion resistant soils were the ones with cohesive sediment type (silt/clay) combined with high belowground biomass, specifically higher root density, found in marshes. However, sandy soils with dense root networks and organic content were also resistant to topsoil erosion. In contrast, vegetated soils with sandy non-cohesive sediment type and/or with low root density and/or low organic content,

such as dunes, pioneer sandy marsh with low organic content and seagrass from deeper depths in fluffy muddy sediment and low root density, were the most vulnerable to both lateral and top erosion. Finally, one important aspect to add is that in normal conditions, the topsoil is protected by the vegetation canopy, which reduces water flow and waves and creates a shield layer reducing shear stress at the soil surface (Nepf 2012). Although not studied in this thesis (the aboveground vegetation was clipped in our marsh erosion experiments), we also expect this to contribute to erosion resistance, especially because the marsh vegetation does not fully disappear in winter, only in the pre-pioneer and pioneer zones in some cases (chapter 2).

Grazing management can reduce marsh lateral erosion sensitivity

Wave flume experiments, described in chapter 6, revealed that lateral erodibility of the marshes (i.e. resistance to cliff erosion) is affected by grazing management in combination with marsh age and marsh elevation. First, the depth of the cohesive top layer of silt, clay, organic matter and roots (Fig. 3), develops stronger at intermediate elevations, due to more exposure to floods, when vegetation can trap fine particles, and in older marshes which had longer time to develop and accrete organic matter (Olff et al. 1997; Van de Koppel et al. 2005, chapter 6). Overall, we showed that marshes with a thin cohesive top layer, such as found in high elevations or young or very low marshes, are more vulnerable to cliff erosion because they collapse as soon as the sandy subsoil is eroded. Secondly, the erosion-resistance of the cohesive top layer is enhanced by management practices that promote i) large grazers (cattle), in agreement with Pagés et al. (2018), which compact the soil by trampling and reduce soil-bioturbating arthropods, ii) mowing, which reduce soil-bioturbating arthropods and iii) small grazers (hares, geese) which promote vegetation types with higher root densities (Fig. 6). However, compaction by large grazers simultaneously leads to thinner cohesive top layers and lower soil elevation, potentially leading to more inundation under sea-level rise. This may be a problem in marshes without enough sediment supply to accrete vertically and keep up with sea level rise (Kirwan et al. 2016).

Although cattle grazing can reduce the silty soils erosion rate (chapter 6), cliff erosion at the marsh edge by toppling of blocks (larger scale) (Francalanci et al. 2013), which was not addressed in our experiment, may be differently affected by grazing. In other words, the fact that the soil itself becomes more cohesive and more resistant to gradual lateral erosion, may not be related to the block toppling in the marsh edge fronting the tidal flats. For example, marshes in Ameland, a barrier island in the Dutch Wadden Sea, are retreating even being grazed (personal communication with a nature manager). Cliff erosion in grazed marshes may be explained by natural cyclic alternations between retreat and marsh expansion due to differences in elevation between the tidal flat and the accreted marsh edge (Van de Koppel et al. 2005), tidal flat erosion dynamics (Bouma et al. 2016, chapter 2) or sediment shortage (Ladd et al. 2019). Therefore, although cattle grazing may reduce erosion rates, all these other large scale factors may be overruling the grazing effect. In order to determine if grazing also reduces large scale erosion (i.e. mass failure) in the marsh edge adjacent to tidal flats, future research should

focus on the grazing effect on a bigger scale, following the work done by Wang et al. (2017) and Pagés et al. (2018).



Fig. 6. Example of grazers found in salt marshes: hare, geese and cattle (top). Enclosure in a salt marsh grazed by hare and gees (bottom-left) and a salt marsh grazed by cattle (bottom-right). Erosion sensitivity of the soil was reduced with both types of grazing.

'Green' management options to change the tidal flat bathymetry

Higher and convex foreshores may lead to higher wave attenuation and longer distance from wave breaking points toward the potential pioneer marsh zone (Mariotti and Fagherazzi 2013; Hu et al. 2015). This would reduce erosion in the pioneer vegetation zone of a salt marsh (Mariotti and Fagherazzi 2013; Hu et al. 2015; Bouma et al. 2016; Willemsen et al. 2017) as well as reduce wave run-up on the dikes (chapter 2). For this reason, management should not focus only on marshes but also on the tidal flats in front of the dikes or the marshes. A more ecological valuable alternative to 'grey' solutions for tidal flat management may be the restoration and protection of sedimentation-promoting foundation species (Angelini et al. 2011; van de Koppel et al. 2015; Schoonees et al. 2019) such as eelgrass meadows or mussel beds. These natural communities could attenuate waves and currents, provide an elevated and stable soil as well as changing tidal flat profile (e.g. Meyer et al. 1997; Borsje et al. 2011; Donker et al. 2013; Walles et al. 2016). In return, this could potentially aid marsh expansion (Chowdhury et al. 2019).

SYNTHESIS

Hence, we tested the use of biodegradable artificial reefs, which were aimed as precursors to restore mussel beds, on wave attenuation and tidal flat stabilization in an exposed location (chapter 7). The results show that the structures, which were 20 cm high, reduced wave heights when the mean water level was < 50 cm. Furthermore, the reefs promoted local sediment accretion (Fig. 7), even when the structures were lower due to degradation as a result of harsh weather conditions including ice sheets. Lower structures were not as effective in wave attenuation, and the explanation for enhanced local sediment trapping even being low elevated may have been by their flow attenuation (Fivash et al. 2021). The effects on sediment dynamics was local (~ 10 m from the reefs). Therefore, an even larger implementation scale would be needed to affect long-term tidal flat morphology and promotion of large-scale connectivity between tidal flats and high intertidal systems such as salt marshes. Furthermore, large bedform dynamics should be considered when designing the dimensions of the reefs to expand their sediment trapping effect. Higher and more resistant structures may be useful to attenuate more waves in exposed locations but not necessarily for sediment trapping due to the possible enhanced scouring (chapter 7). Furthermore, in very exposed locations, stable mussel beds may not be able to develop (Paoli et al. 2015). This highlights the importance of distinguishing the application of these solutions depending on the aim: ecological (e.g. mussel bed restoration) or engineering (wave attenuation and stabilization of the tidal flat) (Morris et al. 2019, chapter 7). In some cases, both aims may just not be possible to combine.



Fig. 7. Effect of the biodegradable artificial reefs on tidal flat accretion. At this stage the reefs were already lower due to degradation, but still accreted sediment.

MANAGEMENT IMPLICATIONS AND APPLICATIONS WITHIN THE DUTCH FLOOD PROTECTION PROGRAM (HWBP)

Benefits from salt marshes for nature-based coastal defence

Salt marshes should be protected and/or restored because they provide stable soils that are resistant to erosion (chapters 3, 4 and 6). Resistant soils provided by marshes may reduce breach dimensions if a dike fails (Zhu et al. 2020, chapter 3). Furthermore, these stable marsh soils effectively reduce wave run-up on the dikes independently of the vegetation species (chapter 2). Wider marshes (> 300 m) or more elevated marshes (> 1.5 m NAP) provide further reduction of wave loads in the dikes (chapter 2). Wave run-up reduction is important for preventing water flowing over the dike during storms (dike overtopping) and to reduce wave impact on the dike during more frequent moderate storms (Vuik et al. 2019). In this thesis we included a wide range of vegetation species (from short grazed marshes to reed marshes with high vegetation), so the effect of marsh width in reducing run-up may apply to other locations although the magnitude may differ.

In the context of The Netherlands, historical land reclamation works in the Dutch Wadden Sea strongly promoted salt marshes in the past and also explain where are current salt marshes located (Dijkema et al. 2011) (chapter 2, Fig. 8). Similarly, marshes have developed with human intervention in the Western Scheldt, although more natural marshes can be found there compared to the Wadden Sea (Van der Wal et al. 2008) (Fig. 4). We found variation in the marsh sediment type depending on the site (chapter 3, 4, 6): in the mainland saltmarshes of the Wadden Sea, the sediment was mostly silty and cohesive, while in Schiermonnikoog (barrier island) and Griend (fetch-limited island), we could distinguish an erosion-resistant top layer accreted on the top of readily erodible coarse sand (Fig. 3 and 4). In the Scheldt delta, few locations had soil profiles with only sand, such as Ritthem and Rilland and the others were silty and cohesive (Fig. 4). Silty marshes with cohesive soils are the most resistant to topsoil and lateral erosion (chapter 3 and 4). Finally, although sandy marshes may be less resistant to lateral erosion, they can still attenuate waves by the vegetation and higher soil elevation (Shepard et al. 2011) and therefore provide coastal protection.

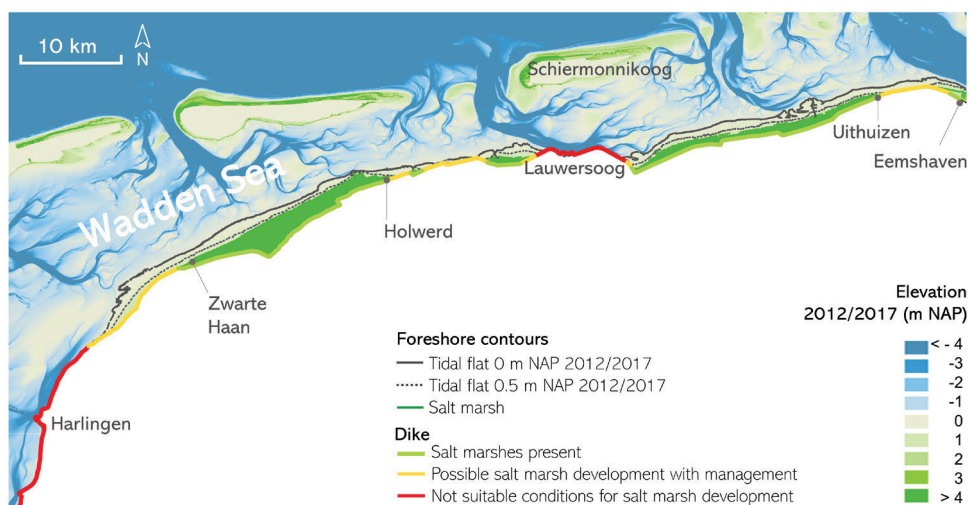


Fig. 8. Map of the potential locations where salt marsh could develop with management efforts, based on the location of the elevated tidal flats and current salt marsh presence.

Grazing management on salt marshes for coastal protection

Low intensity cattle grazing or rotational livestock grazing is recommended because it increases lateral erosion resistance of silty/peaty marsh soils (chapter 6) and provides other benefits such as increased biodiversity and carbon storage (Davidson et al. 2017). In contrast, topsoil erosion under fast-water flow was not affected by grazing although we could expect that in the case of a dike breach, cattle grazed soil would be more compact and more resistant to damages (chapter 3). High intensity cattle grazing should be avoided because it could be a risk for land subsidence due to soil compaction and have negative effects on soil properties (Nolte et al. 2013; Davidson et al. 2017; Keshta et al. 2020). This will be especially important in organogenic marshes with low sediment input sensitive to sea level rise as found in North America (Davidson et al. 2017). Extensive grazing is also preferred from their impact on diversity of plants (Bakker 1989), invertebrates (van Klink et al. 2015; Davidson et al. 2020) and breeding birds (Mandema et al. 2013). In European marshes dominated by *Elytrigia atherica*, like in Europe, promotion of small herbivores (e.g. hare and geese) in areas where they have declined (Dokter et al. 2018) could be investigated to avoid the encroachment of this species which has low root density and is related to less erosion resistance (chapter 6). However, in other marshes dominated by less palatable species such as *Spartina* spp. as found in America (Davidson et al. 2017), the effect of the small grazers may be different.

Marshes grazed by livestock, which have shorter vegetation (i.e. Uithuizen, den Andel and Zwarte Haan), still reduce more waves and wave run-up on the dikes compared to the bare mudflats (chapter 2). This attenuation is due to the higher elevation and the roughness of the vegetation, even during winter state (chapter 2). Therefore, grazing does not suppose a risk for

the efficiency of marshes protecting the dikes, although marshes with taller vegetation may be even more effective (e.g. Möller et al. 1999; Bouma et al. 2010; Ysebaert et al. 2011).

Management of tidal flats for coastal protection (i.e. marsh expansion)

A limitation from the ecosystem-based coastal defence is that marshes may not be able to develop along all the foreshore, as discussed in chapter 2. One of the limiting factors for having a continuous marsh along all the dikes is that tidal flats with enough elevation for marsh establishment do not occur everywhere in front of the dikes (chapter 2). This is especially important in areas modified by humans where the foreshores have been engineered and the space for the ecosystems to develop is limited (Doody 2013). Furthermore, worldwide analysis show that tidal flats are being lost due to coastal development, reduced sediment input, sinking of riverine deltas, increased coastal erosion and sea level rise (Murray et al. 2019). These areas without elevated tidal flats have too high flooding frequency and inundation time for marsh to develop in addition to more wave and current exposure that can prevent seedling establishment (e.g. Hu et al. 2015; Balke et al. 2016; Bouma et al. 2016; Silinski et al. 2016).

In the case of the Dutch Wadden Sea, natural landward marsh migration is limited by the dikes, which results in coastal squeeze (Doody 2013). Our results support the conclusions in the map of potential saltmarsh formation in the Dutch Wadden Sea proposed by van Loon-Steensma (2015). Areas fronting the dikes with low elevations (< 0 m NAP), such as near Harlingen and Lauwersoog, may not be suitable for marsh development even with human intervention due to the lack of natural sediment deposition and/or high exposure, which is necessary to sustain long-term marsh development (Fig. 8, Box 1) (van Loon-Steensma 2015; Wang et al. 2018; Hu et al. 2021). These areas where marshes are not able to develop would need more reinforcement than areas with a dike protected by a marsh. In areas with elevated tidal flats but where marshes are currently missing or are very narrow, marsh expansion seaward could be facilitated by increasing the elevation of tidal flat, reducing incoming waves and supporting sediment supply (Hu et al. 2021), thus creating favourable conditions for marsh establishment (Box 1). This could be done for example at the south of Zwarte Haan, east of Holwerd or the west of Eemshaven (Fig. 8). However, it should be also taken into account that the creation of new marshes would go at the expenses of open mudflats which are important as feeding areas for migratory birds and for mussel beds among others (Compton et al. 2013).

In the past, marsh expansion through increasing the elevation of the tidal flats and reducing waves and currents has been achieved by interventions like building wave-breaking brushwood groynes (Fig. 9), digging drainage channels, or applying dredging material to create a wave attenuating foreshore (Dijkema et al. 2011; Hu et al. 2015; van Loon-Steensma 2015). Restoring stabilizing ecosystems like seagrass beds (chapter 5) or shellfish reefs (chapter 7) could be an alternative for hard engineering to attenuate waves and currents, increase tidal flats accretion (i.e. increase in elevation) and simultaneously increase ecological value (e.g. Meyer et al. 1997; Borsje et al. 2011; Donker et al. 2013; Walles et al. 2016). However, combining ecological aims (restoring an ecosystem) and engineering aims (reducing waves and trapping

SYNTHESIS

sediment to promote suitable conditions for marsh expansion) may not always be possible (Morris et al. 2019, chapter 7). For example, in our experiment with biodegradable artificial reefs (chapter 7), the site was too exposed for the reefs to persist and develop into a stable mussel bed. Larger scale reefs, more resistant materials and the installation at higher elevations may be needed to resist the harsh conditions and have a larger effect on wave attenuation and tidal flat sedimentation. However these alternative characteristics may not be suitable for mussel bed restoration (Paoli et al. 2015). Unfortunately, most of the exposed locations that may benefit from marsh expansion may not be suitable for mussel or seagrass restoration as a management solution due to the high exposure. In these situations, other measures such as sedimentation fields with brushwood groynes (Fig. 9) (De Groot and Van Duin 2013), sediment nourishments (Baptist et al. 2019) or a combination of these 'grey' measures with the restoration of seagrass beds and shellfish reefs as an hybrid solution may be an option. Finally, the use of structures to facilitate marsh expansion may be temporal if the aim is to create a window of opportunity for the first stages of marsh establishment (Hu et al. 2015) (Box 1). However, in situations of coastal squeeze, where the space for ecosystem development is lacking, or is a very exposed area, such structures should be maintained to prevent marsh erosion (Bakker 2014; Siemes et al. 2020). For instance, in the Wadden Sea, management of the tidal flats should be continued to preserve a minimum marsh width in front of the dikes (e.g. ~ 300 m, chapter 2).



Fig. 9. Effects of brushwood groynes on sediment trapping and marsh vegetation establishment. The right side is the lee of the brushwood groyne (facing landwards), more sheltered and where more sediment has been trapped leading to an increase in marsh vegetation.

Lastly, in addition to restoring soil stabilising ecosystems or using man-made solutions for marsh expansion, it is recommended to continue monitoring the evolution of the sediment dynamics over time (e.g. with bathymetric and satellite maps) and detect the areas where tidal flats are eroding or accreting (chapter 2). This may be a predictor of future salt marsh retreat. Furthermore, suspended sediment in the water column should also be monitored at higher

spatial and temporal resolution, which is important for coastal ecosystems to keep up with sea level rise. In other words, we can focus on stabilising the tidal flats, but if sediment availability is reduced (Mariotti and Fagherazzi 2013; Ladd et al. 2019; Murray et al. 2019), ecosystems may have a problem to build up and keep up with sea level rise, especially if the ecosystems are not able to migrate inland due to human constructions (Doody 2013). Sediment shortage due human activities such as the creation of dams or river dredging is a current cause for tidal flats and marsh loss (Mariotti and Fagherazzi 2013; Murray et al. 2019). Therefore foreshore management may require actions in the land watershed such as opening upstream dams. If this is not possible, sediment nourishments in combination with the previous measures mentioned may be an option to consider (Baptist et al. 2019; Hu et al. 2021).

Further recommendations for salt marsh restorations

For future soil nourishments aimed at marsh restoration, using fine-grained sediment (mud), which will become more cohesive and erosion resistant, is recommended rather than the use of coarse sand that is non cohesive and erodes easily (chapter 3, 4, 6). This may not be possible in all the places due to the local sediment source, but it is recommended when fine sediment is available. Restored sandy marshes may take longer to become erosion resistant (chapter 3 and 6). Therefore future research could focus on sediment-type management, how long would it take for a sandy location to become stable and whether sediment-type management could have ecological impacts. Furthermore, marsh restorations should include a good drainage system with creeks to provide enough sediment supply (Reed et al. 1999) and promote the accretion of thicker erosion-resistant top layers (chapter 4).

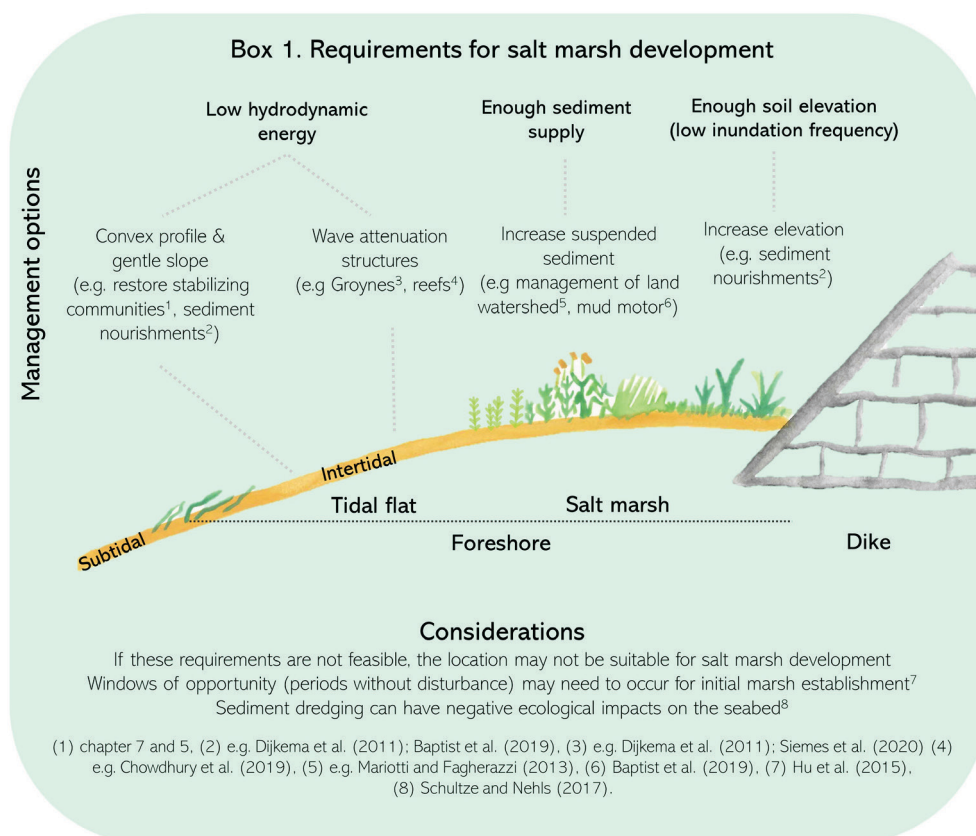
CONCLUDING SUMMARY ON ECOSYSTEM-BASED COASTAL DEFENCE

Based on our findings together with previous studies, I conclude that marshes, compared to bare tidal flats, play an important role on coastal protection independently of the vegetation type or if they are in winter state (chapter 2, 3, 4, 6). Therefore, they should be included in coastal protection schemes. Marshes will be stable and attenuate more waves loads onto the dikes compared to bare tidal flats even if they are grazed (chapter 2). Furthermore, grazing may be interesting to reduce lateral erosion rates (chapter 6), but further research should focus on if there is an effect of grazing on reducing cliff erosion in form of toppling blocks, therefore at a larger scale. Nevertheless, I find very important to avoid high intensity grazing which can lead to land subsidence and affect the biodiversity.

A limitation of the nature-based protection by salt marshes is that they cannot be implemented everywhere, because their establishment is very location-specific and depends on environmental conditions (e.g. sediment availability, elevation profiles and wave exposure Box 1, Hu et al. 2021, chapter 2). When possible, ecosystem-based coastal defence should integrate connected ecosystems lower in the tidal range (for example tidal flats, seagrass beds and shellfish reefs), which can stabilise the soil and reduce waves (chapter 5 and 7), both

SYNTHESIS

processes positively related to marsh expansion and increased ecological value. Unfortunately, restoration of mussel or seagrass beds in exposed locations is often difficult (chapter 7). In cases where natural options like restoring seagrass beds and shellfish reefs are not feasible, marsh expansion could be promoted by minimal engineering actions (e.g. building brushwood groynes) until a stable marsh able to withstand waves has developed. In locations with high exposure or low sediment supply, where marshes are not able to migrate inland, such measures should be maintained long-term to prevent marsh erosion. In some case ecosystem-based solutions combining marshes and dikes may be too costly, not achievable, or going at the expense of other ecological values, such as causing the loss of mudflats that are important for migratory birds (chapter 2). In these situations, 'hard engineering' solutions may remain necessary. Finally, I believe that future research and management should go towards how to maintain coastal ecosystems in face of climate change (i.e. sea level rise and increased storms) and to monitoring sediment dynamics and sediment availability to be able to predict where the marshes may start eroding in order to have time to plan a response to that.



BOX 2. SUMMARY OF RESEARCH QUESTIONS AND ANSWERS

Chapter 2

Questions: Are marshes growing where we need them most? Which factors drive differences of run-up and beach wrack levels across different foreshore types?

Answer: Marshes were associated with higher elevations of adjacent tidal flats (above ~ 0.5 m NAP). Furthermore, marsh expansion offshore was associated with the accretion of the adjacent tidal flats. Marshes effectively protected dikes from wave loading, but also sites that are most vulnerable to high wave run-up were found in those areas where marshes typically do not develop spontaneously due to too low soil elevations and high hydrodynamic exposure.

Chapter 3

Questions: How do different foreshore types resist to fast flow erosion, which could occur during a dike breach?

Answer: Almost all types of saltmarshes, including marshes with sandy subsoil, were resistant to topsoil erosion under fast water flow thanks to the presence of an erosion resistant top layer of organic matter, roots and/or fine sediment accreted by the marsh vegetation. Only pioneer vegetation in sandy places was found without this resistant top layer and therefore were completely eroded. Furthermore, not a single tidal flat soil was erosion resistant.

Chapter 4

Questions: How resistant are soft-sediment ecosystems from fetch-limited barrier island to top and lateral erosion in relation to its management?

Answer: Neither higher dune soil nor bare tidal flat soils were resistant to lateral or top erosion. However, a salt marsh developed in the sheltered side of the dunes, creating an erosion-resistant top soil layer through the accumulation of fine sediment, organic matter and roots. Lateral soil stability increased when the marsh was nearer to a creek and at low elevations, due to more fine sediment deposition and thus thicker erosion-resistant top layers.

Chapter 5

Questions: What is the role of eelgrass on bed-load transport and sediment resuspension under wave conditions?

Answer: Dense root-mat forming seagrass, like *Zostera marina* growing in shallow waters, effectively reduced bedload transport of sandy sediment. However, small patches did not reduce water turbidity.

Chapter 6

Questions: How does grazing management in combination with abiotic factors, such as marsh age, marsh elevation and sediment layering, affect the susceptibility of marsh edges to lateral erosion?

Answer: Grazing by cattle and small herbivores (i.e. hare and geese) can reduce the erodibility of fine-grained soils, making salt marshes more resilient to lateral erosion. However, compaction by livestock simultaneously results into lower soil elevation, potentially leading to more inundation under sea level rise.

Chapter 7

Questions: Can we develop nature-based management on the tidal flats to stabilize the marshes?

Answer: Biodegradable artificial reefs have the potential to attenuate waves and change tidal flat morphology. However, to benefit connected foreshore ecosystems like salt marshes, the dimensions of the reefs should be larger and the structures should be more resistant.



References

A

- Aberle, J., V. Nikora, and R. Walters. 2004. Effects of bed material properties on cohesive sediment erosion. *Mar. Geol.* 207: 83–93. doi:10.1016/j.margeo.2004.03.012
- Adams, M. P., R. K. Hovey, M. R. Hipsey, and others. 2016. Feedback between sediment and light for seagrass: Where is it important? *Limnol. Oceanogr.* 61: 1937–1955. doi:10.1002/lno.10319
- Adolph, W., H. Farke, S. Lehner, and M. Ehlers. 2018. Remote sensing intertidal flats with TerraSAR-X. A SAR perspective of the structural elements of a tidal basin for monitoring the Wadden Sea. *Remote Sens.* 10. doi:10.3390/rs10071085
- Albers, T. S. 2014. Emergency closure of dike breaches. Delft University of Technology.
- Allaoui, N. El, T. Serra, J. Colomer, M. Soler, and X. Casamitjana. 2016. Interactions between Fragmented Seagrass Canopies and the Local Hydrodynamics. 1–19. doi:10.1371/journal.pone.0156264
- Alldred, M., A. Liberti, and S. B. Baines. 2017. Impact of salinity and nutrients on salt marsh stability. *Ecosphere* 8. doi:10.1002/ecs2.2010
- Allen, J. R. L. 1989. Evolution of salt-marsh cliffs in muddy and sandy systems: A qualitative comparison of British West-Coast estuaries. *Earth Surf. Process. Landforms* 14: 85–92. doi:10.1002/esp.3290140108
- Allen, J. R. L. 2000. Morphodynamics of Holocene salt marshes : a review sketch from the Atlantic and Southern North Sea coasts of Europe. *Quat. Sci. Rev.* 19: 1155–1231. doi:10.1016/S0277-3791(99)00034-7
- Altomare, C., T. Suzuki, X. Chen, T. Verwaest, and A. Kortenhaus. 2016. Wave overtopping of sea dikes with very shallow foreshores. *Coast. Eng.* 116: 236–257. doi:10.1016/j.coastaleng.2016.07.002
- Amos, C. L., T. Feeney, T. F. Sutherland, and J. L. Luternauer. 1997. The Stability of Fine-grained Sediments from the Fraser River Delta. *Estuar. Coast. Shelf Sci.* 45: 507–524. doi:10.1006/ecss.1996.0193
- Amos, C. L., J. Grant, G. R. Daborn, and K. Black. 1992. Sea Carousel-A benthic, annular flume. *Estuar. Coast. Shelf Sci.* 34: 557–577. doi:10.1016/S0272-7714(05)80062-9
- Andrews, J. E., D. Burgess, R. R. Cave, E. G. Coombes, T. D. Jickells, D. J. Parkes, and R. K. Turner. 2006. Biogeochemical value of managed realignment, Humber estuary, UK. *Sci. Total Environ.* 371: 19–30. doi:10.1016/j.scitotenv.2006.08.021
- Angelini, C., A. H. Altieri, B. R. Silliman, and M. D. Bertness. 2011. Interactions among foundation species and their consequences for community organization, biodiversity, and conservation. *Bioscience* 61: 782–789. doi:10.1525/bio.2011.61.10.8
- Arens, S. M., J. P. M. Mulder, Q. L. Slings, L. H. W. T. Geelen, and P. Damsma. 2013. Geomorphology Dynamic dune management , integrating objectives of nature development and coastal safety : Examples from the Netherlands. *Geomorphology* 199: 205–213. doi:10.1016/j.geomorph.2012.10.034

B

- Baets, S. De, J. Poesen, G. Gyssels, and A. Knapen. 2006. Effects of grass roots on the erodibility of topsoils during concentrated flow. *Geomorphology* 76: 54–67. doi:10.1016/j.geomorph.2005.10.002

REFERENCES

- Baets, S. De, J. Poesen, A. Knapen, and P. Galindo. 2007. Impact of root architecture on the erosion-reducing potential of roots during concentrated flow. *Earth Surf. Process. Landforms* 32: 1323–1345. doi:10.1002/esp.1470
- Bakker, J. P. 1989. *Nature management by grazing and cutting*, Kluwer.
- Bakker, J. P. 2014. Ecology of salt marshes: 40 years of research in the Wadden Sea, Wadden Academy.
- Bakker, J. P., K. J. Nielsen, J. Alberti, and others. 2015. Bottom-up and top-down interactions in coastal interface systems, T.C. Hanley and K.J. La Pierre [eds.]. Cambridge University Press.
- Bakker, J. P., M. Schrama, P. Esselink, P. Daniels, N. Bhola, S. Nolte, R. M. Veeneklaas, and M. Stock. 2020. Long-Term Effects of Sheep Grazing in Various Densities on Marsh Properties and Vegetation Dynamics in Two Different Salt-Marsh Zones. *Estuaries and Coasts* 43: 293–315. doi:10.1007/s12237-019-00680-5
- Bakker, J. P., and Y. de Vries. 1992. Germination and Early Establishment of Lower Salt-Marsh Species in Grazed and Mown Salt Marsh. *J. Veg. Sci.* 3: 247–252. doi:10.2307/3235686
- Bale, A. J., J. Widdows, C. B. Harris, and J. A. Stephens. 2006. Measurements of the critical erosion threshold of surface sediments along the Tamar Estuary using a mini-annular flume. *Cont. Shelf Res.* 26: 1206–1216. doi:10.1016/j.csr.2006.04.003
- Balke, T., T. J. Bouma, E. M. Horstman, E. L. Webb, P. L. A. Erftemeijer, and P. M. J. Herman. 2011. Windows of opportunity: Thresholds to mangrove seedling establishment on tidal flats. *Mar. Ecol. Prog. Ser.* 440: 1–9. doi:10.3354/meps09364
- Balke, T., M. Stock, K. Jensen, T. J. Bouma, and M. Kleyer. 2016. A global analysis of the seaward salt marsh extent: The importance of tidal range. *Water Resour. Res.* 52: 3775–3786. doi:10.1111/j.1752-1688.1969.tb04897.x
- Baptist, M. J., T. Gerkema, B. C. van Prooijen, and others. 2019. Beneficial use of dredged sediment to enhance salt marsh development by applying a ‘Mud Motor.’ *Ecol. Eng.* 127: 312–323. doi:10.1016/j.ecoleng.2018.11.019
- Barbier, E. B., S. D. Hacker, C. Kennedy, E. W. Kock, A. C. Stier, and R. S. Brian. 2011. The value of estuarine and coastal ecosystem services. *Ecol. Monogr.* 81: 169–193. doi:10.1890/10-1510.1
- Bartholdy, J., J. B. T. Pedersen, and A. T. Bartholdy. 2010. Autocompaction of shallow silty salt marsh clay. *Sediment. Geol.* 223: 310–319. doi:10.1016/j.sedgeo.2009.11.016
- Bates, D., M. Mächler, B. M. Bolker, and S. C. Walker. 2014. Fitting linear mixed-effects models using lme4. *J. Stat. Softw.*
- De Battisti, D., M. S. Fowler, S. R. Jenkins, M. W. Skov, M. Rossi, T. J. Bouma, P. J. Neyland, and J. N. Griffin. 2019. Intraspecific Root Trait Variability Along Environmental Gradients Affects Salt Marsh Resistance to Lateral Erosion. *Front. Ecol. Evol.* 7: 1–11. doi:10.3389/fevo.2019.00150
- De Battisti, D., J. N. Griffin, S. Park, and S. Sa. 2020. Below-ground biomass of plants, with a key contribution of buried shoots, increases foredune resistance to wave swash. 325–333. doi:10.1093/aob/mcz125
- Bishop, M. J., M. Mayer-Pinto, L. Airoldi, and others. 2017. Effects of ocean sprawl on ecological connectivity: impacts and solutions. *J. Exp. Mar. Bio. Ecol.* 492: 7–30. doi:10.1016/j.jembe.2017.01.021
- Boere, G. C., and T. Piersma. 2012. Flyway protection and the predicament of our migrant birds: A critical look at international conservation policies and the Dutch Wadden Sea. *Ocean Coast. Manag.* 68: 157–168. doi:10.1016/j.ocecoaman.2012.05.019
- Borsje, B. W., B. K. van Wesenbeeck, F. Dekker, P. Paalvast, T. J. Bouma, M. M. van Katwijk, and M. B. de Vries. 2011. How ecological engineering can serve in coastal protection. *Ecol. Eng.* 37: 113–122. doi:10.1016/j.ecoleng.2010.11.027
- Bos, A. R., T. J. Bouma, G. L. J. de Kort, and M. M. van Katwijk. 2007. Ecosystem engineering by annual intertidal seagrass beds: Sediment accretion and modification. *Estuar. Coast. Shelf Sci.* 74: 344–348. doi:10.1016/j.ecss.2007.04.006
- Bos, A. R., and M. M. Van Katwijk. 2007. Planting density, hydrodynamic exposure and mussel beds affect survival of transplanted intertidal eelgrass. *Mar. Ecol. Prog. Ser.* 336: 121–129. doi:10.3354/meps336121

- Bos, D., J. P. Bakker, Y. de Vries, and S. van Lieshout. 2002. Long-term vegetation changes in experimentally grazed and ungrazed back-barrier marshes in the Wadden Sea. *Appl. Veg. Sci.* 5: 45–54. doi:10.1658/140210.1111/j.1654-109X.2002.tb00534.x
- Bouchard, V., M. Tessier, F. Digaïre, J. P. Vivier, L. Valéry, J. C. Gloaguen, and J. C. Lefeuvre. 2003. Sheep grazing as management tool in Western European saltmarshes. *Comptes Rendus - Biol.* 326: 148–157. doi:10.1016/s1631-0691(03)00052-0
- Bouma, T. J., J. van Belzen, T. Balke, and others. 2014. Identifying knowledge gaps hampering application of intertidal habitats in coastal protection: Opportunities & steps to take. *Coast. Eng.* 87: 147–157. doi:10.1016/j.coastaleng.2013.11.014
- Bouma, T. J., J. van Belzen, T. Balke, and others. 2016. Short-term mudflat dynamics drive long-term cyclic salt marsh dynamics. *Limnol. Oceanogr.* 61: 2261–2275. doi:10.1002/lno.10374
- Bouma, T. J., L. A. van Duren, S. Temmerman, T. Claverie, A. Blanco-Garcia, T. Ysebaert, and P. M. J. Herman. 2007. Spatial flow and sedimentation patterns within patches of epibenthic structures: Combining field, flume and modelling experiments. *Cont. Shelf Res.* 27: 1020–1045. doi:10.1016/j.csr.2005.12.019
- Bouma, T. J., M. Friedrichs, P. Klaassen, and others. 2009a. Effects of shoot stiffness, shoot size and current velocity on scouring sediment from around seedlings and propagules. *Mar. Ecol. Prog. Ser.* 388: 293–297. doi:10.3354/meps08130
- Bouma, T. J., M. Friedrichs, B. K. Van Wesenbeeck, S. Temmerman, G. Graf, and P. M. J. Herman. 2009b. Density-dependent linkage of scale-dependent feedbacks: a flume study on the intertidal macrophyte *Spartina anglica*. *Oikos* 118: 260–268. doi:10.1111/j.1600-0706.2008.16892.x
- Bouma, T. J., M. B. De Vries, E. Low, and others. 2005a. Flow hydrodynamics on a mudflat and in salt marsh vegetation: Identifying general relationships for habitat characterisations. *Hydrobiologia* 540: 259–274. doi:10.1007/s10750-004-7149-0
- Bouma, T. J., M. B. De Vries, E. Low, G. Peralta, I. C. Tanczos, J. Van De Koppel, and P. M. J. Herman. 2005b. Trade-offs related to ecosystem engineering: A case study on stiffness of emerging macrophytes. *Ecology* 86: 2187–2199. doi:10.1890/04-1588
- Bouma, T., M. De Vries, and P. Herman. 2010. Comparing Ecosystem Engineering Efficiency of 2 Plant Species With Contrasting Growth Strategies. *Ecology* 91: 100125221703024--100125221703024. doi:10.1890/09-0690
- Bouwer, L. M., and P. Vellinga. 2007. On the flood risk in the Netherlands. doi:10.1007/978-1-4020-4200-3
- Brasseur, S., A. de Groot, G. Aarts, E. Dijkman, and R. Kirkwood. 2015. Pupping habitat of grey seals in the Dutch Wadden Sea.
- Brooks, H., I. Möller, S. Carr, and others. 2020. Resistance of salt marsh substrates to near-instantaneous hydrodynamic forcing. *Earth Surf. Process. Landforms* 46: 67–88. doi:10.1002/esp.4912
- Brouwer, G. A., J. van Dieren, L. Feekes, and others. 1950. *Griend. Het vogeleiland in de IJladdenzee*, Martinus Nijhoff, 's-Gravenhage.
- Brown, J., A. Colling, D. Park, J. Phillips, D. Rothery, and J. Wright. 1995. *Waves, Tides and Shallow-Water Processes*, Fourth. G. Bearman [ed.]. The Open University.
- Burylo, M., R. Freddy, N. Mathys, and D. Thierry. 2012. Plant root traits affecting the resistance of soils to concentrated flow erosion. *Earth Surf. Process. Landforms* 37: 1463–1470. doi:10.1002/esp.3248

C

- Cahoon, D. R. 2006. A review of major storm impacts on coastal wetland elevations. *Estuaries and Coasts* 29: 889–898. doi:10.1007/BF02798648
- Cahoon, D. R., P. F. Hensel, T. Spencer, D. J. Reed, K. L. McKee, and N. Saintilan. 2006. Coastal wetland vulnerability to relative sea-level rise: wetland elevation trends and process controls..
- Cahoon, D. R., B. C. Perez, B. D. Segura, and J. C. Lynch. 2011. Elevation trends and shrink-swell response of wetland soils to flooding and drying. *Estuar. Coast. Shelf Sci.* 91: 463–474. doi:10.1016/j.ecss.2010.03.022

REFERENCES

- Callaghan, D. P., T. J. Bouma, P. Klaassen, D. van der Wal, M. J. F. Stive, and P. M. J. Herman. 2010. Hydrodynamic forcing on salt-marsh development: Distinguishing the relative importance of waves and tidal flows. *Estuar. Coast. Shelf Sci.* 89: 73–88. doi:10.1016/j.ecss.2010.05.013
- Castagno, K. A., A. M. Jiménez-Robles, J. P. Donnelly, P. L. Wiberg, M. S. Fenster, and S. Fagherazzi. 2018. Intense Storms Increase the Stability of Tidal Bays. *Geophys. Res. Lett.* 45: 5491–5500. doi:10.1029/2018GL078208
- Chen, Q., J. P. Bakker, J. Alberti, and C. Smit. 2020. Long-term management is needed for conserving plant diversity in a Wadden Sea salt marsh. *Biodivers. Conserv.* 29: 2329–2341. doi:10.1007/s10531-020-01976-w
- Chen, Q., R. A. Howison, J. P. Bakker, J. Alberti, D. P. J. Kuijper, H. Olf, and C. Smit. 2019. Small herbivores slow down species loss up to 22 years but only at early successional stage. *J. Ecol.* 00: 1–9. doi:10.1111/1365-2745.13236
- Chen, S. C., H. C. Chan, and Y. H. Li. 2012. Observations on flow and local scour around submerged flexible vegetation. *Adv. Water Resour.* 43: 28–37. doi:10.1016/j.advwatres.2012.03.017
- Chowdhury, M. S. N., B. Walles, S. Sharifuzzaman, M. Shahadat Hossain, T. Ysebaert, and A. C. Smaal. 2019. Oyster breakwater reefs promote adjacent mudflat stability and salt marsh growth in a monsoon dominated subtropical coast. *Sci. Rep.* 9. doi:10.1038/s41598-019-44925-6
- Christianen, M. J. A., J. van Belzen, P. M. J. Herman, M. M. van Katwijk, L. P. M. Lamers, P. J. M. van Leent, and T. J. Bouma. 2013. Low-Canopy Seagrass Beds Still Provide Important Coastal Protection Services. *PLoS One* 8. doi:10.1371/journal.pone.0062413
- Christianen, M. J. A., T. van der Heide, S. J. Holthuijsen, K. J. van der Reijden, A. C. W. Borst, and H. Olf. 2017a. Biodiversity and food web indicators of community recovery in intertidal shellfish reefs. *Biol. Conserv.* 213: 317–324. doi:10.1016/j.biocon.2016.09.028
- Christianen, M. J. A., J. J. Middelburg, S. J. Holthuijsen, and others. 2017b. Benthic primary producers are key to sustain the Wadden Sea food web : stable carbon isotope analysis at landscape scale. 98: 1498–1512. doi:10.1002/ecy.1837
- Clarke, K. Robert. 1993. Nonparametric Multivariate Analyses of Changes in Community Structure. *Aust. J. Ecol.* 18: 117–143. doi:10.1111/j.1442-9993.1993.tb00438.x
- Colden, A. M., K. A. Fall, G. M. Cartwright, and C. T. Friedrichs. 2016. Sediment Suspension and Deposition Across Restored Oyster Reefs of Varying Orientation to Flow: Implications for Restoration. *Estuaries and Coasts* 39: 1435–1448. doi:10.1007/s12237-016-0096-y
- Compton, T. J., S. Holthuijsen, A. Koolhaas, and others. 2013. Distinctly variable mudscapes: Distribution gradients of intertidal macrofauna across the Dutch Wadden Sea. *J. Sea Res.* 82: 103–116. doi:10.1016/j.seares.2013.02.002
- Conery, I., J. P. Walsh, and D. Reide Corbett. 2018. Hurricane Overwash and Decadal-Scale Evolution of a Narrowing Barrier Island, Ocracoke Island, NC. *Estuaries and Coasts* 41: 1626–1642. doi:10.1007/s12237-018-0374-y
- Cooper, J. A. G. 2013. Mesoscale geomorphic change on low energy barrier islands in Chesapeake Bay, U.S.A. *Geomorphology* 199: 82–94. doi:10.1016/j.geomorph.2012.06.019
- Cooper, J. A. G., O. H. Pilkey, and D. A. Lewis. 2007. Islands behind islands: An unappreciated coastal land form category. *J. Coast. Res.* 907–911.
- Coops, H., H. J. Verheij, and R. Boeters. 1996. Interactions between waves, bank erosion and emergent vegetation: an experimental study in a wave tank. 53: 187–198.
- Cox, R., R. A. Wadsworth, and A. G. Thomson. 2003. Long-term changes in salt marsh extent affected by channel deepening in a modified estuary. *Cont. Shelf Res.* 23: 1833–1846. doi:10.1016/j.csr.2003.08.002
- Craft, C. B., E. D. Seneca, and S. W. Broome. 1991. Loss on ignition and kjeldahl digestion for estimating organic carbon and total nitrogen in estuarine marsh soils: Calibration with dry combustion. *Estuaries* 14: 175–179. doi:10.2307/1351691

D

- Dahl, M., E. Infantes, R. Clevesjö, H. W. Linderholm, M. Björk, and M. Gullström. 2018. Increased current flow enhances the risk of organic carbon loss from *Zostera marina* sediments: insights from a flume experiment. *Limnol. Oceanogr.*
- Davidson, K. E., M. S. Fowler, M. W. Skov, S. H. Doerr, N. Beaumont, and J. N. Griffin. 2017. Livestock grazing alters multiple ecosystem properties and services in salt marshes: A meta-analysis. *J. Appl. Ecol.* 54: 1395–1405. doi:10.1111/1365-2664.12892
- Davidson, K. E., M. S. Fowler, M. W. Skov, D. Forman, J. Alison, M. Botham, N. Beaumont, and J. N. Griffin. 2020. Grazing reduces bee abundance and diversity in saltmarshes by suppressing flowering of key plant species. *Agric. Ecosyst. Environ.* 291: 106760. doi:10.1016/j.agee.2019.106760
- Dennison, W. C. 1987. Effects of light on seagrass photosynthesis, growth and depth distribution. *Aquat. Bot.* 27: 15–26. doi:10.1016/0304-3770(87)90083-0
- Dennison, W. C., R. J. Orth, K. a Moore, J. C. Stevenson, V. Carter, S. Kollar, P. W. Bergstrom, and R. a Batiuk. 1993. Assessing Water Quality with Submersed Aquatic Vegetation Habitat requirements as barometers of Chesapeake Bay health. *Bioscience* 43: 86–94.
- Derksen-Hooijberg, M., C. Angelini, J. R. H. Hoogveld, and others. 2019. Repetitive desiccation events weaken a salt marsh mutualism. *J. Ecol.* 107: 2415–2426. doi:10.1111/1365-2745.13178
- Didier, D., C. Caulet, M. Bandet, P. Bernatchez, D. Dumont, E. Augereau, and F. Floc. 2020. Wave runup parameterization for sandy , gravel and platform beaches in a fetch-limited , large estuarine system. *Cont. Shelf Res.* 192: 104024. doi:10.1016/j.csr.2019.104024
- Dijkema, K. S., W. E. van Duin, E. M. Dijkman, and others. 2011. Vijftig jaar monitoring en beheer van de Friese en Groninger kwelderwerken: 1960-2009. *Wettelijk Onderz. Nat. Milieu WOt-werkdo*: 96.
- Dokter, A. M., H. P. Van Der Jeugd, W. Fokkema, B. S. Ebbinge, H. Olff, and B. A. Nolet. 2018. Agricultural pastures challenge the attractiveness of natural saltmarsh for a migratory goose. *J. Appl. Ecol.* 55: 2707–2718. doi:10.1111/1365-2664.13168
- Donadi, S., T. van der Heide, T. Piersma, and others. 2015. Multi-scale habitat modification by coexisting ecosystem engineers drives spatial separation of macrobenthic functional groups. 1502–1510. doi:10.1111/oik.02100
- Donadi, S., T. van der Heide, E. M. van der Zee, and others. 2013. Cross-habitat interactions among bivalve species control community structure on intertidal flats.pdf. 94: 489–498.
- Donker, J. J. A., M. Van Der Vegt, and P. Hoekstra. 2013. Wave forcing over an intertidal mussel bed. *J. Sea Res.* 82: 54–66. doi:10.1016/j.seares.2012.08.010
- Doody, J. P. 2013. Coastal squeeze and managed realignment in southeast England , does it tell us anything about the future? *Ocean Coast. Manag.* 79: 34–41. doi:10.1016/j.ocecoaman.2012.05.008
- Duarte, C. M. 1991. Seagrass depth limits. *Aquat. Bot.* 40: 363–377. doi:10.1016/0304-3770(91)90081-F
- Duarte, C. M., I. J. Losada, I. E. Hendriks, I. Mazarrasa, and N. Marbà. 2013. The role of coastal plant communities for climate change mitigation and adaptation. *Nat. Clim. Chang.* 3: 961–968. doi:10.1038/nclimate1970
- Durán Vinent, O., and L. J. Moore. 2015. Barrier island bistability induced by biophysical interactions. *Nat. Clim. Chang.* 5: 158–162. doi:10.1038/nclimate2474

E

- Eerd, M. M. V. A. N. 1985. Salt marsh cliff stability in the oosterschelde. *Earth Surf.* 10: 95–106. doi:10.1002/esp.3290100203
- Einstein, H. A., A. G. Anderson, and J. W. Johnson. 1940. A distinction between bed-load and suspended load in natural streams. *Eos, Trans. Am. Geophys. Union* 21: 628–633. doi:10.1029/TR021i002p00628

REFERENCES

- Elias, E. P. L., A. J. F. Van Der Spek, Z. B. Wang, and J. De Ronde. 2012. Morphodynamic development and sediment budget of the Dutch Wadden Sea over the last century. 293–310.
- Elschot, K., J. P. Bakker, S. Temmerman, J. Van De Koppel, and T. J. Bouma. 2015. Ecosystem engineering by large grazers enhances carbon stocks in a tidal salt marsh. *Mar. Ecol. Prog. Ser.* 537: 9–21. doi:10.3354/meps11447
- Elschot, K., T. J. Bouma, S. Temmerman, and J. P. Bakker. 2013. Effects of long-term grazing on sediment deposition and salt-marsh accretion rates. *Estuar. Coast. Shelf Sci.* 133: 109–115. doi:10.1016/j.ecss.2013.08.021
- Engelstad, A., B. G. Ruessink, P. Hoekstra, and M. van der Vegt. 2018. Sand Suspension and Transport During Inundation of a Dutch Barrier Island. *J. Geophys. Res. Earth Surf.* 123: 3292–3307. doi:10.1029/2018JF004736
- EurOtop. 2018. Manual on wave overtopping of sea defences and related structures. <http://www.overtopping-manual.com/>.

F

- Fagherazzi, S., G. Mariotti, N. Leonardi, A. Canestrelli, W. Nardin, and W. S. Kearney. 2020. Salt Marsh Dynamics in a Period of Accelerated Sea Level Rise. *J. Geophys. Res. Earth Surf.* 125: 1–31. doi:10.1029/2019JF005200
- Feagin, R. A., J. Figlus, J. C. Zinnert, and others. 2015. Going with the flow or against the grain? The promise of vegetation for protecting beaches, dunes, and barrier islands from erosion. *Front. Ecol. Environ.* 13: 203–210. doi:10.1890/140218
- Feagin, R. A., M. Furman, K. Salgado, and others. 2019. The role of beach and sand dune vegetation in mediating wave run up erosion. *Estuar. Coast. Shelf Sci.* 219: 97–106. doi:10.1016/j.ecss.2019.01.018
- Feagin, R. A., S. M. Lozada-Bernard, T. M. Ravens, I. Mo, K. M. Yeager, and A. H. Baird. 2009a. Does vegetation prevent wave erosion of salt marsh edges? *PNAS* 106: 10109–10113. doi:10.1073/pnas.0901297106
- Fivash, G. S., J. van Belzen, R. J. M. Temmink, K. Didderen, W. Lengkeek, T. van der Heide, and T. J. Bouma. 2020. Elevated micro-topography boosts growth rates in *Salicornia procumbens* by amplifying a tidally driven oxygen pump: Implications for natural recruitment and restoration. *Ann. Bot.* 125: 353–364. doi:10.1093/aob/mcz137
- Fivash, G. S., R. J. M. Temmink, M. D'Angelo, and others. 2021. Restoration of biogeomorphic systems by creating windows of opportunity to support natural establishment processes. *Ecol. Appl.* 0: 1–16. doi:10.1002/eap.2333
- Folmer, E., H. Büttger, M. Herlyn, A. Markert, G. Millat, K. Troost, and A. Wehrmann. 2017. Beds of blue mussels and Pacific oysters. In: *Wadden Sea Quality Status Report 2017*. Common Wadden Sea Secretariat.
- Fonseca, M. S., and J. A. Cahalan. 1992. A preliminary evaluation of wave attenuation by four species of seagrass. *Estuar. Coast. Shelf Sci.* 35: 565–576. doi:10.1016/S0272-7714(05)80039-3
- Fonseca, M. S., and M. A. R. Koehl. 2006. Flow in seagrass canopies: The influence of patch width. *Estuar. Coast. Shelf Sci.* 67: 1–9. doi:10.1016/j.ecss.2005.09.018
- Ford, H., A. Garbutt, C. Ladd, J. Malarkey, and M. W. Skov. 2016. Soil stabilization linked to plant diversity and environmental context in coastal wetlands. *J. Veg. Sci.* 27: 259–268. doi:10.1111/jvs.12367
- Francalanci, S., M. Bendoni, M. Rinaldi, and L. Solari. 2013. Geomorphology Ecomorphodynamic evolution of salt marshes: Experimental observations of bank retreat processes. *Geomorphology* 195: 53–65. doi:10.1016/j.geomorph.2013.04.026
- Friese, J., A. Temming, and A. Dänhardt. 2018. Grazing management affects fish diets in a Wadden Sea salt marsh. *Estuar. Coast. Shelf Sci.* 212: 341–352. doi:10.1016/j.ecss.2018.07.014

G

- Gailani, J. Z., L. Jin, J. McNeil, and W. Lick. 2001. Effects of Bentonite Clay on Sediment Erosion Rates. DOER Tech. Notes Collect. (ERDC TN-DOER-N9), U.S. Army Eng. Res. Dev. Cent.
- Gambi, M. C., A. R. M. Nowell, and P. A. Jumars. 1990. Flume Observations on Flow Dynamics in *Zostera marina* (Eelgrass) Beds. *Mar. Ecol. Prog. Ser.* 61: 159–169. doi:10.3354/meps061159
- Ganthy, F., L. Soissons, P. G. Sauriau, R. Verney, and A. Sottolichio. 2015. Effects of short flexible seagrass *Zostera noltei* on flow, erosion and deposition processes determined using flume experiments. *Sedimentology* 62: 997–1023. doi:10.1111/sed.12170
- Gedan, K. B., B. R. Silliman, and M. D. Bertness. 2009. Centuries of Human-Driven Change in Salt Marsh Ecosystems. *Ann. Rev. Mar. Sci.* 1: 117–141. doi:10.1146/annurev.marine.010908.163930
- Gelman, A., A. Jakulin, M. G. Pittau, and Y. S. Su. 2008. A weakly informative default prior distribution for logistic and other regression models. *Ann. Appl. Stat.* 2: 1360–1383. doi:10.1214/08-AOAS191
- Gijsman, R., E. M. Horstman, D. van der Wal, D. A. Friess, A. Swales, and K. M. Wijnberg. 2021. Nature-Based Engineering: A Review on Reducing Coastal Flood Risk With Mangroves. *Front. Mar. Sci.* 8. doi:10.3389/fmars.2021.702412
- Gillis, L. G., T. J. Bouma, C. G. Jones, M. M. Van Katwijk, I. Nagelkerken, C. J. L. Jeuken, P. M. J. Herman, and A. D. Ziegler. 2014. Potential for landscape-scale positive interactions among tropical marine ecosystems. *Mar. Ecol. Prog. Ser.* 503: 289–303. doi:10.3354/meps10716
- González-Ortiz, V., L. G. Egea, R. Jiménez-Ramos, F. Moreno-Mariñ, J. L. Pérez-Lloréns, T. J. Bouma, and F. G. Brun. 2014. Interactions between seagrass complexity, hydrodynamic flow and biomixing alter food availability for associated filter-feeding organisms. *PLoS One* 9. doi:10.1371/journal.pone.0104949
- Govers, L. L., and V. C. Reijers. 2021. Griend: Een bewogen eiland, KNNV Uitgeverij.
- Grabowski, R. C., I. G. Droppo, and G. Wharton. 2011. Earth-Science Reviews Erodibility of cohesive sediment: The importance of sediment properties. *Earth Sci. Rev.* 105: 101–120. doi:10.1016/j.earscirev.2011.01.008
- Gracia, A., N. Rangel-Buitrago, J. A. Oakley, and A. T. Williams. 2018. Use of ecosystems in coastal erosion management. *Ocean Coast. Manag.* 156: 277–289. doi:10.1016/j.ocecoaman.2017.07.009
- Granata, T. C., T. Serra, J. Colomer, X. Casamitjana, C. M. Duarte, and E. Gacia. 2001. Flow and particle distributions in a nearshore seagrass meadow before and after a storm. *Mar. Ecol. Prog. Ser.* 218: 95–106. doi:10.3354/meps218095
- De Groot, A. V., and W. E. Van Duin. 2013. Best practices for creating new salt marshes in an estuarine setting, a literature study. 39.

H

- Hansen, J. C. R., and M. A. Reidenbach. 2012. Wave and tidally driven flows in eelgrass beds and their effect on sediment suspension. *Mar. Ecol. Prog. Ser.* 448: 271–287. doi:10.3354/meps09225
- Van Der Heide, T., E. H. Van Nes, G. W. Geerling, A. J. P. Smolders, T. J. Bouma, and M. M. Van Katwijk. 2007. Positive feedbacks in seagrass ecosystems: Implications for success in conservation and restoration. *Ecosystems* 10: 1311–1322. doi:10.1007/s10021-007-9099-7
- Himmelstoss, E. A., R. E. Henderson, M. G. Kratzmann, and A. S. Farris. 2018. Digital Shoreline Analysis System (DSAS) Version 5.0 User Guide.
- Le Hir, P., W. Roberts, O. Cazaillet, M. Christie, P. Bassoullet, and C. Bacher. 2000. Characterization of intertidal flat hydrodynamics. *Cont. Shelf Res.* 20: 1433–1459. doi:10.1016/S0278-4343(00)00031-5
- Houwing, E.-J. J. 1999. Determination of the critical erosion threshold of cohesive sediments on intertidal mudflats along the Dutch Wadden Sea coast. *Estuarine, Coast. Shelf Sci.* 49: 545–555. doi:10.1006/ecss.1999.0518

REFERENCES

- Howes, N. C., D. M. Fitzgerald, Z. J. Hughes, I. Y. Georgiou, M. A. Kulp, M. D. Miner, J. M. Smith, and J. A. Barras. 2010. Hurricane-induced failure of low salinity wetlands. 107: 14014–14019. doi:10.1073/pnas.0914582107
- Howison, R. A., H. Olff, J. van de Koppel, and C. Smit. 2017. Biotically driven vegetation mosaics in grazing ecosystems: the battle between bioturbation and biocompaction. *Ecol. Monogr.* 87: 363–378. doi:10.1002/ecm.1259
- Howison, R. A., H. Olff, R. Steever, and C. Smit. 2015. Large herbivores change the direction of interactions within plant communities along a salt marsh stress gradient. 26: 1159–1170. doi:10.1111/jvs.12317
- Hu, Z., J. Van Belzen, D. Van Der Wal, T. Balke, Z. B. Wang, M. Stive, and T. J. Bouma. 2015. Windows of opportunity for salt marsh vegetation establishment on bare tidal flats: The importance of temporal and spatial variability in hydrodynamic forcing. *J. Geophys. Res. G Biogeosciences* 120: 1450–1469. doi:10.1002/2014JG002870
- Hu, Z., B. W. Borsje, J. Van Belzen, P. W. J. M. Willemssen, and H. Wang. 2021. Mechanistic modelling of marsh seedling establishment provides a positive outlook for coastal wetland restoration under global climate change. *Geophys. Res. Lett.* 1–19.
- Human, L. R. D., G. C. Snow, J. B. Adams, G. C. Bate, and S. C. Yang. 2015. The role of submerged macrophytes and macroalgae in nutrient cycling: A budget approach. *Estuar. Coast. Shelf Sci.* 154: 169–178. doi:10.1016/j.ecss.2015.01.001

I

- Infantes, E., A. Orfila, G. Simarro, J. Terrados, M. Luhar, and H. Nepf. 2012. Effect of a seagrass (*Posidonia oceanica*) meadow on wave propagation. *Mar. Ecol. Prog. Ser.* 456: 63–72. doi:10.3354/meps09754
- Infantes, E., J. C. De Smit, E. Tamarit, and T. J. Bouma. 2021. Making realistic wave climates in low-cost wave mesocosms: A new tool for experimental ecology and biogeomorphology. 10425. doi:10.1002/lom3.10425
- IPCC. 2014. Climate Change 2014: Synthesis Report. Contribution of Working Groups I, II and III to the Fifth Assessment Report of the Intergovernmental Panel on Climate Change.

J

- Janssen-Stelder, B. 2000. A system analysis of salt marsh development along the mainland coast of the Dutch Wadden Sea. Dr. Thesis 1–125.
- Jonge, V. N. De, K. Essink, and R. Boddeke. 1993. The Dutch Wadden Sea : a changed ecosystem. 45–71.

K

- Kamrath, P., M. Disse, M. Hammer, and J. Köngeter. 2006. Assessment of discharge through a dike breach and simulation of flood wave propagation. *Nat. Hazards* 38: 63–78. doi:10.1007/s11069-005-8600-x
- van Katwijk, M. M., A. Thorhaug, N. Marbà, and others. 2016. Global analysis of seagrass restoration: The importance of large-scale planting. *J. Appl. Ecol.* 53: 567–578. doi:10.1111/1365-2664.12562
- Kearney, M. S., and R. E. Turner. 2016. Microtidal Marshes: Can These Widespread and Fragile Marshes Survive Increasing Climate–Sea Level Variability and Human Action? *J. Coast. Res.* 319: 686–699. doi:10.2112/JCOASTRES-D-15-00069.1
- Keimer, K., D. Schürenkamp, F. Miescke, V. Kosmalla, O. Lojek, N. Goseberg, and M. Asce. 2021. Ecohydraulics of Surrogate Salt Marshes for Coastal Protection : Wave – Vegetation Interaction

- and Related Hydrodynamics on Vegetated Foreshores at Sea Dikes. 147: 1–14. doi:10.1061/(ASCE)WW.1943-5460.0000667
- Keshta, A., K. Koop-Jakobsen, J. Titschack, P. Mueller, K. Jensen, A. Baldwin, and S. Nolte. 2020. Ungrazed salt marsh has well connected soil pores and less dense sediment compared with grazed salt marsh: a CT scanning study. *Estuar. Coast. Shelf Sci.* 245: 106987. doi:10.1016/j.ecss.2020.106987
- Kiesel, J., L. R. Macpherson, M. Schuerch, and A. T. Vafeidis. 2021. Can Managed Realignment Buffer Extreme Surges? The Relationship Between Marsh Width, Vegetation Cover and Surge Attenuation. *Estuaries and Coasts*. doi:10.1007/s12237-021-00984-5
- Kirwan, M. L., and G. R. Guntenspergen. 2012. Feedbacks between inundation, root production, and shoot growth in a rapidly submerging brackish marsh. *J. Ecol.* 100: 764–770. doi:10.1111/j.1365-2745.2012.01957.x
- Kirwan, M. L., S. Temmerman, E. E. Skeehan, G. R. Guntenspergen, and S. Fagherazzi. 2016. Overestimation of marsh vulnerability to sea level rise. *Nat. Clim. Chang.* 6: 253–260. doi:10.1038/ndclimate2909
- van Klink, R., S. Nolte, F. S. Mandema, D. D. G. Lagendijk, M. F. WallisDeVries, J. P. Bakker, P. Esselink, and C. Smit. 2016. Effects of grazing management on biodiversity across trophic levels—The importance of livestock species and stocking density in salt marshes. *Agric. Ecosyst. Environ.* 235: 329–339. doi:10.1016/j.agee.2016.11.001
- van Klink, R., F. van der Plas, C. G. E. T. van Noordwijk, M. F. Wallisdevries, and H. Olff. 2015. Effects of large herbivores on grassland arthropod diversity. *Biol. Rev.* 90: 347–366. doi:10.1111/brev.12113
- van de Koppel, J., T. van der Heide, A. H. Altieri, B. K. Eriksson, T. J. Bouma, H. Olff, and B. R. Silliman. 2015. Long-Distance Interactions Regulate the Structure and Resilience of Coastal Ecosystems. *Ann. Rev. Mar. Sci.* 7: 139–158. doi:10.1146/annurev-marine-010814-015805
- Van de Koppel, J., D. Van der Wal, J. P. Bakker, and P. M. J. Herman. 2005. Self-Organization and Vegetation Collapse in Salt Marsh Ecosystems. *Am. Nat.* 165: 1–12. doi:10.1086/426602
- Koppenaar, P., E. C. Esselink, W. E. van Duin, and J. P. Bakker. 2021. Temporal and Spatial Accretion Patterns and the Impact of Livestock Grazing in a Restored Coastal Salt Marsh. *Estuaries and Coasts*. doi:10.1007/s12237-021-00963-w
- Kroon, A. 1994. Sediment transport and morphodynamics of the beach and nearshore zone near Egmond, The Netherlands. University of Utrecht.
- Kuijper, D., and J. Bakker. 2005. Top-down control of small herbivores on salt-marsh vegetation along a productivity gradient. *Ecology* 86: 914–923. doi:10.1890/04-0693

L

- Ladd, C. J. T., M. F. Duggan-Edwards, T. J. Bouma, J. F. Pagès, and M. W. Skov. 2019. Sediment Supply Explains Long-Term and Large-Scale Patterns in Salt Marsh Lateral Expansion and Erosion. *Geophys. Res. Lett.* 46: 11178–11187. doi:10.1029/2019GL083315
- Ladd, C. J. T., M. F. Duggan-Edwards, J. F. Pagès, and M. W. Skov. 2021. Saltmarsh Resilience to Periodic Shifts in Tidal Channels. *Front. Mar. Sci.* 8: 1–13. doi:10.3389/fmars.2021.757715
- Lai, S., L. H. L. Loke, M. J. Hilton, T. J. Bouma, and P. A. Todd. 2015. The effects of urbanisation on coastal habitats and the potential for ecological engineering: A Singapore case study. *Ocean Coast. Manag.* 103: 78–85. doi:10.1016/j.ocecoaman.2014.11.006
- Van Ledden, M., W. G. M. Van Kesteren, and J. C. Winterwerp. 2004. A conceptual framework for the erosion behaviour of sand-mud mixtures. *Cont. Shelf Res.* 24: 1–11. doi:10.1016/j.csr.2003.09.002
- Lefebvre, A., C. E. L. Thompson, and C. L. Amos. 2010. Influence of *Zostera marina* canopies on unidirectional flow, hydraulic roughness and sediment movement. *Cont. Shelf Res.* 30: 1783–1794. doi:10.1016/j.csr.2010.08.006

REFERENCES

- Leonardi, N., I. Carnacina, C. Donatelli, N. K. Ganju, A. J. Plater, M. Schuerch, and S. Temmerman. 2018. Dynamic interactions between coastal storms and salt marshes: A review. *Geomorphology* 301: 92–107. doi:10.1016/j.geomorph.2017.11.001
- Leonardi, N., and S. Fagherazzi. 2015. Effect of local variability in erosional resistance on large-scale morphodynamic response of salt marshes to wind waves and extreme events. *Geophys. Res. Lett.* 5872–5879. doi:10.1002/2015GL064730.Received
- Leonardi, N., N. K. Ganju, and S. Fagherazzi. 2016. A linear relationship between wave power and erosion determines salt-marsh resilience to violent storms and hurricanes. *Proc. Natl. Acad. Sci.* 113: 64–68. doi:10.1073/pnas.1510095112
- Li, Y., X.-M. Zhu, and J.-Y. Tian. 1991. Effectiveness of plant roots to increase the anti-scourability of soil on the Loess Plateau. *Chinese Sci. Bull.* 36: 077–2082.
- Lilley, R. J., and R. K. F. Unsworth. 2014. Atlantic Cod (*Gadus morhua*) benefits from the availability of seagrass (*Zostera marina*) nursery habitat. *Glob. Ecol. Conserv.* 2: 367–377. doi:10.1016/j.gecco.2014.10.002
- Liu, Z., S. Fagherazzi, and B. Cui. 2021. Success of coastal wetlands restoration is driven by sediment availability. *Commun. Earth Environ.* 2: 1–9. doi:10.1038/s43247-021-00117-7
- Lo, V. B., T. J. Bouma, J. van Belzen, C. Van Colen, and L. Airoidi. 2017. Interactive effects of vegetation and sediment properties on erosion of salt marshes in the Northern Adriatic Sea. *Mar. Environ. Res.* 131: 32–42. doi:10.1016/j.marenvres.2017.09.006
- van Loon-Steensma, J. M. 2015. Salt marshes to adapt the flood defences along the Dutch Wadden Sea coast. *Mitig. Adapt. Strateg. Glob. Chang.* 20: 929–948. doi:10.1007/s11027-015-9640-5
- van Loon-Steensma, J. M., H. A. Schelfhout, M. E. A. Broekmeyer, M. P. C. P. Paulissen, W. T. Oostenbrink, C. Smit, and E. Jolink. 2014a. Nadere verkenning Groene Dollard Dijk. 90.
- van Loon-Steensma, J. M., H. A. Schelfhout, and P. Vellinga. 2014b. Green adaptation by innovative dike concepts along the Dutch Wadden Sea coast. *Environ. Sci. Policy* 44: 108–125. doi:10.1016/j.envsci.2014.06.009
- Van Loon-steensma, J. M., and P. A. Slim. 2013. The Impact of Erosion Protection by Stone Dams on Salt-Marsh Vegetation on Two Wadden Sea Barrier Islands Stable URL : <http://www.jstor.org/stable/23486550> Linked references are available on JSTOR for this article : The Impact of Erosion Protection by Sto. *J. Coast. Res.* 29: 783–796.
- Loonstra, A. H. J., T. Piersma, and J. Reneerkens. 2016. Staging Duration and Passage Population Size of Sanderlings in the Western Dutch Wadden Sea. *Ardea* 104: 49–61. doi:10.5253/arde.v104i1.a4

M

- Mandema, F. S., J. M. Tinbergen, B. J. Ens, and J. P. Bakker. 2013. Livestock grazing and trampling of birds' nests: An experiment using artificial nests. *J. Coast. Conserv.* 17: 409–416. doi:10.1007/s11852-013-0239-2
- Marani, M., C. Da, and A. D. Alpaos. 2013. Vegetation engineers marsh morphology through multiple competing stable states. doi:10.1073/pnas.1218327110
- Marchand, P., and D. Gill. 2018. waver: Calculate Fetch and Wave Energy.
- Marin-Diaz, B., G. S. Fivash, J. Nauta, and others. 2021. On the use of large-scale biodegradable artificial reefs for intertidal foreshore stabilization. 170. doi:10.1016/j.ecoleng.2021.106354
- Mariotti, G., and S. Fagherazzi. 2013. Critical width of tidal flats triggers marsh collapse in the absence of sea-level rise. *Proc. Natl. Acad. Sci.* 110: 5353–5356. doi:10.1073/pnas.1219600110
- Mateos-Naranjo, E., S. Redondo-Gómez, C. J. Luque, E. M. Castellanos, A. J. Davy, and M. E. Figueroa. 2008. Environmental limitations on recruitment from seed in invasive *Spartina densiflora* on a southern European salt marsh. *Estuar. Coast. Shelf Sci.* 79: 727–732. doi:10.1016/j.ecss.2008.06.017
- Maxwell, P. S., J. S. Eklöf, M. M. van Katwijk, and others. 2017. The fundamental role of ecological feedback mechanisms for the adaptive management of seagrass ecosystems – a review. *Biol. Rev.* 92: 1521–1538. doi:10.1111/brv.12294

- McBride, R. A., M. J. Taylor, and M. R. Byrnes. 2007. Coastal morphodynamics and Chenier-Plain evolution in southwestern Louisiana, USA: A geomorphic model. *Geomorphology* 88: 367–422. doi:10.1016/j.geomorph.2006.11.013
- McLeod, E., G. L. Chmura, S. Bouillon, and others. 2011. A blueprint for blue carbon: Toward an improved understanding of the role of vegetated coastal habitats in sequestering CO₂. *Front. Ecol. Environ.* 9: 552–560. doi:10.1890/110004
- Menéndez, M., and P. L. Woodworth. 2010. Changes in extreme high water levels based on a quasi-global tide-gauge data set. *J. Geophys. Res. Ocean.* 115: 1–15. doi:10.1029/2009JC005997
- Meyer, D. L., E. C. Townsend, and G. W. Thayer. 1997. Erosion Control Value of Oyster Cultch for Intertidal Marsh. 5: 93–99.
- Moksnes, P. O., L. Eriander, E. Infantes, and M. Holmer. 2018. Local Regime Shifts Prevent Natural Recovery and Restoration of Lost Eelgrass Beds Along the Swedish West Coast. *Estuaries and Coasts* 1–20. doi:10.1007/s12237-018-0382-y
- Möller, I. 2006. Quantifying saltmarsh vegetation and its effect on wave height dissipation : Results from a UK East coast saltmarsh. *Estuar. Coast. Shelf Sci.* 69: 337–351. doi:10.1016/j.ecss.2006.05.003
- Möller, I., M. Kudella, F. Rupprecht, and others. 2014. Wave attenuation over coastal salt marshes under storm surge conditions. *Nat. Geosci.* 7. doi:10.1038/ngeo2251
- Möller, I., and T. Spencer. 2002. Wave dissipation over macro-tidal saltmarshes: Effects of marsh edge typology and vegetation change. *J. Coast. Res.* 36: 506–521. doi:ISSN:0749-0208
- Möller, I., T. Spencer, J. R. French, D. J. Leggett, and M. Dixon. 1999. Wave Transformation Over Salt Marshes : A Field and Numerical Modelling Study from North Norfolk , England. *Estuarine, Coast. Shelf Sci.* 411–426.
- Morris, J. T., P. V. Sundareshwar, C. Nietch, B. Kjerfve, and D. R. Cahoon. 2002. Responses of coastal wetlands to rising sea level. *Ecology* 83: 2869–2877.
- Morris, R. L., D. M. Bilkovic, M. K. Boswell, and others. 2019. The application of oyster reefs in shoreline protection: Are we over-engineering for an ecosystem engineer? *J. Appl. Ecol.* 56: 1703–1711. doi:10.1111/1365-2664.13390
- Morris, R. L., A. Boxshall, and S. E. Swearer. 2020. Climate-resilient coasts require diverse defence solutions. *Nat. Clim. Chang.* 10: 485–487. doi:10.1038/s41558-020-0798-9
- Morris, R. L., T. M. Konlechner, Ghisalberti, and S. E. Swearer. 2018. From grey to green : Efficacy of eco-engineering solutions for nature-based coastal defence. *Glob. Chang. Biol.* 24: 1827–1842. doi:10.1111/gcb.14063
- Murray, N. J., S. R. Phinn, M. DeWitt, and others. 2019. The global distribution and trajectory of tidal flats. *Nature* 565: 222–225. doi:10.1038/s41586-018-0805-8

N

- La Nafie, Y. A., C. B. de los Santos, F. G. Brun, M. M. van Katwijk, and T. J. Bouma. 2012. Waves and high nutrient loads jointly decrease survival and separately affect morphological and biomechanical properties in the seagrass *Zostera noltii*. *Limnol. Oceanogr.* 57: 1664–1672. doi:10.4319/lo.2012.57.6.1664
- Narayan, S., M. W. Beck, B. G. Reguero, and others. 2016. The effectiveness, costs and coastal protection benefits of natural and nature-based defences. *PLoS One* 11: 1–18. doi:10.1371/journal.pone.0154735
- Neal, A., J. Richards, and K. Pye. 2002. Structure and development of shell cheniers in Essex, southeast England, investigated using high-frequency ground-penetrating radar. *Mar. Geol.* 185: 435–469. doi:10.1016/S0025-3227(01)00239-0
- Nepf, H. M. 2012. Flow and Transport in Regions with Aquatic Vegetation. *Annu. Rev. Fluid Mech.* 44: 123–142. doi:10.1146/annurev-fluid-120710-101048
- Nicholls, R. J., S. Hanson, C. Herweijer, N. Patmore, S. Hallegatte, J. Corfee-Morlot, J. Chateau, and R. Muir-Wood. 2007. Ranking of The World's Cities Most Exposed to Coastal Flooding Today Executive Summary. *Organ. Econ. Coop. Dev.*

REFERENCES

- Nieuwhof, A., and P. C. Vos. 2018. New data from terp excavations on sea-level index points and salt marsh sedimentation rates in the eastern part of the Dutch Wadden Sea. *Geol. en Mijnbouw/Netherlands J. Geosci.* 97: 31–43. doi:10.1017/njg.2018.2
- Nieuwhof, S., P. M. J. Herman, N. Dankers, K. Troost, and D. Van Der Wal. 2015. Remote sensing of epibenthic shellfish using synthetic aperture radar satellite imagery. *Remote Sens.* 7: 3710–3734. doi:10.3390/rs70403710
- Nolte, S., E. C. Koppenaar, P. Esselink, K. S. Dijkema, M. Schuerch, A. V. De Groot, J. P. Bakker, and S. Temmerman. 2013. Measuring sedimentation in tidal marshes: A review on methods and their applicability in biogeomorphological studies. *J. Coast. Conserv.* 17: 301–325. doi:10.1007/s11852-013-0238-3
- Nordstrom, K. F., and N. L. Jackson. 2012. Physical processes and landforms on beaches in short fetch environments in estuaries, small lakes and reservoirs: A review. *Earth-Science Rev.* 111: 232–247. doi:10.1016/j.earscirev.2011.12.004

O

- Oertel, G. F. 1985. The barrier island system. *Mar. Geol.* 63: 1–18. doi:10.1016/0025-3227(85)90077-5
- Oksanen, J., F. G. Blanchet, R. Kindt, P. Legendre, P. R. Minchin, R. B. O'hara, &..., and H. Wagner. 2018. *vegan: Community Ecology Package*. R package version 2.5-6. 2–5.
- Olf, H., J. De Leeuw, J. P. Bakker, R. J. Platerink, and H. J. van Wijnen. 1997. Vegetation Succession and Herbivory in a Salt Marsh: Changes Induced by Sea Level Rise and Silt Deposition Along an Elevational Gradient. *J. Ecol.* 85: 799. doi:10.2307/2960603
- Olf, H., and M. E. Ritchie. 1998. Effects of herbivores on grassland plant diversity. *Trends Ecol. Evol.* 13: 261–265. doi:https://doi.org/10.1016/S0169-5347(98)01364-0
- Ondiviela, B., I. J. Losada, J. L. Lara, M. Maza, C. Galván, T. J. Bouma, and J. van Belzen. 2014. The role of seagrasses in coastal protection in a changing climate. *Coast. Eng.* 87: 158–168. doi:10.1016/j.coastaleng.2013.11.005
- Orth, R. J., T. J. B. Carruthers, W. C. Dennison, and others. 2006. A Global Crisis for Seagrass Ecosystems. *Bioscience* 56: 987–996. doi:10.1641/0006-3568(2006)56[987:agcfse]2.0.co;2
- Osswald, F., T. Dolch, and K. Reise. 2019. Remobilizing stabilized island dunes for keeping up with sea level rise? *J. Coast. Conserv.* 23: 675–687.
- Otvos, E. G. 2020. Coastal barriers - fresh look at origins, nomenclature and classification issues. *Geomorphology* 355: 107000. doi:10.1016/j.geomorph.2019.107000

P

- Pagés, J., S. R. Jenkins, T. J. Bouma, E. Sharps, J. F. Page, and M. W. Skov. 2018. Opposing Indirect Effects of Domestic Herbivores on Saltmarsh Erosion. *Ecosystems* 22: 1055–1068. doi:10.1007/s10021-018-0322-5
- Paoli, H. De, J. Van De Koppel, E. Van Der Zee, A. Kangeri, and J. Van Belzen. 2015. Processes limiting mussel bed restoration in the Wadden-Sea. *J. Sea Res.* 103: 42–49. doi:10.1016/j.seares.2015.05.008
- Paul, M., and N. B. Kerpen. 2021. Erosion protection by winter state of salt marsh vegetation. *J. Ecohydraulics* 0: 1–10. doi:10.1080/24705357.2021.1938252
- Perkins-Kirkpatrick, S. E., and S. C. Lewis. 2020. Increasing trends in regional heatwaves. *Nat. Commun.* 11: 1–8. doi:10.1038/s41467-020-16970-7
- Phillips, J. D. 1986. Coastal Submergence and Marsh Fringe Erosion. *J. Coast. Res.* 2: 427–436.
- Piazza, B. P., P. D. Banks, and M. K. La Peyre. 2005. The potential for created oyster shell reefs as a sustainable shoreline protection strategy in Louisiana. *Restor. Ecol.* 13: 499–506. doi:10.1111/j.1526-100X.2005.00062.x

- Piersma, T., R. Hoekstra, A. Dekinga, A. Koolhaas, P. Wolf, P. Battley, and P. Wiersma. 1993. Scale and intensity of intertidal habitat use by knots *Calidris canutus* in the Western Wadden Sea in relation to food, friends and foes. *Netherlands J. Sea Res.* 31: 331–357. doi:10.1016/0077-7579(93)90052-T
- Pilkey, O. H., J. A. G. Cooper, and D. A. Lewis. 2009. Global distribution and geomorphology of fetch-limited barrier islands. *J. Coast. Res.* 25: 819–837. doi:10.2112/08-1023.1
- Pinsky, M. L., G. Guannel, and K. K. Arkema. 2013. Quantifying wave attenuation to inform coastal habitat conservation. *Ecosphere* 4: art95. doi:10.1890/ES13-00080.1
- Polidoro, A. 2014. Wave run-up on shingle beaches: A new method.
- Priestas, A. M., G. Mariotti, N. Leonardi, and S. Fagherazzi. 2015. Coupled Wave Energy and Erosion Dynamics along a Salt Marsh Boundary, Hog Island Bay, Virginia, USA. *Mar. Sci. Eng.* 3: 1041–1065. doi:10.3390/jmse3031041

R

- R Development Core Team. 2018. R: A language and environment for statistical computing.
- Redfield, A. C., E. Monographs, and N. Spring. 1972. Development of a New England Salt Marsh. *Ecol. Monogr.* 42: 201–237. doi:10.2307/1942263
- Reed, D. J., T. Spencer, A. L. Murray, J. R. French, and L. Leonard. 1999. Marsh surface sediment deposition and the role of tidal creeks: Implications for created and managed coastal marshes. *J. Coast. Conserv.* 5: 81–90. doi:10.1007/BF02802742
- Reise, K., M. Baptist, P. Burbridge, N. Dankers, L. Fischer, B. Flemming, A. P. Oost, and C. Smit. 2010. The Wadden Sea - A Universally Outstanding Tidal Wetland: The Wadden Sea Quality Status Report Synthesis Report 2010. *Wadden Sea Ecosyst.* 29: 7–24.
- van Rijn, L. C. 2019. Erodibility of Mud–Sand Bed Mixtures. *J. Hydraul. Eng.* 146: 04019050. doi:10.1061/(asce)hy.1943-7900.0001677
- Van Rijn, L. C. 1984a. Sediment transport, Part I: bed load transport. *J. Hydraul. Eng.* 110: 1431–1456. doi:10.1061/(ASCE)0733-9429(1987)113:9(1187)
- Van Rijn, L. C. 1984b. Sediment transport, Part II: Suspended Load Transport. 110: 655–664.
- Ritz, C., F. Baty, J. C. Streibig, and D. Gerhard. 2015. Dose-Response Analysis Using R. *PLoS One* 10.
- Ros, À., J. Colomer, T. Serra, D. Pujol, M. Soler, and X. Casamitjana. 2014. Experimental observations on sediment resuspension within submerged model canopies under oscillatory flow. *Cont. Shelf Res.* 91: 220–231. doi:10.1016/j.csr.2014.10.004
- RWS. 2013. Kenmerkende waarden. Getijgebied 2011.0.

S

- Salvador de Paiva, J. N., B. Walles, T. Ysebaert, and T. J. Bouma. 2018. Understanding the conditionality of ecosystem services : The effect of tidal flat morphology and oyster reef characteristics on sediment stabilization by oyster reefs. *Ecol. Eng.* 112: 89–95. doi:10.1016/j.ecoleng.2017.12.020
- Scheres, B., and H. Schüttrumpf. 2019. Enhancing the ecological value of sea dikes. *Water (Switzerland)* 11. doi:10.3390/w11081617
- Scheres, B., and H. Schüttrumpf. 2020. Investigating the Erosion Resistance of Different Vegetated Surfaces for Ecological Enhancement of Sea Dikes. *J. Mar. Sci. Eng.* 8: 519. doi:10.3390/jmse8070519
- Schneider, C. A., W. S. Rasband, and K. W. Eliceiri. 2012. HISTORICAL commentary NIH Image to ImageJ : 25 years of image analysis. *Nat. Methods* 9: 671–675. doi:10.1038/nmeth.2089
- Schoonees, T., A. Gijón Mancheño, B. Scheres, T. J. Bouma, R. Silva, T. Schlurmann, and H. Schüttrumpf. 2019. Hard Structures for Coastal Protection, Towards Greener Designs. *Estuaries and Coasts* 42: 1709–1729. doi:10.1007/s12237-019-00551-z

REFERENCES

- Schotanus, J., J. J. Capelle, E. Paree, G. S. Fivash, J. van de Koppel, and T. J. Bouma. 2020. Restoring mussel beds in highly dynamic environments by lowering environmental stressors. *Restor. Ecol.* 1–11. doi:10.1111/rec.13168
- Schrama, M., L. A. van Boheemen, H. Olff, and M. P. Berg. 2015. How the litter-feeding bioturbator *Orchestia gammarellus* promotes late-successional saltmarsh vegetation. *J. Ecol.* 103: 915–924. doi:10.1111/1365-2745.12418
- Schrama, M., P. Heijning, J. P. Bakker, H. J. Van Wijnen, M. P. Berg, and H. Olff. 2013. Herbivore trampling as an alternative pathway for explaining differences in nitrogen mineralization in moist grasslands. *Oecologia* 172: 231–243. doi:10.1007/s00442-012-2484-8
- Schuerch, M., T. Dolch, K. Reise, and A. T. Vafeidis. 2014. Unravelling interactions between salt marsh evolution and sedimentary processes in the Wadden Sea (southeastern North Sea). *Prog. Phys. Geogr.* 38: 691–715. doi:10.1177/0309133314548746
- Schüttrumpf, H., and H. Oumeraci. 2005. Layer thicknesses and velocities of wave overtopping flow at seadikes. *Coast. Eng.* 52: 473–495. doi:10.1016/j.coastaleng.2005.02.002
- Schwarz, C., T. J. Bouma, L. Q. Zhang, S. Temmerman, T. Ysebaert, and P. M. J. Herman. 2015. Geomorphology Interactions between plant traits and sediment characteristics in influencing species establishment and scale-dependent feedbacks in salt marsh ecosystems. *Geomorphology* 250: 298–307. doi:10.1016/j.geomorph.2015.09.013
- Schwimmer, R. A., R. Bay, and R. A. Schwimmer. 2001. Rates and Processes of Marsh Shoreline Erosion in Rehoboth Bay, Delaware, U.S.A. *J. Coast. Researc* 17: 672–683.
- Sharma, S., J. Goff, R. M. Moody, and others. 2016. Effects of shoreline dynamics on saltmarsh vegetation. *PLoS One* 11. doi:10.1371/journal.pone.0159814
- Shepard, C. C., C. M. Crain, and M. W. Beck. 2011. The protective role of coastal marshes: A systematic review and meta-analysis. *PLoS One* 6. doi:10.1371/journal.pone.0027374
- Siemes, R. W. A., B. W. Borsje, R. J. Daggenvoorde, and S. J. M. H. Hulscher. 2020. Artificial structures steer morphological development of salt marshes: A model study. *J. Mar. Sci. Eng.* 8. doi:10.3390/JMSE8050326
- Silinski, A., E. Fransen, T. J. Bouma, P. Meire, and S. Temmerman. 2016. Unravelling the controls of lateral expansion and elevation change of pioneer tidal marshes. *Geomorphology* 274: 106–115. doi:10.1016/j.geomorph.2016.09.006
- Silinski, A., M. Heuner, J. Schoelynck, and others. 2015. Effects of wind waves versus ship waves on tidal marsh plants: A flume study on different life stages of *Scirpus maritimus*. *PLoS One* 10: 1–16. doi:10.1371/journal.pone.0118687
- Silliman, B. R., J. De Van Koppel, M. D. Bertness, L. E. Stanton, and I. A. Mendelssohn. 2005. Drought, snails, and large-scale die-off of Southern U.S. salt marshes. *Science* (80-). 310: 1803–1806. doi:10.1126/science.1118229
- Silliman, B. R., E. Schrack, Q. He, and others. 2015. Facilitation shifts paradigms and can amplify coastal restoration efforts. *Proc. Natl. Acad. Sci.* 112: 14295–14300. doi:10.1073/pnas.1515297112
- Soil Science Division Staff. 2017. *Soil Survey Manual*.
- Spencer, K. L., and G. L. Harvey. 2012. Understanding system disturbance and ecosystem services in restored saltmarshes: Integrating physical and biogeochemical processes. *Estuar. Coast. Shelf Sci.* 106: 23–32. doi:10.1016/j.ecss.2012.04.020
- Spencer, T., S. M. Brooks, B. R. Evans, J. A. Tempest, and I. Möller. 2015. Southern North Sea storm surge event of 5 December 2013: Water levels, waves and coastal impacts. *Earth Sci. Rev.* 146: 120–145. doi:10.1016/j.earscirev.2015.04.002
- Spencer, T., I. Möller, F. Rupprecht, and others. 2016. Salt marsh surface survives true-to-scale simulated storm surges. *Earth Surf. Process. Landforms* 41: 543–552. doi:10.1002/esp.3867
- Syvitski, J. P. M., A. J. Kettner, I. Overeem, and others. 2009. Sinking deltas due to human activities. *Nat. Geosci.* 2: 681–686. doi:10.1038/ngeo629

T

- Temmerman, S., P. Meire, T. J. Bouma, P. M. J. Herman, T. Ysebaert, and H. J. De Vriend. 2013. Ecosystem-based coastal defence in the face of global change. *Nature* 504: 79–83. doi:10.1038/nature12859
- Temmink, R. J. M. 2020. The restoration of wetlands dominated by habitat modifiers. PhD Thesis, University of Groningen (<https://repository.ubn.ru.nl/handle/2066/225923>).
- Temmink, R. J. M., M. J. A. Christianen, G. S. Fivash, and others. 2020. Mimicry of emergent traits amplifies coastal restoration success. *Nat. Commun.* 1–9. doi:10.1038/s41467-020-17438-4
- Terrados, J., and J. Borum. 2004. Why are seagrasses important? - Goods and services provided by seagrass meadows. *Eur. seagrasses an Introd. to Monit. Manag.* 8–10.
- Timmons, E. A., A. B. Rodriguez, C. R. Mattheus, and R. DeWitt. 2010. Transition of a regressive to a transgressive barrier island due to back-barrier erosion, increased storminess, and low sediment supply: Bogue Banks, North Carolina, USA. *Mar. Geol.* 278: 100–114. doi:10.1016/j.margeo.2010.09.006
- Törnqvist, T. E., K. L. Jankowski, Y. X. Li, and J. L. González. 2020. Tipping points of Mississippi Delta marshes due to accelerated sea-level rise. *Sci. Adv.* 6: eaaz5512. doi:10.1126/sciadv.aaz5512
- Türker, U., O. Yagci, and M. S. Kabdasli. 2019. Impact of nearshore vegetation on coastal dune erosion : assessment through laboratory experiments. *Environ. Earth Sci.* 78: 1–14. doi:10.1007/s12665-019-8602-8
- Twomey, A. J., M. I. Saunders, D. P. Callaghan, T. J. Bouma, Q. Han, and K. R. O'Brien. 2021. Lateral sediment erosion with and without the non-dense root-mat forming seagrass *Enhalus acoroides*. *Estuar. Coast. Shelf Sci.* 253: 107316. doi:10.1016/j.ecss.2021.107316

V

- Vannoppen, W., S. De Baets, J. Keeble, Y. Dong, and J. Poesen. 2017. How do root and soil characteristics affect the erosion-reducing potential of plant species? *Ecol. Eng.* 109: 186–195. doi:10.1016/j.ecoleng.2017.08.001
- Veeneklaas, R., A. Bockelman, T. Reusch, and J. Bakker. 2011. Effect of grazing and mowing on the clonal structure of *Elytrigia atherica* : a long-term study of abandoned and managed sites. *Preslia* 83: 455–470.
- Vinent, O. D., B. E. Schaffer, and I. Rodriguez-Iturbe. 2021. Stochastic dynamics of barrier island elevation. *Proc. Natl. Acad. Sci. U. S. A.* 118: 6–11. doi:10.1073/pnas.2013349118
- Vousdoukas, M. I., L. Mentaschi, E. Voukouvalas, M. Verlaan, S. Jevrejeva, L. P. Jackson, and L. Feyen. 2018. Global probabilistic projections of extreme sea levels show intensification of coastal flood hazard. 9: 1–12. doi:10.1038/s41467-018-04692-w
- Vroom, J., B. van Maren, M. Ibanez, M. de L. Pardo, H. Winterwerp, and L. Sittoni. 2014. Mud dynamics in the Ems-Dollard, phase 2.
- Vuik, V., B. W. Borsje, P. W. J. M. Willemsen, and S. N. Jonkman. 2019. Salt marshes for flood risk reduction: Quantifying long-term effectiveness and life-cycle costs. *Ocean Coast. Manag.* 171: 96–110. doi:10.1016/j.ocecoaman.2019.01.010
- Vuik, V., S. N. Jonkman, B. W. Borsje, and T. Suzuki. 2016. Nature-based flood protection: The efficiency of vegetated foreshores for reducing wave loads on coastal dikes. *Coast. Eng.* 116: 42–56. doi:10.1016/j.coastaleng.2016.06.001
- Vuik, V., H. Y. Suh Heo, Z. Zhu, B. W. Borsje, and S. N. Jonkman. 2017. Stem breakage of salt marsh vegetation under wave forcing: A field and model study. *Estuar. Coast. Shelf Sci.* doi:10.1016/j.ecss.2017.09.028
- Vuik, V., H. Y. Suh Heo, Z. Zhu, B. W. Borsje, and S. N. Jonkman. 2018. Stem breakage of salt marsh vegetation under wave forcing: A field and model study. *Estuar. Coast. Shelf Sci.* 200: 41–58. doi:10.1016/j.ecss.2017.09.028

REFERENCES

- van der Wal, D., and K. Pye. 2004. Patterns, rates and possible causes of saltmarsh erosion in the Greater Thames area (UK). *Geomorphology* 61: 373–391. doi:10.1016/j.geomorph.2004.02.005
- Van der Wal, D., A. Wielemaker-Van den Dool, and P. M. J. Herman. 2008. Spatial patterns, rates and mechanisms of saltmarsh cycles (Westerschelde, The Netherlands). *Estuar. Coast. Shelf Sci.* 76: 357–368. doi:10.1016/j.ecss.2007.07.017

W

- Walles, B., F. J. Fodrie, S. Nieuwhof, O. J. D. Jewell, P. M. J. Herman, and T. Ysebaert. 2016a. Guidelines for evaluating performance of oyster habitat restoration should include tidal emersion: Reply to Baggett et al. *Restor. Ecol.* 24: 4–7. doi:10.1111/rec.12328
- Walles, B., J. Salvador de Paiva, B. C. van Prooijen, T. Ysebaert, and A. C. Smaal. 2015. The Ecosystem Engineer *Crassostrea gigas* Affects Tidal Flat Morphology Beyond the Boundary of Their Reef Structures. *Estuaries and Coasts* 38: 941–950. doi:10.1007/s12237-014-9860-z
- Walles, B., K. Troost, D. van den Ende, S. Nieuwhof, A. C. Smaal, and T. Ysebaert. 2016b. From artificial structures to self-sustaining oyster reefs. *J. Sea Res.* 108: 1–9. doi:10.1016/j.seares.2015.11.007
- Wang, C., and S. Temmerman. 2013. Does biogeomorphic feedback lead to abrupt shifts between alternative landscape states?: An empirical study on intertidal flats and marshes. *J. Geophys. Res. Earth Surf.* 118: 229–240. doi:10.1029/2012JF002474
- Wang, H., D. van der Wal, X. Li, and others. 2017. Zooming in and out: scale-dependence of extrinsic and intrinsic factors affecting salt marsh erosion. *J. Geophys. Res. Earth Surf.* 122: 1455–1470. doi:10.1002/2016JF004193
- Wang, Z. B., E. P. L. Elias, A. J. F. Van Der Spek, and Q. J. Lodder. 2018. Sediment budget and morphological development of the Dutch Wadden Sea: Impact of accelerated sea-level rise and subsidence until 2100. *Geol. en Mijnbouw/Netherlands J. Geosci.* 97: 183–214. doi:10.1017/njg.2018.8
- Ward, L. G., W. Michael Kemp, and W. R. Boynton. 1984. The influence of waves and seagrass communities on suspended particulates in an estuarine embayment. *Mar. Geol.* 59: 85–103. doi:10.1016/0025-3227(84)90089-6
- van Wesenbeeck, B. K., W. de Boer, S. Narayan, W. R. L. van der Star, and M. B. de Vries. 2016. Coastal and riverine ecosystems as adaptive flood defenses under a changing climate. *Mitig. Adapt. Strateg. Glob. Chang.* 1–8. doi:10.1007/s11027-016-9714-z
- Weston, N. B. 2014. Declining Sediments and Rising Seas: An Unfortunate Convergence for Tidal Wetlands. *Estuaries and Coasts* 37: 1–23. doi:10.1007/s12237-013-9654-8
- Widdows, J., N. D. Pope, M. D. Brinsley, H. Asmus, and R. M. Asmus. 2008. Effects of seagrass beds (*Zostera noltii* and *Z. marina*) on near-bed hydrodynamics and sediment resuspension. *Mar. Ecol. Prog. Ser.* 358: 125–136. doi:10.3354/meps07338
- Wiehe, P. O. 1935. A Quantitative Study of the Influence of Tide Upon Populations of *Salicornia Europea*. 3: 222–230.
- Willemsen, P. W. J. M., B. W. Borsje, S. J. M. H. Hulscher, and others. 2017. Quantifying Bed Level Change at the Transition of Tidal Flat and Salt Marsh : Can We Understand the Lateral Location of the Marsh Edge ? *J. Geophys. Res. Earth Surf.* 2509–2524. doi:10.1029/2018JF004742
- Willemsen, P. W. J. M., B. W. Borsje, V. Vuik, T. J. Bouma, and S. J. M. H. Hulscher. 2020. Field-based decadal wave attenuating capacity of combined tidal flats and salt marshes. *Coast. Eng.* 156: 103628. doi:10.1016/j.coastaleng.2019.103628
- Woodworth, P. L., W. R. Gehrel, and R. S. Nerem. 2011. Nineteenth and Twentieth Century Changes in Sea Level. *Oceanography* 24: 80–93. doi:10.5670/oceanog.2011.29.COPYRIGHT

Y

- Yang, S. L., B. W. Shi, T. J. Bouma, T. Ysebaert, and X. X. Luo. 2012. Wave Attenuation at a Salt Marsh Margin: A Case Study of an Exposed Coast on the Yangtze Estuary. *Estuaries and Coasts* 35: 169–182. doi:10.1007/s12237-011-9424-4
- Ysebaert, T., S. L. Yang, L. Zhang, Q. He, T. J. Bouma, and P. M. J. Herman. 2011. Wave attenuation by two contrasting ecosystem engineering salt marsh macrophytes in the intertidal pioneer zone. *Wetlands* 31: 1043–1054. doi:10.1007/s13157-011-0240-1

Z

- Zanuttigh, B., R. Nicholls, R. Thompson, Jean-Paul Vanderlinden, and H. Burcharth. 2015. *Coastal Risk Management in a Changing Climate*, Elsevier.
- van Zelst, V. T. M., J. T. Dijkstra, B. K. van Wesenbeeck, D. Eilander, E. P. Morris, H. C. Winsemius, P. J. Ward, and M. B. De Vries. 2021. Cutting the costs of coastal protection by integrating vegetation in flood defences. *Nat. Commun.* 6533. doi:10.1038/s41467-021-26887-4
- Zhu, Z., J. Van Belzen, Q. Zhu, J. Van De Koppel, and T. J. Bouma. 2019. Vegetation recovery on neighboring tidal flats forms an Achilles' heel of saltmarsh resilience to sea level rise. 1–12. doi:10.1002/lno.11249
- Zhu, Z., V. Vuk, P. J. Visser, and others. 2020. Historic storms and the hidden value of coastal wetlands for nature-based flood defence. *Nat. Sustain.* 3: 853–862. doi:10.1038/s41893-020-0556-z



Summary

SUMMARY

Many coastal communities are currently facing flood risks due to accelerating sea level rise, land subsidence and extreme events such as storms surges, which will probably become more frequent with climate change. As a result, increasing investment in coastal defence is needed worldwide. Hard engineering structures such as dikes are commonly used for coastal protection, nevertheless they are often associated with negative impacts on natural functioning and biodiversity of coastal ecosystems and their ecosystem services. Furthermore, because conventional hard engineering is static, it can be challenged by climate change and the maintenance may become very costly. Alternatives to hard engineering are the hybrid nature-based coastal defence systems which combine conventional hard engineered barriers with coastal ecosystems.

Hybrid nature-based defences can be a more sustainable, ecologically valuable and cost-effective alternative to hard engineering alone. In other words, combining coastal ecosystems with conventional hard infrastructures such as dikes may improve the coastal protection while preserving natural ecosystems. Coastal ecosystems such as marshes, mangroves, coral reefs, shellfish reefs and seagrass meadows provide coastal protection by attenuating waves, preventing coastal erosion and potentially keeping up with sea level rise. However, uncertainties about the actual effectiveness of these nature-based measures still hampers their practical implementation.

In this thesis I focussed on investigating coastal ecosystem dynamics in relation to their coastal protection role, as well as investigating nature management strategies in order to optimize both the coastal protection services and the ecological value of these ecosystems. This thesis is mainly focused on salt marshes, which are salt-tolerant vegetated areas at the transition between the land and sea subject to periodic flooding; seagrasses meadows, which are meadows of vegetation adapted to grow below the water; and tidal flats, which are soft sediment environments regularly flooded by the tides in intertidal areas.

FORESHORE ECOSYSTEM IMPACTS ON WAVE ATTENUATION AND RUN-UP

To understand the effect of foreshores on wave attenuation and wave run-up reduction onto the dikes, we require in depth understanding of *i)* which locations are suitable for salt marshes and *ii)* how effective are such vegetated foreshores in reducing wave run-up including contrasting foreshore types (i.e. different wind exposure, vegetation, tidal range and bathymetry).

In **Chapter 2**, through the analysis of vegetation and bathymetry maps of the Dutch Wadden Sea from the last two decades, we found that marshes grow next to tidal flats where sediment is deposited with sufficient elevation. Furthermore, we show that marsh retreat in the past decade was related to the erosion of the tidal flats in front of the marsh. In contrast, accretion of tidal flats was correlated to an expansion of the marsh edge. In addition, by conducting field measurements during 3 years, **Chapter 2** shows that wave run-up on the dikes is always reduced in dikes fronted by salt marshes compared to dikes facing bare mudflats, even when the marshes have short vegetation. This effect was mainly driven by the fact that salt

marsh vegetation traps sediment, and over time thus change the foreshore elevation, leading to increased wave reduction. Overall **Chapter 2** highlights the importance of foreshore morphology and sediment dynamics in both *i)* run-up reduction by wave attenuation (reducing dike failure risk) and *ii)* marsh development (i.e. low wave exposure and minimum elevation for specific flooding regime necessary for the vegetation to establish)

FORESHORE SEDIMENT STABILITY

In line with **Chapter 2**, soil stability of coastal ecosystems is of key importance for maintaining stable and elevated foreshores which in turn will provide increased coastal protection. In **Chapters 3, 4, 5 and 6** we studied the resistance of salt marshes, tidal flats, seagrass and dunes to erosion by water. We utilised different flumes, including wave flumes to test top and lateral erosion and a fast flow flume to test top erosion under fast water conditions that are representative of dike breach conditions. In **Chapter 3** we show that salt marsh vegetation creates a cohesive top layer that is highly resistant to fast water flow, which is important to reduce the breach depth in case of a dike failure. Only pioneer vegetation in sandy places was not erosion resistant, comparable to bare mudflats (**Chapter 3**). Furthermore, marshes with sandy subsoil can be resistant to top erosion but are sensitive to lateral erosion (**Chapter 3, 4 and 6**). Thus, marshes that are created for flood safety should not be built with sand. In **Chapter 4** we show that management of sandy islands by creating sheltered conditions for marsh development can lead to more stable soils. Dune soil was not resistant to lateral or top erosion due to the lack of cohesive sediment. Nevertheless, a salt marsh formed in the sheltered side of the dunes, creating a cohesive erosion-resistant topsoil layer through the accumulation of fine sediment, organic matter and roots by the marsh vegetation. Finally, ecosystems lower in the tidal range such as seagrass are also important for maintaining high and stable tidal flats and seabed. In **Chapter 5** we found that seagrass beds with high root density reduce soil erosion, and therefore play an important role on the stability of the seabed.

GRAZING MANAGEMENT ON SALT MARSHES FOR COASTAL PROTECTION

Lateral erodibility of marshes with fine-grained soils can be reduced by grazing of *i)* small herbivores (e.g., hares, geese) through the promotion of vegetation types with higher root densities, and *ii)* large herbivores (i.e., cattle) through soil compaction and reduced soil-bioturbating arthropods as a result of trampling (**Chapter 6**). Intensive cattle grazing may however lead to lower soil elevations, which may negatively impact the marsh resilience to sea level rise in areas with low sediment supply. Extensive grazing is also preferential for impacts on biodiversity. These results provide novel insight for understanding the effect of grazing by both large and small herbivores on marsh width, marsh elevation and marsh retreat.

MANAGEMENT OPTIONS FOR TIDAL FLATS TO PROMOTE MARSH EXPANSION

Wider marshes and elevated tidal flats can provide more coastal protection compared to low-lying bare foreshores (**Chapter 2**). Marsh expansion can be promoted by stabilizing and trapping sediment on the connected systems such as bare tidal flats. This can be achieved by

SUMMARY

hard engineering or by restoring natural ecosystems such as seagrass beds and mussel reefs as a nature-based alternative. In **Chapter 7** we tested the use of biodegradable artificial reefs for salt marshes expansion by accreting the fronting mudflats. Our experiment showed that there is potential to change tidal flat morphology. However, the dimensions of the reefs should be larger and the selection of materials should be matched with the hydrodynamic exposure.

CONCLUSIONS

In conclusion, salt marshes, compared to bare tidal flats, play an important role on coastal protection independently of the vegetation type or if they are in winter state (**Chapter 2, 3, 4, 6**). Therefore, they should be included in coastal protection schemes. Marshes will be stable and attenuate more waves loads onto the dikes compared to bare tidal flats even if they are grazed (**Chapter 2**). Furthermore, grazing by hare, geese and cattle may be interesting for reducing lateral erosion rates (**Chapter 6**). Nevertheless, high intensity cattle grazing should be avoided because it can lead to land subsidence and impact biodiversity. A limitation of the nature-based protection by salt marshes is that they cannot be implemented everywhere, because salt marsh establishment is very location-specific and depends on environmental conditions (e.g. sediment availability, elevation profiles and wave exposure, **Chapter 2**).

To create new marshes or to prevent the erosion of the existing marshes, focus should be put on managing the elevation of the fronting tidal flats and stimulate their net sediment accretion. When possible, ecosystem-based coastal defence should integrate connected ecosystems lower in the tidal range (for example tidal flats, seagrass beds and shellfish reefs), which can stabilise the soil, reduce waves arriving to the marsh edge (**Chapter 5 and 7**) and at the same time increase the ecological value of the area. Both processes, sediment stabilization and wave attenuation, are positively related to marsh expansion.

Unfortunately, restoration of mussel or seagrass beds in exposed locations is often difficult (**Chapter 7**). In cases where natural options like restoring seagrass beds and shellfish reefs are not feasible, marsh expansion could be promoted by minimal engineering actions (e.g. building brushwood groynes) until a stable marsh able to withstand waves has developed. In locations with high exposure or low sediment supply, where marshes are not able to migrate inland, such measures should be maintained long-term to prevent marsh erosion. In some cases, ecosystem-based solutions combining marshes and dikes may be too costly, not achievable, or going at the expense of other ecological values, such as causing the loss of mudflats that are important for migratory birds (**Chapter 2**). In these situations, 'hard engineering' solutions will remain the main applicable solution.



Samenvatting

SAMENVATTING

Veel kustgebieden kampen momenteel met risico's op overstroming door versnelde zeespiegelstijging, grondverzakking en extreme weersomstandigheden, wat mogelijk toe zal nemen met klimaatverandering. Hierdoor zal kustbescherming wereldwijd moeten worden verbeterd. Technische structuren zoals dijken worden gewoonlijk gebruikt als kustbescherming, maar kunnen een negatieve impact hebben op het natuurlijk functioneren en de biodiversiteit van kustecosystemen. Verder kan klimaatverandering deze statische structuren schade toebrengen waardoor het onderhoud prijzig wordt. Hybride, natuurgerichte bescherming waarbij techniek gecombineerd wordt met kustecosystemen biedt een alternatief.

Hybride, natuurgerichte kustbescherming kan een duurzamere, ecologisch waardevollere en goedkopere oplossing bieden. In andere woorden, het combineren van kustecosystemen met technische barrières zoals dijken verbetert de kustbescherming, evenals het behoud van natuurlijke ecosystemen. Kustecosystemen zoals moerassen, mangroves, koraalriffen en zeegrasweiden dragen bij aan kustbescherming door golfenergie te verlagen en hiermee kusterosie te voorkomen. Echter, onzekerheden over de effectiviteit belemmert nog altijd de toepassing hiervan. In deze thesis heb ik mij gefocust op de dynamiek van kustecosystemen in relatie tot hun rol in kustbescherming, evenals op strategieën om kustbescherming en de ecologische waarde van de ecosystemen te optimaliseren. Deze thesis is vooral gefocust op zoutmoerassen, zouttolerante gebieden op de grens van land en zee en onderhevig aan periodieke overstromingen; zeegrasweiden, vegetatie die is aangepast om onder water te kunnen groeien; en wadden, gebieden met zacht sediment die regelmatig overstromen door de getijden.

DE IMPACT VAN INTERGETIJDENGEBIEDEN OP DEMPING EN “RUN-UP” VAN GOLVEN

Om het effect van intergetijdengebieden op de demping van golven en de vermindering van run-up op dijken te begrijpen is kennis nodig van i) welke locaties geschikt zijn voor zoutmoerassen en ii) hoe effectief deze begroeide intergetijdengebieden zijn in het verminderen van run-up. In **Hoofdstuk 2**, blijkt dat moerassen groeien naast wadden waar sediment met voldoende verheffing wordt afgezet. Dit aan de hand van een vegetatieanalyse en bathymetrie kaarten van de Waddenzee van de afgelopen twintig jaar. Verder laten we zien dat de afname van moerassen in de afgelopen tien jaar te maken heeft met de erosie op wadden voor het moeras. Daarentegen is accumulatie van wadden gecorreleerd aan uitbreiding van de buitenste grens van moerassen. Hierbij laat Hoofdstuk 2 ook zien, aan de hand veldmetingen van de afgelopen drie jaar, dat run-up van golven op dijken altijd minder is bij aanwezigheid van een zoutmoeras voor deze dijk. Dit komt vooral doordat zoutmoerasvegetatie sediment afzet, wat zorgt voor verandering in de hoogte van intergetijdengebieden en hiermee bijdraagt aan golfdemping. Hoofdstuk 2 benadrukt het belang van de morfologie van intergetijdengebieden en sediment in i) run-up vermindering door golfdemping (wat het risico op dijkdoorbraken verlaagd) en ii) ontwikkeling van moerassen (b.v. minder blootstelling aan golven).

SEDIMENTSTABILITEIT VAN INTERGETIJDENGEBIEDEN

Sedimentstabiliteit van kustecosystemen is belangrijk voor het behoud van stabiele intergetijdengebieden, welke zo betere kustbescherming kunnen bieden. In **Hoofdstuk 2, 3, 4, 5 en 6** is de weerstand van zoutmoerassen, wadden, zeegrassen en duinen tegen erosie door water onderzocht. Verschillende golf tanks zijn gebruikt om erosie te testen onder verschillende golf omstandigheden, welke bijvoorbeeld vergelijkbaar waren met de omstandigheden bij een dijkdoorbraak. In **Hoofdstuk 3** laten we zien dat zoutmoerasvegetatie een bindende toplaag kan vormen die bestand is tegen snelle waterstroom. Alleen pioniersvegetatie in zandgebieden, zoals een wad, is niet bestand tegen erosie. Verder zijn moerassen met een zandondergrond bestand tegen toperosie maar niet tegen laterale erosie (**Hoofdstuk 3, 4 en 6**). Moerassen die gemaakt worden om te beschermen bij overstromingen moeten dus niet met zand worden gemaakt. In **Hoofdstuk 4** laten we zien dat bij zandeilanden het creëren van beschutting bij moerasontwikkeling kan leiden tot stabielere bodems. Duingrond was niet bestand tegen erosie door een tekort aan vast sediment. Bij een zoutmoeras aan de beschutte kant van de kust werd een vaste topsediment laag gevormd door de accumulatie van fijn sediment, organisch materiaal en wortels van de moerasvegetatie. Tot slot zijn ecosystemen lager in het getijdenverschil zoals zeegrassen ook belangrijk voor het behoud van hoge en stabiele wadden. In Hoofdstuk 5 hebben wij gevonden dat zeegrasweiden met een hoge worteldichtheid gronderosie verminderen en daarbij een belangrijke rol spelen in de stabiliteit van dit systeem.

HET BEHEER VAN GRAZERS IN ZOUTMOERASSEN VOOR KUSTBESCHERMING

Erosie van moerassen met fijn sediment kan verminderd worden door het laten grazen van i) kleine herbivoren (b.v. hazen, ganzen) welke vegetatie met hogere worteldichtheid stimuleren en ii) grote herbivoren (vee) welke de grond compacter maken en het aantal geleedpotigen doen verminderen (**Hoofdstuk 6**). Intensieve afgrazing door vee kan echter ook leiden tot terreinheffing, wat bij zeespiegelstijging een negatief effect kan hebben op de veerkracht van moerassen met weinig sedimenttoevoer. Deze resultaten geven nieuwe inzichten in het effect van grazers op moerasverbreding, -verhoging en -afname.

HET BEHEER VAN WADDEN EN DE VERBREIDING VAN MOERASSEN

Bredere moerassen en hogere wadden kunnen meer kustbescherming bieden dan kale, lage intergetijdengebieden (**Hoofdstuk 2**). Het stabiliseren en afzetten van sediment in verbonden systemen zoals wadden kan moerasverbreding tot gevolg hebben. Dit kan worden bereikt door technische structuren of door het natuurlijke ecosysteem te herstellen als een natuurgericht alternatief. In Hoofdstuk 7 hebben wij afbreekbare kunstmatige riffen getest voor zoutmoerasverbreding en dit liet zien dat het mogelijk is om de morfologie van het wad te veranderen. Echter zouden de riffen groter moeten zijn en de materialen die gebruikt worden zouden beter moeten passen bij de hydrodynamische omstandigheden waar zij aan blootgesteld worden.

CONCLUSIES

Om samen te vatten spelen zoutmoerassen, vergeleken met wadden, een belangrijke rol bij kustbescherming, onafhankelijk van het vegetatietype en het seizoen (**Hoofdstuk 2, 3, 4, 6**). Daarom moeten moerassen betrokken worden bij kustbeschermingsprogramma's. In vergelijking met wadden zijn zij stabiel en kunnen zij meer golven dempen op dijken, ook als zij begraasd worden (**Hoofdstuk 2**). Ook zou begrazing door hazen, ganzen en vee interessant kunnen zijn voor het verminderen van erosie (**Hoofdstuk 6**), alhoewel een hoge intensiteit aan begrazing door vee voorkomen moet worden door het bijkomend risico op grondverzakking en het effect op de biodiversiteit. Een nadeel van de natuurgerichte bescherming van zoutmoerassen is dat dit niet overal geïmplementeerd kan worden door de specifieke ecologische omstandigheden en locatie die dit ecosysteem nodig heeft (b.v. beschikbaarheid van sediment, blootstelling aan golven, **Hoofdstuk 2**). Om moeraserosie tegen te gaan en om nieuwe moerassen te creëren is het beheer van wadhoogte en stimulatie van sedimentaccumulatie belangrijk. Waar mogelijk moet ecosysteemgerichte kustbescherming ecosystemen die lager in het getijdenverschil liggen (b.v. zeegrasweiden) integreren. Deze ecosystemen kunnen de bodem stabiliseren en golven verminderen (**Hoofdstuk 5 en 7**), beide iets dat een positief effect heeft op moerasverbreding en de ecologische waarde. Helaas is het herstellen van zeegras- of mosselbedden in open locaties vaak moeilijk (**Hoofdstuk 7**). Wanneer natuurlijke oplossingen niet mogelijk zijn zou moerasverbreding kunnen plaatsvinden door minimale technische implicaties (b.v. bezinkvelden) totdat een stabiel moeras is ontstaan. Op onbeschutte locaties of locaties met weinig toevoer van sediment kunnen zulke maatregelen een lange termijn oplossing bieden om moeraserosie tegen te gaan. In sommige gevallen kunnen ecosysteemgerichte oplossingen waarbij moerassen en dijken gecombineerd worden prijzig of onhaalbaar zijn, of ten koste van andere ecologische waarden gaan zoals het verlies van wadden die belangrijk zijn voor migrerende vogels (**Hoofdstuk 2**). In zulke gevallen zullen 'technische structuur' oplossingen de meest toepasbare oplossing blijven.



Resumen

RESUMEN

Actualmente, muchas comunidades costeras están en riesgo de inundación debido al aumento acelerado del nivel del mar, el hundimiento de la tierra y eventos extremos, como las marejadas ciclónicas, los cuales probablemente serán más frecuentes con el cambio climático. Por lo que es necesario aumentar la inversión en defensa costera en todo el mundo. Las estructuras de ingeniería rígida tradicionales, como los diques, se usan comúnmente para la protección costera, sin embargo, a menudo se asocian con impactos negativos en el funcionamiento natural y la biodiversidad de los ecosistemas costeros. Además, debido a que la ingeniería rígida convencional es estática, puede verse desafiada por el cambio climático y el mantenimiento puede volverse muy costoso. Como alternativas a la ingeniería rígida tenemos los sistemas híbridos de defensa costera basados en la naturaleza o infraestructura “verde”, los cuales combinan barreras convencionales de ingeniería rígida con ecosistemas costeros.

Las defensas híbridas basadas en la naturaleza pueden ser una alternativa más sostenible, ecológicamente valiosa y rentable comparada con la ingeniería rígida por sí sola. En otras palabras, la combinación de ecosistemas costeros con infraestructuras rígidas convencionales, como por ejemplo la combinación de diques con marismas, puede mejorar la protección costera al mismo tiempo que se preservan los ecosistemas naturales costeros y sus servicios ecosistémicos (ver figuras 1 y 2 en el Capítulo 1 - Introducción). Algunos de estos ecosistemas costeros son las marismas, los manglares, arrecifes de coral, los arrecifes de ostras o de mejillones y las praderas marinas. Estos ecosistemas brindan protección costera al atenuar las olas, prevenir la erosión de la costa y, potencialmente, mantener la elevación del suelo al ritmo del aumento del nivel del mar. Sin embargo, las incertidumbres sobre la efectividad real de estas medidas basadas en la naturaleza aún dificultan su implementación práctica.

En esta tesis me he centrado en investigar la dinámica de los ecosistemas costeros en relación a su papel en la protección costera, así como en investigar estrategias de gestión de la naturaleza para optimizar tanto los servicios de protección costera como el valor ecológico de estos ecosistemas. Esta tesis se centra principalmente en las marismas intermareales, que son áreas con vegetación tolerante a la inundación por agua salada que crece en zonas intermareales sujetas a inundaciones periódicas; praderas de fanerógamas marinas, que son praderas de vegetación adaptada a crecer sumergidas en el agua marina; y planicies intermareales de barro, que son ambientes de sedimentos blandos sin vegetación inundados periódicamente por las mareas en las zonas intermareales (ver Box 1 en el Capítulo 1 - Introducción).

EFFECTOS DE LOS ECOSISTEMAS COSTEROS EN LA ATENUACIÓN DE LAS OLAS Y “RUN-UP”

“Run-up” se describe como el recorrido de las olas al chocar contra la costa o diques en relación al nivel promedio del mar (ver figura 3 en el Capítulo 1 - Introducción). Para comprender el efecto de los ecosistemas costeros como las marismas o las planicies intermareales de barro en la atenuación de las olas y la reducción del “run-up” en los diques, necesitamos comprender *i)* qué ubicaciones son adecuadas para el crecimiento y desarrollo de las marismas y *ii)* cómo de efectivas son dichas marismas con vegetación reduciendo las olas y “run-up”, comparando

diferentes tipos de marismas (ej. diferente exposición al viento, tipo de vegetación, rango de mareas y batimetría).

En el **Capítulo 2**, a través del análisis de mapas de vegetación y batimetría del Mar de Wadden Holandés de las últimas dos décadas, encontramos que las marismas crecen junto a las planicies intermareales de barro donde se depositan sedimentos con suficiente elevación, ya que una mínima elevación respecto al nivel del mar es necesaria para el crecimiento de la vegetación de marisma. Zonas demasiado inundadas por el mar no son aptas para el crecimiento de la vegetación de marisma. Además, mostramos que el retroceso de la marisma en la última década estuvo relacionado con la erosión de las planicies intermareales de barro frente a la marisma. Por el contrario, el incremento en elevación de las planicies intermareales gracias a la acumulación de sedimentos se correlacionó con una expansión de las marismas. Esto podría deberse a que las planicies intermareales más elevadas en frente de las marismas reducen más las olas que llegan al borde de las marismas, protegiéndolas así de la erosión. En el **Capítulo 2** además hice mediciones de campo durante 3 años, las cuales muestran que las olas y el "run-up" siempre fueron más atenuados en los diques que en frente tenían marismas con vegetación comparado con diques enfrentados por planicies intermareales de barro sin vegetación, incluso cuando las marismas tenían vegetación corta. Este efecto fue debido principalmente al hecho de que la vegetación de las marismas atrapa sedimentos y, con el tiempo, incrementa la elevación de la costa, lo que lleva a una mayor reducción de las olas. En general, el **Capítulo 2** destaca la importancia de la morfología de la costa y la dinámica de los sedimentos tanto en *i*) la reducción de las olas y "run-up" en los diques (reduciendo así el riesgo de "falla" del dique) como en *ii*) el desarrollo de las marismas intermareales (es decir, una elevación mínima permitirá el crecimiento de la vegetación de marisma gracias a una menor exposición a las olas y una frecuencia de inundación adecuada).

ESTABILIDAD DE LOS SEDIMENTOS COSTEROS

De acuerdo con el **Capítulo 2**, la estabilidad del suelo proporcionada por los ecosistemas costeros es de importancia clave para mantener las zonas costeras estables y elevadas, lo que a su vez brindará una mayor protección costera a través de una mayor atenuación de las olas. En los **Capítulos 3, 4, 5 y 6** hemos estudiado la resistencia a la erosión por olas y corrientes de agua de los suelos de marismas intermareales, planicies intermareales de barro, pastos marinos y dunas. En estos experimentos utilizamos canales de olas para medir la erosión superior y lateral de los sedimentos, y un canal de flujo rápido para medir la erosión superior en condiciones de corrientes de agua rápida que podrían ocurrir durante la ruptura de un dique. En el **Capítulo 3**, mostro que la vegetación de las marismas crea una capa superior cohesiva con mucha materia orgánica, raíces y/o sedimentos finos atrapados por la vegetación que es altamente resistente a la erosión por flujo rápido de agua, lo cual es importante para reducir la profundidad de la brecha en el caso de que un dique se rompa durante una tormenta. Las marismas con subsuelo arenoso pueden ser resistentes a la erosión superficial gracias a la capa superior cohesiva, pero son sensibles a la erosión lateral, ya que la arena sin mucha materia orgánica y baja densidad de raíces se erosiona fácilmente (**Capítulos 3, 4 y 6**). Sólo la vegetación de marisma pionera en lugares arenosos no fue resistente a ningún tipo de erosión experimental, al igual que las planicies intermareales de barro (**Capítulo 3**). Por lo tanto, se

RESUMEN

debería evitar construir nuevas marismas para la protección costera con arena y, por el contrario, utilizar sedimentos más finos como el limo y la arcilla.

En el **Capítulo 4** muestro que la gestión de islas arenosas mediante la creación de dunas que proveen protección frente a las olas para el desarrollo de marismas, puede dar como resultado suelos más estables. Los experimentos de erosión mostraron que el suelo de las dunas no es resistente a la erosión lateral o superior debido a la falta de sedimento cohesivo. Sin embargo, se formó una marisma en el lado protegido de las dunas, creando una capa cohesiva de suelo resistente a la erosión a través de la acumulación de sedimentos finos, materia orgánica y raíces por parte de la vegetación de la marisma. Finalmente, en el **Capítulo 5** encontramos que las praderas marinas con alta densidad de raíces también reducen la erosión del suelo y, por lo tanto, juegan un papel importante en la estabilidad del lecho marino. Por lo tanto, los ecosistemas más sumergidos que se encuentran a menos elevación respecto al nivel del mar, como los pastos marinos, también son importantes para mantener las planicies intermareales de barro y los fondos marinos elevados y estables.

GESTIÓN DEL PASTOREO EN LAS MARISMAS PARA LA MEJORAR LA PROTECCIÓN COSTERA

En el **Capítulo 6** muestro cómo la erosión lateral de las marismas con suelos de grano fino puede reducirse mediante el pastoreo por i) pequeños herbívoros (ej., liebres y gansos) gracias a la promoción de tipos de vegetación con mayor densidad de raíces, y ii) grandes herbívoros (ej., vacas) a través de la compactación del suelo y reducción de artrópodos bioturbadores del suelo como resultado del pisoteo. Sin embargo, el pastoreo de ganado intensivo puede reducir la elevación del suelo, lo cual puede tener un impacto negativo en la resistencia de las marismas al aumento del nivel del mar, sobre todo en áreas donde el suministro de nuevos sedimentos a la marisma es bajo. El pastoreo extensivo también es preferible por sus impactos sobre la biodiversidad. Estos resultados brindan una perspectiva novedosa para comprender el efecto que el pastoreo de herbívoros grandes y pequeños puede tener en la erosión lateral de las marismas y su elevación.

OPCIONES DE GESTIÓN PARA LAS PLANICIES INTERMAREALES DE BARRO CON OBJETIVO DE PROMOVER LA EXPANSIÓN DE LAS MARISMAS

Las marismas más anchas y las planicies intermareales de barro más elevadas pueden proporcionar una mayor protección costera en comparación a las zonas costeras con menor elevación y/o sin vegetación (**Capítulo 2**). La expansión de las marismas se puede promover mediante la estabilización y el incremento en elevación de los ecosistemas conectados, como las planicies intermareales de barro que se encuentran delante de las marismas. Esto se podría lograr mediante ingeniería rígida como los espigones, o con alternativas basadas en la naturaleza, por ejemplo restaurando ecosistemas naturales como las praderas marinas y los arrecifes de mejillones que pueden atrapar sedimento y elevar el lecho marino. En el **Capítulo**

7, hemos probado el uso de arrecifes artificiales biodegradables para aumentar la elevación de las planicies intermareales y así promover la expansión de las marismas. Nuestro experimento mostró que existe potencial para cambiar la morfología de las planicies intermareales usando arrecifes artificiales. Sin embargo, las dimensiones de los arrecifes deben ser mayores a los que utilizamos en el experimento y los materiales deberían de resistir las condiciones hidrodinámicas de la zona en concreto donde se vayan a utilizar.

CONCLUSIONES

En conclusión, las marismas intermareales con vegetación, en comparación a las planicies intermareales sin vegetación, juegan un papel muy importante en la protección costera, independientemente del tipo de vegetación presente o si se encuentran en estado invernal, cuando la cubierta de vegetación es menor y más corta (**Capítulo 2, 3, 4, 6**). Por lo tanto, las marismas intermareales deberían incluirse en los esquemas de protección costera. Las marismas serán estables y atenuarán más “run-up” en los diques en comparación a las planicies intermareales, incluso cuando hay pastoreo de ganado, el cual mantiene la vegetación más corta (**Capítulo 2**). Además, el pastoreo de liebres, gansos y ganado puede ser interesante para reducir las tasas de erosión lateral (**Capítulo 6**). Sin embargo, el pastoreo de ganado de alta intensidad debe evitarse porque puede provocar el hundimiento de la tierra y afectar la biodiversidad. Una limitación de la protección basada en la naturaleza por parte de las marismas es que no se puede implementar en todas partes, ya que el establecimiento de las marismas es muy específico y depende de las condiciones ambientales del lugar (ej., disponibilidad de sedimentos, perfiles de elevación y exposición a las olas, **Capítulo 2**).

Para la creación de nuevas marismas o para evitar la erosión de las marismas existentes, la atención se debe centrar en gestionar la elevación de las planicies intermareales de barro que se encuentran delante de las marismas y estimular su acumulación neta de sedimentos. Cuando sea posible, la defensa costera basada en ecosistemas debería integrar ecosistemas conectados a menores elevaciones en el rango de mareas (por ejemplo, planicies intermareales, praderas marinas y arrecifes), que pueden estabilizar el suelo, reducir las olas que llegan a las marismas (**Capítulos 5 y 7**) y a la vez que aumentar el valor ecológico de la zona. Ambos procesos (estabilización del suelo y reducción de las olas) están relacionados positivamente con la expansión de marismas.

Desafortunadamente, la restauración de arrecifes de mejillones u ostras y de praderas marinas en lugares muy expuestos a olas suele ser difícil (**Capítulo 7**). En los casos en que las opciones naturales, como la restauración de las praderas marinas y los arrecifes de mejillones u ostras no sean factibles, la expansión de la marisma podría promoverse mediante acciones temporales de ingeniería “blandas”, como, por ejemplo, la construcción de espigones hechos con matorral en vez de cemento, hasta que se desarrolle una marisma estable capaz de resistir las olas. En lugares con alta exposición a olas o bajo suministro de sedimentos, donde las marismas no pueden migrar hacia el interior del plano intermareal, dichas medidas deben mantenerse a largo plazo para evitar la erosión de las marismas. En algunos casos, las marismas no se desarrollan naturalmente aun poniendo medidas “blandas” de ingeniería, y por lo tanto

RESUMEN

las soluciones basadas en la naturaleza podrían ser demasiado costosas o inviables. En otros casos, la creación de nuevas marismas podría ir a expensas de otros valores ecológicos, como causar la pérdida de planicies intermareales de barro que son importantes para las aves migratorias (**Capítulo 2**). En estas dos últimas situaciones, las soluciones de "ingeniería rígida" seguirán siendo la principal solución frente a las inundaciones.



Acknowledgements

ACKNOWLEDGEMENTS

A PhD is not something you do alone, a PhD is not possible without the help and support of so many people. That's why I want to give thanks...

...To my PhD promotors Tjeerd, Han, Daphne and Laura. Thank you for giving me the opportunity to work with you and guide me through this adventure that is a PhD, including the good times but also the rough ones, especially with a pandemic in between. Your feedback has been always very valuable and I'm very grateful to have learnt from such talented scientists. Although 4 supervisors may seem a lot, I liked to have different opinions, you complemented each other with your own specializations on different topics. Special thanks to Laura, my daily supervisor, with who I've got more time to share experiences. You have inspired me in many ways to become better in what I do. Your tips have been always super helpful, and I appreciate all your support during my PhD. I also appreciate your effort to always make people aware of taking care of themselves.

...To the colleagues from the faculty in Groningen with who I started and the ones that came later and with I shared most of the moments there, Lis, Izzy, Drew, Guido, Nadia, Yvonne, Nico, Koosje, Max, Janne, Katrin, Kasper, Rik, Karin, Inger, Annelies, Karen, Bjorn, Hacen, Xueali, Ruth, Oscar, Fee; to the new colleagues in the office 443 and the 5th floor from the last year, which I could meet few times but where very nice; and to all the others at the CONSECO group. You made such a nice environment, I really enjoyed working there. I already miss you, our lunch breaks and ~~coffee~~ cake breaks!

...To Ingeborg and Joyce from the RUG, for being such nice persons and very helpful with the administration in the RUG. And to Matty Berg for the conversations about Orchestia at the beginning of the PhD

...To Lis and Izzy, for accepting being my paranymphs. After having shared office and friendship since pre-corona times, I'm very happy to have you by my side during this process! You are awesome persons! Also thanks Lis for helping me with the layout of the cover and Izzy for helping in the field and being the new mama of Hami 🐾

...To the colleagues (& partners of colleagues) that became close friends in Groningen. You made the living abroad much more fun and became my second family in Groningen. I loved our BBQs, the dinners and parties at home, the hotpots (thanks Drew!! I discovered them thanks to you!), the outings to Walibi were so much fun, the trainings with Bombi team, the reglettes, that day eating bugs for the first time (these were bad haha), the days swimming in the lake (I wish we would have had more nice weather days for this haha), our meetings in the grass field during corona times (with social distancing) playing games, volley and frisbee (I learnt how dangerous it can be thanks to Rik haha), the Carnival in Venlo (it was very cool to experience this with our local friend Guido), the arts and crafts days... and much more. Unfortunately we could not do some things we wanted due to covid... but we managed to do nice things anyways

😊 I miss you all!!!

...To the technicians from NIOZ and Groningen, Lennart, Bert, Daniel, Jan, Jacob, Nelly... for your help provided during the experiments.

...To the people I met from the NIOZ Yerseke during my stays there. Although for short periods, it was nice to meet new colleagues. Also thanks to the staff that has supported me during my PhD and which made paperwork and administration an easy task.

...To the Griend Team, Laura, Tjisse, Karin, Jannes, Marjolin, Valérie, Ralph, Greg, Janne, Emma, Maarten, Nadia, Han, Peter and all the volunteers. The biggest experiment I've been involved. The expeditions were so much fun, it was very nice sharing those days, sleeping in the Ambulant and being able to just walk from the boat to the sea bed when the tide was low. Special thanks to Sien and Saar for the amazing food and Jouke the captain!

... To Roselle Spaargaren for translating the summary to Dutch

... To the colleagues from the AllRisk project and the end users. It was very enriching to be involved with researchers and stakeholders related to other topics different from ecology. I appreciate all the input and insights from the meetings and I really enjoyed the outings we did every year as a team.

...To the people from The Fieldwork Company, Jannes, Maarten, Gabriela, Diewuke, Marga, Henk, Jan ... for sharing nice moments in the field collecting seagrass, in Griend, nice dinners and company.

...To the bachelor and master students that did projects with me and the ones who volunteered some days to do fieldwork: Marc Santsusagna, Rebecca Christiaanse, Anne Bauw, Rens Riggers, Tjalf van Minnen, Geert- Jan Sieperda, Leon Kaptein, Fabris van der Zee, Linda Meijers, Panagiota Stergiou, Santiago Amaya, Lissie de Groot, Michelle Jongenelen, Arne van Eerden, Tessel Lagerwerf, Isabella Hosftede, Thijs Zuidewind, Lucia Irazabal Gonzalez and Sarah Paulson. None of the projects would have been feasible without you. Thank you for the moments shared in the field, mostly fun, other times also feeling a bit miserable under the cold rain in winter sinking in the mud but always with good spirit haha, others like the rescue in the mudflat of Holwerd (you know who you are haha) , luckily I had a wooden board, which I never thought I would use, but glad I had it in the car haha.

...To Eduardo Infantes, his family in Sweden and the colleagues I met in Kristineberg Marine Station (Sweden) . There I did my master project and performed the experiment that became my first paper, included in this thesis. I spent an awesome time there, enjoying the amazing Swedish nature and seagrass, only by 50 meters from my door! We were very few people there but I loved the environment, it felt like a little family.

... A mi familia, en especial a vosotros, papa, mama e Iván, por siempre creer en mí y apoyarme en todas mis decisiones. Por no parar mi curiosidad y ganas de explorar, aunque eso significara irme a vivir a otro país. Porque siempre habéis intentado venir a verme allá donde esté. Siempre

ACKNOWLEDGEMENTS

os llevo conmigo, suerte que la tecnología hoy en día hace más fácil mantener el contacto, eso hace más llevadero estar lejos. Os quiero mucho!

... A todos mis amig@s en Barcelona, l@s de siempre, l@s de la uni, las de waterpolo y l@s nuevos que conocí gracias al Pol (en realidad no tan nuevos despues de más de 8 años ya jaja). Porque siempre que vuelvo a casa es como si no hubiera pasado el tiempo entre nosotr@s y nunca me van a faltar cosas por hacer y eso me encanta! Haceis que desconecte y recargue las baterias al 100%! Os echo de menos!

... A la Tere i la Marina, per acollir-me com part de la vostra familia cada cop que vaig a casa vostra (bé, ara ja sí que som familia legal haha) i pels bons moments cada cop que ens reunim.

... I per últim però no menys important, al Pol, per donar-me suport incondicional, fins i tot mudar-te a un altre país. Has sigut una part clau en tot el doctorat. A part del suport moral, m'has ajudat molt amb el treball de camp, sobretot durant els mesos amb restriccions pel covid, on no ens podíem juntar amb altra gent i et vas convertir en el meu únic ajudant de camp. Gràcies per ficar-te al fang apestos i enganxifos amb mi haha. T'estimo molt i em sento molt afortunada de poder compartir la vida amb tu.









Curriculum vitae

CURRICULUM VITAE

Beatriz Marin Diaz has dedicated her education and early career to making a positive connection between humans and the natural environment. She was born in Ripollet, Barcelona, Spain, on the 23rd of January 1992, and always loved being in nature, especially in the water. After finishing high school in 2010, she started a degree in Environmental Biology at the Autonomous University of Barcelona. This was a new degree in Spain that centered on the part of the biology that studies the relationship among biological systems, in all of its complexity and diversity, within their natural environment, also including environmental management and conservation. For 4 years she gained knowledge about all the ecosystems, from high mountains to the sea, with special focus on the Mediterranean region. For her internship, she spent the summer of 2013 at the Center for Recovery of Marine Species (CREM) in Ibiza, a beautiful island in the Mediterranean. There, she took care of the fish in the Center, learned how to rescue turtles and dolphins and worked as an environmental educator with both international tourists and local kids from the island. She also censused marine species with scuba, with particular attention to sea urchins and seagrass.

After finishing her Bachelor's degree, she did further training to become a technician of rehabilitation and recuperation of wild animals, in Madrid, Spain. Then she volunteered in a wildlife recovery center in Barcelona. While there, she also led a Scouts group and worked as an environmental educator and adventure sports leader in summer camps for kids and families. Her favourite activity was introducing visitors to the Mediterranean Sea through snorkel tours.

Driven by the eagerness to conserve and restore natural ecosystems, in 2015 Beatriz pursued a Master's degree in Ecology, Environmental Management and Restoration at the University of Barcelona. At the same time, she volunteered for a whale monitoring project between Barcelona and Mallorca. She also obtained an Erasmus grant to initiate her final research project in Sweden on seagrass. She conducted an experiment to examine the role of eelgrass in reducing soil erosion, which led to her first scientific paper. She also participated in seagrass seed collection for restoration projects and did data analysis of the causes preventing the success of seagrass restoration projects.

One of Beatriz's biggest motivations was to play an active role in the real-world conservation and restoration of coastal ecosystems by developing and applying scientific knowledge. In line with these interests, in 2017, she applied for a joint PhD position in the Netherlands between The Royal Netherlands Institute for Sea Research (NIOZ) and the University of Groningen. The project aimed to address knowledge gaps on the effectiveness of coastal ecosystems on shoreline protection to encourage their conservation and inclusion in coastal protection schemes. Her work was a bridge between the practical application of engineering with nature and ecology. During her PhD, she has collaborated with a wide range of stakeholders that included engineers, nature managers and policy makers. She has presented 3 posters at national conferences in the Netherlands, and 4 oral presentations, 2 of which were in international conferences. She received the 1st prize for her oral presentation at the Netherlands Annual Ecology Meeting in 2020. She has supervised 11 students, including 4 master's projects. She has also given lectures on ecosystem-based coastal defence for the Master's Degree program in Marine Biology from the University of Groningen in 2020 and

2021. In addition to her thesis, her love for seagrass compelled her to engage with seagrass restoration projects with colleagues at the University of Groningen.

Since March 2022, Beatriz has worked as a Post-Doc in the Center for Coastal Solutions at the University of Florida. She has started a scientific diving course and will perform monitoring and restoration experiments in seagrass meadows, oyster beds and marshes on the west coast of Florida as part of a coastal resilience through nature-based solutions project.

CONTACT INFORMATION

bea.marin.diaz@gmail.com

ORCID: 0000-0003-4820-4662

www.linkedin.com/in/beatriz-marin-diaz

www.researchgate.net/profile/Beatriz-Marin-Diaz

Twitter [@BeatrizMarin_](https://twitter.com/BeatrizMarin_)



List of publications

PUBLISHED PAPERS

Marin-Diaz, B., Govers, L. L., van der Wal, D., Olff, H., & Bouma, T. J. (2022). The importance of marshes providing soil stabilization to resist fast-flow erosion in case of a dike breach. *Ecological Applications*, e2622. <https://doi.org/10.1002/eap.2622>

Temmink, R.J.M., Fivash, G.S., Govers, L. L., Nauta J., **Marin-Diaz, B.**, Cruijnsen, P.P.M.J.M., Reijers V.C., Didderen, K., Penning, E., Olff, H., Heusinkveld, J.H.T., Lamers L.P.M., Lengkeek, W., Christianen, M.J.A., Bouma, T. J. & van der Heide, T., (2022). Initiating and upscaling mussel reef establishment with life cycle informed restoration: Successes and future challenges. *Ecological Engineering*, 175, 106496. <https://doi.org/10.1016/j.ecoleng.2021.106496>

Marin-Diaz, B., Fivash, G.S., Nauta J., Temmink, R.J.M., Hijner N., Reijers V.C., Cruijnsen, P.P.M.J.M., Didderen, K., Heusinkveld, J.H.T., Penning, E., Maldonado-Garcia, G., van Belzen, J., Christianen, M.J.A., van der Heide, T., Daphne van der Wal, D., Olff, H., Bouma, T. J. & Govers, L. L. (2021). On the use of large-scale biodegradable artificial reefs for intertidal foreshore stabilization. *Ecological Engineering*, 170, 106354. <https://doi.org/10.1016/j.ecoleng.2021.106354>

Marin-Diaz, B., Govers, L. L., van der Wal, D., Olff, H., & Bouma, T. J. (2021). How grazing management can maximize erosion resistance of salt marshes. *Journal of Applied Ecology*, 58(7), 1533-1544. <https://doi.org/10.1111/1365-2664.13888>

Marin-Diaz, B., Bouma, T. J., & Infantes, E. (2019). Role of eelgrass on bed-load transport and sediment resuspension under oscillatory flow. *Limnology and Oceanography*, (2), 426–436. <https://doi.org/10.1002/lno.11312>

SUBMITTED PAPERS

Marin-Diaz, B., Daphne van der Wal, Leon Kaptein, Pol Martinez-Garcia, Christopher H. Lashley, Kornelis de Jong, Jan Willem Nieuwenhuis, Laura L. Govers, Han Olff, Tjeerd J. Bouma (under review). Using salt marshes for coastal protection: effective but hard to get where most needed.

PENDING SUBMISSION

Marin-Diaz, B., Reijers, V. C., Meijers, L., van der Wal, D., Olff, H., Bouma, T. J. & Govers, L. L. (in prep.). Quantifying the resistance to cliff and sheet erosion across vegetation zones on a sandy back-barrier island

Nauta J., Christianen, M.J.A., Temmink, R.J.M., Fivash, G.S., **Marin-Diaz, B.**, Reijers V.C., Penning, E., Borst, A., Didderen, K., Heusinkveld, J.H.T., Zwarts, M., Cruijnsen, P.P.M.J.M., Hijner, N., Lengkeek, W., Lamers L.P.M., van der Heide, T., Bouma, T. J., van der Wal, D., Olff, H., Govers, L. L. (in prep.). Enhanced food web complexity and biodiversity through artificial reefs in an intertidal soft-sediment ecosystem

NON PEER-REVIEWED REPORTS

Habitat-overstijgende interacties in het Waddengebied. Govers, L., Reijers, V., Smeele, Q., Olf, H., van der Zee, E., Temmink, R., **Marin Diaz, B.**, Fivash, G., Nauta, J. & van der Heide, T., 2021, Driebergen: VBNE, Vereniging van Bos- en Natuurterreineigenaren. 52 p.

CONFERENCE PRESENTATIONS

Marin-Diaz, B., Fivash, G.S., Nauta J., Temmink, R.J.M., Hijner N., Reijers V.C., Crujisen, P.P.M.J.M., Didderen, K., Heusinkveld, J.H.T., Penning, E., Maldonado-Garcia, G., van Belzen, J., Christianen, M.J.A., van der Heide, T., Daphne van der Wal, D., Olf, H., Bouma, T. J. & Govers, L. L. On the use of large-scale biodegradable artificial reefs for intertidal foreshore stabilization. 9th World Conference on Ecological Restoration (SER), 2021, Canada (online due to covid-19)

Marin-Diaz, B., Govers, L. L., van der Wal, D., Infantes, E., Olf, H., & Bouma, T. J. Unravelling foreshore ecosystem dynamics: applications for ecosystem-based coastal defence. 6th International EcoSummit Congress: Building a sustainable and desirable future: Adapting to a changing land and sea-scape, 2021, Australia (online due to covid-19)

Marin-Diaz, B., Govers, L. L., van der Wal, D., Infantes, E., Olf, H., & Bouma, T. J. Unravelling foreshore ecosystem dynamics: applications for ecosystem-based coastal defence. Netherlands Annual Ecology Meeting (NAEM), 2020, the Netherlands (1st prize oral presentation)

Marin-Diaz, B., Govers, L. L., van der Wal, D., Olf, H., & Bouma, T. J. Saltmarsh elevation, age and grazing as predictors for cliff erosion. Coastal Ecology Workshop, Wales, 2018.

POSTER PRESENTATIONS

Marin-Diaz, B., Govers, L. L., van der Wal, D., Infantes, E., Olf, H., & Bouma, T. J. Unravelling foreshore ecosystem dynamics: applications for ecosystem-based coastal defence. Netherlands Annual Ecology Meeting (NAEM), 2019 and LIFE Congress, The Netherlands, 2019

Marin-Diaz, B., Govers, L. L., van der Wal, D., Olf, H., & Bouma, T. J. How to manage foreshore ecosystems to gain both coastal protection and ecological value?. Netherlands Annual Ecology Meeting (NAEM), 2018.

ORGANIZATION OF SEMINARS

"Forelands: useful for flood risk management or just beautiful nature?", as part of the All-Risk Webinar series, including an oral presentation (29th June 2021, The Netherlands)

